Examination of mechanisms underlying the effect of single-session exercise on cortical plasticity

by

Jonathan S. Thacker

A thesis
presented to the University of Waterloo
in fulfillment of the
thesis requirement for the degree of
Doctor of Philosophy
in
Kinesiology

Waterloo, Ontario, Canada, 2018

Examining Committee Membership

The following served on the Examining Committee for this thesis. The decision of the Examining Committee is by majority vote.

External Examiner	NAME **Dr. Tak Pan Wong** Title: **Associate Professor**
Supervisor(s)	NAME **Dr. John G. Mielke** Title **Associate Professor** NAME **Dr. W. Richard Staines** Title **Professor, Associate Dean - Research**
Internal Member	NAME **Dr. A Russell Tupling** Title **Professor, Associate Chair - Undergraduate** NAME **Dr. Robin Duncan** Title **Assistant Professor**
Internal-external Member	NAME **Dr. Michael Beazely** Title **Associate Professor**
Other Member(s)	NAME **N/A**

Authors Declaration

This thesis consists of material all of which I authored or co-authored: see Statement of Contributions included in the thesis. This is a true copy of the thesis, including any required final revisions, as accepted by my examiners.

I understand that my thesis may be made electronically available to the public.

Statement of Contributions

I declare that my contribution includes the majority of research design, data collection, data analysis and data interpretation in Chapters 2-5, and writing of the thesis. Both supervisors, Dr. W. Richard Staines, and Dr. John G. Meilke, are the primary co-authors on all published manuscripts derived from this thesis. Dr. Eric Bombardier assisted with collection of VO_2 data in Chapter 2. Yuyi Xu and Cerise Tang contributed to the data collection in chapters 3-4.

Abstract

Individuals who routinely participate in physical activity are the beneficiaries of a wide array of health benefits. As well, recent observations in humans have identified that even a single session of aerobic exercise can enhance the receptivity of the primary motor cortex (M1) to within-session motor skill training, a phenomenon referred to as "priming". However, the biochemical mechanisms that account for exercise-induced priming of M1 remain relatively unexplored. Thus, the current thesis presents 4 studies that aimed to uncover the biochemical signature responsible for exercise-induced priming of M1 following a single bout of aerobic exercise. Given the notion that a single exercise exposure primes M1 for learning, it is likely this change would manifest on a molecular level and mirror adaptations stereotypically observed during early synaptic plasticity. In the first study, no observable differences in plasticity-related protein expression were found in the M1 of male, Sprague-Dawley rats following either acclimatization, or a graded exercise test to exhaustion. These data suggest treadmill acclimatization, or exhaustive exercise are not likely, by themselves, to evoke the required sort of change within M1. Consequently, a more likely candidate for exercise-induced priming was pursued; that is, post-translational modification of the already established proteome. In study 2, significant increases of both AMPA (GluA1, 2) and NMDA (GluN2A, B) receptor subunit phosphorylation were observed only after a single session of moderate exercise. Phosphorylation changes of the observed direction and magnitude have previously indicated alterations in the localization of these receptors at the cellular surface, however, whether these changes are confined to synaptic densities remains uncertain. Presently, few techniques exist with the specificity and precision required to adequately assess the synaptic surface fraction. As a result, in study 3, we developed a novel approach to enrich synaptic surface proteins by combining two well-established techniques (biotinylation + synaptoneurosome

isolation). Using Western blot analysis, we confirmed that our biotinylated-synaptoneurosome fraction showed strong agreement with the presumptive presence of synaptic membrane-bound proteins, while excluding negative-control proteins. Moreover, we displayed the sensitivity of this approach to detect synaptic receptor trafficking events by chemically inducing long-term potentiation in M1 slices. Following the development of this technique, we redirected our efforts to explore the priming effects within M1. Specifically, we assessed the efficacy of priming M1 using two molecules (Corticosterone + BDNF) previously demonstrated to be released during and after a single session of exercise. We incubated M1 slices either in combination, or alone, with each of the two hormones and found significant changes in synaptic surface expression of either NMDA, or AMPA receptor subunits. In addition, we observed large increases in AMPA receptor subunit phosphorylation and total AMPA receptor presence within synaptic fractions, suggesting priming of M1 may be reflected as the accumulation of receptors within synapses, which would serve to provide a receptor pool at the synaptic density ready for insertion. In combination, the 4 studies provide the first evidence for a mechanism that may account for exercise-induced priming following a single session of moderate aerobic exercise.

Acknowledgments

The words on the page may be mine, but between every line is the support of a mentor, a colleague, a family member, and a friend. I share in my success of this thesis with these individuals, for it is they who provided me with the unwavering support and encouragement to pursue my dreams.

First, I would like to thank my mentors Dr. W Richard Staines, and Dr. John G Mielke; to this day I still cannot believe I convinced you both to undertake this endeavor. Rich, you took a chance on that naïve undergraduate student in your neuroanatomy class, introduced him to the scientific method and fostered his ability for inquiry, for this I will be forever grateful. John, our long conservations in your office and in the laboratory about life and science are some of the most meaningful moments of my Ph.D., your guidance has instilled a confidence in me that will remain with me always. Although I will forever consider you both as mentors, it is now my privilege to call you both my colleagues, and my friends.

To my committee, Dr. Robin Duncan and Dr. Russ Tupling: your combined expertise, and continued feedback were central to the development of this thesis. I thoroughly enjoyed our conversations about science whenever, and wherever they took place, be it in the office, laboratory or on the ice. You collectively challenged me to think critically of my data, question the boundaries of my research, and instilled in me what it means to be a great researcher, a lesson I will not take for granted. In addition, I would also specifically like to thank Dr. Mike Beazely and Dr. Tak Pan Wong, for both the donation of their time and expertise to the thesis process.

To my colleagues and friends: from our scientific debates and distracted office discussions, from the lab to the rink, Bourbon St. to Mission Bay, we have developed friendships and memories

to last a lifetime. I am incredibly fortunate to have been surrounded by such an amazing group of individuals, I want you to know that each and every one of you continues to inspire me.

To my loving parents and sisters: you are a force of stability and encouragement in my world, constantly pushing me forward. To my parents, your relentless support, hard work, and countless sacrifices have rewarded me the opportunity to pursue my dreams, and for this, I am eternally grateful. To my family-in-law, your continuous encouragement and open availability for de-stress weekends at “the cottage” were integral to the completion of this thesis, thank you.

To my loving wife Rebecca and son Arley, I am at a loss for words that could accurately express my gratitude towards you both, which is odd considering this thesis is not short on any. I will say this; Rebecca I am so lucky to have discovered such a loving and supportive partner. I couldn’t imagine experiencing this crazy journey with anyone else. You and Arley are the reason why I get up every morning on purpose. I hope our next adventures can only be half as fun as our first one. Love you.

Table of Contents

List of Figures

and CaMKII which together results in the vesicular migration and insertion into the perisynaptic membrane. Unknown (?) components of this model include how TrkB may mediate GluA2 phosphorlyation and whether trkb activation results in an increase GluA1 at post synaptic densities. Alternative model is related to the spiked response of peripheral corticosterone resulting from exercise. CORT rapidly perfuses the blood-brain barrier where it can, under a concentration-gradient specificity, activate membrane bound MRs. MR have the capacity to activate SFKs such as SRC that are known to upregulate the phosphorylation and Ca^{2+} conductance of GluN2-containing NMDARs. Moreover, SRC has been shown to mediadte GluA2 phosphorylation resulting in an internalization of surface GluA2-containing AMPARs. Furthermore, MR activation modulates GPCR activity resulting in the increased activity of adenylyl cyclase, increasing the local levels of cAMP. Increased cAMP acts as a second messenger activator of PKA which is known to be critical for the phosphorylation, vesicular migration and perisynaptic insertion of GluA1.

Figure 3.16 Sequential mechanism through which CaMKII can act as an LTP-independent primer. Activation of CaMKII at T286 by the temporal release of intracellular Ca^{2+} or PKC-mediated activation results in CaMKII accumulation around post-synaptic densities, PP1 remains dormant. In particular, pCaMKII form associations with GluN2-containing NMDARs where they phosphorylate GluN2 at various sites. Under conditions of low post-synaptic densities and high PKA activation, PP1 phosphatase dephosphorylates CaMKII at T286, causing it to dissociate from the GluN2 complex, leaving behind the phosphorylated GluN2.

Figure 4.1 Illustration of the procedure for producing biotinylated synaptoneurosomes (BioSyn), which in theory yield an enriched homogenate of synaptic surface proteins. Slices (350 µm) from either SMCx, or HP were incubated with 1 mg/mL of biotin for 40 minutes at 4oC. Following homogenization, the whole homogenate (WH) was passed through a sequence of filters to isolate the synaptoneurosome preparation. The SNPs were then lysed and homogenates incubated with neutravidin beads for 4 h at 4oC

List of Tables

List of Abbreviations

AC – Acclimatization control

ACSF – Artificial cerebral spinal fluid

AMPAR- α-amino-3-hydroxy-5-methyl-4-isoxazolepropionic acid receptors

BDA – Biotinylated dextran amine

BDNF – Brain-derived neurotrophic factor

BioSyn – Biotinylated synaptoneurosome

BSA – Bovine serum albumin

CA – cornu Ammonis

CAMKII - calcium-calmodulin-dependent protein kinase II

cAMP – cyclic adenosine monophosphate

CNS – Central nervous system

DG – Dentate Gyrus

fEPSP – field excitatory postsynaptic potential

GABAR- γ-aminobutyric acid receptor

GC – Glucocorticoid Receptor

GFAP – glial fibrillary acidic protein

GRIP – Glutamate-receptor-interacting protein

GXT – Graded exercise test

HP – Hippocampus

LTP – Long-Term Potentiation

M1 – Primary Motor Cortex

MC – Mineralocorticoid Receptor

mEPSP – miniature excitatory postsynaptic potential

mGluR – metabotropic glutamate receptors

MOD – Moderate exercise group

NMDAR- N-methyl-D-aspartate receptors

PBP – primed burst potentiation

PKA – Protein Kinase A

PKC – Protein Kinase C

PND – Post-natal Day

PSD95 – Postsynaptic density protein 95

PTM – Post-translational modifications

PTP – Post-tetanic potentiation

pTyr – Total phosphor-tyrosine

RER – Respiratory exchange ratio

SED – Sedentary group

Ser – Serine

SNP – Synaptoneurosome preparation

Src - Proto-oncogene tyrosine-protein kinase

TARP – transmembrane AMPA receptor regulatory protein

TBST – Tris-buffered saline with Tween-20

TC- Treadmill control

TEA – tetraethylammonium

Thr – Threonine

Trk – tropomyosin-related kinase

TTX – tetrodotoxin

Tyr – Tyrosine

VCO_2- Carbon dioxide production

VDCC – Voltage-dependent calcium channel

VO_2 – Oxygen consumption

WH – Whole homogenate

1. REVIEW OF RELEVANT LITERATURE

1.1 THESIS OVERVIEW & GENERAL OBJECTIVES

Neuroplasticity is a process by which neurons are able to refine their structure and function in an effort to perform optimally within a given environment. With regards to acquiring a novel motor skill (i.e., motor learning), neuroplasticity is thought to induce cellular mechanisms, one of which is known as long-term potentiation (LTP) (Ziemann et al., 2004). LTP may be broken down into early (receptor trafficking and post-translational modification) and late (protein synthesis) phases. Emerging evidence suggests that chronic exercise can enhance the synthesis of growth factors and their respective receptors (Voss et al., 2013). However, it is unclear how short-term plasticity may be affected by acute exercise, and further, how this may promote the transition from the early phase to late phase LTP. Interestingly, acute bouts of aerobic exercise can have a robust modulatory effect on the concentration and uptake of plasticity-related growth factors (Vaynman, 2003). The following series of studies investigated the possibility that aerobic exercise may have a priming effect on early phases of LTP within cortical motor neurons, leading to more efficient and sustained motor skill acquisition. The research in this thesis aimed to provide a mechanistic foundation for the use of acute bouts of aerobic exercise to enhance motor learning through the following research questions:

(1) Does acclimatization to the use of a treadmill or maximal exhaustive exercise alter plasticity-related protein expression in motor cortex?

(2) Does acute aerobic exercise modify post-translational signaling within the motor cortex in a way that would promote plasticity?

(3) Does exercise promote the movement of receptors that alter the synaptic content in a way that favors plasticity?

1.2 ANATOMICAL STRUCTURES

1.2.1 Primary Motor Cortex

The term motor cortex is a common nomenclature used to represent the collection of frontal areas that contribute to the production of movement. Specifically, in humans, the primary motor cortex (M1) is broadly defined as the region of cortical tissue responsible for producing cortical efferent information that evokes voluntary movement (Penfield and Boldrey, 1937). The M1 can be dissociated from other motor regions anatomically as the precentral gyrus, or by the decreased threshold required to elicit a motor response. Cytoarchitecturally M1, is often referred to as either Brodmann Area 4 or agranular cortex, stemming from the absence of a granular layer (layer IV). At the cellular level, the cortical orientation can be broken into 6 vertical layers, numbered superficially to deep. These layers are defined by either the presence or absence of cellular bodies. Input into M1 is generally associated with layer IV while the output is associated with I and II locally, and V globally. Layer V principally consists of large excitatory pyramidal cells whose axons produce the corticospinal tract. These features consequentially yield a thicker layer V within M1, with a relatively smaller layer IV compared to other primary afferent receiving regions, such as the primary somatosensory cortex (Geyer, Schleicher, & Zilles, 1999).

Unlike the human primary somatosensory cortex, where representations are parceled into distinct smooth overlapping regions (dependent on the sensitivity, or innervation density of varying regions of the body), M1's representation appears to be less resolved and far more pixelated, coding for organized movements rather than individual muscle representations (Chouinard and Paus, 2006). Research in the area of micro and transcranial magnetic stimulation has provided insight into the substantial overlap that exists in the initiation of different movements (Wilson et al., 1993). This overlap has been confirmed using intracortical recordings in macaque

monkeys, showing a single upper motor neuron activating a collection of lower motor neuron pools representing many individual muscles (Murray and Oulter, 1981). Coding of muscular movements in this way allows for a variety of simple and complex actions with an impressive level of adaptability.

This way of categorizing movement is not a unique primate trait; laboratory rat species have highly evolved motor systems that display similar, albeit more rudimentary, behaviors. However, at roughly 1000^{th} the size of a human brain, identifying definitive cortical regions in rat brain can be complicated. Specifically, rat cortex is lissencephalic with fewer prominent gross anatomical features, and segregated cortical fields (Hall and Lindholm, 1974). For this reason, cortical structures are commonly referenced to bregma: a juncture between coronal and sagittal sutures of the skull. When considering the inherent variability in bone structure, bregma is remarkably consistent and rarely deviates more than 0.5 mm in rodents when age, sex, and weight are fixed (Paxinos et al., 1985). The inherent reliability of bregma allows for relative specificity when identifying brain regions, especially with the use of a stereotaxic coordinating system.

Histological staining of rat brain slices reveals cortical regions similar in cytoarchitecture to that of humans, including an agranular cortex (Paxinos and Watson, 1982; Zilles, 1985). Further evidence suggests rat agranular cortex can be further divided into medial (AG_m) and lateral (AG_l) fields (Donoghue and Wise, 1982). Although retrograde labeling of the cervical cortico-spinal tract yields positive results in both agranular cortices, microstimulation of these areas would suggest thresholds to be lower in AG_l (Donoghue and Wise, 1982). Unlike human M1, rat electrophysiological data display significantly more overlap in responsiveness between the motor and sensory representations (Hall and Lindholm, 1974). For this reason, debate still persists about the true boundaries of M1 in rats. However, for the purpose of this thesis the superior frontoparietal

region containing agranular cortices AG_m and AG_l in rats will be considered synonymous with M1 of humans. In the mature rat, this M1 characterization corresponds to the cortical tissue constrained by the boundaries of 2.7 mm rostral and 3.3 mm caudal of bregma (Paxinos and Watson, 1982).

1.2.2 Hippocampus

The term hippocampus (HP) stems from the Greek, *hippókampos* meaning sea monster, or classical mythological seahorse, and is a reference to its structural appearance from the intraventricular view. All known vertebrates have evolved two hippocampi, which are specialized regions of cortex encapsulated within each cortical hemisphere. In humans, each HP arcs from the hippocampal head laterally, embedded within the temporal lobe (temporal pole), to the tail medially along the posterior septum (septal pole), resulting in an overall crescent-shaped appearance. The HP is a bilaminar structure consisting of the dentate gyrus and cornu Ammonis separated by a thin vestigial hippocampal sulcus. The lamina folds into one another, emerging as two interlocking U-shaped layers when viewed coronally.

The dentate gyrus (DG) can be parceled into 3 cytoarchitectural layers collectively known as allocortex: *strata molecular, granulosum,* and *polymorphic.* The most prominent, *strata granulosum* are comprised of densely packed granular cells: the primary efferent neuron of the DG. The DG receives almost all of its afferent projections from the entorhinal cortex, with fewer than 15% of synapses stemming from other subcortical structure (Nafstad, 1967; Simonsen and Jeune, 1972; Steward, 1976; Köhler, 1985). Collectively, these projections materialize into the historically characterized “perforant” pathway whose unilateral mossy fibers must pierce or “perforate” the cortical layers of subiculum along its axis in order to synapse upon the DG (Lorente De Nó, 1939; Simonsen and Jeune, 1972). The consequence of these projections on DG appears to be predominately excitatory, as a majority of perforant synapses are glutamatergic (White et al.,

1977). The activation of the DG granule neurons is the first stage of the intrahippocampal trisynaptic pathway (described later).

The cornu Ammonis (CA), or hippocampus proper, is more complex cytoarchitecturally than the DG, consisting of 6 layers. CA layers are appropriately named for their appearance following Nissl staining. Primary interest surrounds the *stratum pyramidale* (layer III) which, unlike the DG, houses pyramidal cells, the chief functional cell of the CA. The CA is comprised of 3 functional subfields: CA1-CA3 (although CA4 is sometimes characterized) (Lorente De Nó, 1934). Each subfield is distinguished by the size and density of the pyramidal cell somata. For example, CA1 pyramidal neurons appear scattered with small soma, whereas CA2 soma is larger and more compact, forming a thin dense layer (Dam, 1979). The CA3 comprises the second stage of the trisynaptic pathway, and thus receives a majority of the primary excitatory afferents from the DG mossy fibers (Witter, 2006). CA3 pyramidal neurons are morphologically distinct, in addition to their traditional single axon projection, they contain an extra axonal branch known as a Schaffer collateral that stems from the apical dendrite and projects directly to CA1. The innervation of CA1 by CA3 Schaffer collaterals is remarkably exclusive and completes the intrahippocampal trisynaptic loop (Simonsen and Jeune, 1972). In summary, the trisynaptic sequence is initiated by entorhinal perforant activation of the DG, which, via mossy fibers, stimulates the CA3 Schaffer collateral projections to CA1 (Andersen et al., 1971). The prevailing consensus on trisynaptic loop projections is that they are exclusively excitatory and rely on regional GABAergic inhibitory interneurons to regulate their activation (Cobb et al., 1995; Freund and Gulyás, 1997). The complexity of this pathway is heavily associated with hippocampal-dependent learning processes and interfering species, or in any combination, with DG, CA3, and

CA1 nodes has detrimental effects on episodic, spatial and declarative memory across various species (see reviews, Squire, 1992; van Strien et al., 2009).

The conservation of hippocampal cytoarchitectural features both within and across species, combined with studies illustrating hippocampal involvement in learning and memory, has contributed to the extensive scientific focus on this structure as a neurological model. Many of these findings can be attributed to the advent of the acute brain slice preparation, which allows metabolic and electrophysiological properties of the nervous system to be evaluated *ex vivo* (McIlwain, 1951; Gibson et al., 1965; Yamamoto and McIlwain, 1966). This model has many distinct advantages, including the complete control of the chemical microenvironment, specific stimulation/measurement of a brain region and the reproducibility of slices from the same animal (Teyler, 1980). HP tissue performs particularly well with this preparation as the conservation of the trisynaptic hippocampal architecture in each slice provides a unique scientific advantage. This unique set of peculiarities allow electrophysiological stimulation to be assessed within a single *in vivo* established network on each slice, a characteristic that led directly to the discovery of long-term potentiation (described later) (Lømo, 2003). The culmination of each of these aforementioned features (hippocampal learning and memory, trisynaptic circuitry, ease of electrophysiological recordings) is the reason nearly all neurobiological research in animal models of the past half-century have utilized the HP (Brodmann and Garey, 2006).

1.2.3 Anatomical and Physiological Variation between M1 and HP

Although heavy dedication has centered around the whole HP as a model of neuronal function, the HP's unique features draw caution to its generalizability across other brain regions. As well, emerging evidence illustrates a heterogeneity of function and injury susceptibility even across the longitudinal axis of the HP (See reviews, Fanselow and Dong, 2010; Strange et al.,

2014). Human and animal lesion studies suggest a dichotomy in function between ventral (temporal) and dorsal (septal) HP, with the former having strong correlations with emotional responses and the latter being related to spatial learning (Nadel, 1968; Moser et al., 1993; Ito and Lee, 2016). These functional distinctions may be partially due to the divergence in anatomical projections from HP subregions (septal and temporal) to varying cortical and subcortical structures (Swanson and Cowan, 1977). More compelling support of the longitudinal axis hypothesis, are acute rodent HP slice preparations illustrating differential susceptibility to anoxic injury (Ashton et al., 1989; Rami et al., 1997). One explanation that has emerged is biochemical data demonstrating a preferential expression gradient of key glutamatergic receptors (AMPAR and NMDAR) across the HP axis (Martens et al., 1998). Taken together these data suggest a noteworthy difference in underlying subfield physiology across the hippocampal axis that should be considered when assessing HP data.

In a similar way, caution is warranted when extrapolating HP data to other cortical regions. Although comparisons may be drawn between HP and some cortical regions, such as M1, there are important differences. First, the total and synaptic proteome between cortex and HP tissue are substantially different (Fountoulakis et al., 2005; Witzmann et al., 2005; Hirano et al., 2006). Specifically, the subunit composition and distribution of key transmitter receptors (NMDAR, AMPAR, and GABAR) have been shown to be unique to each brain region (Bowery et al., 1987; Martin et al., 1993; Wenzel et al., 1995; Goebel and Poosch, 1999). These differences are reflected in the total density (synapses per neuron) and type (whether excitatory, or inhibitory) of synapses on an individual pyramidal cells in each cortical region (Carlin et al., 1980; Keller, 1993; Somogyi et al., 1998; Gulyás et al., 1999; Tang et al., 2001). Lastly, the overall presence and concentration of supporting glial cells show regional discrepancies. The density of astrocytes appears greatest in

the hippocampus, and considerably less so in the cortex; conversely, microglia are more uniformly distributed (Lawson et al., 1990; Savchenko et al., 1997). However, debate persists as to whether subpopulations of microglia exist, and whether regional differences of diverse microglia contribute to changes in tissue phenotype (Hanisch and Kettenmann, 2007; Olah et al., 2011). One study argues the latter, with data showing microglial cultured from HP intensely express inflammatory proteins compared to other cultured cortical and subcortical regions (Ren et al., 1999). This HP specific phenotypic adaptation has been shown to have a considerable influence on the role of microglia to actively alter the synaptic network within this region in response to inflammatory stimuli (Ji et al., 2013). The noted differences between cortex and HP, in the proteome, synapse density, and type, as well as relative concentrations of glia, most likely contribute to the divergent functions of these two regions and may have an impact on the responsiveness of these tissues to insult, injury or learning paradigms.

1.2 NEUROPLASTICITY

Neuroplasticity is a form of cellular adaptation by which neurons alter their structure and function to perform optimally under a given set of environmental or behavioral constraints. There is overwhelming agreement that these processes are heavily reliant on the remodeling and refining of neuronal connections in an activity-dependent fashion (Bailey and Kandel, 1993; Bruel-Jungerman et al., 2007). This phenomenon occurs throughout the central nervous system, including cortical, subcortical and spinal regions (Eccles and McIntyre, 1951; Johansson, 2000; Parker, 2001). However, discussion persists regarding the temporal nature and defining characteristics of the events surrounding neuroplasticity. Thus, the term neuroplasticity often encompasses upstream events, such as post-translational modifications of proteins and gene transcription, and downstream (long-term) changes in neuronal architecture and behavior. There

is prevailing agreement that these events are not mutually exclusive, but are dependent processes that occur in parallel or in sequence with one another.

In the context of traditional motor learning (e.g. the practice of a novel skill over multiple sessions), the acquisition of a novel motor skill promotes the reorganization of cortical muscle representations in an effort to yield a greater efficiency of trained movements (Kleim et al., 1998; Willingham, 1998; Plautz et al., 2000). Numerous studies, utilizing various species, have consistently demonstrated this reorganization as regionally exclusive and highly specific, with expansion to cortical representations of only specific muscle groups utilized during the training and no effects in non-use limbs or uninvolved muscle groups of the same limb (e.g., flexors versus extensors) (Elbert et al., 1995; Nudo and Milliken, 1996; Plautz et al., 2000; Schieber, 2001). This specificity is reflected as an augmentation of dendritic spine growth (synaptogenesis) of neuronal populations involved in the trained motor representation (Kleim et al., 2002; Xu et al., 2009). The maturation, or stabilization of these spines with subsequent training sessions is thought to be the underlying mechanism driving the persistence of memory with motor training (Kleim et al., 2004; Xu et al., 2009; Hayashi-Takagi et al., 2015).

Further evidence suggests that rapid motor cortical adaptations can occur within a single session of training. Muellbacher and colleagues (2002) noted significant enhancement in the trained movement behavior and cortical excitability of M1 in humans following only 20 minutes of brief motor practice. Furthermore, the authors observed disruptions of skill acquisition following initial training when M1 was exposed to either an additional novel skill training session, or repetitive transcranial magnetic stimulation (a protocol that is known to interfere with basal neuronal communication) (Huang et al., 2005). However, this disruption was not exhibited if the interfering protocol was introduced 6 hours after the initial training. Remarkably, this “time-

window" for memory consolidation appears to be conserved across brain regions, as amygdala-based fear memories can be abolished with the administration of protein synthesis inhibitors during the same 6-hour window (Nader et al., 2000). Together, these data suggest a generic phasic neuronal mechanism: an initial labile state (<6 hours) independent of protein synthesis and a mature state (> 6 hours) dependent upon protein synthesis. To date, the most promising cellular mechanisms explaining these states are the phenomena surrounding excitatory glutamatergic synapses known as long-term potentiation and depression.

1.2.1 Key Plasticity Receptors

1.2.1.1 AMPARs

Basal excitatory synaptic transmission is predominately governed by glutamate receptors, in particular, α-amino-3-hydroxy-5-methyl-4-isoxazolepropionic acid receptors (AMPARs) (Huganir and Nicoll, 2013). To date, the most prevalent model for the study of AMPAR function has been displayed using post-natal cultured neurons in the absence of glia, or transfected human embryonic kidney cells 293 (HEK 293). Although these models involve the use of artificial environments they agree with more recent *in vivo* genetic knockout and knockdown models (Huganir and Nicoll, 2013).

Based on these models, it is now well understood that AMPARs are transmembrane ionotropic glutamate receptors, that assemble as homo- or hetero-tetrameric complexes of any combination of subunits (GluA1-4). In principal cells, the native AMPARs of the postsynaptic density (PSDs) are those that contain Ca^{2+} impermeable GluA2 subunits (Jonas et al., 1994; Geiger et al., 1995). These receptors function as ligand-gated Na^{+} pores that facilitate synaptic transmission. All AMPARs are capable of undergoing post-translational modification on either serine (Ser), tyrosine (Tyr) and threonine (Thr) residues. Phosphorylation of these sites alters their

biophysical properties (e.g., enhancing glutamate gating and channel opening), and/or facilitates the internalization or surface localization of the receptor within the PSD, thus regulating surface expression of AMPARs (Song and Huganir, 2002; Huganir and Nicoll, 2013). As an example, GluA2-containing AMPARs are constitutively cycled through the PSD during the steady-state synaptic function. Phosphorylation of Ser 880 by protein kinase C (PKC) regulates the scaffolding of GluA2 with postsynaptic density protein 95 (PSD95), while Tyr site activation by Src family kinases at 869, 873, 876 has a persuasive influence on the migration and internalization of the receptor (Chung et al., 2000; Hayashi and Huganir, 2004). Phosphorylation and dephosphorylation are governed by the frequency of synaptic transmission, and aid in the ongoing maintenance and integrity of the synapse (Shi et al., 2001).

There is now wide acceptance supporting the roles of native-GluA2 AMPARs at excitatory synapses, however, GluA2-lacking AMPARs have been discovered to have a direct role in the development of NMDAR-dependent and NMDAR-independent forms of LTP phenomenon as well as ischemic-induced excitotoxicity (Pellegrini-Giampietro et al., 1997; Mahanty and Sah, 1998; Hayashi et al., 2000). Data supporting divergent rules governing the trafficking of GluA1-containing and GluA2-containing AMPARs suggest various functions for each AMPAR subunit type within a single excitatory synapse (Shi et al., 2001; Lee et al., 2004). In favour of this hypothesis are two important pieces of data: (1) GluA1 are often found to have a considerably lower contribution than GluA2 at homeostatic synapses and (2) GluA1 are disproportionally sensitive to activation by Ca^{2+} (Geiger et al., 1995; Hayashi et al., 1997; Petralia et al., 1999; Lee et al., 2004). This sensitivity stems from a dependency of the phosphorylation sites Ser 831 and 845 on protein kinase A (PKA) and calcium-calmodulin-dependent protein kinase II (CaMKII), respectively. Activation of these two sites has been shown to be adequate for the mobilization of

vesicular GluA1 AMPARs towards the peri-synaptic membrane (Shi et al., 1999; Hayashi et al., 2000; Diering et al., 2016). Additionally, the activation of CaMKII and PKA are contingent on Ca^{2+} binding calmodulin and rise of cyclic adenosine monophosphate (cAMP) as a result of NMDAR bulk Ca^{2+} (discussed later), which is readily present during high-frequency stimulation. These data suggest a role for GluA1-containing AMPARs in the persistence of the LTP phenomena by increasing their relative surface expression in an activity-dependent manner (Hayashi et al., 2000). Moreover, the unveiling of silent synapses, a process believed to govern some forms of learning, has been suggested to be a GluA1 dependent process (Isaac et al., 1995; Hayashi et al., 2000; Malinow et al., 2000).

1.2.1.2 NMDARs

N-methyl-D-aspartate receptors (NMDAR) are another subtype of ionotropic glutamate receptors that are most often considered as the critical intermediary of neuronal plasticity, with the capability of translating complex patterns of neuronal activity into long-term changes in synaptic morphology and function (Paoletti et al., 2013). NMDARs are heterodimers formed by 2 obligatory NR1 subunits and 2 phenotypically varied GluN2, or GluN3 subunits (GluN2A, B, C, D; NR3 A, B) (Dingledine et al., 1999; Paoletti et al., 2013). NMDAR activation is dependent on two temporally sensitive events: (1) the ligand-binding of glutamate to its receptor site in the presence of glycine and (2) the voltage-dependent removal of a Mg^{2+} blockade of its channel pore. The requirement for synchronization (as would occur with high-frequency synaptic activation) between these events is why many consider NMDARs to be neuronal coincidence indicators of synaptic potentiation/depression (Tsien, 2000). The stringent regulation of NMDAR activation is vital to neuronal health and function, as activation leads to a prolonged Ca^{2+} permeability resulting

from slow receptor kinetics and retarded glutamate unbinding (Lester et al., 1990; Cull-Candy et al., 2001).

The robust flux of Ca^{2+} into synapses following NMDAR activation is driven by the almost 20,000 fold gradient of [Ca^{2+}] between intracellular and extracellular environments (Clapham, 2007). Under resting conditions, the cytosol is actively deprived of intracellular [Ca^{2+}], since Ca^{2+} triggers changes in both charge and conformational properties of countless proteins (Clapham, 2007; Mattson, 2007). For example, basally dormant CaMKII becomes active upon Ca^{2+}-Calmodulin interaction, undergoing rapid autophosphorylation that persists beyond the initial Ca^{2+} stimulus (Miller and Kennedy, 1986; Giese et al., 1998). The perpetuating nature of some Ca^{2+}-dependent proteins has a profound influence on intracellular signaling pathways, synaptic modulation, and genomic transcription factors, making proteins like CaMKII both sufficient and necessary for some forms of LTP/LTD phenomena (Giese et al., 1998; Morris, 2013; Nicoll and Roche, 2013).

The vast array of Ca^{2+} sensitive proteins within a cell is responsible for the heavy regulation and less variability of NMDARs in PSDs compared to their AMPAR counterpart (Takumi et al., 1999). NMDAR subunit expression can be considerably influenced by stage of development and brain region (Paoletti et al., 2013). Convincing evidence from both human and rat brain displays GluN2B mRNA predominates in prenatal neurons, whereas GluN2A expression rapidly increases around the time of birth; arguments persist as to whether this is related to the rise in total or relative GluN2A content at synapses (Watanabe et al., 1992; Monyer et al., 1994; Sheng et al., 1994; Tovar and Westbrook, 1999, 2002; Ritter et al., 2001; Law et al., 2003). Although global GluN2B quickly decreases during the post-natal period, its expression remains relative to that of GluN2A in some brain regions, notably, hippocampus and frontal cortex (Monyer et al., 1994). A prevailing

hypothesis from neuron cultures and slice preparations derived from various brain regions (hippocampal, spinal, and cerebellar) suggests that GluN2B-containing NMDARs vacate post-natal synapses and migrate extrasynaptically, while GluN2A-containing NMDARs become the native synaptic residents (Stocca and Vicini, 1998; Rumbaugh and Vicini, 1999; Tovar and Westbrook, 1999; Momiyama, 2000).

However, a more in-depth analysis reveals that individual pyramidal neurons from the frontal cortex and hippocampus are capable of expressing NMDAR subunits in a synapse-specific manner. Specifically, it has been found that commissural/associational synapses on apical dendrites of CA3 are strongly affected by mutations to GluN2A, whereas the basal dendrite synapse is influenced by GluN2B mutation (Ito et al., 1997). A follow-up study entertained the notion that this dichotomy of subunit expression may be related to the pre-synaptic origin (Ito et al., 2000). It was discovered that GluN2A and GluN2B subunits were more potently expressed at synapses opposite that of ipsilateral and contralateral hemispheric input, respectively (Ito et al., 2000). Intriguing, this is in contrast to pyramidal neurons isolated from the frontal cortex that display GluN2A-containing NMDARs at post-synaptic sites of transcallosal input, while GluN2B-containing NMDARs dominate intracortical synapses (Kumar and Huguenard, 2003). This level of intricacy has a profound impact on the way neurons interpret incoming signals, and may provide a mechanism by which neurons gauge or control the contribution from a given network on its behavior.

The biophysical properties of GluN2A-containing (fast kinetics) and GluN2B-containing (slow kinetics) NMDARs undoubtedly contribute differently to the genesis of neuroplasticity (Foster et al., 2010). The delayed pore closing of GluN2B following activation increases the temporal window and thus the likelihood of summation with a successive stimulus (Erreger et al.,

2005). In combination, these characteristics make GluN2B-containing NMDARs highly efficient integrators that produce significantly higher excitatory post-synaptic potentials (EPSPs) and more readily bring neurons toward a firing threshold (Kumar and Huguenard, 2003). Conversely, GluN2A-containing NMDARs have a higher opening probability and are far superior at fluxing Ca^{2+} rapidly (Erreger et al., 2005). These properties allow GluN2A-containing NMDARs to be exceptional coincidence indicators, as they must be repeatedly activated within a temporally sensitive window (Kumar and Huguenard, 2003). Subunit-dependent phenotypes of this nature yield distinct bulk Ca^{2+} signatures which can be interpreted in different ways by intracellular proteins (Chen et al., 1999). As mentioned previously, CaMKII is an important intracellular chaperone of LTP that is extremely sensitive to Ca^{2+} influx via the Ca^{2+}-calmodulin interaction (Lisman et al., 2012). In HEK293 cells, Ca^{2+}-calmodulin has been shown to have a duality of facilitation, or inhibition on Ca^{2+} channels that is dependent on the rate and range of bulk Ca^{2+} flux (Demaria et al., 2001). This evidence alongside divergence in subunit kinetics has led some to speculate opposing associations between GluN2A with LTP and GluN2B with LTD (Liu et al., 2004; Massey, 2004). However, it remains unclear whether the divergence is due to embedded properties of the receptors, phosphorylation state of the receptors or slight alterations in receptor microenvironment (e.g. synapse-specific protein complexes). Additionally, it is uncertain whether the tendency of GluN2A, and GluN2B-containing receptors to induce LTP or LTD is modified by brain region.

1.2.2 Long-Term Potentiation

Although the discovery of long-term potentiation (LTP) occurred over 50 years ago, it is a term that has yet to be consistently defined in the literature (Lømo, 2003). Many consider it to be a long-term (>30 min) augmentation of synaptic transmission that outlasts experimentally induced

high-frequency synaptic stimulation (Nicoll and Roche, 2013). LTP is considered an experimental model that artificially mimics the assumed natural physiological phenomenon of synaptic potentiation. Almost all experimental investigations probing LTP phenomenon have done so using hippocampal Schaffer collateral or CA1 glutamatergic neurons; however this phenomenon has been displayed in excitatory neurons in other cortical regions (Teyler and DiScenna, 1987; Iriki et al., 1989; Kirkwood et al., 1993; Rioult-Pedotti et al., 2000b). There is now convincing evidence that LTP-type phenomenon is directly responsible for certain forms of learning, with reports drawing substantial parallels between the two processes (Rioult-Pedotti et al., 2000b; Whitlock et al., 2006). Specifically, Whitlock and colleagues (2006) displayed that a single-trial inhibitory avoidance learning task enhanced CA1 specific synaptic transmission and induced adaptations in AMPAR signaling in a similar way to experimentally induced LTP. These data were further supported by the demonstration of this particular learning task to obstruct additional potentiation, suggesting LTP had saturated within the trained region of CA1 (Whitlock et al., 2006). These data are suggestive that a common mechanism is shared by LTP and some forms of learning.

Experimental induction of LTP is predominately achieved through repetitive electrical stimulation applied presynaptically, and measured post-synaptically. This induction is heavily dependent on the frequency, pattern, and strength of stimulation, as a wide range of each has been shown to simulate various physiological states (Albensi et al., 2007; Nicoll and Roche, 2013). Following high-frequency stimulation, there is a brief (≈90s), but robust, post-tetanic potentiation (PTP) (Bliss and Lomo, 1973). PTP is characterized by an enhancement in miniature excitatory postsynaptic potential (mEPSP) frequency in the absence of an intensification in amplitude, which is reflective of a pre-synaptic accumulation of Ca^{2+} causing a surge in vesicular mobilization and neurotransmitter release, rather than an enhanced responsiveness of the post-synaptic cell (Eliot et

al., 1994; Bao et al., 1997). According to Teyler and DiScenna (1987), there are three plausible fates of PTP: (1) PTP may mature into either short-term potentiation (STP) or LTP, (2) experience a brief post-tetanic depression as a result of neurotransmitter depletion, before replenishing and maturing to LTP, or (3) PTP can fail to induce LTP (Teyler and DiScenna, 1987; Zucker and Regehr, 1989). Anecdotally, LTP failure is often referenced as a common experimental nuisance that is heavily unreported in the literature. When LTP failure is reported, it is most often attributed to lack of slice viability, or technical variation within the study. Although some advocate for a physiological basis for the failure of LTP (Roth-Alpermann et al., 2006), it has yet to be systematically or adequately investigated.

Unlike PTP that is driven through a presynaptic mechanism, most models of LTP are contingent on post-synaptic adaptations. There is a general consensus that the persistence of LTP originates from a shift in receptor dynamics, early LTP (E-LTP), to a protein synthesis-dependent late LTP (L-LTP) phase (Nguyen et al., 2016). The most studied form of LTP involves the family of excitatory glutamate receptors NMDAR and AMPAR. The importance of these receptors during LTP is attributable to the observation that LTP can be negated by the application of amino-phosphono-valeric acid (NMDAR inhibitor) prior to high-frequency stimulation while no effect was observed when given after LTP induction (Collingridge et al., 1983). Additional data from various knockout and knockdown models of NMDAR in mice further support the central role of NMDAR in LTP phenomenon and learning in general (Cui et al., 2004). These data proposed that NMDARs may be necessary for the initiation of LTP, but not sufficient for its maintenance (Collingridge et al., 1983). The following section discusses the relative contribution of these two receptors in NMDAR-dependent LTP.

Under high-frequency stimulation, hyperactivity of GluA2-containing AMPAR increases the likelihood of NMDARs will release the Mg^{2+} block, and thus fluxing Ca^{2+} into the synapse. The accumulation of individual NMDAR "sparks" create a Ca^{2+} nanodomain within the PSD that under high-frequency activation summate into a bulk Ca^{2+} wave that propagates through the synapse activating proteins like CaMKII (via calmodulin), PKA, and PKC (Bliss and Collingridge, 1993; Berridge, 2006). The proceeding cascade of events initiates the migration of AMPARs (containing GluA1, 3, or 4) towards the peri-synaptic membrane, which is a process governed by the activation of CaMKII. Once the AMPAR containing vesicles are within the vicinity of the perisynaptic membrane, Ser 845 is phosphorylated by PKA and AMPARs are embedded within the membrane. AMPARs then associate with the voltage-dependent calcium channel (VDCC) and transmembrane AMPA receptor regulatory protein (TARP) family member stargazin, promoting the migration towards the PSD (Chen et al., 2000; Tomita et al., 2005; Bats et al., 2007).

The conservation of PSD integrity is thought to be achieved by the stabilization of AMPARs and NMDAs within theoretical "slots". The anchoring assemblies regulate the number of total AMPARs present during basal transmission (Nicoll and Roche, 2013). However, during E-LTP, basal GluA2-containing AMPARs have been shown to be sequestered and replaced with readily available, calcium-permeable, GluA2-lacking AMPARs present in the perisynapse. The "capture" of GluA2-lacking AMPARs within the PSD is a process that is dependent on the phosphorylation of stargazin by CaMKII (Opazo and Choquet, 2011). Additional data support not only differences in receptor composition, but also the drastic increases in receptor density compared to before LTP induction (Hayashi et al., 2000). The present model suggests CaMKII associates with NMDARs by scaffolding to it, and this, in turn, contributes additional binding sites for AMPA channel anchoring assemblies, which results in the supplementary capture of AMPARs

within the PSD (Lisman et al., 2002). The increased density of GluA2-lacking or Ca^{2+} permeable AMPARs at PSDs has the impact of enhancing the capacity for Ca^{2+} flux, perpetuating AMPAR trafficking until theoretical saturation, at which time further potentiation is not possible. The above processes occur in rapid succession and result in the abrupt induction of LTP that lasts roughly 30 minutes (Lisman et al., 2002).

Further maintenance of LTP, lasting >30 minutes does not appear to be a result of the GluA2-lacking AMPARs. As LTP develops, GluA2-lacking AMPARs are once again sequestered and replaced with GluA2-containing AMPARs (Plant et al., 2006). However, the aforementioned AMPAR binding assemblies persist, producing a net increase in the number of AMPARs present in the PSD (Derkach et al., 2007). Newly inserted GluA2-containing AMPARs produce a far more stable form of LTP, with potentiation lasting up to 3 hours before decaying (Sutton and Schuman, 2006). During this period, synaptic processes, including increased synapse-specific ribosomal activity, produce proteins that incorporate into the native synaptic architecture, resulting in semi-permanent changes in the functioning of the cytoskeleton and mitochondria, that accommodate the enhanced synaptic efficiency (Sutton and Schuman, 2005). The transitional period from receptor-dependent to protein synthesis-dependent LTP signifies the establishment of L-LTP. Eventually, even L-LTP saturates, upon which time the neuron is believed to undergo the extraordinary ability to foster a greater integration with the presynaptic cell via synaptogenesis.

1.3 PRIMING PLASTICITY

The natural ability of neurons to incorporate incoming stimuli by means of functional and structural adaptation is the hallmark processes that underlie novel skill acquisition and recovery from injury. As mentioned, strong support implements LTP as a primary proponent of this phenomenon and as such, the regulation of these processes is integral to healthy brain function.

Both the impairment and hyperactivity of LTP have been shown to have a profound impact on brain functioning, including being associated with the pathogenesis of many diseases (Johnston, 2004). Therefore, mechanisms must have evolved that exert an influence over the induction of LTP in order to provide a high degree of specificity and minimize rampant plasticity from occurring, especially during periods of increased memory encoding. The dynamic regulation of plasticity expression, whether the regulation is spatial, temporally, or the degree to which plasticity is able to be induced within a given brain region is termed metaplasticity.

In particular, metaplasticity is related to the physiological or biochemical "state" of a synapse, neuron or population of neurons that render them more or less receptive to LTP induction (Abraham, 2008). This modified biochemical signature is a temporally sensitive event that is preceded experimentally by a triggering or priming stimulus and has been shown to decay anywhere from a few minutes to days in rat hippocampus (Abraham et al., 2001). Generally, there are three primary characteristics of a priming stimulus: (1) the stimulus does not by itself induce LTP (some exceptions), (2) the priming response must outlast the original stimulus, and (3) these priming responses must be sufficient to alter the induction of either LTP at a future time point (Hulme et al., 2013). These features make metaplasticity unique, whereas traditional modulators of plasticity are often applied concurrently with LTP induction, metaplastic stimuli can be applied in advance. As an example, tetraethylammonium (TEA) and tetrodotoxin (TTX) are popular experimental modulators of LTP induction, but whose *in vivo* application is hindered by either their pharmacokinetics (TEA does not cross the blood-brain barrier) or acute toxicity (TTX is a potent neurotoxin)(Gruhzit et al., 1947; Saoudi et al., 2010). These characteristics limit their investigative potential during learning paradigms and restrict their use to *in vitro* models. Conversely, the non-synchronous application requirement of metaplastic stimuli with tetanus to

influence LTP provides a promising alternative that could benefit *in vivo* investigations and may be more advantageous both experimentally and therapeutically to traditional methods.

The mechanism for the expression of metaplasticity at the level of individual neurons is a topic of fierce debate (Abraham, 2008). The most likely candidates for metaplastic change are post-translational modifications of the synaptic proteome, specifically the phosphorylation state of membrane-bound receptors and intracellular protein cascades (Klann, 2002; Rodríguez-Durán and Escobar, 2014). The receptor hypothesis stems from findings of numerous receptors, including subclasses of metabotropic (mGluRs) and ionotropic (AMPAR and NMDAR) glutamate receptors, as well as, GABAergic receptors that have been implicated in the metaplastic phenomenon. As mentioned previously, ionotropic glutamate receptors have a capacity for phosphorylation at multiple sites that have been shown to prominently modulate their ability to flux Na^+ and Ca^{2+}, making LTP more or less likely (Song and Huganir, 2002; Morris, 2013). With regards to mGluRs, their activation appears to indirectly downregulate Ca^{2+} activated K^+ channel activity producing slow afterhyperpolarization, in turn promoting LTP persistence following high-frequency stimulation (Cohen et al., 1999). Less well understood are the roles inhibitory receptors, such as γ-aminobutyric acid receptors (GABAR), have in metaplastic processes. GABAergic synapses are chiefly expressed by interneurons whose activation has a potent inhibitory influence on principal cells. Their role seems to be involved with the synchrony of incoming inhibitory and excitatory inputs on principal cells and can have a profound impact on whether or not plasticity occurs in neighboring synapses; as blocking GABAergic inputs drastically lowers the threshold for LTP induction (Wigstrom and Gustafsson, 1983). Together strong support exists for a receptor-mediated mechanism of metaplasticity.

Conversely, these changes may likely be indicative of the downstream processes resulting from intracellular regulation of activity at the level of synaptic Src family kinases and phosphatases (Yang et al., 2011). However, most heavily studied are intracellular Ca^{2+} sensing molecules, such as CaMKII, whose primed or active state has been shown to not only phosphorylate ionotropic receptors but to facilitate receptor migration (Lisman et al., 2012). These molecules may provide attractive candidates for metaplasticity, but it is less clear how they are able to upregulate their activity in the absence of LTP induction (Abraham, 2008). Whichever the mechanism, there has been widespread interest in exploring the various stimulation patterns and behavioral interventions that may induce metaplasticity (Fiuza-Luces et al., 2013; Cassidy et al., 2014).

1.3.1 Stress as a Mediator of Metaplasticity

Metaplasticity likely evolved to balance the stability and adaptability of neuronal networks in such a fashion as to be successful within a given set of environmental circumstances. As such, environmental cues are powerful manipulators of neuronal behavior. Stressful events are those that perturb an organism's homeostasis. Often these environmentally adverse events initiate a shift in biological state that is optimized for the detection, identification and generation of appropriate behaviors that deal with either a psychological, or physical threat. These stress responses recruit primitive brain regions including the hypothalamic-pituitary-adrenal axis (HPA), that initiate a cascade of biological processes whose aim is to return the organism to homeostatic equilibrium. The simultaneous response, coordinated across numerous bodily tissues, is chaperoned by the secretion of hormonal factors, including corticotropin-releasing factor, vasopressin and glucocorticoids. The release of these hormones following stressful stimuli demonstrates a high degree of evolutionary conservatism as responses are similar across species and lifespan (Chang and Hsu, 2004; Dean and Thornton, 2007). Due to brains active role in the detection and

determination of appropriated response action to stressful stimuli, it is not surprising it contains an abundance of glucocorticoid receptor expression, making brain especially susceptible to circulating levels of glucocorticoids, notably in regions such as the hippocampus (Aronsson et al., 1988). For these reasons, many have investigated the role glucocorticoids may have in promoting, or interfering with learning processes.

Circulating levels of glucocorticoids, such as cortisol or corticosterone, are heavily regulated by diurnal rhythm in both humans and rats, respectively (Harrington and Hooton, 1985; Cauter and Turek, 1995; Windle et al., 1998; Selmaoui and Touitou, 2003; Joels et al., 2012). Under basal conditions, roughly 80% of cortisol is transported through circulation bound to corticosteroid-binding globulin (high affinity, low capacity), and 15% by albumin (low affinity, high capacity), while the remainder is free or unbound cortisol (Perogamvros et al., 2012). As a steroid derived hormone, unbound cortisol is the only bioactive form, and freely bypasses capillary vasculature, where it enters cells via simple diffusion (Pardridge, 1981; Mendel, 1992). Once cortisol gains access to the cytosol it binds to one of two subclasses of receptors, either low-affinity glucocorticoid (GC), or high-affinity mineralocorticoids (MC) (Funder, 1997; Kim and Yoon, 1998). The activation of either GC, or MCs by cortisol promotes migration of the receptor to the nucleus causing upregulation, or suppression of gene transcription, a process known as transactivation or transrepression (Hanawalt and Hanawalt, 1993).

Although slow genomic actions of GC and MCs have been traditionally investigated, more recent evidence suggests a possibility for rapid steroid action (Joels et al., 2012). Specifically, acute physical stress exposure, or corticosterone application causes enhanced presynaptic release of glutamate in hippocampal slices(Karst et al., 2005). Using selective MR knockout mice, Karst and colleagues (2005) were able to display this presynaptic release as MR-dependent.

Furthermore, these responses could be elicited at a 10 nM dose of corticosterone, a concentration previously shown to be only available at circadian peak, or following an acute stressor in mice (Cauter and Turek, 1995; Linthorst et al., 2000). In line with others, the authors speculate the existence of two MR pools, cytosolic MRs that are responsible for slow acting genomic effects, and membrane-bound MRs coupled to G-protein complexes that elicit rapid non-genomic effects (Tasker et al., 2006; Prager et al., 2010). Although the existence of membrane-bound or membrane incorporated GRs and MRs at synaptic terminals is still subject to debate, there is growing consensus that this receptor pool is responsible for the dramatic acute effects of glucocorticoids at synapses (Popoli et al., 2012). This notion of dual populations of MR and GRs may help to explain the differences often reported following repeated or chronic exposure to environmental stress and the response following a single stressor.

In particular, chronic exposure to social, psychological or physical stress has been shown to have a profound negative impact on learning and memory; this phenomenon occurs throughout the lifespan and across various brain regions (Diamond et al., 1996; Frisone et al., 2002; Lupien et al., 2009). There are strong arguments linking these negative effects to corticosterone exposure, as both chronic stress and chronic corticosterone injection yield a persistent elevation circulating levels producing similar learning outcomes (Mcewen and Magarinos, 1997; de Quervain et al., 1998). Conversely, the opposing phenomenon (enhanced LTP and learning behavior) has been reported following single exposure to many of the above-listed stressors or acute corticosterone administration in naïve rats (Shors, 2001; Yuen et al., 2009; Russell et al., 2014). However, these acute effects are dose-dependent, as an inverted-U relationship between hippocampal primed burst potentiation (PBP) and circulating corticosterone has been observed (Diamond et al., 1992). Follow-up investigations demonstrate high levels of corticosterone foster a preferential switch

from hippocampal LTP (downregulated) to LTD (upregulated) at CA1 and dentate neurons, suggesting glucocorticoids may directly or indirectly influence NMDAR activity (Pavlides et al., 1993, 1995). This relationship may be related to the differential affinity of the two receptor types, as MC activation at low to moderate (15-20 µg/dL) levels of circulating corticosterone has been associated with enhanced PBP and LTP, whereas MC saturation and GC activation experienced at high corticosterone (>25 µg/dL) promotes long-term synaptic depression and PBP repression (Diamond et al., 1992; Pavlides et al., 1993). These native characteristics of corticosterone signaling make it a prominent target for metaplastic manipulation in an effort to favor learning and recovery.

1.3.1 Exercise as a Unique Body Stressor

There is overwhelming evidence that transitory increases in metabolic rate due to dynamic movements of large muscle groups causes a perturbation in organism homeostasis. This category of physical stressors is generally referred to as exercise and has been traditionally separated into two types. Resistance exercises are those that favor the production of force under low repetition and predominately recruit anaerobic respiration; a combination that stimulates skeletal muscle growth and strength. The other form, aerobic exercise, is often continuous, rhythmical muscle contractions under comparatively lower forces for a duration that exceeds the capacity of anaerobic respiration (>10 min). This type of exercise promotes a greater efficiency and capacity of the aerobic respiratory system. By virtue, adaptation following resistance exercise is myo-centric, whereas aerobic exercise promotes adaptation across various body tissues. Tissues with a high resting metabolic rate appear to be the most sensitive to adaptation following chronic aerobic exercise exposure (Gallagher et al., 1998; Fiuza-Luces et al., 2013). The human brain is one of the most metabolically active tissues; while it only constitutes about 2% of an adult human's body

weight, it accounts for roughly 20% of resting metabolism (Sokoloff, 1960). Thus, it is likely that in addition to cardiovascular and musculoskeletal adaptation, the brain is a site of active change following aerobic exercise exposure.

Unlike chronic exposure to other physical stressors, chronic aerobic exercise has been demonstrated to exert a profound positive influence on brain biochemistry, physiology and fitness (Cotman et al., 2007; Stranahan et al., 2007; Hillman et al., 2008). Individuals who regularly participate in aerobic exercise are the beneficiaries of improvements in cognitive fitness and a delay in age-related brain atrophy (Hillman et al., 2008). Moreover, aerobic training in naïve older adults increases hippocampal volume and improves scores on spatial memory tasks (Erickson et al., 2011). When aerobic exercise is provided in combination with a negative stressor or CNS injury, it has the remarkable ability to negate detrimental effects and even enhance recovery across various species (Tillerson et al., 2003; Vaynman, 2005; Ploughman et al., 2007; Kiuchi et al., 2012; Mang et al., 2013b; Lee et al., 2015; Sage, 2015; Murdoch et al., 2016). Although these effects are contrary to other stressors, data suggest that they both stem from similar mechanisms; through either stimulating or suppressing cellular pathways that underlie synaptogenesis and neurogenesis (Stranahan et al., 2006; Pereira et al., 2007; Dietrich et al., 2008; Nadel et al., 2013). The way in which aerobic exercise is able to selectively promote a positive influence over these pathways is still the subject of ongoing research, with some causal associations being recently made; most notably, the neurotrophic hypothesis.

1.3.1.1 Neurotrophic Hypothesis

In the long term, repeated bouts of both voluntary and forced aerobic exercise have been shown to decrease circulating corticosterone levels in rats, while at the same time enhancing neurotrophic factor presence (Hackney, 2006). Neurotrophins are a family of signaling growth

factors that are involved in the survival, development and ongoing maintenance of neurons (Cotman et al., 2007). Their roles at synapses are well documented, and they can actively participate in the process and persistence of neuroplasticity including certain forms of LTP (Poo, 2001). Neurotrophic factors are able to achieve this through a family of membrane-bound tropomyosin-related kinase (Trk) receptors. Once bound, receptor dimerization activates kinase activity at tyrosine residues, promoting the docking of adaptor proteins that facilitate interaction with intracellular signaling cascades (Patapoutian and Reichardt, 2001). Although there is conservation across numerous tyrosine residues of Trk receptors (TrkA: Y490, Y674/Y675, Y785; TrkB: Y512, Y706/Y707, Y816), terminal sites are most associated with intracellular interaction as they exist external to the kinase activation domain (Obermeier et al., 1993; Segal et al., 1996; Pierotti and Greco, 2006). These sites have been shown to be independently activated following various treatments, leading to the versatility amongst signaling patterns and interactions of these receptors (Minichiello et al., 2002; Ernfors and Bramham, 2003). Additionally, a bias exists amongst the family of Trk receptors following chronic exercise. TrkB receptors expression is selectively modulated, most likely due to augmented ligand interaction, as brain-derived neurotrophic factor (BDNF) expression and release is augmented in aerobically trained animals (Neeper et al., 1996). More recently, it has been discovered that muscle-derived irisin is a potent regulator of BDNF expression in hippocampus and is released into circulation following short bouts of high intensity and long bouts of endurance aerobic exercise (Wrann et al., 2013; Xu, 2013; Zhang and Zhang, 2016).

1.3.1.1 Brain-Derived Neurotrophic Factor

Since the discovery that BDNF is released peripherally the following exercise, BDNF-TrkB has been by far the most popular hypothesis explaining chronic exercise-induced effects.

BDNF is an attractive candidate for metaplastic effects following exercise, it is expressed in all regions of the brain, which is across numerous species (Zoladz and Pilc, 2010). There are thought to be 3 primary sources of BDNF in the brain; presynaptic neurons, postsynaptic neurons and active accumulation from circulation. Neuronally derived BDNF has limited bioavailability as it is expressed in low amounts, basally stored in vesicles and presynaptic release is dependent on neuronal activity (Kohara et al., 2001). Circulating BDNF is thought to be heavily expressed vascular endothelial cells, stored in platelets, and under high levels of stretch or injury released into the periphery (Nakahashi et al., 2000; Fujimura et al., 2002; Kermani et al., 2005). Additionally, BDNF has two active forms, a glycosylated precursor, proBDNF (32 kDa), which binds to low-affinity nerve growth factor receptor (p75), and a post-translationally cleaved mature BDNF (13 kDa) form with high affinity for TrkB. Both active forms counterbalance one another as p75 activation promotes apoptosis, while TrkB which promotes neurogenesis and neuronal differentiation (Lu et al., 2005).

Additionally, a prevalent (30%) polymorphism caused by a single nucleotide substitution, valine-to-methionine at codon 66 (Val66Met polymorphism) has a profound impact on BDNF function (Egan et al., 2003). Although Val66Met BDNF has similar bioactivity, it has drastically reduced bioavailability due to its inability to interact with the vesicular sorting protein sortilin (Chen et al., 2005). As a consequence, Met carriers display markedly reduced responses to experience-dependent neuroplasticity in both the motor cortex and hippocampus (Egan et al., 2003; Kleim et al., 2006). Based on these data, it is clear that increased levels of BDNF from chronic exercise are beneficial for long-term neuronal function and that any hindrance to either its availability or action can have detrimental consequences. Although chronic exercise is beneficial for long-term brain health and preventing cognitive decline, it lacks obvious practicality as a

potential aid in the recovery of the brain from injury. Thus, exploiting the influence of single session exercise on neuroplastic change in the brain may offer a more appropriate avenue for recovery.

Similar to glucocorticoids, acute BDNF exposure has a pronounced influence on both early and late phases of neuroplasticity. Incubation of hippocampal slices with BDNF potently upregulates synaptic transmission in Schaffer collateral axons (Kang and Schuman, 1995). Furthermore, deletion of the BDNF gene in mice disrupts the induction of E-LTP that can be rescued with BDNF application in hippocampal slices (Korte et al., 1995; Pozzo-Miller et al., 1999). These detriments were found to be the result of drastic decreases in vesicular docking, altered synaptic protein arrangement, and increased synaptic fatigue (Pozzo-Miller et al., 1999). Moreover, BDNF application in hippocampal slices prior to a non-LTP inducing weak stimulation results in a robust E-LTP generation (Kovalchuk et al., 2002). Although, BDNF application alone has been shown to be insufficient to induce E-LTP, it does appear sufficient for the transition to L-LTP expression (Boulanger and Poo, 1999; Pang et al., 2004). Previous data heavily supports L-LTP to be dependent on protein synthesis (Sutton and Schuman, 2006). BDNF administration following LTP induction in the presence of a protein synthesis inhibitor (anisomycin) fully recovers the L-LTP phenomenon, suggesting BDNF as the key regulator of this process. Taken together these data strongly advocate for BDNF as a modulator of metaplastic change in brain and thus treatments that acutely enhance the release of BDNF provide potential avenues to improve recovery following CNS injury.

The transient release of peripheral BDNF following acute bouts of exercise has been consistently displayed in the literature (Rojas Vega et al., 2006; Winter et al., 2007; Tang et al., 2008; Rasmussen et al., 2009; Schmolesky et al., 2013). In the same way as glucocorticoids, BDNF

release from exercise increases as both intensity and duration increase, when measured in a population of healthy subjects (Rojas Vega et al., 2006; Schmolesky et al., 2013). Circulating BDNF levels reach peak concentration immediately following cessation of exercise and have been shown to remain elevated for a transient period of time before decaying to resting values in blood serum within 10-60 minutes (Knaepen et al., 2010). The finding that peripheral BDNF is stored in platelets and released upon stimulation suggests that the decay in peripheral BDNF may be a result of increased uptake by tissues or reabsorption by platelets. However, analysis of platelet-derived BDNF prior to and following single session exercise has yet to be evaluated. Considering BDNF bidirectionally crosses the blood-brain barrier, it is a likely possibility that the brain may be a site of active absorption of peripheral BDNF following exercise (Poduslo and Curran, 1996). Although chronic exercise is known to enhance BDNF expression in neurons, it is less clear if peripheral BDNF stimulated by acute aerobic exercise has a direct influence in the brain.

1.4 RESEARCH OBJECTIVES

Model Development

(1) To establish a model of single session aerobic exercise for the exploration of neuroplasticity related proteins within rat sensorimotor cortex.

(2) To determine if varying intensities of single session aerobic exercise differentially influence the priming of various regions of the brain, specifically the hippocampus and motor cortex, for neuroplasticity.

Mechanism of Priming

(3) To investigate the possible interaction of aerobic exercise with the phosphorylation state of proteins involved in neuroplasticity

(4) To explore the influence aerobic exercise has upon the trafficking of plasticity-related receptors within sensorimotor cortex and hippocampus.

(5) To establish a biochemical technique for the isolation and specific capture of synaptic membrane-bound proteins.

(6) To investigate the possible role BDNF and CORT have on exercise-induced priming within sensorimotor cortex and hippocampus.

2. Single Session, High-Intensity Aerobic Exercise Fails to Affect Plasticity-Related Protein Expression in the Rat Sensorimotor Cortex

Adapted from Accepted Manuscript: "Thacker JS, Yeung D, Chambers PJ, Tupling AR, Staines WR, Mielke JG (2018) Single Session, High-Intensity Aerobic Exercise Fails to Affect Plasticity-Related Protein Expression in the Rat Sensorimotor Cortex. Behav Brain Res"

2.1 ABSTRACT

Typical responses in muscle following acute aerobic exercise have been well documented, but the responses in the brain have remained relatively unexplored. Recent reports suggest that a single bout of aerobic exercise can prime motor regions of the human brain to experience use-dependent plasticity, however, the mechanisms underlying this priming phenomenon are unclear. As a result, we asked whether a graded test to exhaustion (GXT), the most widely employed test to examine relationships between exercise and integrated responses within the musculoskeletal, cardiopulmonary, and neuropsychological systems, would be able to upregulate the expression of plasticity-related proteins in sensorimotor cortex in rats. We examined immediate responses in animals following either a GXT, or two resting conditions: non-exercising treadmill controls (TC), and acclimatization controls (AC). Young, male Sprague-Dawley rats (n = 20) on a reverse light cycle (12h/12h) were exposed to a treadmill acclimatization procedure consisting of 8 days of increasing exercise intensity (10 m/min up to 25 m/min) for 10 minutes at the same time each day. The acclimatization was followed by 2 days of rest to reduce any carryover effects. On testing day, rats performed either a GXT, or rested (TC and AC), were then sacrificed and sensorimotor cortex dissected. Homogenates were probed for a physiological marker of stress (HSP 70), and plasticity-related proteins (CaMKII, GluN2A, GluN1, GluA1, GluA2) by Western blotting analysis. Both our acclimatization protocol and single event GXT yielded no observable differences in protein expression, suggesting that single session exercise does not prime brain via altered plasticity-related protein expression.

2.2 INTRODUCTION

There is overwhelming agreement that physical activity promotes adaptations that improve human performance and reduce mortality. In particular, previous investigations have revealed the ability of long-term aerobic exercise to induce remodeling of cardiac and skeletal muscle, while simultaneously stimulating genetic pathways that promote metabolic protein expression (see reviews: Flück and Hoppeler, 2003; Fluck, 2006). As well, research over the past decade has shown the contractile history of a muscle can profoundly influence its use-dependent adaptation (Petriz et al., 2017). Specifically, when an exercise bout is preceded by a sub-exhaustive "priming" exercise, notable improvements are observed in a number of physiological measures (e.g., oxygen utilization, or VO_2; (Bishop, 2003; Bailey et al., 2009; Maloney et al., 2014)), which are thought to be the result of changes at the level of post-translational modifications, protein translocation, and DNA methylation within the muscle (Flück and Hoppeler, 2003; Fluck, 2006; Rockl et al., 2008; Barrès et al., 2012).

Importantly, a growing body of evidence suggests that not all exercise-induced adaptations are myo-centric, for the central nervous system has displayed a variety of beneficial changes following aerobic training (Radak et al., 2001; Ferreira et al., 2010; Fiuza-Luces et al., 2013). For example, adult mice with access to a running wheel show enhanced neurogenesis, strengthened long-term potentiation (LTP), and improved spatial learning (van Praag et al., 1999). Moreover, chronic exercise leads to a general augmentation of protein synthesis within both cortex and hippocampus (Nadel et al., 2013), which can be reflected in widespread changes in neuronal architecture, such as increased dendritic arborization and spine density (Stranahan et al., 2007).

Along with our growing awareness that chronic exercise can affect neural structure and function, an emerging view is that preconditioning exercise can prime within session performance

in the brain (Roig et al., 2012; McDonnell et al., 2013; Skriver et al., 2014). In a previous report, Statton and colleagues (Statton et al., 2015), provide evidence that a single bout of moderately intense exercise can condition motor regions to facilitate within-session motor skill acquisition. Furthermore, a number of studies report that this conditioning is not related to changes in basal neuronal transmission, but modulations to intracortical facilitation and inhibition within motor cortices that produce a favorable environment for plasticity (Yamaguchi et al., 2012; Singh et al., 2014a; Smith et al., 2014; Neva et al., 2017). Taken together, these studies suggest that, in a manner similar to the effects of preconditioning exercise on muscle, the brain can be primed for use-dependent plasticity. In other words, exercise can prime motor regions for learning; however, the mechanisms underlying this phenomenon have not been identified.

Chronic exercise (>7 days of access to a running wheel) has been shown to consistently increase the expression of hippocampal genes (Tong et al., 2001; Molteni et al., 2002; Makatsori et al., 2003; Farmer et al., 2004; Lou et al., 2008) and proteins (Park et al., 2014) known to play a role in plasticity, including α-amino-3-hydroxy-5-methyl-4-isoxazolepropionic acid (AMPA) receptor and N-methyl-D-aspartate (NMDA) receptor subunits. Additional work also suggests >7 days of treadmill exercise training can elevate AMPA receptor subunit expression in cerebellum, striatum, and motor cortices (Real et al., 2010, 2015); notably, however, the minimal dose of exercise required to induce these expression changes remains unclear. Therefore, we sought to determine whether exercise-induced priming following a single session of exercise could take the form of increased expression of postsynaptic ionotropic receptors and intracellular signaling intermediaries that have been previously shown to influence synaptic plasticity. Specifically, the NMDAR subunits GluN1 and GluN2A, AMPAR subunits GluA1 and GluA2, and Ca^{2+}/calmodulin-dependent protein kinase II (CaMKII) are known to be altered following chronic

exercise (Real et al., 2010, 2015; Cassilhas et al., 2012; Park et al., 2014), and are strongly associated with not only the induction of certain types of plasticity (such as long-term potentiation), but are also involved in synaptic processes that alter the likelihood of plasticity occurring (Abraham, 2008).

2.3 MATERIALS & METHODS

2.3.1 Animals

Male Sprague-Dawley rats (*Rattus norvegicus)* were purchased from Envigo™ at 6 weeks of age (weight 250-350 g). Throughout the study, animals were group housed in a temperature-controlled room on a reverse 12 : 12 light-dark cycle, and allowed free access to both water and standard rodent chow. Each animal was handled for 10 minutes a day for 5 days following arrival and prior to treadmill acclimatization. Animals were used in accordance with procedures approved by the University of Waterloo animal care committee.

2.3.2 Treadmill Acclimatization

All rats were randomly separated into three groups [Figure 2.1; treadmill control (TC), acclimatization control (AC), and graded exercise test (GXT)], before being habituated to a metabolic modular treadmill (Cat#1012R-1, Columbus Instruments, Columbus, OH, USA). All acclimatization periods were conducted 2 hours into the dark cycle (10 am) with each exposure lasting a total of 10 minutes/day for 8 consecutive days; our protocol was similar to that used by others (Soya et al., 2007; Betik et al., 2009). The AC and GXT groups were acclimatized with the treadmill on and fixed at a 10^{o} incline. Running was motivated by a brief electrical stimulus to the foot when rats contacted the probe at the back of the treadmill.

On day 11, AC and GXT rats ran at a constant speed of 10 m/min for the total duration of the acclimation period (10 minutes). On subsequent days (12-18), greater terminal speeds were achieved by gradually decreasing the total time spent at 10 m/min; in particular, speed was increased by 1 m/min every 30 seconds until, by the 7^{th} day, a terminal speed of 25 m/min was achieved within 10 minutes (Table 1). On the 8^{th} day animals again experienced 10 m/min for 10

minutes and were considered acclimated if no shocks were applied. The objective of this protocol was to train the animals to the mechanics of the treadmill without causing any exercise effects. Additionally, rats experienced 2 days of no treadmill exposure after the acclimatization period in an attempt to remove any sessional carryover effects that may have developed during acclimatization. TC animals were provided with the same opportunity to explore the treadmill (10 min/day) with the treadmill turned off and the electrical grid active.

2.3.3 GXT Treadmill Exercise

On the day of sacrifice, animals experienced either complete rest (TC & AC), or a graded bout of treadmill exercise to exhaustion (GXT). As a result, TC (N = 4) and AC (N = 6) animals experienced no running compartment exposure on day 21, while approximately 2 hours into the dark cycle (10 am) GXT (N = 10) animals were placed inside the metabolic treadmill apparatus. Baseline oxygen consumption (VO_2) measures were assessed over the first 2.5 minutes. Afterward, the treadmill was set at 10 m/min at a 10^o incline. Each recording for each speed interval lasted 2 minutes (VO_2 sampled once every 30 seconds) after which the speed was increased by an additional 2-3 m/min until fatigue (Table 2). Exhaustion was determined when the animal was unable to maintain pace and contacted the probe more than 3 times in a 5 second period; VO_2 corresponding to this time point was classified as peak VO_2. Following exhaustion, rats were removed from the treadmill housing and immediately anesthetized by CO_2 and then euthanized by decapitation.

2.3.4 Preparation of Sensorimotor Cortex

Following decapitation, brains were immediately removed and placed within an adult rat coronal brain matrix (Ted Pella, Inc., Redding, CA, USA) submerged in ice-cold artificial cerebral spinal fluid (ACSF) that contained (in mM): 127.0 NaCl (Sigma, Oakville, ON, Canada; all

subsequent reagents from Sigma, unless otherwise noted), 26.0 $NaHCO_3$, 10.0 glucose, 2.0 $CaCl_2$, 2.0 KCl, 2.0 $MgSO_4$, and 1.2 KH_2PO_4, and was equilibrated with carbogen (95% O_2/5% CO_2), at a pH of 7.37–7.43. The most rostral 6 mm of the cortex (prefrontal cortex) was removed by a coronal cut at a position roughly corresponding to atlas plate 9 (Paxinos and Watson, 1997) (Figure 2.3). Two additional coronal cuts were made at positions 9 and 12, yielding two 3 mm thick slices (matrix positions 6-9 / 9-12), encompassing an area between plates 9-21 of the Paxinos & Watson atlas. Slices were further dissected by a transverse cut along the apex of the corpus callosum to yield an area we and others have defined as sensorimotor cortex; the area contained medial and lateral agranular cortices (motor cortex) and primary somatosensory cortex (S1) (Heffner et al., 1980). All efforts were made to remove white matter from each slice. The sensorimotor cortex dissected from each hemisphere was pooled and manually homogenized in non-ionizing lysis buffer (10 mM Tris, 25 mM ethylenediaminetetraacetic acid [EDTA], 100 mM NaCl, 1% [v/v] Triton X-100, and 1% [v/v] NP-40, pH 7.4; protease inhibitor cocktail added on day of experiment), over ice with a Potter-Elvehjem homogenizer, and then centrifuged at 1000 x g for 10 min at 4ºC. Supernatants were collected, protein concentrations determined with a Bio-Rad DC protein assay kit according to the manufacturer's recommended protocol, and aliquots stored at -80ºC until further analysis.

2.3.5 Histological Staining and Imaging

A single TC rat was sacrificed to help confirm the ability of the dissection technique to isolate the sensorimotor region (Figure 2.4). Following the procedure noted above, rostral and caudal 3 mm thick slices were prepared for Hematoxylin and Eosin (H&E) staining. Each slice was embedded in Optimal Cutting Temperature compound (Tissue-Tek), frozen in liquid nitrogen-cooled isopentane, and cut into 10 µm thick sections with a cryostat (Thermo Electronic)

maintained at -20ºC. Slices were mounted on glass slides prior to H&E staining as previously described (Fajardo et al., 2016). Images were acquired with a brightfield Nikon microscope linked to a PixeLink digital camera and stitched together using ImageJ.

2.3.6 Western Blotting

Samples were thawed on ice and then denatured in sample buffer (0.0625 M Tris, 2% [v/v] glycerol, 5% [w/v] sodium dodecyl sulfate [SDS], 5% [v/v] β-mercaptoethanol, and 0.001% [w/v] bromophenol blue, pH 6.8) at 95ºC for 5 min. Proteins (10-20 µg) were separated electrophoretically using a 10, or 15% SDS-polyacrylamide gel at 200 V, or 150 V, respectively for 1 h, and were then electroblotted onto PVDF membranes via wet transfer (35 V at 4ºC for 16 h). Blots were then incubated with Ponceau S solution, washed with deionized water, air dried, and then imaged.

Membranes were blocked using either 5% (w/v) bovine serum albumin (BSA), or 5% (w/v) non-fat milk in Tris-buffered saline with Tween-20 (TBST) for 1 h at room temperature and incubated with relevant antibodies overnight at 4ºC. All primary antibodies (from Cell Signaling Technology unless otherwise stated) were diluted to 1:1000 in blocking buffer specific to the application. The following monoclonal antibodies were used to assess whether the acclimatization protocol, or single session exercise had an influence on the cellular expression of plasticity-related proteins: anti-GluA1 (#13185S), anti-GluA2 (#13607), anti-GluN1 (#5704), anti-GluN2A (#4205), anti-CaMKII (#11945). Heat shock protein, anti-HSP70 (SC-32239; Santa Cruz) was also used. On the following day, membranes were incubated with either rabbit (#7074), or mouse (SC-2005; Santa Cruz) IgG antibody (1:5000) conjugated to horseradish peroxidase and immunoblotted using Luminata Crescendo ECL substrate (Millipore) for 2 minutes. Optical densities were captured and analyzed as previously described (Thacker et al., 2016, Appendix I). Briefly, optical

densities were normalized to whole lane Ponceau S staining images in order to control for loading variation. Within each blot, the optical density: Ponceau S ratios for each condition were then normalized to a similar ratio constructed for an internal control (IC; an amount of whole brain sample equal to the experimental samples) to account for inter-blot variability.

2.3.7 Statistical Analysis

All statistical analyses were performed using GraphPad Prism. All Western blot data for TC – AC – GXT samples were compared using the Kruskal-Wallis test (a non-parametric version of the one-way ANOVA). Pre-planned comparisons between AC – GXT rats were conducted using a Mann-Whitney U test (a non-parametric version of the Student's t-test). A linear regression analysis was conducted on VO_2 as a function of speed. Baseline and peak VO_2 values following GXT were compared using the Wilcoxon matched-pairs signed rank test. All dependent measures are presented as the mean ± SEM and were analyzed for statistical significance with $p < 0.05$. Standardized effect sizes (Cohen's d) are presented when $p \leq 0.05$.

2.4 RESULTS & DISCUSSION

2.4.1 Physiological Inquiries

All AC and GXT rats completed acclimatization with minimal (≤ 1 count) foot shocks by the 8th day of training, and no rats were excluded. An average baseline VO_2 of 40.7 ± 6.9 mL/kg/min and peak VO_2 of 95.6 ± 4.5 mL/kg/min for GXT rats (N = 10) suggest a significant increase in oxygen consumption during exercise (Figure 2.2: $p < 0.002$, $d = 4.27$). The peak VO_2 observed in this study is comparable to previously reported VO_{2max} values determined under equivalent conditions (10º incline) with similarly aged treadmill naïve Sprague-Dawley rats, although a visible plateau in VO_2 was not observed as expected (Wisløff et al., 2001; Høydal et al., 2007). One possible explanation for the absence of an observed VO_2 plateau may be related to how we defined exhaustion. Unlike other reports (Bedford et al., 1979; Hilty et al., 1989; Wranne and R. D. Woodson., 2013), we chose a more conservative classification for exhaustion (3 shocks in 5 seconds), in an effort to reduce discomfort and the number of noxious stimuli often required to motivate animals to continue running at extreme intensities. Our use of less intense criteria to classify exhaustion may have led to the termination of the exercise session prior to an observable VO_2 plateau. An additional explanation may be related to observations by Wisløff and colleagues (Wisløff et al., 2001) that an optimal incline angle of 25º is required to achieve the highest possible rat VO_{2max} with a distinct VO_2 plateau. The authors note that 25° may recruit the optimal level of muscle mass, balanced by a slower cadence (Wisløff et al., 2001). The present study used an incline of 10°, which may have increased cadence at the expense of recruiting the amount of muscle mass necessary to observe a VO_2 plateau.

In this study, GXT rats achieved peak VO_2 within an average of 22.7 ± 4.2 min at an average speed of 33.6 ± 5.0 m/min. Previous research has supported the use of speed as a proxy

for VO_2 at lower intensities (Høydal et al., 2007), thus a linear regression analysis was used to predict the influence of speed on VO_2 (Figure 2.2). Although individual rats displayed a large range for total duration (15.6 min, 28.3 min) and terminal speed (24 m/min, 40 m/min), the GXT protocol resulted in a strong linear relationship ($F(1,6) = 111.0$, $p < 0.0001$) between speed and VO_2 ($R^2 = 0.9487$). The clear relationship of VO_2 intensity with speed may allow for the selection of speeds for sub-max exercise intensities in single session investigations in rodents without the need for prior VO_2 testing.

The use of speed as a predictor for single session exercise intensity has numerous advantages over other methods, such as measuring blood lactate, that do not require VO_{2max} testing; in particular, approaches that require the continuous collection of blood throughout the exercise bout may introduce additional stress that could interfere with the interpretation of the neurological data. Moreover, the collection of blood requires the animal to cease exercising for brief periods, which may alter the exercise dose. Additionally, the terminal speed achieved by our rats (33.6 ± 5.0 m/min) would also suggest lactate threshold was reached, for others have shown this to occur at, or around, 30 m/min (2 rats in our study did not surpass 30 m/min). Overall, the GXT protocol performs well as a single session exercise model in young Sprague-Dawley rats and, as others have suggested, speed may be an adequate means of selecting the intensity of a moderate bout of single session exercise in future studies.

2.4.2 Anatomical Inquiries

Coronal slices from brain matrix positions 6-9 and 9-12 display gross anatomical resemblance to the relevant regions depicted by plates 9 and 21 of Paxinos and Watson (Figure 2.3) (Paxinos and Watson, 1997). Light microscopic examination of H&E stained 10 µm sections from cortical slices bordering our presumptive sensorimotor region (Figure 2.4 A, B) show

morphological consistency with wheat germ agglutinin conjugated horseradish peroxidase (WGA-HRP) (Figure 2.4C) and biotinylated dextran amine (BDA) (Figure 2.4D) tracer studies of areas previously described as sensorimotor cortical regions (Donoghue and Parham, 1983; Zakiewicz et al., 2011). Taken together, the qualitative comparisons of our slices to both the Paxinos and Watson atlas and functional tracer studies confirm our procedure reliably isolated rat sensorimotor cortex (Zakiewicz et al., 2011).

2.4.3 Biochemical Investigations

Our selection of forced exercise on a metabolic treadmill was based on its ability to control individual rodent exercise dose over a single session. However, the forced exercise paradigm requires animals to be acclimatized to the treadmill prior to the study of a single session. Since aerobic exercise requires the direct activation of muscle via projections from motor centers in the brain, the possibility exists that acclimatizing to a treadmill may induce protein expression in these areas. As a result, when assessing the biochemical signature that follows single session exercise, accounting for adaptation that may have occurred in response to the acquisition of treadmill skill is important. We attempted to account for potential skill acquisition effects by allowing the animals only 10 minutes/day of treadmill exposure, and through the addition of two days of rest prior to the day of sacrifice. However, the literature is unclear with regards to the minimal dose of aerobic exercise needed to induce adaptation in the brain. A primary marker for muscle and brain adaptation following aerobic training is the expression of heat shock protein 70 (HSP70) (Walters et al., 1998a; Milne et al., 2002; Melling et al., 2007). Notably, HSP70 is a marker of physiological stress, and its expression is induced in muscular tissue in response to a single event exercise. In addition, HSP70 expression is directly correlated with the level of muscle adaptation to aerobic training (Milne et al., 2002; Melling et al., 2007). To determine whether our acclimatization

protocol induced exercise training-like effects in the brain, we measured HSP70 expression in the sensorimotor cortex (Figure 2.5). Comparing HSP70 expression between TC-AC revealed no significant differences (normalized to IC; TC: 0.76 ± 0.05, AC: 0.67 ± 0.05; p = 0.37). Moreover, upon comparing AC-GXT no significant increases in the sensorimotor cortex were observed (AC: 0.67 ± 0.05, GXT: 0.82 ± 0.05; p = 0.17), which is similar to previous reports of single session exercise evaluating HSP70 in the brain (Walters et al., 1998b). Together, these data suggest that the acclimatization protocol is below the threshold required to stimulate HSP70 expression in sensorimotor cortex while maintaining the acquisition of treadmill skill.

To examine whether the acclimatization period was sufficient to induce exercise-like effects (Real et al., 2010), we investigated the expression of AMPAR subunits GluA1 and GluA2, NMDAR subunits GluN1 and GluN2A, and the kinase CaMKII, which are proteins consistently associated with synaptic plasticity (Lisman and Zhabotinsky, 2001; Lisman et al., 2002; Barria and Malinow, 2005; Huganir and Nicoll, 2013). As expected, AC and TC did not significantly differ with regards to the total protein expression of either GluA1 (TC: 1.10 ± 0.14, AC: 1.19 ± 0.17; p = 0.93), GluA2 (TC: 1.57 ± 0.14, AC: 1.36 ± 0.20; p = 0.68), GluN1 (TC: 2.99 ± 0.46, AC: 2.54 ± 0.38; p = 0.41), GluN2A (TC: 3.65 ± 0.93, AC: 3.75 ± 0.43; p = 0.64), or CaMKII (TC: 2.68 ± 0.32, AC: 2.41 ± 0.31; p = 0.77) (Figures 2.5-2.7). These data reinforce the notion that the treadmill acclimation protocol is appropriate for use in studying single session effects as it does not appear to elicit significant changes in expression of key plasticity-related proteins. Moreover, the addition of a single session GXT following acclimatization did not modify the amount of cellular GluA1 (AC: 1.04 ± 0.07, GXT: 1.27 ± 0.11; p = 0.28), GluA2 (AC: 1.36 ± 0.20, GXT: 1.32 ± 0.18; p = 0.99), GluN1 (AC: 2.54 ± 0.38, GXT: 3.03 ± 0.41; p = 0.43), GluN2A (AC: 3.75

± 0.43, GXT: 4.00 ± 0.46; p = 0.63), or CaMKII (AC: 2.41 ± 0.31, GXT: 2.38 ± 0.34; p = 0.87) in sensorimotor cortex compared to AC animals (Figures 2.5-2.7).

Overall, our observations provide evidence that the expression of these plasticity-related proteins is not immediately altered following exhaustive exercise; notably, had we sampled at a delayed time point (e.g., 30-90 minutes) after exercise, we might have observed differences. Moreover, the expression of these plasticity-related proteins may require chronic (> a week) exercise exposure to achieve measurable differences (Ferreira et al., 2010; Real et al., 2010, 2015; Park et al., 2014). Nonetheless, if a delay is required to alter protein expression in a manner that would promote plasticity, then this particular possible mechanism is not compatible with data from human studies showing immediate priming within motor cortex. Another possibility may be that priming takes shape at the molecular level as increases in transcription factors (immediate early genes), altered neurotransmitter/neuromodulator release, or, most likely, the post-translational modification of AMPA receptor and NMDA receptor subunit proteins.

2.5 CONCLUSION

Herein, we present a model for the exploration of acute physiological responses to single session exercise in rat sensorimotor cortex. The animals (after acclimatization + single exercise bout) displayed a minimal change in stress marker protein expression in response to treadmill acclimatization, and stable plasticity-related protein expression, suggesting the expression of these proteins does not account for post-exercise priming. These features, combined with our qualitative anatomical assessment of a technique to isolate the motor cortex, and method for the selection of exercise intensity for a single session, provide a novel set of tools to further study single session exercise effects in the rat sensorimotor cortex.

FIGURE LEGEND

Figure 2.1. Timeline illustrating study protocol from arrival at the animal facility to the day of euthanasia. Upon arrival, animals were randomly separated into three groups: treadmill control (TC; N = 4), acclimatization control (AC; N = 6), and graded exercise test (GXT; N = 10).

Figure 2.2. (A) Average baseline and peak VO2 (mean ± SEM) following maximal graded exercise in GXT rats (N = 10). *denotes significance following both a Mann-Whitney U test ($p < 0.0001$) and calculation of a standardized effect size ($d = 4.27$). (B) Individual VO2 data as a function of incremental speed in GXT rats.

Figure 2.3. Illustrations depicting isolation of sensorimotor cortex. (A) Plate 9 from Paxinos & Watson (2007) indicates the rostral border of sensorimotor cortex, while Plate 21 from Paxinos & Watson (2007) indicates the caudal border of sensorimotor cortex (Paxinos and Watson, 1997). In both plates, the dashed lines denote the region dissected and used for analysis. (B) Cortical view of the functional motor and sensory map overlays as displayed following electrical stimulation (Hall and Lindholm, 1974). Blue shaded area defines the boundaries of cortical tissue isolated as sensorimotor cortex in this study.

Figure 2.4. H&E staining of coronal slices (10 µm) caudal to brain matrix position 6 (A) and rostral to position 12 (B) The slices illustrate the borders of our presumptive sensorimotor cortex; notably, only tissue above the dashed lines was used to prepare tissue homogenates. (C) For comparison, we have provided a photomicrograph of WGA-HRP staining following in vivo electrostimulation guided injection of the lateral agranular cortex (AG_l) (Donoghue and Parham, 1983) and (D) a photomicrograph of in vivo BDA-injected Primary Somatosensory Cortex (S1) counterstained with neutral red (Zakiewicz et al., 2011).

Figure 2.5. Western blot data for CaMKII and HSP70. Summary graphs for each protein are shown along with representative immunoblots and their respective Ponceau-stained membrane from individual cohorts; TC (N = 4), AC (N = 8), GXT (N = 10). In both graphs, the bars present the mean ± SEM. All values are normalized to an internal control (IC; whole brain).

Figure 2.6. Western blot data for GluA1 and GluA2. Summary graphs for each protein are shown along with representative immunoblots and their respective Ponceau-stained membrane from individual cohorts; TC (N = 4), AC (N = 8), GXT (N = 10). In both graphs, the bars present the mean ± SEM. All values are normalized to an internal control (IC; whole brain).

Figure 2.7. Western blot data for GluN1 and GluN2A. Summary graphs for each protein are shown along with representative immunoblots and their respective Ponceau-stained membrane from individual cohorts; TC (N = 4), AC (N = 8), GXT (N = 10). In both graphs, the bars present the mean ± SEM. All values are normalized to an internal control (IC; whole brain).

Figure 2.1

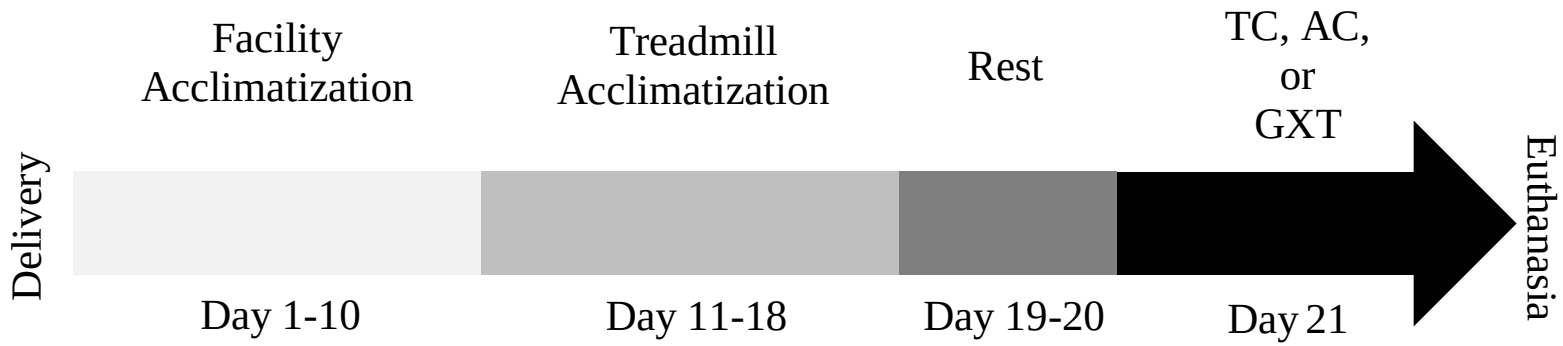
Facility Acclimatization
Treadmill Acclimatization
Rest
TC, AC, or GXT
Delivery
Euthanasia
Day 1-10
Day 11-18
Day 19-20
Day 21

Figure 2.2

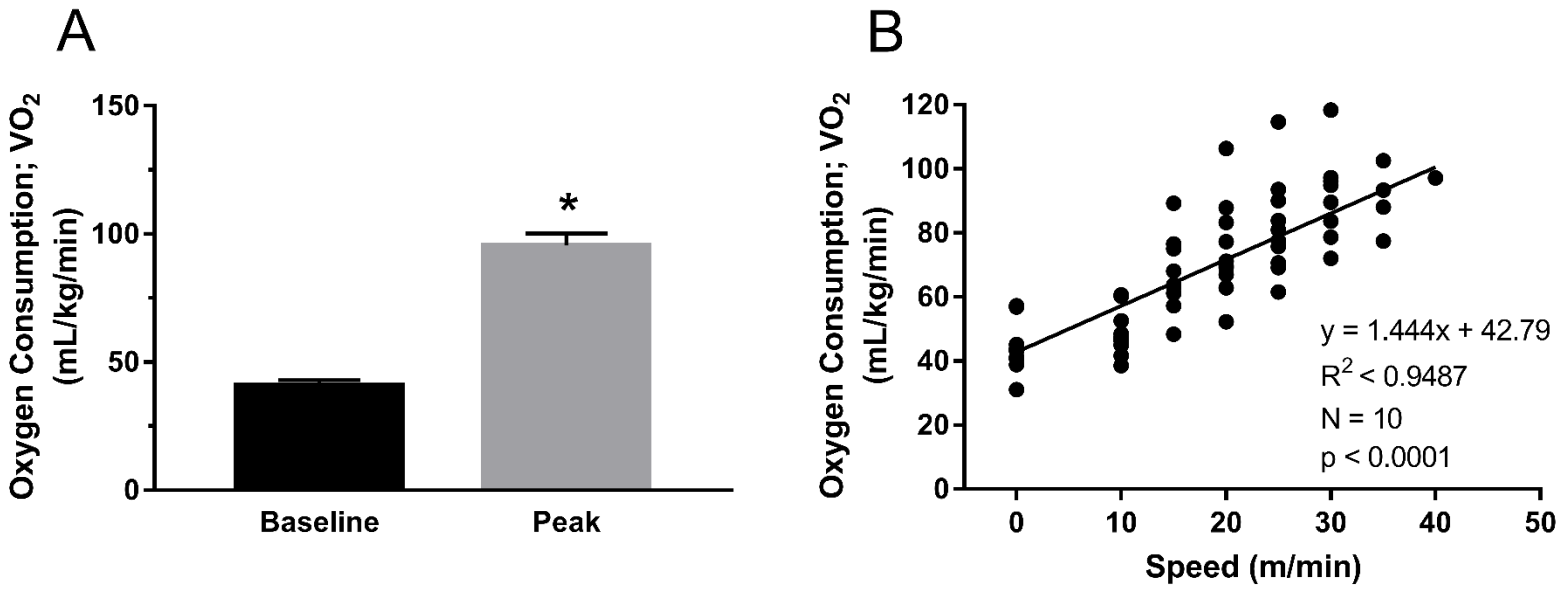
A
Oxygen Consumption; VO2 (mL/kg/min)
150
100
50
0
*
Baseline
Peak
B
Oxygen Consumption; VO2 (mL/kg/min)
120
100
80
60
40
20
0
0
10
20
30
40
50
Speed (m/min)
y = 1.444x + 42.79
R2 < 0.9487
N = 10
p < 0.0001

Figure 2.3

A

Plate 9

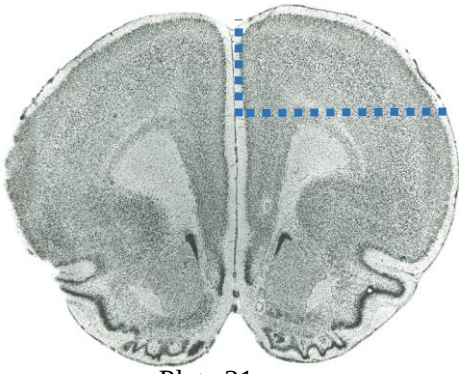

Plate 21

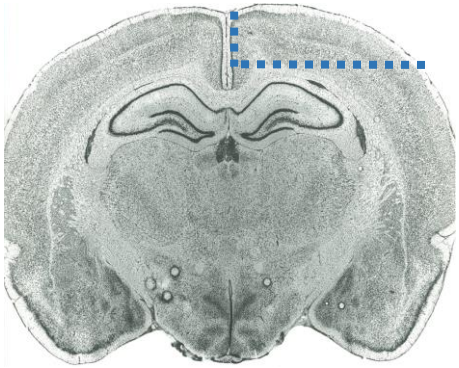

B

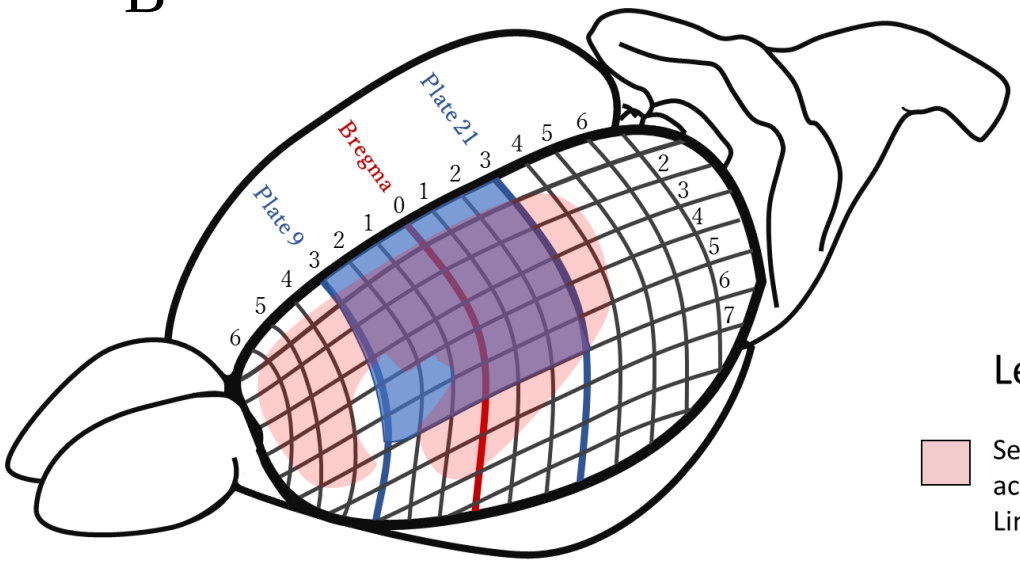

Legend

Sensorimotor Cortex according to Hall & Lindholm (1976)

Region isolated in current study

Figure 2.4

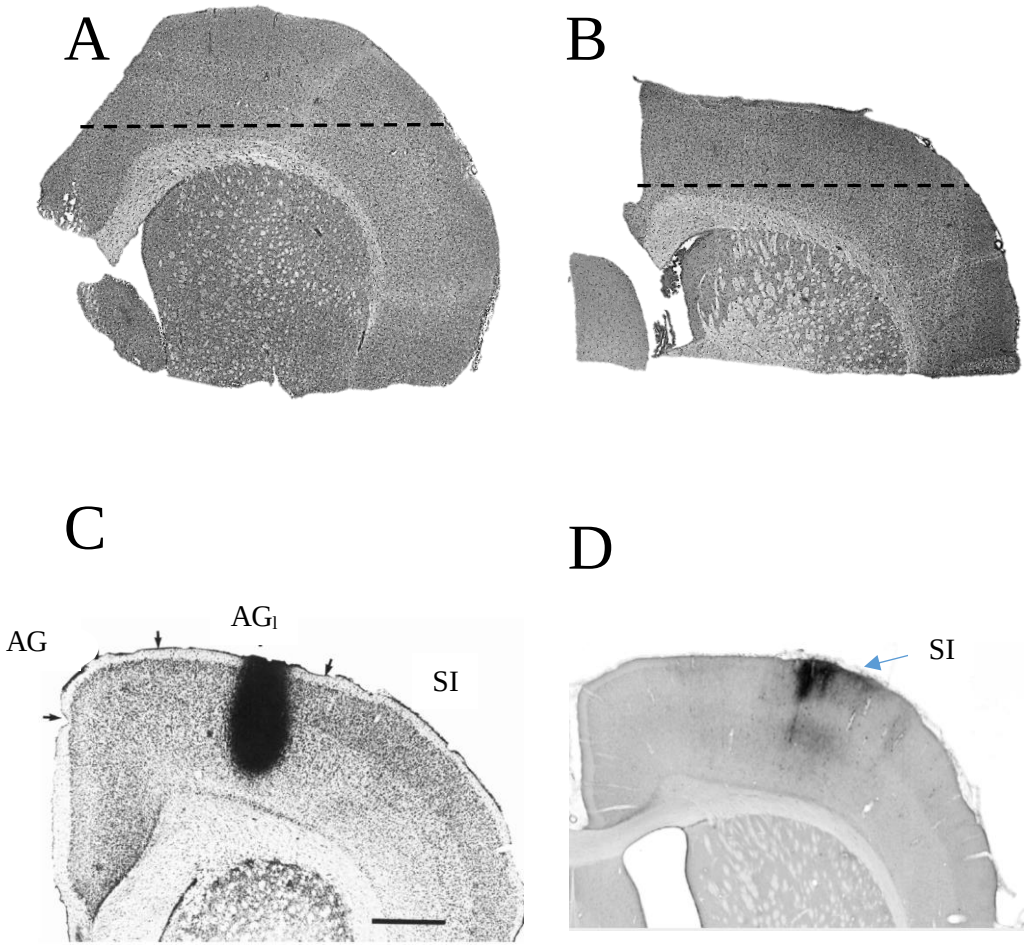

Figure 2.5

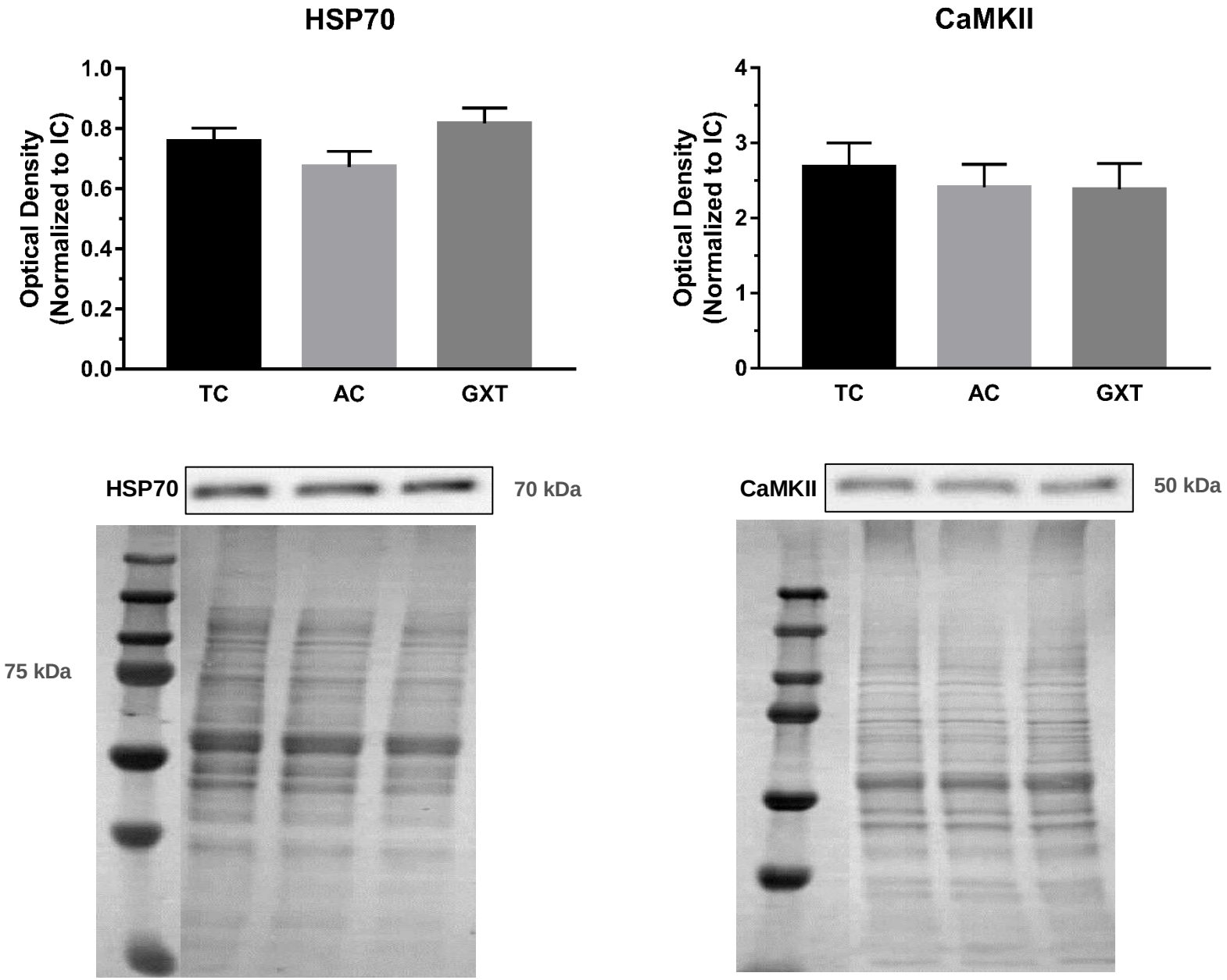
HSP70
Optical Density (Normalized to IC)
1.0
0.8
0.6
0.4
0.2
0.0
TC
AC
GXT
CaMKII
Optical Density (Normalized to IC)
4
3
2
1
0
TC
AC
GXT
HSP70
70 kDa
75 kDa
CaMKII
50 kDa

Figure 2.6

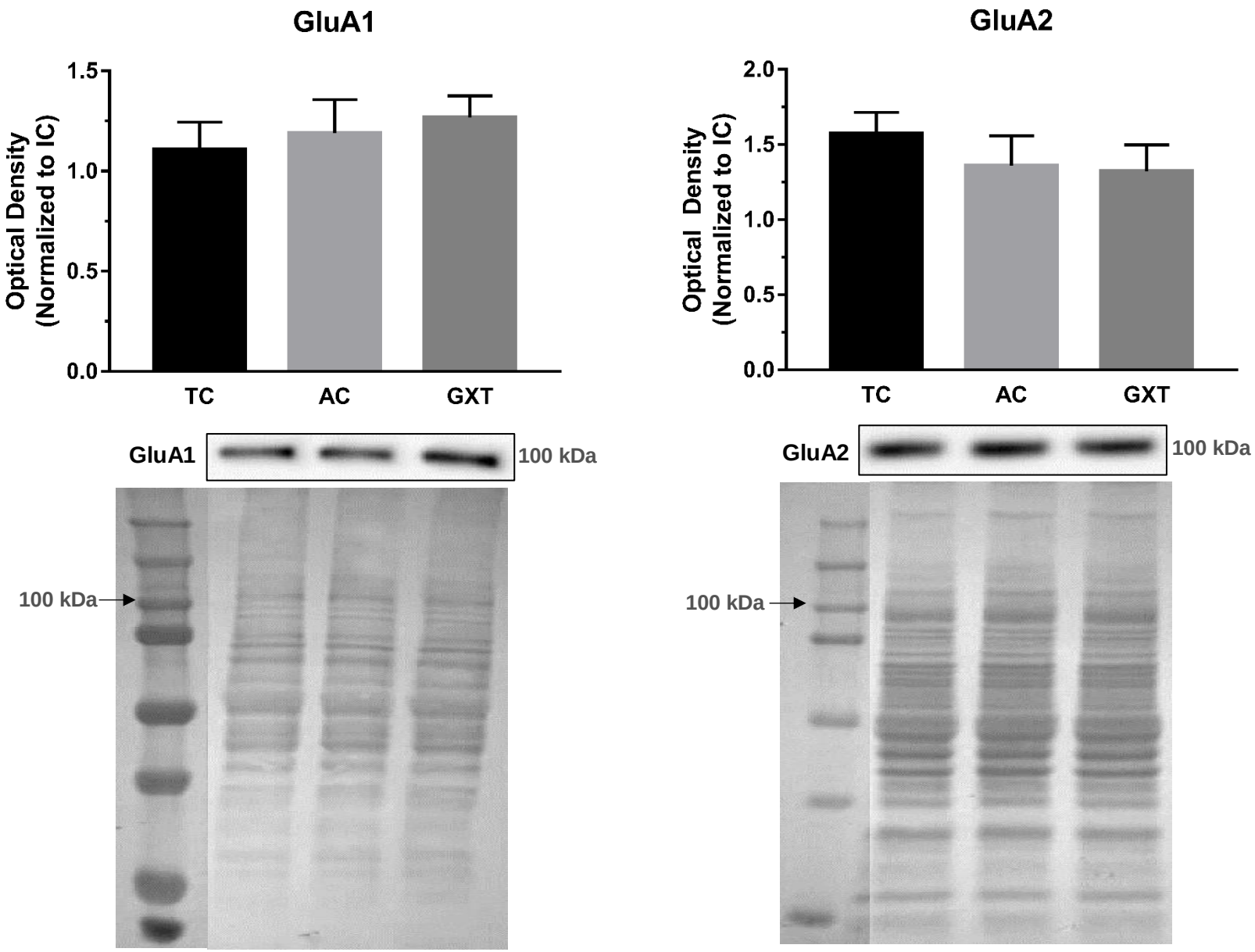
GluA1
Optical Density (Normalized to IC)
1.5
1.0
0.5
0.0
TC
AC
GXT
GluA1
100 kDa
100 kDa
GluA2
Optical Density (Normalized to IC)
2.0
1.5
1.0
0.5
0.0
TC
AC
GXT
GluA2
100 kDa
100 kDa

Figure 2.7

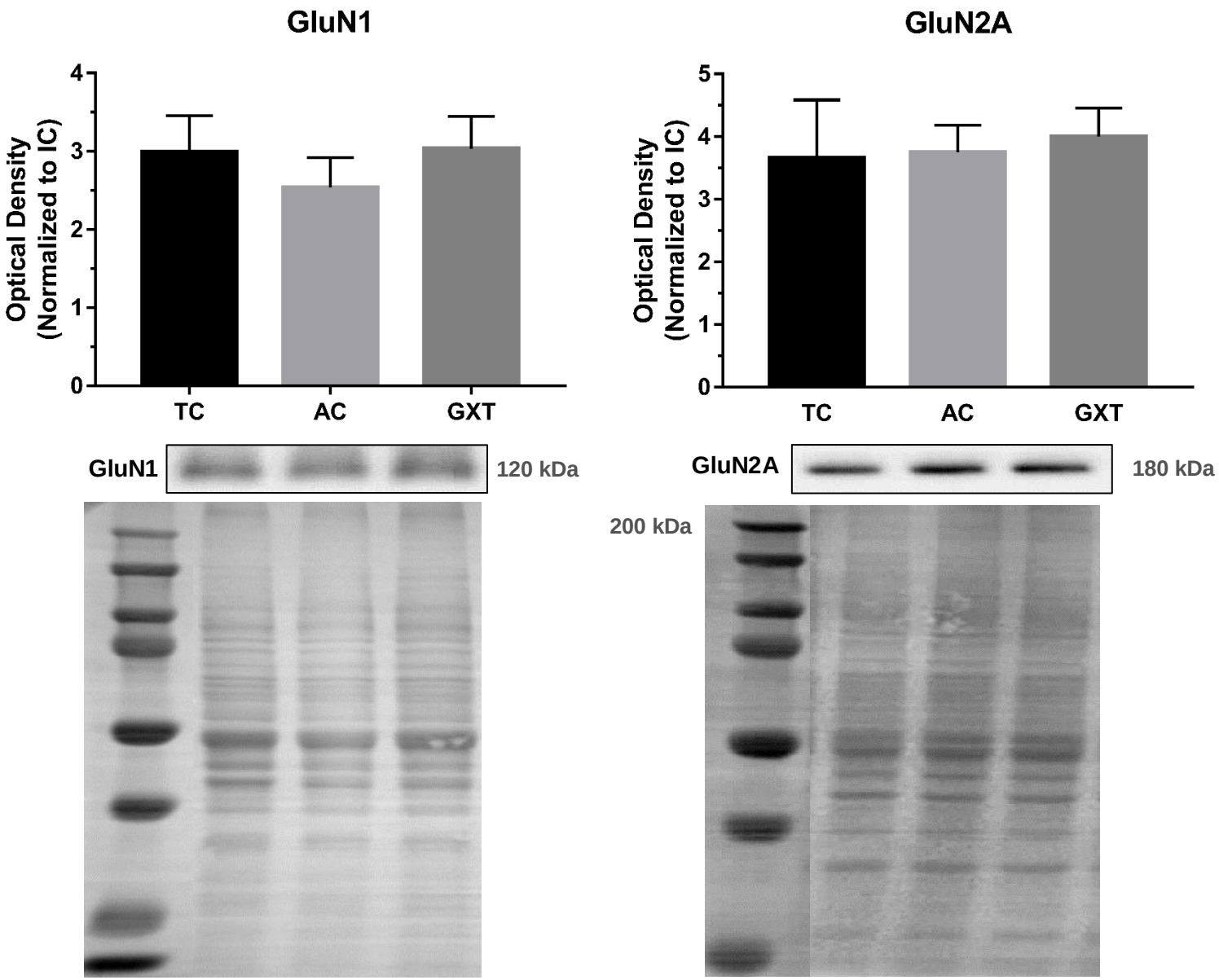
GluN1
Optical Density (Normalized to IC)
0
1
2
3
4
TC
AC
GXT
GluN1
120 kDa
GluN2A
Optical Density (Normalized to IC)
0
1
2
3
4
5
TC
AC
GXT
GluN2A
180 kDa
200 kDa

3. A Single Session of Aerobic Exercise Mediates Plasticity-Related Phosphorylation in both the Motor Cortex and Hippocampus

Adapted from Submitted Manuscript: "Thacker JS, Yuyi Xu, Cerise Tang, A Russel Tupling, W Richard Staines, John G Mielke (2018). A Single Session of Aerobic Exercise Mediates Plasticity-Related Phosphorylation in both the Motor Cortex and Hippocampus. JNeurosci"

3.1 ABSTRACT

A single session of aerobic exercise may offer one means to "prime" motor regions to be more receptive to the acquisition of a motor skill, however, the mechanisms whereby this priming may occur are not clear. One possible explanation may be related to the post-translational modification of plasticity-related receptors and intracellular signaling molecules, given that both of these sets of proteins are integral to the development of synaptic plasticity. In particular, phosphorylation governs the biophysical properties (e.g. Ca^{2+} conductance) and the migratory patterns (i.e., trafficking) of plasticity-related receptors by altering the relative contribution of specific receptor subunits at synapses. We hypothesized that a single session of exercise would alter the subunit phosphorylation of plasticity-related receptors (AMPA receptors, NMDA receptors) and intracellular signaling molecules (PKA/CaMKII) in a manner that would serve to prime the motor cortex. Young, male Sprague-Dawley rats (n = 24) on a reverse light cycle were randomly assigned to either exercise (Moderate, Exhaustion), or non-exercising (Sedentary) groups. Immediately following a single session of treadmill exercise, rats were euthanized and whole homogenates were prepared from both the motor cortex and hippocampus. We observed a robust (1.2 – 2.0x greater than sedentary) increase in tyrosine phosphorylation of AMPAR (GluA1,2) and NMDAR (GluN2A, B) subunits, and a clear indication that exercise preferentially affects pPKA over pCaMKII. The changes were found, specifically, following moderate, but not maximal, an acute aerobic exercise in both the motor cortex and hippocampus to varying degrees. Given the requirement for these proteins during the early phases of plasticity induction, the possibility exists exercise-induced priming may occur by altering the phosphorylation state of plasticity-related receptors.

3.2 INTRODUCTION

Studies with various species have revealed clear adaptations in brain regions such as the hippocampus (HP) following long-term exercise interventions. Furthermore, even acute (≈ 20 minutes) bouts of moderately intense exercise can have a transient modulatory influence on excitability in the human motor cortex (Thacker et al., 2014; Singh and Staines, 2015; Neva et al., 2017). Exercise-dependent changes in excitability may be indicative of a "primed" state allowing motor regions to more readily facilitate the acquisition of a novel skill (Roig et al., 2012; McDonnell et al., 2013; Stavrinos and Coxon, 2014; Statton et al., 2015), however, the biochemical changes caused by a single session of exercise remain relatively unexplored.

As with other areas of brain, plasticity in the motor cortex is the result of precisely coordinated changes at the neuronal level (Kleim et al., 1996, 1998; Sanes and Donoghue, 2000; Xu et al., 2009), and the best-characterized mechanism for this plasticity is the persistent enhancement of synaptic transmission (long-term potentiation; LTP) at the involved synapses (Bliss and Lomo, 1973). Although the induction of LTP at synapses has been shown to require numerous biochemical changes, the most thoroughly understood involves the excitatory glutamatergic receptors (Morris, 2013; Nicoll and Roche, 2013). If a single session of exercise truly results in the priming of plasticity in the motor cortex, then this change would most likely be reflected in adaptations at the level of glutamate receptors.

The early phases of LTP induction require the activation of glutamatergic N-methyl-D-aspartate receptors (NMDARs), which are heterotetramers formed from 2 obligatory GluN1 subunits and 2 varied GluN2, or GluN3 subunits (GluN2A-D; GluN3A-B) (Dingledine et al., 1999; Paoletti et al., 2013). Although numerous combinations of NMDAR subunits are possible, the GluN2A and GluN2B subunits appear to predominate in regions such as motor cortex and

hippocampus (Monyer et al., 1994; Goebel and Poosch, 1999; Sun et al., 2000). Notably, these particular GluN2 subunits are distinguished by their unique intracellular C-termini, which allow interaction with an assortment of cytosolic kinases and scaffolding proteins that govern biophysical properties, such as channel conductance, Mg^{2+} sensitivity, and open probability (Erreger et al., 2005; Wyllie et al., 2013).

Although the induction of LTP requires the NMDAR, its persistence is thought to rest upon the migration, peri-synaptic insertion, and synaptic capture of glutamatergic α-amino-3-hydroxy-5-methyl-4-isoxazolepropionic acid receptors (AMPAR) (Huganir and Nicoll, 2013). Like the NMDAR, AMPARs form as hetero-tetrameric complexes by any combination of phenotypically diverse subunits (GluA1-4), with GluA1 and GluA2 being most heavily expressed. Data now support divergent rules governing the trafficking of the GluA1-containing and GluA2-containing AMPARs, suggesting various functions each AMPAR subunit type within a single excitatory synapse (Shi et al., 2001; Lee et al., 2004).

Long-term exercise increases both NMDAR and AMPAR subunit protein expression in hippocampus (Real et al., 2010; Park et al., 2014), however, we, and others, have found that a single session of high-intensity exercise (lasting no longer than 30 minutes) does not have such an effect (Real et al., 2010; Thacker et al., 2018). Thus, changes in the expression of subunit proteins is not a likely explanation for the priming effects caused by a single session of exercise. More likely, are post-translational modifications, which present rapidly and alter the biophysical properties, and trafficking, of excitatory glutamatergic receptors in a fashion that favors LTP induction.

Acute physical stress often yields a positive effect on synaptic plasticity by upregulating the release of neuroactive substances into the periphery (Garcia, 2001; Yuen et al., 2009;

Whitehead et al., 2013). For example, human studies note that a graded exercise test to exhaustion causes robust changes in circulating levels of brain-derived neurotrophic factor (BDNF) (Rojas Vega et al., 2006; Ferris et al., 2007), which has repeatedly displayed to increase the activity (i.e. firing rate) influence over glutamatergic-dependent forms of plasticity (Lu, 2003; Bramham and Messaoudi, 2005; Lu et al., 2005). Additionally, the glucocorticoid corticosterone/cortisol is robustly released following acute exercise in naïve or unfit subjects (Rojas Vega et al., 2006; Hill et al., 2014; Radahmadi et al., 2014, 2015), and a variety of studies have shown that either acute stress exposure, or bath application of corticosterone enhances experimentally induced LTP in both the rodent hippocampus and cortex (Windle et al., 1998; Groc et al., 2008a; Whitehead et al., 2013; Treccani et al., 2014; Kula et al., 2016). We hypothesized that a single session of exercise would prime plasticity within the hippocampus and motor cortex through a combination of tyrosine phosphorylation-mediated changes to glutamatergic receptors in the hippocampus and sensorimotor cortex. Moreover, we thought that any observed changes would correspond with an increased release of either peripheral BDNF, and/or corticosterone.

3.3 METHODS

3.3.1 Animals

Male Sprague-Dawley rats (*Rattus norvegicus)* were purchased from Envigo™ at 6 weeks of age (weight = 250-350 g). All animals were group housed (N = 3, 1 animal/condition) in a temperature-controlled room on a reverse 12 : 12 light-dark cycle, and were allowed free access to both water and standard rodent chow (Teklad 22/5, Envigo, Cat# 8640). Each animal was handled by an individual researcher for 10 minutes a day, for 5 days, following adjustment to the facility and prior to treadmill acclimatization. Animals were used in accordance with procedures approved by the University of Waterloo animal care and ethics committee.

3.3.2 Treadmill Acclimatization

All rats were habituated to a metabolic modular treadmill (Columbus Instruments, Columbus, OH, USA) following a previously published protocol (Thacker et al., 2018, Chapter 2). Briefly, 2 hours into the dark cycle (10 am), on each of 8 consecutive days, rats in either the sedentary (SED), moderate (MOD), or graded exercise test (GXT) groups were individually placed in a metabolic modular treadmill. Sedentary rats were placed in the treadmill for 10 minutes with the treadmill off, whereas MOD and GXT rats ran for 10 minutes per day, with increasing treadmill speed on each consecutive day. Two days of rest were given to reduce any carryover effects of acclimatization on the single session testing day. In total, 1 rat was excluded from the study as it failed to acclimate to the use of the treadmill (did not produce a running behavior) by the end of the 8^{th} day.

3.3.3 Treadmill Exercise

Following the 2 rest days, all animals were placed in the metabolic treadmill using group-specific intensities. The experiments were carried out in a random order of treatment (SED, MOD, GXT), with the first animal being placed inside the treadmill 2 hours into the dark cycle (10 am). All baseline VO_2 measures were assessed over the first 2.5 minutes in the treadmill apparatus. The total duration (22.5 minutes) of SED (N = 8) and MOD (N = 7) treadmill exposure was determined by the average duration of a sub-sample (N = 10) of GXT animals (Thacker et al., 2018, Chapter 2). In addition, previous work has suggested that speed may be used as a predictor of VO_2 for the purpose of selecting intensity, and for this reason, MOD animals ran at 60% of the average terminal speed based on the same sub-sample of rats (N = 10) previously noted (Thacker et al., 2018, Chapter 2). On the day of testing, SED animals were placed in the metabolic chamber with the treadmill switched off for the duration of the protocol. Following baseline measures, MOD animals started at 10 m/min at a 10^o graded incline, with a gradual increase in speed every 30 seconds (2 m/min) until a terminal speed of 20 m/min was achieved and maintained for 20 minutes. The GXT (N = 7) animals were placed in the treadmill apparatus and, following baseline VO_2, the treadmill was then set at 10 m/min at a 10^o graded incline. Each recording interval lasted 2 minutes, at which time the speed was increased by an additional 2.5 m/min until fatigue was observed. Exhaustion was taken to be the point when the animal was unable to maintain pace and encroached towards the back of the treadmill, contacting the probe more than 3 times in a 5 second period. Determination of steady state (SED and MOD) VO_2 at baseline and termination (VO_{2Peak}) was determined by the average of the first and last 4 sample points, respectively. VO_{2Peak} for GXT rats was taken as a point sample measured over the last 30 seconds prior to exhaustion. Following either the SED, MOD or GXT protocols, rats were removed from the treadmill housing and sacrificed.

3.3.4 Isolation of Tissue Homogenates from the Sensorimotor Cortex and Hippocampus

Immediately following either the SED, MOD or GXT protocols, rats were anesthetized with CO_2 and euthanized by decapitation. Brains were immediately removed and placed within an adult rat coronal brain matrix (Ted Pella, Inc., Redding, CA, USA) submerged in ice-cold artificial cerebral spinal fluid (ACSF) that contained (in mM): 127.0 NaCl (Sigma, Oakville, ON, Canada; all subsequent reagents from Sigma, unless otherwise noted), 26.0 $NaHCO_3$, 10.0 glucose, 2.0 $CaCl_2$, 2.0 KCl, 2.0 $MgSO_4$, and 1.2 KH_2PO_4 and was equilibrated with carbogen (95% O_2/5% CO_2), pH 7.37–7.43. Sensorimotor cortex was dissected as previously described (Thacker et al., 2018, Chapter 2). Briefly, guided by the use of a brain matrix, coronal cuts were made 6 mm and 12 mm from the rostral pole, which encompassed a region previously identified as sensorimotor cortex (Hall and Lindholm, 1974; Heffner et al., 1980) The section of tissue was further dissected by a transverse cut along the apex of the corpus callosum to yield an area limited to only cortical layers. The remaining caudal portion of the brain was used to extract both hippocampi from each hemisphere in a fashion similar to that previously described (Madison and Edson, 2001). Tissue isolated from each hemisphere was pooled and manually homogenized in non-ionizing lysis buffer (containing 10 mM Tris, 25 mM ethylenediaminetetraacetic acid [EDTA], 100 mM NaCl, 1% [v/v] Triton X-100, and 1% [v/v] NP-40, pH 7.4; protease inhibitor cocktail and sodium orthovanadate added on day of experiment) over ice with a Potter-Elvehjem homogenizer, and then centrifuged at 1000 x g for 10 min at 4ºC. Supernatants were collected, protein concentrations were determined with a Bio-Rad DC protein assay kit according to the manufacturer's recommended protocol, and aliquots were stored at -80ºC.

3.3.5 Enzyme-linked Immunosorbent Assay (ELISA)

Trunk blood was collected in 1.5 mL Eppendorf tubes following decapitation and allowed to rest for 20 minutes at room temperature to clot. Tubes were then centrifuged at 2,000 x g for 10 minutes at 4ºC. The supernatants (representing the serum portion of the blood) were collected and pooled in a clean glass test tube, vortexed for 5 seconds and immediately aliquoted for storage at -80ºC. BDNF was investigated using ChemiKine™ sandwich ELISA (#CYT306, EMD Millipore, USA) according to the manufacturer's instructions. All samples were run in duplicate at 2x and 5x dilutions. Corticosterone was assessed using competitive ELISA (#501320, Cayman Chemicals, Ann Arbor, MI, USA) according to the manufacturer`s instructions. Serum was run in triplicate at empirically determined dilutions for each treatment; SED (50x, 100x), MOD and GXT (250x, 500x). All attempts were taken to limit the amount of freeze-thaw cycles for each sample.

3.3.6 Western Blotting

Samples were thawed on ice and then denatured in sample buffer (0.0625 M Tris, 2% [v/v] glycerol, 5% [w/v] sodium dodecyl sulfate [SDS], 5% [v/v] β-mercaptoethanol, and 0.001% [w/v] bromophenol blue, pH 6.8) at 95ºC for 5 min. Samples (10-20 µg) were loaded in triplicate and separated electrophoretically using a 10, or 15% SDS-polyacrylamide gel at 200, or 150 V, respectively, for 1 h, and were then electroblotted onto PVDF membranes via wet transfer (35 V at 4ºC for 16 h). Blots were then incubated with Ponceau S solution, washed with deionized water, air dried, and then imaged.

Membranes were blocked using either 5% (w/v) bovine serum albumin (BSA), or 5% (w/v) non-fat milk in Tris-buffered saline with Tween-20 (TBST) for 1 h at room temperature, and then incubated with relevant antibodies overnight. All primary antibodies were diluted to 1:1000 in blocking buffer specific to the application. All antibodies were purchased from Cell Signaling

unless otherwise stated. The following polyclonal antibodies were used: anti-BDNF (SC-546) from Santa Cruz, anti-phospho (Y869, Y873, Y876)-GluA2 (#3921), anti-phosphoY1472-NMDAR2B (#4208), anti-NMDAR2B (#4207). Monoclonal antibodies used included: anti-phosphotyrosine (#05-321X; from Millipore), anti-phosphoS845-GluA1 (#8084), anti-GluA1 (#13185S), anti-GluA2 (#13607). On the following day, membranes were incubated in either rabbit (SC-2004), or mouse (SC-2005) IgG antibodies (1:5000) conjugated to horseradish peroxidase from Santa Cruz and immunoblotted using Luminata Classico, or Crescendo ECL substrate (Millipore) for 2 minutes. Optical densities were captured, normalized to Ponceau staining and analyzed as previously described (Thacker et al., 2016, Appendix I).

3.3.7 Statistics

Based on our sample size, we could not appropriately assume a normalized distribution for samples, and, as such, all sample means were compared using non-parametric statistical analyses in GraphPad Prism™ 7. Specifically, for comparisons where MOD and GXT were not normalized to SED (VO_2 and both ELISAs), or where MOD was compared to GXT (Fig. 2a, b), a Mann-Whitney U test (a distribution-free equivalent of the 2-sample Student`s t-test) was performed. In all other comparisons involving Western blot data where MOD and GXT were normalized to SED, comparisons were made using the Wilcoxon-signed-ranked test (the distribution-free equivalent of the 1-sample Student`s t-test) with a hypothetical value of 1.0 as the comparator. Statistical analyses were considered significant if they achieved a $p < 0.05$. Finally, effect size and 95% confidence intervals were calculated using the ESCI as previously described (Cumming and Finch, 2001).

3.4 RESULTS

3.4.1 Exercise of Varying Intensity Causes a Graded Effect upon VO_2

All of the MOD and GXT rats (with the exception of 1 GXT animal) completed the acclimatization period with minimal (≤ 1) foot shocks, and proceeded on to the exercise portion of the study. Notably, neither the body weight (data not shown), nor the baseline VO_2 measures were significantly different between MOD ($p = 0.79$, $d = 0.43$), or GXT ($p = 0.90$, $d = 0.20$) groups and the SED group. During the 20 minutes of exercise, MOD rats achieved a mean VO_{2Peak} of 75.3 ± 5.7 mL/kg/min, while GXT rats attained a VO_{2Peak} of 81.8 ± 6.5 mL/kg/min within an average time of 26.7 ± 2.5 minutes. Following a single session of exercise, both MOD and GXT animals experienced a significant increase in mean VO_{2Peak} relative to their respective baseline values (MOD: $p = 0.016$, $d = 2.58$; GXT: $p = 0.0313$, $d = 3.63$), whereas the SED group showed no appreciable change (SED: $p = 0.999$, $d = 0.06$) (Figure 3.1). As well, when the raw $VO2_{Peak}$ findings were considered relative to baseline (GXT rats: 199 ± 9.5% of baseline; MOD rats: 159 ± 9.8% of baseline; $p = 0.0303$, $d = 1.73$; Figure 3.2), the normalized data indicate the MOD rats maintained an exercise intensity that was approximately 60% that of the GXT group, which was a primary aim of the protocol.

3.4.2 Exercise Affects the Cellular Level of Tyrosine Phosphorylation in a Region and Intensity Specific Fashion

Since numerous studies have confirmed the importance of tyrosine phosphorylation (pY) to the development of early phase LTP (Barria et al., 1997; Esteban et al., 2003; Hayashi and Huganir, 2004), we aimed to measure the extent to which an acute bout of exercise changed tyrosine phosphorylation across molecular weights known to contain plasticity-related proteins (i.e., GluN2 ≈180 kDa, GluA1-4 ≈100 kDa, Src-Family Kinases ≈50 kDa). Our data illustrate that,

relative to SED, MOD clearly causes a general pY increase in both the sensorimotor cortex (SMCx; $p = 0.01$, $d = 0.89$; Figure 3.3), and the hippocampus (HP; $p = 0.03$, $d = 1.19$; Figure 3.4). Previous reports noted that pY changes of between 30-50% can profoundly affect cellular functioning and survival following ischemic injury in neocortex (Shamloo and Wieloch, 1999), which supports the possibility that the increases in pY we observed following MOD in sensorimotor cortex (125 ± 11%) and hippocampus (131 ± 9%) may be biologically relevant. Unexpectedly, GXT rats did not display an increase in total pY in either SMCx ($p = 0.58$, $d = 0.30$; Figure 3.3), or HP ($p = 0.81$, $d = 0.49$; Figure 3.4).

When tyrosine phosphorylation at molecular weights corresponding with plasticity-related proteins was examined, the SMCx from the MOD group was found to have a significantly greater signal at pY50 ($p = 0.047$, $d = 0.705$), pY100 ($p = 0.016$, $d = 1.54$), and pY180 ($p = 0.016$, $d = 1.23$), compared to the SED group. Although the MOD-related effects in the HP moved in a similar direction, only the change at pY100 ($p = 0.047$, $d = 0.96$) was notable (pY50: $p = 0.11$, $d = 0.77$; pY180: $p = 0.38$, $d = 0.64$). As expected, given the cellular pY results, there were no observable differences at pY50 (SMCx: $p = 0.16$, $d = 0.723$; HP: $p = 0.81$, $d = 0.269$), pY100 (SMCx: $p = 0.99$, $d = 0.027$; HP: $p = 0.47$, $d = 0.42$), and pY180 (SMCx: $p = 0.38$, $d = 0.375$; HP: $p = 0.81$, $d = 0.22$) within GXT animals.

3.4.3 Acute Exercise Selectively Increases GluN2A & GluN2B Subunit Phosphorylation

The NMDAR plays a pivotal role in the induction of LTP, and the phosphorylation state of its subunits influences the receptor's capacity to affect synaptic potentiation (Cheung and Gurd, 2001). In agreement with our earlier data showing that MOD generally increased pY around 180 kDa, which corresponds to the molecular weight of the GluN2 subunits, we observed notable increases in GluN2A (Y1246) (SMCx: 139 ± 20%, $p = 0.031$, $d = 0.81$; HP: 145 ± 21%, $p = 0.09$,

d = 0.90) and GluN2B (Y1472) (SMCx: 170 ± 30%, p = 0.09, d = 0.90; HP: 168 ± 50%, p = 0.31, d = 0.56) compared to SED (Figure 3.5-3.6). As well, phosphorylation following GXT generally reflects the pattern of cellular pY observed earlier. For example, there is no obvious exercise-mediated change in GluN2B (Y1472) phosphorylation in either SMCx (117 ± 13%, p = 0.99, d = 0.53), or HP (117 ± 13%, p = 0.84, d = 0.10). Although GXT does, at first glance, seem to considerably alter GluN2A phosphorylation in both SMCx (161 ± 27%) and HP (143 ± 23%), which disagrees with our cellular pY results, these changes did not reach thresholds for both statistical and practical significance (SMCx: p = 0.09, d = 0.913; HP: p = 0.16, d = 0.77). Taken together, our data indicate the effect of exercise on pY is NMDAR subunit, brain region, and intensity specific. Additionally, these data support the notion that a single session of moderately intense exercise may prime motor regions of the brain via enhanced phosphorylation of GluN2A (Y1246) and GluN2B (Y1472).

3.4.5 Acute Exercise Influences Phosphorylation of GluA1 & GluA2 in a Region-Specific Manner

Extensive work over the past few decades has revealed that AMPAR trafficking is clearly associated with the induction of synaptic plasticity (Scannevin and Huganir, 2000; Song and Huganir, 2002; Huganir and Nicoll, 2013). Furthermore, strong evidence now exists to implicate site-specific changes in phosphorylation as a key mechanism underlying the initiation of subunit-specific migration (Martin et al., 1993; Shi et al., 2001; Hayashi and Huganir, 2004; Anggono and Huganir, 2012). In particular, phosphorylation of GluA2 at Tyr869/873/876 causes receptor internalization, while phosphorylation at Ser845 of GluA1 causes receptor insertion, changes that, taken together, alter the number of Ca^{2+}-permeable AMPARs at synaptic sites. As a result, in our search to locate a plausible explanation for exercise-induced priming, we assessed the

phosphorylation state of GluA1 at Ser845 and GluA2 at Tyr869/873/876. Western blot analysis revealed large increases in S845 GluA1 phosphorylation in SMCx following both MOD (162 ± 14%) and GXT (141 ± 24%) when compared to SED (Figure 3.7), although only the MOD group crossed the threshold for both statistical ($p = 0.031$) and practical significance ($d = 1.87$). In contrast, the HP displayed a notable decrease in GluA1 (S845) phosphorylation following MOD (73 ± 6%, $p = 0.031$, $d = 1.87$), and little difference following GXT (90 ± 11%, $p = 0.94$, $d = 0.38$). In addition to GluA1, SMCx GluA2 (Y869/873/876) phosphorylation was also clearly enhanced following MOD (127 ± 5%, $p = 0.031$, $d = 2.30$), but not GXT (117 ± 22%, $p = 0.99$, $d = 0.32$) (Figure 3.8). A similar pattern was observed in HP for both MOD (152 ± 33%, $p = 0.06$, $d = 0.65$) and GXT (84 ± 10%, $p = 0.16$, $d = 0.69$). Collectively, these data support the possibility that priming through MOD (most clearly in the SMCx) operates by mediating AMPAR receptor phosphorylation in a way that alters their surface expression to favor plasticity.

3.4.6 Moderate-Intensity Acute Exercise Activates PKA, but Suppresses CaMKII

Phosphorylation of AMPAR and NMDAR subunits results from the coordinated interaction of several intracellular cascades, however, substantial evidence exists implicating two kinases as playing a lead role during the induction of short-term plasticity: CaMKII and PKA (Esteban et al., 2003; Lisman et al., 2012; Murphy et al., 2014; Herring and Nicoll, 2016). The activation of either of these kinases independently has been shown to promote plasticity by augmenting both AMPAR and NMDAR synaptic currents (Esteban et al., 2003; Lisman et al., 2012; Murphy et al., 2014; Herring and Nicoll, 2016). Consequently, we assessed the phosphorylation state of both CaMKII (Thr286) and PKA (Thr197) to determine whether acute exercise activated kinases in a non-specific manner, or favored a specific cascade. Immunoblotting analysis revealed robust activation of PKA following MOD in both SMCx (217 ± 53%, $p = 0.02$,

d = 0.90) and HP (229 ± 40%, p = 0.02, d = 1.22); however, this effect was not observed in GXT animals (SMCx: 118 ± 16%, p = 0.30, d = 0.46; HP: 159 ± 44%, p = 0.30, d = 0.51). Furthermore, the influence of exercise on kinase activity was divergent, for MOD animals displayed significantly down-regulated CaMKII (Thr286) activity in both SMCx (74 ± 6%, p = 0.03, d = 1.78) and HP (61 ± 6%, p = 0.06, d = 1.40). Moreover, these effects were not seen in GXT animals (SMCx: 94 ± 10%, p = 0.99, d = 0.46; HP: 94 ± 4%, p = 0.47, d = 0.52). Collectively, our data suggest that a single session of MOD exercise favors PKA signaling, while suppressing CaMKII signaling.

3.4.7 Corticosterone and BDNF Differ in their Release Pattern Following Aerobic Exercise

The positive effects on neuroplasticity that follow brief physical and psychological stress are well established (McEwen, 2009). Strong evidence from rodent models implicates circulating corticosterone levels as responsible for the swift upregulation of phosphorylation in the hippocampus after acute physical stressors (Karst et al., 2005). However, studies investigating acute aerobic exercise in humans often argue that the enhanced release of BDNF is the primary mediator of its beneficial effects (Vaynman, 2005; Ding et al., 2011). Therefore, we investigated whether rats in our study had elevated levels of either BDNF, or corticosterone to determine whether these may help account for the rise in phosphorylation observed.

Although conflicting results exist, there is general agreement that a single session of moderate to high-intensity exercise, or endurance exercise lasting longer than an hour, will produce a surge in serum levels of mature BDNF (mBDNF) in humans that remain elevated for a period of time following exercise cessation (Rasmussen et al., 2009). As a result, we tested whether our exercise paradigms would cause an increase in the mBDNF release into the circulation. Compared

to SED, neither MOD ($p = 0.59$, $d = 0.30$), nor GXT ($p = 0.79$, $d = 0.13$) rats displayed an observable increase in serum mBDNF immediately following the cessation of exercise (Figure 3.13). Since mBDNF can be released peripherally in response to exercise and centrally in response to neural activity, we next decided to assess mBDNF expression within both HP and SMCx. Our Western blot analysis revealed a clear increase in mBDNF protein within SMCx ($p = 0.03$, $d = 1.70$) after MOD, but not GXT ($p = 0.31$, $d = 0.62$); notably, no change was observed in the HP regardless of exercise intensity (MOD: $p = 0.94$, $d = 0.09$; GXT: $p = 0.94$, $d = 0.11$) (Figure 3.11-3.12).

Since increases in synaptic activity can alter the conversion of proBDNF to mBDNF in hippocampal cultures (Lu et al., 2005; Nagappan et al., 2009), and the conversion from pro to mBDNF is related to cleavage by tissue plasminogen activator (which is elevated following acute exercise; Chandler et al., 1992; Pang et al., 2004), we considered the possibility that exercise may increase mBDNF by enhancing the conversion of pro-BDNF to mBDNF, instead of through upregulating transcription and translation. We tested whether exercise enhanced the mBDNF/proBDNF ratio, which has recently been used as a proxy for conversion rate (Cao et al., 2014). We observed a large increase in mBDNF/proBDNF ratio for MOD ($p = 0.094$, $d = 0.85$) and a large decrease in GXT ($p = 0.094$, $d = 1.02$) in SMCx, although neither change crossed both the required statistical and practical thresholds.

Corticosterone is the predominant glucocorticoid in rodents, and is elevated following either acute, or chronic exposure to environmental stress (Sapolsky et al., 2000). In addition to their well-characterized genomic effects, growing support exists for non-genomic, rapid actions of glucocorticoids, and one of these is as a potent modulator of plasticity(Groeneweg et al., 2011). We observed a dramatic 10-fold increase in serum corticosterone of both MOD ($p = 0.0022$, $d =$

5.77) and GXT ($p = 0.0022$, $d = 3.15$) animals, with no significant differences observed between MOD and GXT animals ($p = 0.70$, $d = 0.078$) (3.14).

3.5 DISCUSSION

Alterations in cortical excitability following a single session of moderate aerobic exercise are conducive to the improved acquisition of a novel motor skill in humans. The use of exercise to improve skill acquisition has the potential to complement a number of contemporary movement rehabilitation therapies, fueling a growing interest to understand the underlying biochemical mechanisms. Herein, we present a novel mechanism by which a single session of aerobic exercise may prime SMCx by altering the phosphorylation signaling cascades that guide the biophysical and trafficking properties of AMPA and NMDA receptors. Specifically, we display a relationship between exercise and the level of AMPA and NMDA receptor phosphorylation that is dependent on both its intensity and the brain region examined (SMCx vs. HP).

3.5.1 Influence of Exercise on BDNF and Corticosterone in SMCx and HP

A single session of aerobic exercise has long been recognized to modulate the global release of neurotransmitters in the brain (Meeusen and Meirleir, 1995; Meeusen et al., 2001). In addition, the increased presence of neuroactive molecules such as corticosterone and BDNF in serum, during and after exercise supports the notion that exercise modulates brain activity globally. The current study noted acute exercise influences tyrosine phosphorylation of plasticity-related proteins in the same direction, but to varying degrees between HP and SMCx, which may reflect both shared a and tissue-specific effect following exercise. The change in magnitude of post-exercise effects may be related to the type of exercise in the given experiment. In particular, whereas exercise requires the continued recruitment of motor neurons within SMCx to maintain movement, treadmill running within an enclosure (the model used in our study) may not actively

engage hippocampal circuitry to the same extent. In other words, the SMCx may be regarded as an active contributor during treadmill exercise, while the HP may be considered as playing a secondary role, which may contribute to the disparity in phosphorylation magnitude observed between the tissues. Our hypothesis is supported by our data displaying the limited change in mBDNF within HP compared to SMCx, as mBDNF is thought to undergo synaptic translation, proteolytic cleavage, and release in response to increased neuronal activity (Lu, 2003). Thus, brain regions that are actively engaged during the course of the exercise may be more likely primed due to an increased release of mBDNF centrally. Interestingly, the forced-treadmill protocols were not able to augment the release of mBDNF peripherally, which a number of studies support (Ferris et al., 2007; Rasmussen et al., 2009; Rojas Vega et al., 2012; Piepmeier and Etnier, 2015). However, these studies have been exclusively conducted in humans, and although chronic exercise augments BDNF transcription and expression within the rodent brain (Gómez-Pinilla et al., 2002; Molteni et al., 2002), we are not aware of any other studies that assess rat serum mBDNF immediately following a single event of exercise. Peripheral mBDNF may not have increased in our study due to the stressful nature of the forced-treadmill exercise in contrast to other forms such as voluntary wheel running , or related to our sampling time immediately after exercise, although others suggest serum mBDNF peaks immediately after exercise in humans (Tang et al., 2008; Rojas Vega et al., 2012). Finally, these results may simply indicate that acute exercise-induced release of mBDNF peripherally is specific to humans, as we did not observe mBDNF differences following either exercise group, however, more data is needed to determine this hypothesis.

Alternatively, the current exercise protocol can be considered as a form of physical stress, and, as such, we would expect a steep rise in serum corticosterone, which we observed (≈20-fold increase in both MOD and GXT). Depending on its characteristics (e.g. type, intensity, and

duration), acute stress can either facilitate, or inhibit the threshold for plasticity and HP-dependent learning (de Kloet et al., 1999). Based on the finding that the HP shows altered phosphorylation similar to SMCx but not significantly compared to SED, it is possible the MOD exercise dose was not optimal to consistently elicit these responses. Previous reports using forced-swim consistently show a rise in tyrosine phosphorylation of intracellular cascade pathways in both HP and neocortex, although the effect is far greater in neocortex than HP (Shen et al., 2004). Forced-swim is a task that has previously been shown to increase mitogen-activated protein kinase (MAPK) phosphorylation (Shen et al., 2004), and alters local circuitry activity within HP (Yarom et al., 2008), which reinforces the notion that exercise-induced priming may be greatest in brain regions activated during exercise. Taken together, our findings show MOD exercise more consistently effects SMCx compared to HP, which may be due to a convergence of corticosterone and mBDNF pathways not present in HP.

3.5.2 Phosphorylation as a Basis for Exercise-Induced Priming

During the early phases of LTP induction, the activity of Src-family kinases is markedly increased, leading to a large increase in protein tyrosine phosphorylation (Wang and Salter, 1994). Notably, Src-family kinases specifically target phosphorylation sites of the glutamatergic receptors, NMDAR GluN2 subunits (≈180 kDa) and AMPAR subunits (≈100 kDa), as well as signaling cascade intermediaries, such as CaMKII and PKA (50 kDa), are well characterized to be sufficient for the induction of LTP (Hayashi et al., 2000; Soderling and Derkach, 2000; Zheng and Keifer, 2009; Lisman et al., 2012; Huang and Hsu, 2014). In particular, tyrosine phosphorylation sites have been repeatedly demonstrated to be one of the most important mediators of signal transduction and regulation, and are implicated heavily in CNS processes such as development and learning, as well as processes that follow injury (Cudmore and Gurd, 1989; Shamloo and

Wieloch, 1999; Hunter, 2010). Arguably, total pY can represent one way to assess the relative "state" of intracellular activity that may reflect a biochemical signature for priming.

The current study reveals that a single session of aerobic exercise increases regional total cellular pY in an intensity-dependent manner. Specifically, MOD exercise uniquely augments total pY in SMCx and HP, whereas pY differences were not observed following GXT. The difference may be attributed to the distinct physiological state the animals achieve by the point of exercise cessation, with GXT animals reaching a point of exhaustion where MOD do not. Since exhaustion is often associated with a depletion of ATP and Ca^{2+}-dysregulation in muscle (Allen et al., 2008, 2018), a similar process may occur in the brain. With this in mind, it can be hypothesized that the increased level of phosphorylation observed during sub-exhaustive exercise (MOD) may fail to be maintained under higher intensities or may reflect a marked increase in phosphatase activity not present under lower intensities (Otmakhova et al., 2000; Winder and Sweatt, 2001), however, these mechanisms remained to be explored. The lack of difference between observed GXT total pY with SED might also represent a neuroprotective mechanism against excessive neuronal excitation that would be required to maintain such high-intensity exercise and signify a possible marker of central fatigue. The notion that phosphorylation might, be a marker of central fatigue has yet to be explored. Nonetheless, the combined MOD, GXT data are in support of a common thread of hypotheses suggesting aerobic exercise intensity obeys an inverted-U relationship with cognitive performance (Kamijo et al., 2004b, 2007; Lambourne and Tomporowski, 2010). In addition to cellular pY, we determined augmented tyrosine phosphorylation at three specific molecular weights that correspond with a number of plasticity-related proteins.

3.5.3 Kinase Phosphorylation and Exercise-Induced Priming

We observed a significant increase in tyrosine phosphorylation of proteins surrounding the 50 kDa molecular weight band, a site representing a majority of kinases. Previous reports suggest the activity of kinases, specifically PKA and CaMKII, can independently sponsor the induction of LTP (Giese et al., 1998; Huang and Kandel, 1998; Hayashi et al., 2000; Lisman et al., 2002; Yang et al., 2011; Kim et al., 2016; Luo et al., 2017). Moreover, both PKA and CaMKII phosphorylation can be regulated by the exogenous application of either mBDNF (via tropomyosin receptor kinase B) (Guo et al., 2014; Itoh et al., 2016a), or corticosterone (via GPCR activated adenylate cyclase) (Chen et al., 2012; Whitehead et al., 2013; Guo et al., 2014; Luo et al., 2017), indicating they may also be modulated by exercise. Our Western blot data support a robust ≈200% increase in pPKA (Thr197) signal and suppression of roughly 25-30% of pCaMKII (Thr286) following MOD, but not GXT. Both of these effects were remarkably consistent across SMCx and HP, suggesting a conserved level of kinase activity following acute exercise. Previous reports have linked PKA activation to the site-specific phosphorylation of Ser845 of GluA1 resulting in its migration towards, and incorporation into peri-synaptic membranes (Shi et al., 2001; Bredt and Nicholl, 2003; Henley et al., 2012). Additional data support increased PKA activity is critical for acute stress-induced priming of LTP (Whitehead et al., 2013). Therefore, it is likely that exercise achieves a similar pattern of priming via increased pPKA (Thr197) in the present study.

However, the suppression of pCaMKII (Thr286) is not as easily explained in the context of priming, as pCaMKII (Thr286) investigations have been limited to observations following LTP induction. During LTP, pCaMKII (Thr286) autophosphorylates in response to levels of NMDAR-dependent Ca^{2+} release and activation of Ca^{2+}-calmodulin (Lisman et al., 2012). The activation of pCaMKII (Thr286) promotes the migration of CaMKII towards synapses where it phosphorylates

various sites on the NMDAR (Soderling and Derkach, 2000; Lisman et al., 2002, 2012). The continued binding of CaMKII is crucial for the potentiation of the synapse to be maintained, as it is believed to be a foundational component of AMPA-receptor anchoring assemblies (Lisman et al., 2002). However, CaMKII's occupancy at the synaptic surface is dependent on the continued presence of high levels of Ca^{2+}, as depleting these levels activates NMDAR-associated protein phosphate 1 (PP1) via a PKA dependent mechanism, resulting in the dephosphorylation and dissociation of CaMKII from NMDARs, while NMDAR phosphorylation is presumably sustained (Soderling and Derkach, 2000). Although CaMKII has not been yet associated with priming, we hypothesize that the suppression of CaMKII (Thr286) signal following MOD exercise may reflect priming at this final stage. For example, exercise may activate pCaMKII (Thr286) independently of LTP through either mBDNF or corticosterone (Chen et al., 2012), resulting in the subsequent migration to and incorporation with NMDAR, whereby CaMKII phosphorylates NMDAR subunits. However, the presence of CaMKII in this state is temporary as PP1 activation is likely under conditions lacking NMDAR-dependent Ca^{2+} and high levels of pPKA (Thr196), resulting in CaMKII (Thr286) dephosphorylation (Colbran, 2004) (See Figure 3.16). The overcompensation in dephosphorylation below baseline observed following MOD, might be accounted for through the robust pPKA activation present in the study and signify a buffer protecting primed synapses from spontaneous LTP, which acts to conserve the specificity of activity-dependent synaptic plasticity. Therefore, it is plausible that an increase in pPKA and a decrease of pCaMKII may result in downstream changes of NMDARs and AMPARs indicative of a primed state.

3.5.4 AMPAR Phosphorylation and Exercise-Induced Priming

We assessed the relative phosphorylation state of pY at the 100 kDa molecular weight band and noted significant increases in phosphorylation, particularly in the SMCx. The band

corresponds with AMPAR subunits integral to the induction of synaptic plasticity. During early phases of LTP GluA2-containing AMPARs are preferentially internalized and replaced with GluA2-lacking AMPARs, a process believed to be accompanied by an increase in phosphorylation of GluA2 (Tyr869/873/876), resulting in internalization, and GluA1 (Ser845), causing membrane insertion (Ehlers, 2000; Collingridge et al., 20005; Shi et al., 2001; Roth et al., 2017). Furthermore, previous data support that acute stress can alter the relative cell surface expression of GluA1-containing AMPARs in a PKA-dependent manner (Whitehead et al., 2013). The present study observed a significant increase in GluA1 (Ser845) and GluA2 (Tyr869/873/876) levels following MOD exercise in SMCx. However, in HP, GluA2 (Tyr869/873/876) is present, but GluA1 (Ser845) was significantly decreased after MOD. These results suggest that exercise may augment the induction of LTP (that is, priming) through altering the surface expression of GluA1 extrasynaptically and GluA2 synaptically, ultimately priming synapses by promoting GluA1/GluA2 substitution (Oh et al., 2006a; Derkach et al., 2007).

With regards to the HP, the combination of decreased pGluA1 (Ser845) and increased pGluA2 (Tyr869/873/876) is suggestive that HP may favor long-term depression (LTD). Previous reports support these conditions are indicative of internalization and subsequent degradation of both receptors by lysosomes (Holman et al., 2007; Fernandez-Monreal et al., 2012). Considering the consistency of data between HP and SMCx with regards to CaMKII and PKA signaling, it is not clear why MOD exercise may favor LTP in SMCx and LTD in HP. One explanation may be linked to the heterogeneity between the tissues. For example, HP expresses 3-5x more mineralocorticoid and glucocorticoid receptors (Reul and De Kloet, 1985; Morimoto et al., 1996; Patel et al., 2001) and more readily absorbs circulating cortisol compared to cortex (McEwen et al., 1969), features which have been shown to increase the susceptibility of this region to stress

and stress-induced priming (McEwen, 1999; Groc et al., 2008a; Mikasova et al., 2017). Moreover, the dose to which acute corticosterone is administered can lead to divergent effects on learning and plasticity-related induction (Sandi and Pinelo-nava, 2007). It stands to reason that the high levels of corticosterone release displayed by exercising animals in this study surpass the threshold for priming LTP within HP, and instead promotes LTD. This hypothesis is supported by a number of studies showing impaired memory recall and reduced LTP following high dose peripheral corticosterone administration in rats (Pavlides et al., 1993; de Quervain et al., 1998). Follow-up studies suggest that under high doses of peripheral corticosterone HP is more likely to undergo LTD, related to MR and GR suppression of glutamate reuptake, producing synaptic spillover and the activation of specifically GluN2B-containing NMDARs, in turn promoting the internalization of GluA2-containing AMPARs (Sandi and Pinelo-nava, 2007; Sandi, 2011). Overall, MOD exercise appears to cause cellular changes that would be expected to promote plasticity within both the HP and SMCx albeit in different directions.

3.5.5 NMDAR Phosphorylation and Exercise-Induced Priming

Finally, we evaluated the relative phosphorylation of pY at 180 kDa and determined increased signaling in SMCx following MOD, which corresponds to the molecular weight of the NMDAR subunits GluN2A and GluN2B. Overwhelming agreement exists that NMDARs are the both necessary, and sufficient for neuronal plasticity, capable of translating complex patterns of neuronal activity into long-term changes in synaptic morphology and function (Paoletti et al., 2013). Moreover, the phosphorylation status of GluN2-containing NMDARs is strongly associated with the relative level of plasticity induction (Takasu et al., 2002; Salter and Kalia, 2004; Wang et al., 2014; Sun et al., 2018). We discovered a general increase in phosphorylation following both exercise intensities corresponding to GluN2A (Tyr1246), whereas GluN2B (Tyr1472) signaling

was selectively increased following only MOD, however, these effects were both found to be similar in magnitude in both HP and SMCx. Thus, exercise may prime plasticity by an increased NMDAR phosphorylation likely through the recruitment of Src family kinases, such as Fyn and Src, whose activity is regulated by BDNF-TrkB (Yamada and Nabeshima, 2003; Itoh et al., 2016b) and corticosterone-MR (Yang et al., 2013), respectively. The activation of GluN2A and GluN2B produces a diversity of function which is dependent on the unique differences between their C-terminal domain and subcellular localization. Specifically, in the adult brain GluN2A is believed to be located synaptically and sponsor LTP, whereas GluN2B promotes LTD and positioned extrasynaptically (Tovar and Westbrook, 2002; Massey, 2004; Foster et al., 2010), although there are some conflicting reports displaying contributions of both GluN2A/B to LTP/LTD (Zhao et al., 2005; Fox et al., 2007). Priming may be directly related to both GluN2A (Tyr1246) and GluN2B (Tyr1472) phosphorylation as these sites are responsible for potentiating Ca^{2+} flux through NMDAR (Takasu et al., 2002). Additionally, tyrosine phosphorylation of both GluN2A and GluN2B has been linked to the trafficking, stabilization and surface expression of NMDARs (Vissel et al., 2001; Wenthold et al., 2003; Prybylowski et al., 2005; Lau and Zukin, 2007). Thus, exercise may, in a similar fashion as AMPARs, provide the conditions to upregulate the activity, and quantity of NMDARs at the neuronal surface. Together, the data presented here support that a single session of MOD exercise produces a favorable environment for plasticity in general (including LTP and LTD).

3.6 CONCLUSIONS

There are a growing number of studies attempting to exploit the priming benefits of single session aerobic exercise to alter the receptivity of motor regions to traditional learning paradigms. To date, there are limited data that support the identity of the mechanism connecting single session exercise and the priming of a subsequent learning event. Our data support that moderately intense exercise upregulates the phosphorylation state of a number of proteins vital to the induction of plasticity. We argue that this set of phosphorylation conditions provides evidence for a biochemical signature responsible for exercise-induced priming (Figure 3.15). Specifically, the convergence of an activity-dependent central release of mBDNF combined with the robust peripheral release in corticosterone yields a positive influence over intracellular cascade activation. Notably, kinase-specific activation (↑PKA, ↓CaMKII) leads to increases in NMDAR and AMPAR phosphorylation, that may provide a basis for which proceeding use-dependent plasticity will be more favorably received. It remains unclear whether priming is restricted to phosphorylation changes or also reflects changes in NMDAR and AMPAR surface expression. Finally, it remains to be investigated whether the phosphorylation conditions of this nature result in augmented learning.

FIGURE LEGENDS

Figure 3.1 Average baseline and VO2Peak following rest, or acute exercise (SED, N = 6; MOD, N = 6; GXT, N = 5). * denotes significant difference ($p < 0.01$) from baseline VO2 within treatment.

Figure 3.2 Mean Peak VO2 as a percentage of baseline following a single session of either rest (SED, N = 6), or acute exercise (MOD, N = 6; GXT, N = 5). * and # denote a significant difference ($p < 0.05$) from SED and MOD, respectively.

Figure 3.3 Tyrosine phosphorylation of all proteins and those at molecular weights corresponding to specific NMDAR subunits (pY180), AMPAR subunits (pY100), and src-family kinases (pY50) within sensorimotor cortex (SMCx) after MOD (n = 7) and GXT (n = 7) treatment. * Denotes statistical significance ($p < 0.05$) following comparison with SED.

Figure 3.4 Tyrosine phosphorylation of all proteins and those at molecular weights corresponding to specific NMDAR subunits (pY180), AMPAR subunits (pY100), and src-family kinases (pY50) within hippocampus (HP) after MOD (n = 7) and GXT (n = 7) treatment. * Denotes statistical significance ($p < 0.05$) following comparison with SED.

Figure 3.5 Y1246 phosphorylation site of the NMDAR subunit GluN2A in sensorimotor cortex (n = 6/group) and hippocampus (n = 6/group). Each MOD and GXT sample pGluN2A optical density is taken as a ratio of total GluN2A and displayed relative to SED pGluN2A/GluN2A. * denotes statistical significance ($p < 0.05$).

Figure 3.6 Y1472 phosphorylation site of the NMDAR subunit GluN2B in sensorimotor cortex (n = 6/group) and hippocampus (n = 6/group). Each MOD and GXT sample pGluN2B optical density is taken as a ratio of total GluN2A and displayed relative to SED pGluN2B/GluN2B. * denotes statistical significance ($p < 0.05$).

Figure 3.7 S845 phosphorylation site of the AMPAR subunit GluA1 in sensorimotor cortex (n = 6/group) and hippocampus (n = 6/group). Each MOD and GXT sample pGluA1 optical density is taken as a ratio of total GluA1 and displayed relative to SED pGluA1/GluA1. * denotes statistical significance ($p < 0.05$).

Figure 3.8 Tyrosine (Y869,Y873,Y876) phosphorylation of the AMPAR subunit GluA2 in sensorimotor cortex (n = 6/group) and hippocampus (n = 6/group). Each MOD and GXT sample pGluA2 optical density is taken as a ratio of total GluA2 and displayed relative to SED pGluA2/GluA2. * denotes statistical significance ($p < 0.05$).

Figure 3.9 T286 phosphorylation site of CaMKII in sensorimotor cortex (n = 6/group) and hippocampus (n = 4/group). Each MOD and GXT sample pCaMKII optical density is taken as a ratio of total CaMKII and displayed relative to SED pCaMKII/CaMKII. * denotes statistical significance ($p < 0.05$).

Figure 3.10 T197 phosphorylation site of PKA in sensorimotor cortex (n = 7/group) and hippocampus (n = 7/group). Each MOD and GXT sample pPKA optical density is taken as a ratio

of total PKA and displayed relative to SED pPKA/PKA. * denotes statistical significance ($p < 0.05$), while † denotes $p = 0.06$.

Figure 3.11 Comparison of optical densities for proBDNF, mBDNF and mBDNF/proBDNF conversion in sensorimotor cortex (n = 7/group). Each MOD and GXT sample optical density is taken as a ratio of whole lane ponceau and displayed relative to SED mBDNF/Ponceau. * denotes statistical significance ($p < 0.05$).

Figure 3.12 Comparison of optical densities for proBDNF, mBDNF and mBDNF/proBDNF conversion in hippocampus (n = 7/group). Each MOD and GXT sample optical density is taken as a ratio of whole lane ponceau and displayed relative to SED mBDNF/Ponceau. * denotes statistical significance ($p < 0.05$).

Figure 3.13 Comparison of levels of mBDNF following SED (n = 6), MOD (n = 6), or GXT (n = 5) treatment. Results are expressed as mean BDNF concentration ± SEM in pg/mL obtained from serum.

Figure 3.14 Comparison of levels of corticosterone following SED (n = 6), MOD (n = 6), or GXT (n = 5) treatment. Results are expressed as mean corticosterone concentration ± SEM in ng/mL obtained from serum.

Figure 3.15 Multiple mechanisms by which exercise might enhance post-synaptic plasticity in SMCx. Exercise results in an increased synaptic activity resulting in a presynaptic release of BDNF. BDNF via its receptor TrkB causes Fyn-mediated phosphorylation of GluN2 subunits both synoptically (GluN2A) and extrasynaptically (GluN2B). TrkB activation also recruits the second messenger system PLCγ1, resulting in the increased activity of PKC. PKC has the dual capacity to phosphorylate GluA1 subunits and CaMKII which together results in the vesicular migration and insertion into the perisynaptic membrane. Unknown (?) components of this model include how TrkB may mediate GluA2 phosphorylation and whether Trkb activation results in an increase GluA1 at postsynaptic densities. An alternative model is related to the spiked response of peripheral corticosterone resulting from exercise. CORT rapidly perfuses the blood-brain barrier where it can, under a concentration-gradient specificity, activate membrane-bound MRs. MR has the capacity to activate SFKs such as SRC that are known to upregulate the phosphorylation and Ca2+ conductance of GluN2-containing NMDARs. Moreover, SRC has been shown to mediate GluA2 phosphorylation resulting in an internalization of surface GluA2-containing AMPARs. Furthermore, MR activation modulates GPCR activity resulting in the increased activity of adenylyl cyclase, increasing the local levels of cAMP. Increased cAMP acts as a second messenger activator of PKA which is known to be critical for the phosphorylation, vesicular migration and perisynaptic insertion of GluA1.

Figure 3.16 Sequential mechanism through which CaMKII can act as an LTP-independent primer. Activation of CaMKII at T286 by the temporal release of intracellular Ca2+ or PKC-mediated activation results in CaMKII accumulation around post-synaptic densities, PP1 remains dormant. In particular, pCaMKII form associations with GluN2-containing NMDARs where they phosphorylate GluN2 at various sites. Under conditions of low post-synaptic densities and high

PKA activation, PP1 phosphatase dephosphorylates CaMKII at T286, causing it to dissociate from the GluN2 complex, leaving behind the phosphorylated GluN2.

Figure 3.1

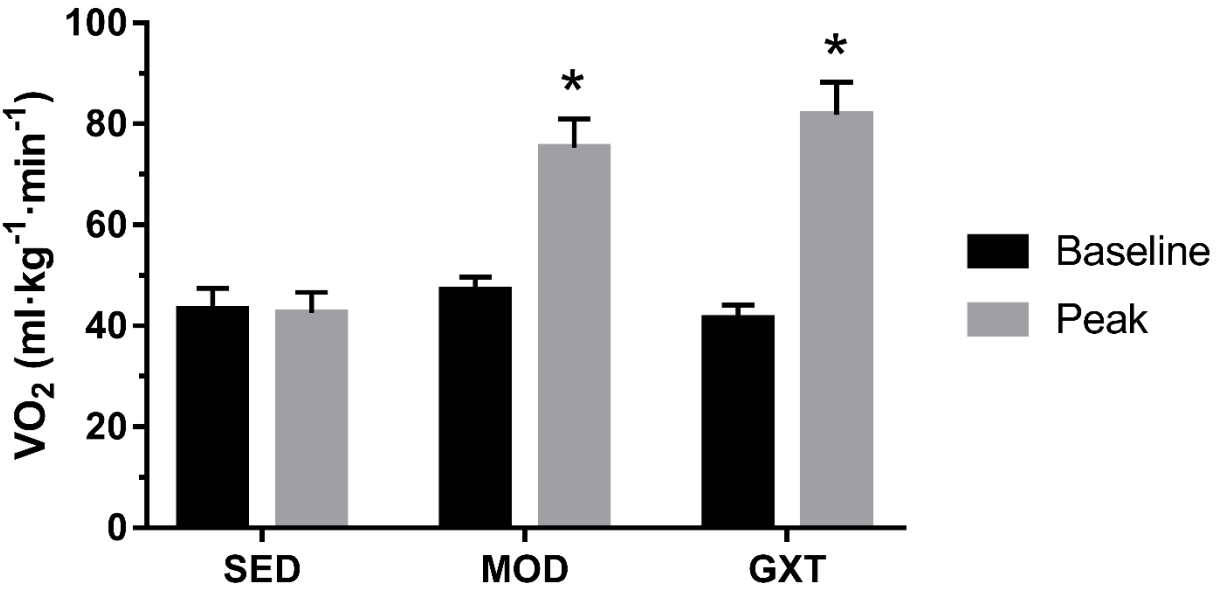

Figure 3.2

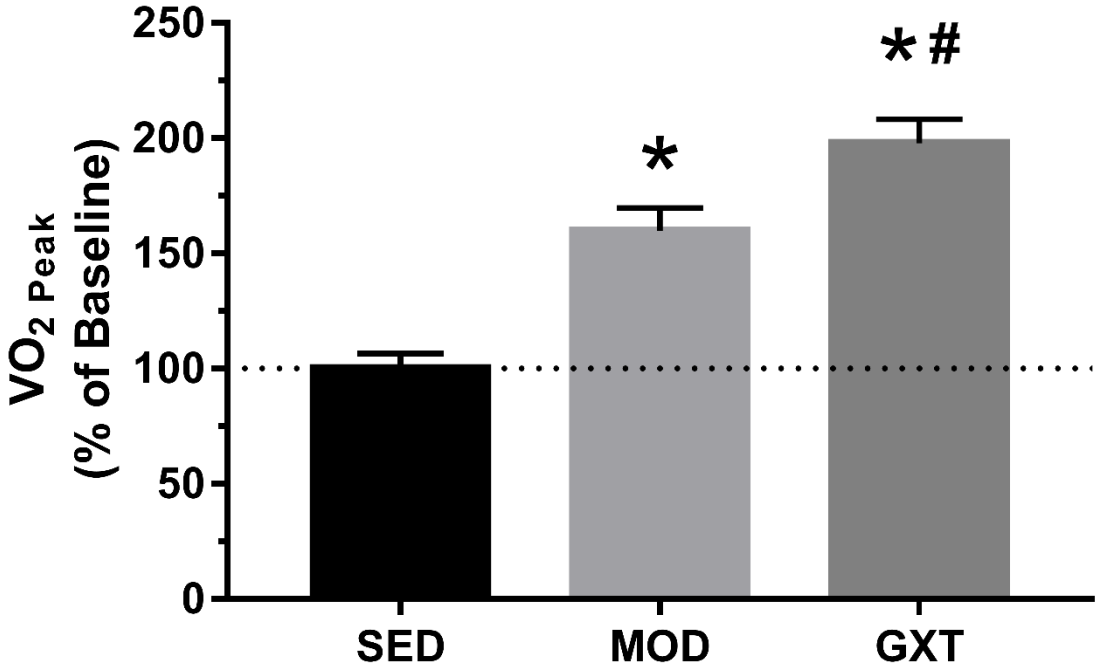

Figure 3.3

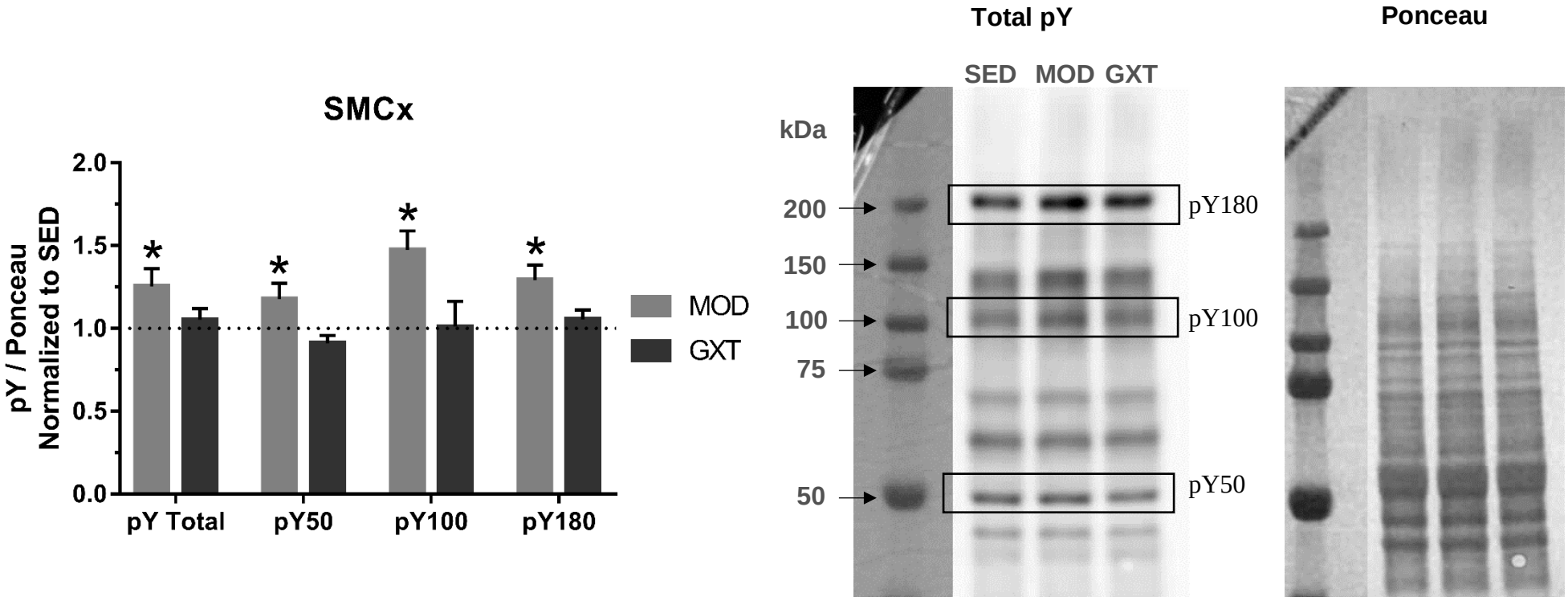
SMCx
pY / Ponceau
Normalized to SED
2.0
1.5
1.0
0.5
0.0
pY Total
pY50
pY100
pY180
MOD
GXT
Total pY
Ponceau
SED MOD GXT
kDa
200
150
100
75
50
pY180
pY100
pY50

Figure 3.4

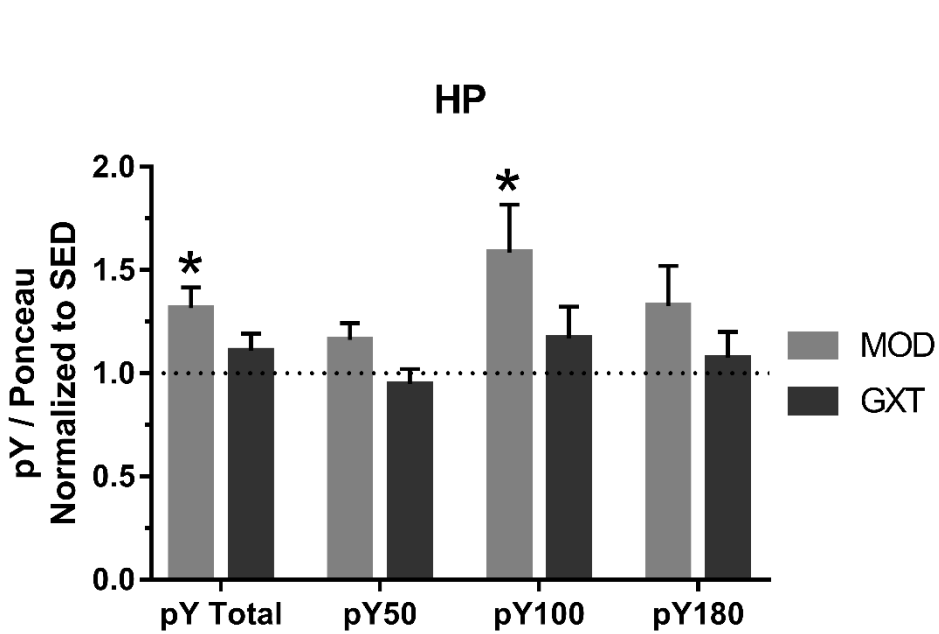
HP
pY / Ponceau
Normalized to SED
2.0
1.5
1.0
0.5
0.0
*
*
pY Total
pY50
pY100
pY180
MOD
GXT

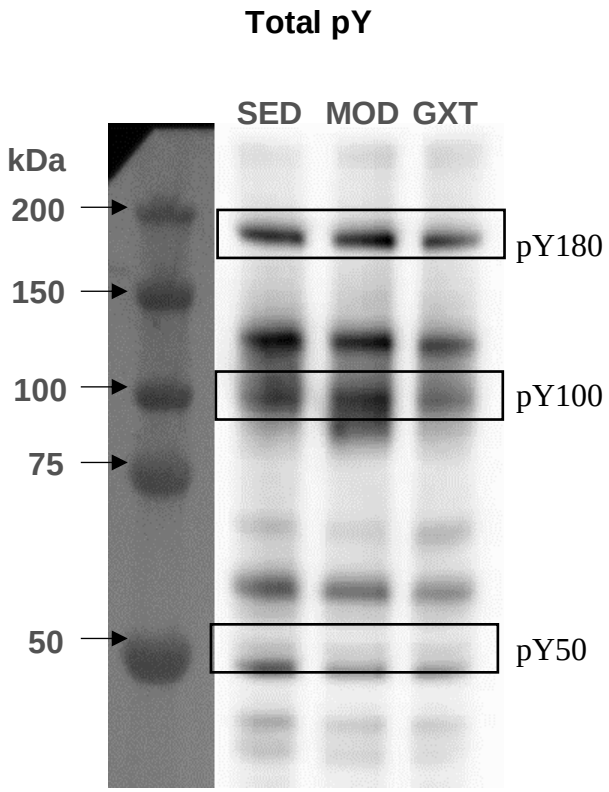
Total pY
SED
MOD
GXT
kDa
200
150
100
75
50
pY180
pY100
pY50

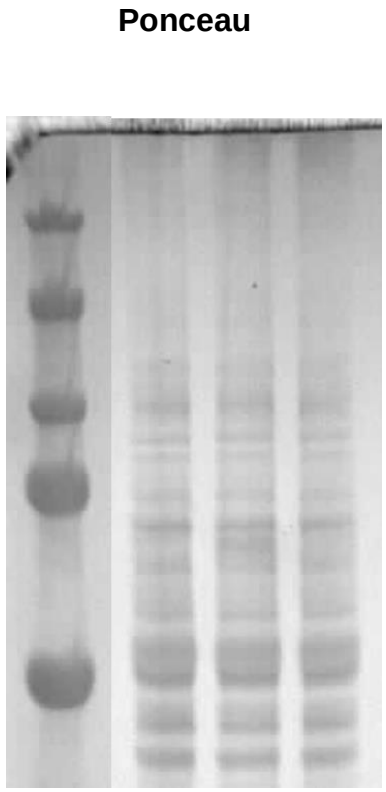
Ponceau

Figure 3.5

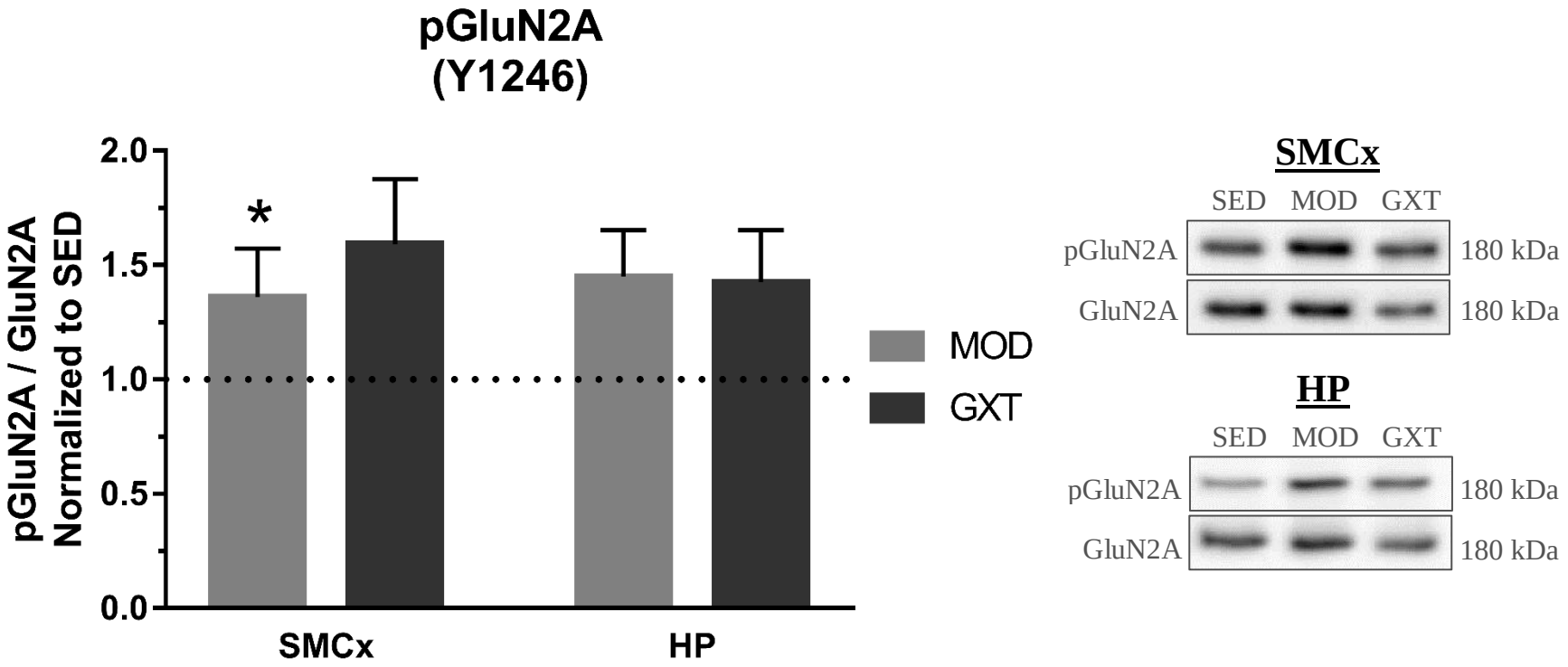
pGluN2A
(Y1246)
pGluN2A / GluN2A
Normalized to SED
2.0
1.5
1.0
0.5
0.0
*
SMCx
HP
MOD
GXT
SMCx
SED MOD GXT
pGluN2A
180 kDa
GluN2A
180 kDa
HP
SED MOD GXT
pGluN2A
180 kDa
GluN2A
180 kDa

Figure 3.6

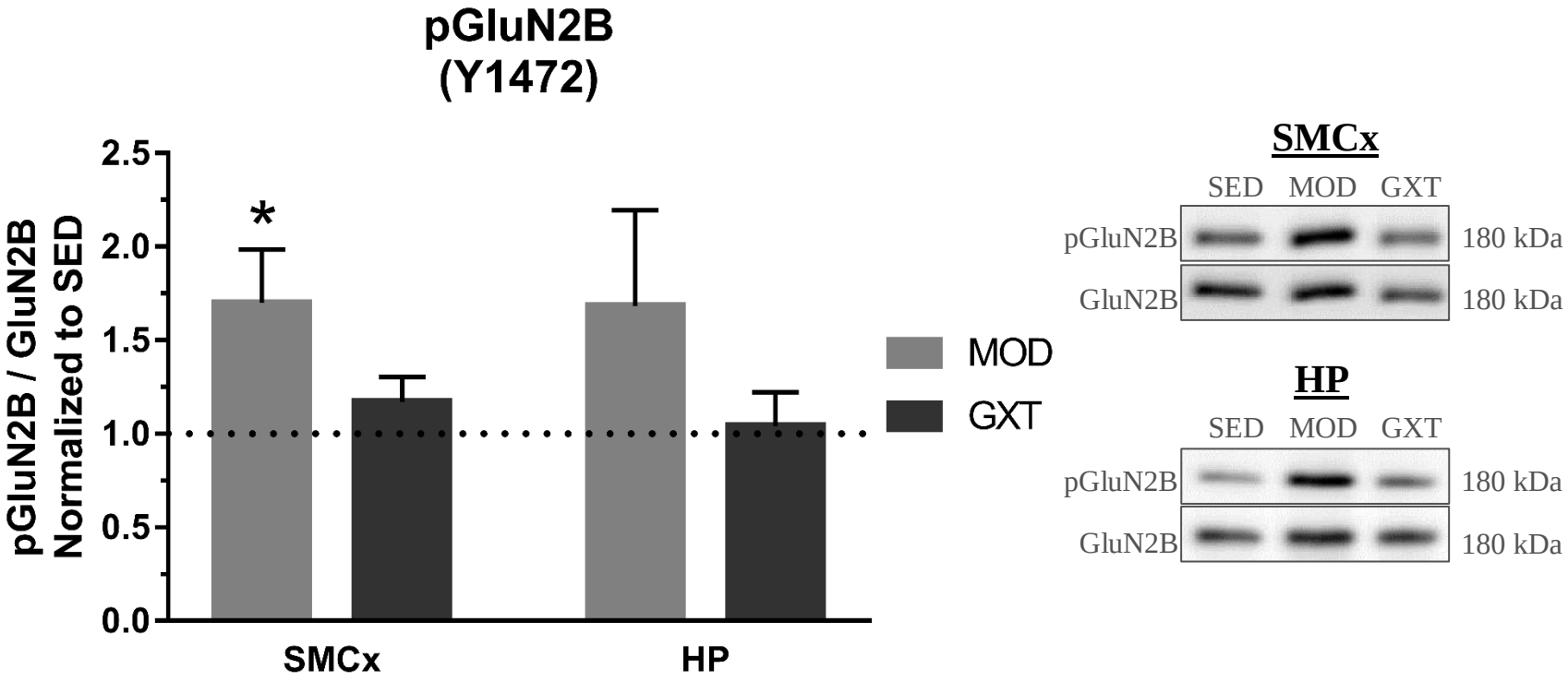
pGluN2B
(Y1472)
pGluN2B / GluN2B
Normalized to SED
2.5
2.0
1.5
1.0
0.5
0.0
*
SMCx
HP
MOD
GXT
SMCx
SED MOD GXT
pGluN2B
180 kDa
GluN2B
180 kDa
HP
SED MOD GXT
pGluN2B
180 kDa
GluN2B
180 kDa

Figure 3.7

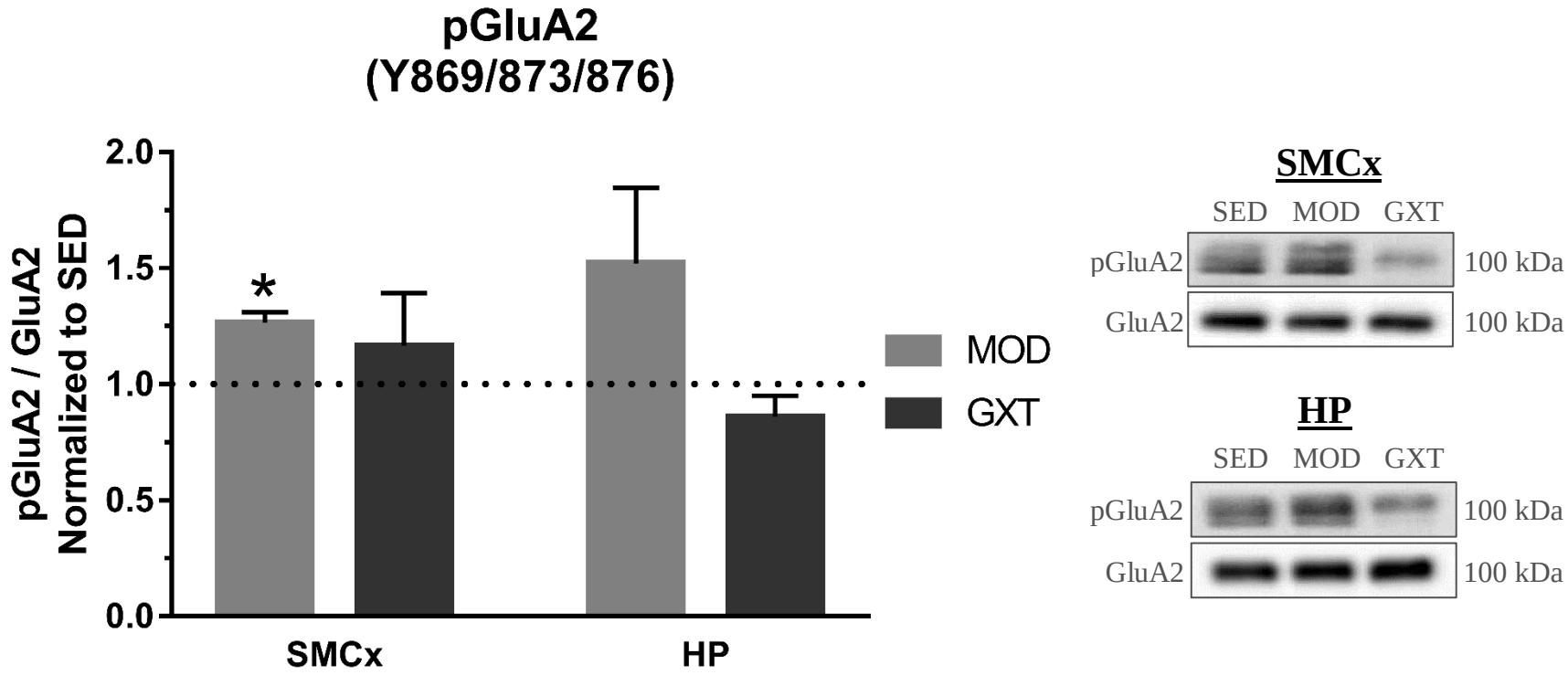
pGluA2
(Y869/873/876)
pGluA2 / GluA2
Normalized to SED
2.0
1.5
1.0
0.5
0.0
*
SMCx
HP
MOD
GXT
SMCx
SED MOD GXT
pGluA2
100 kDa
GluA2
100 kDa
HP
SED MOD GXT
pGluA2
100 kDa
GluA2
100 kDa

Figure 3.8

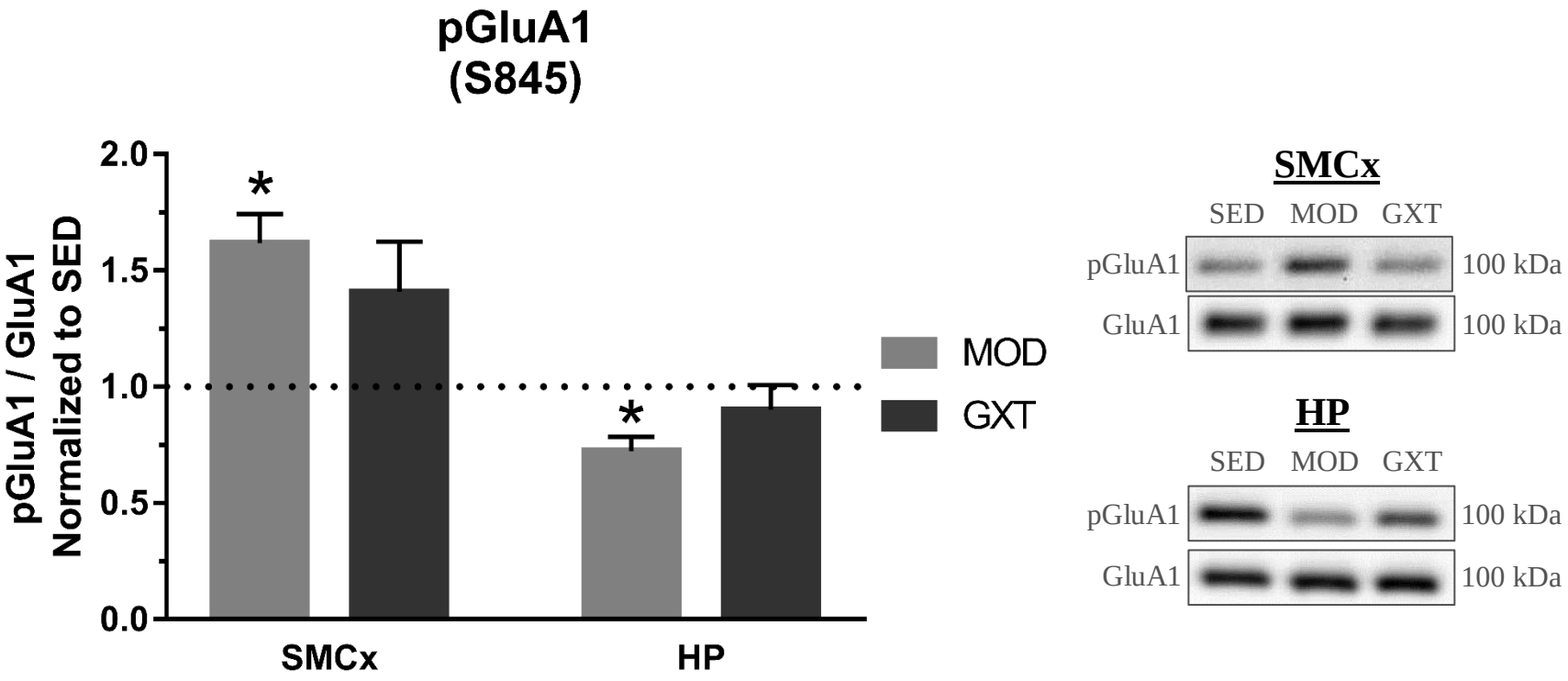
pGluA1
(S845)
pGluA1 / GluA1
Normalized to SED
2.0
1.5
1.0
0.5
0.0
*
*
SMCx
HP
MOD
GXT
SMCx
SED MOD GXT
pGluA1
100 kDa
GluA1
100 kDa
HP
SED MOD GXT
pGluA1
100 kDa
GluA1
100 kDa

Figure 3.9

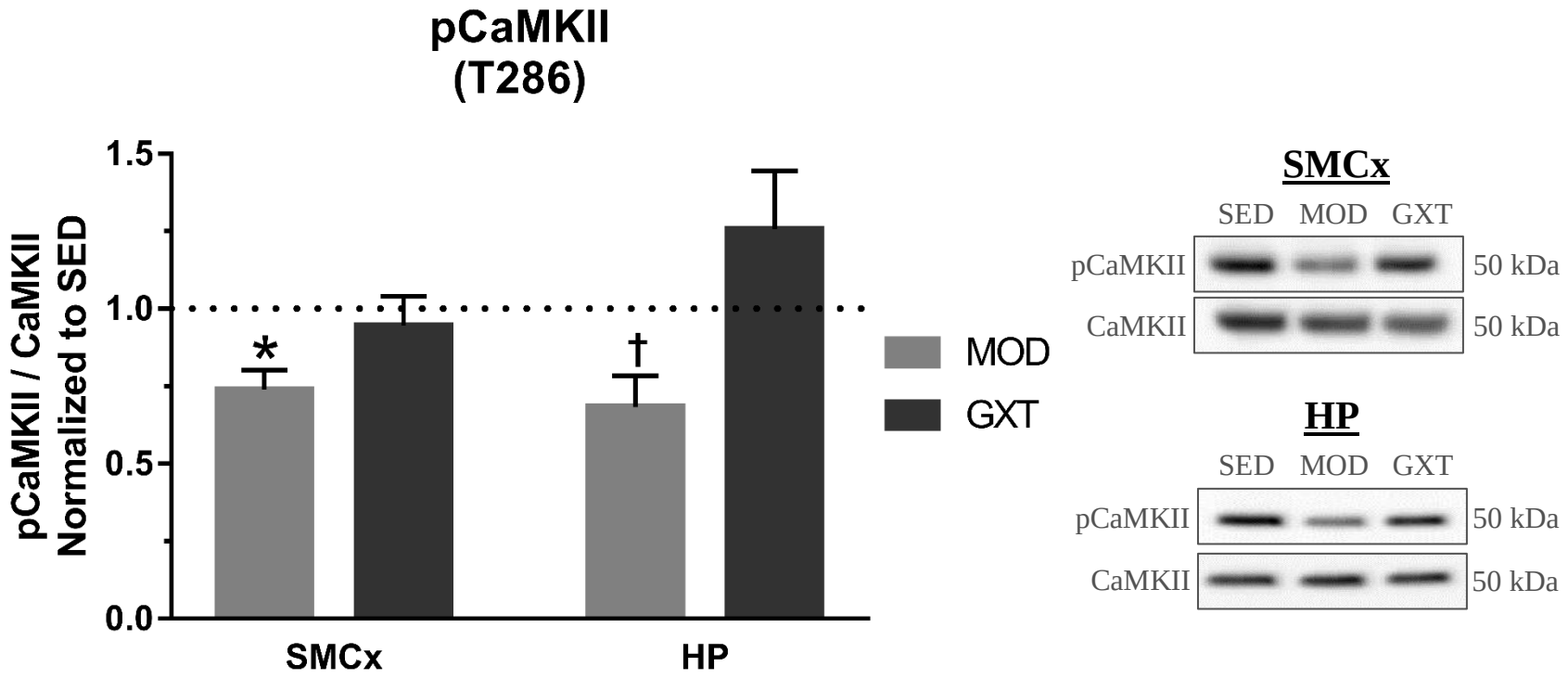
pCaMKII
(T286)
pCaMKII / CaMKII
Normalized to SED
1.5
1.0
0.5
0.0
*
†
SMCx
HP
MOD
GXT
SMCx
SED MOD GXT
pCaMKII
50 kDa
CaMKII
50 kDa
HP
SED MOD GXT
pCaMKII
50 kDa
CaMKII
50 kDa

Figure 3.10

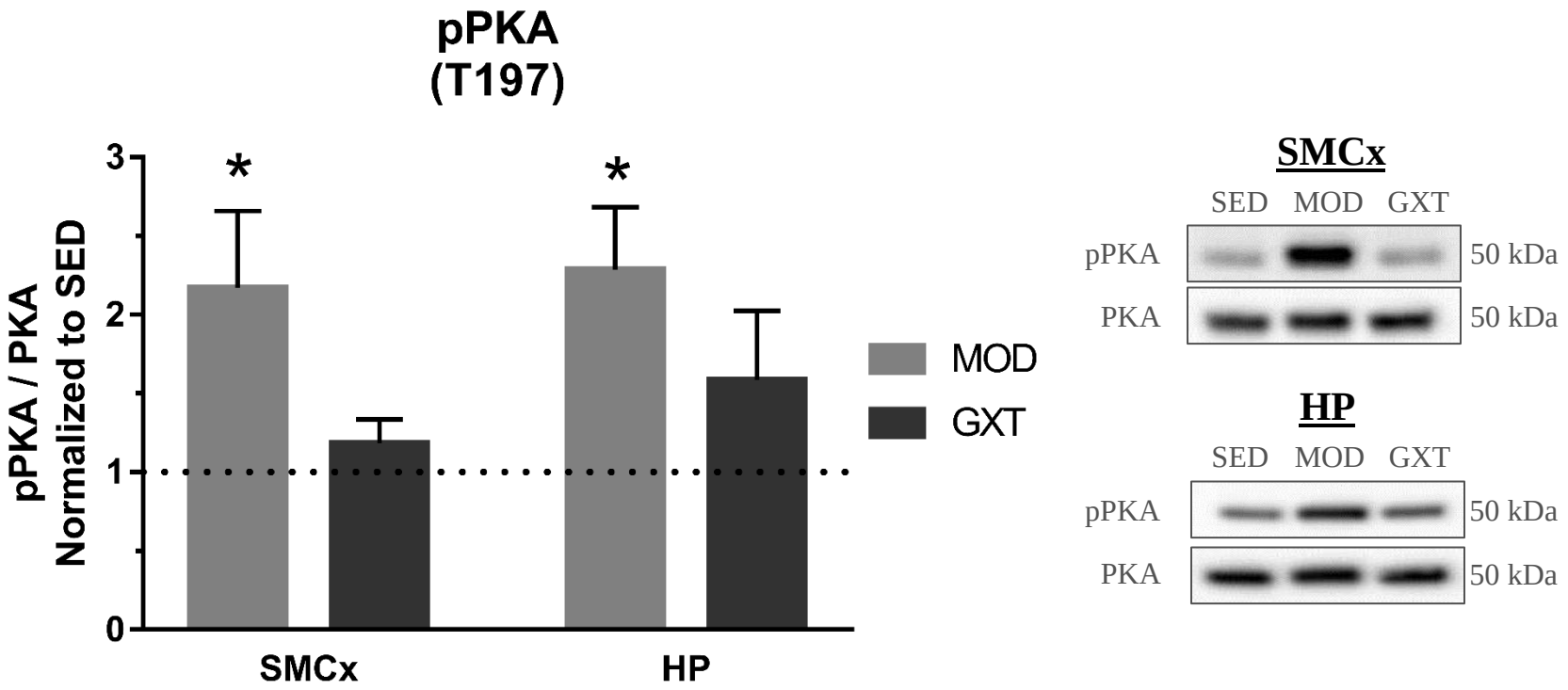
pPKA
(T197)
pPKA / PKA
Normalized to SED
3
2
1
0
*
*
SMCx
HP
MOD
GXT
SMCx
SED MOD GXT
pPKA
50 kDa
PKA
50 kDa
HP
SED MOD GXT
pPKA
50 kDa
PKA
50 kDa

Figure 3.11

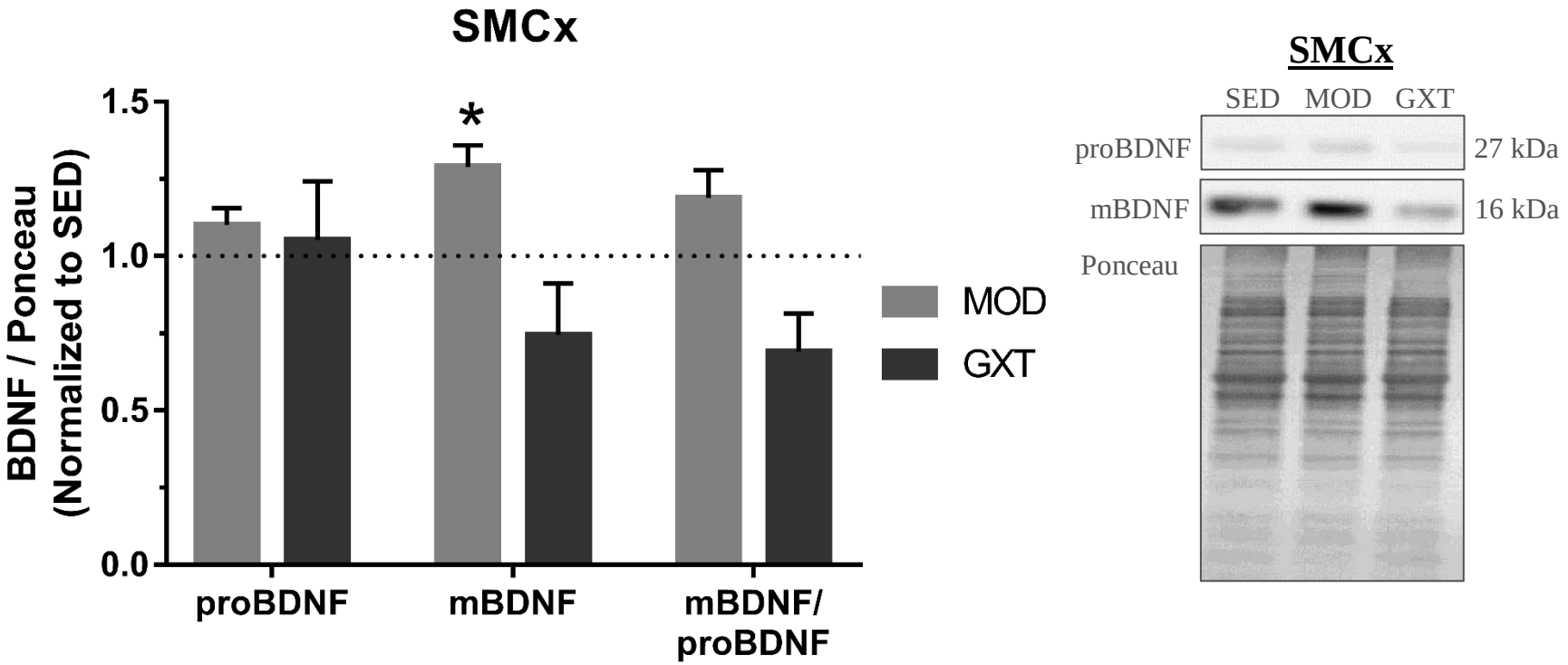
SMCx
BDNF / Ponceau
(Normalized to SED)
1.5
1.0
0.5
0.0
*
proBDNF
mBDNF
mBDNF/
proBDNF
MOD
GXT
SMCx
SED MOD GXT
proBDNF
27 kDa
mBDNF
16 kDa
Ponceau

Figure 3.12

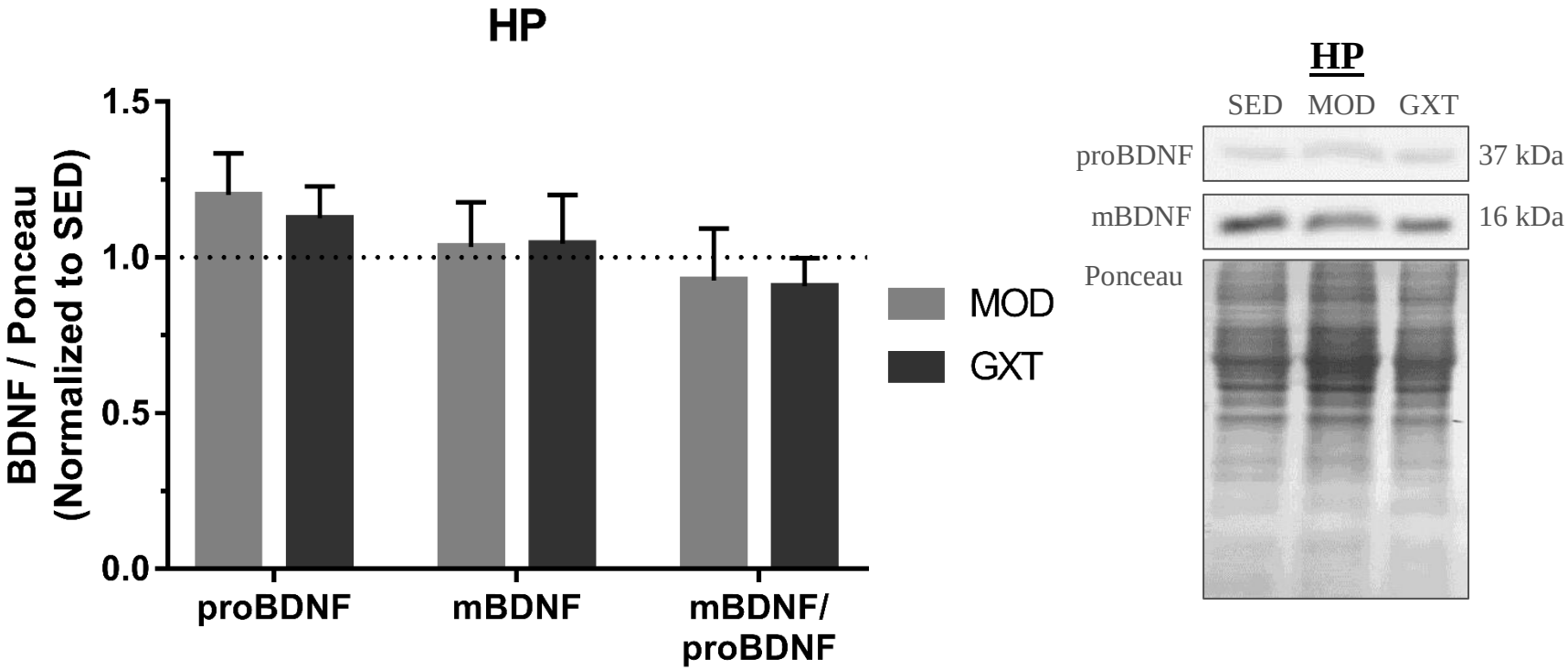
HP
BDNF / Ponceau
(Normalized to SED)
1.5
1.0
0.5
0.0
proBDNF
mBDNF
mBDNF/
proBDNF
MOD
GXT
HP
SED
MOD
GXT
proBDNF
37 kDa
mBDNF
16 kDa
Ponceau

Figure 3.13

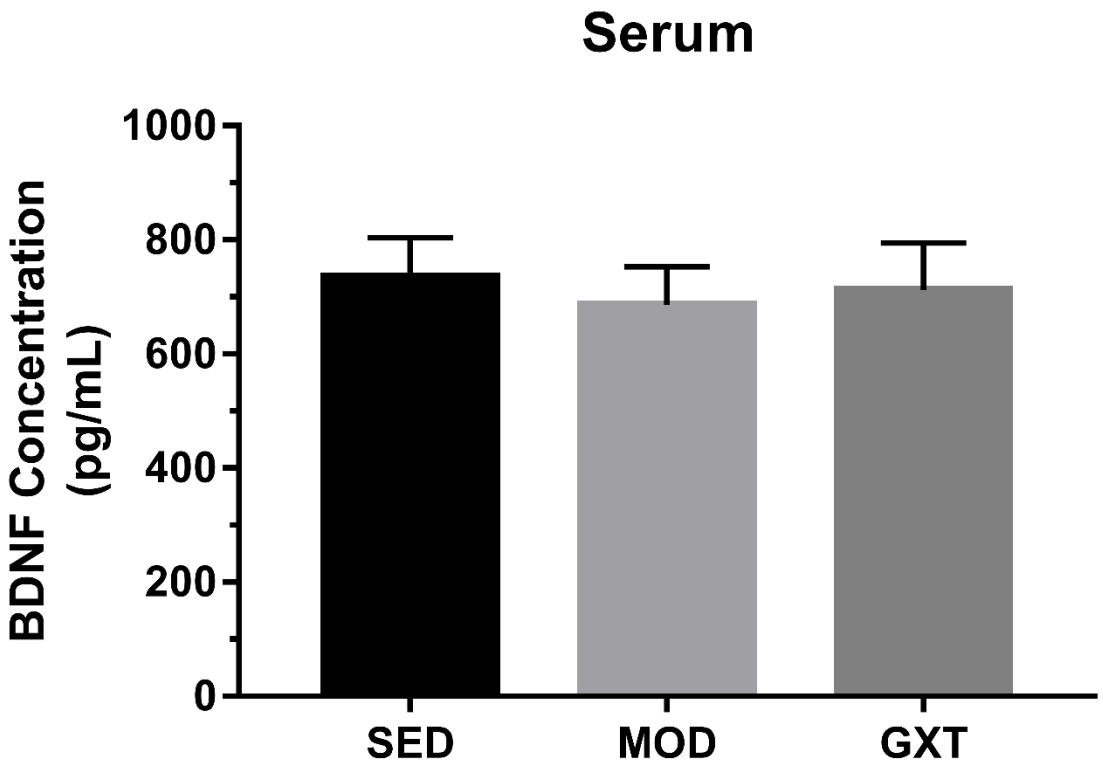
Serum
BDNF Concentration (pg/mL)
1000
800
600
400
200
0
SED
MOD
GXT

Figure 3.14

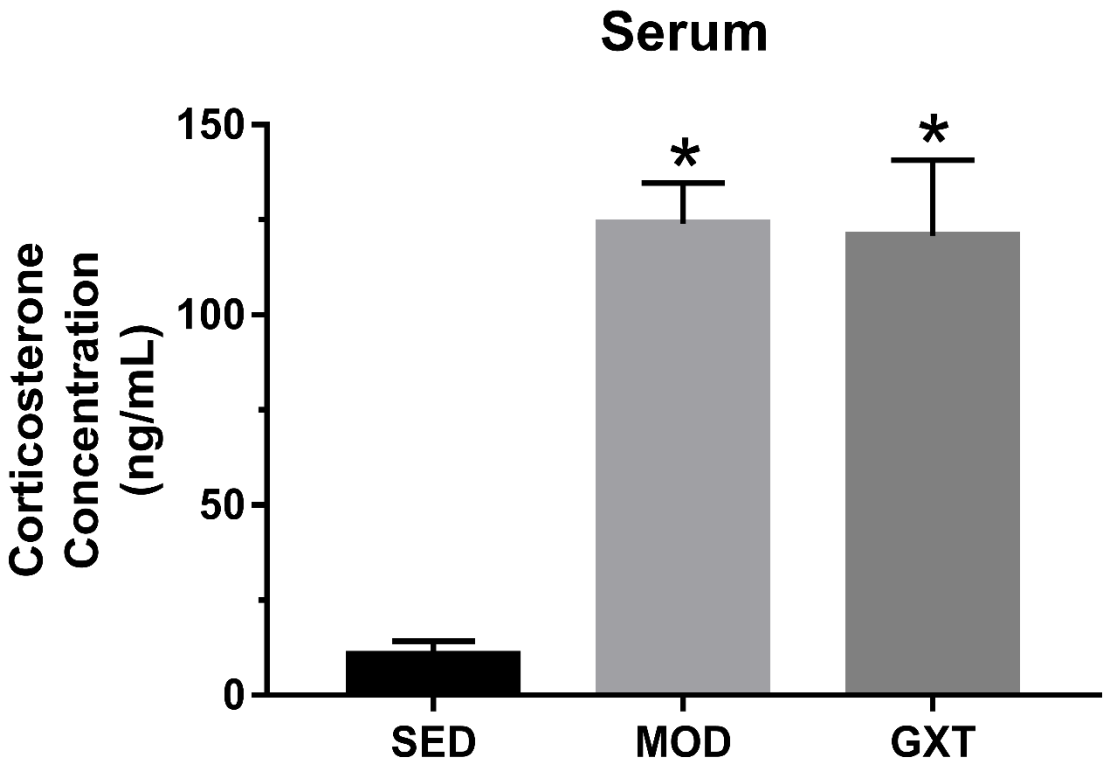
Serum
Corticosterone Concentration (ng/mL)
150
100
50
0
*
*
SED
MOD
GXT

Figure 3.15

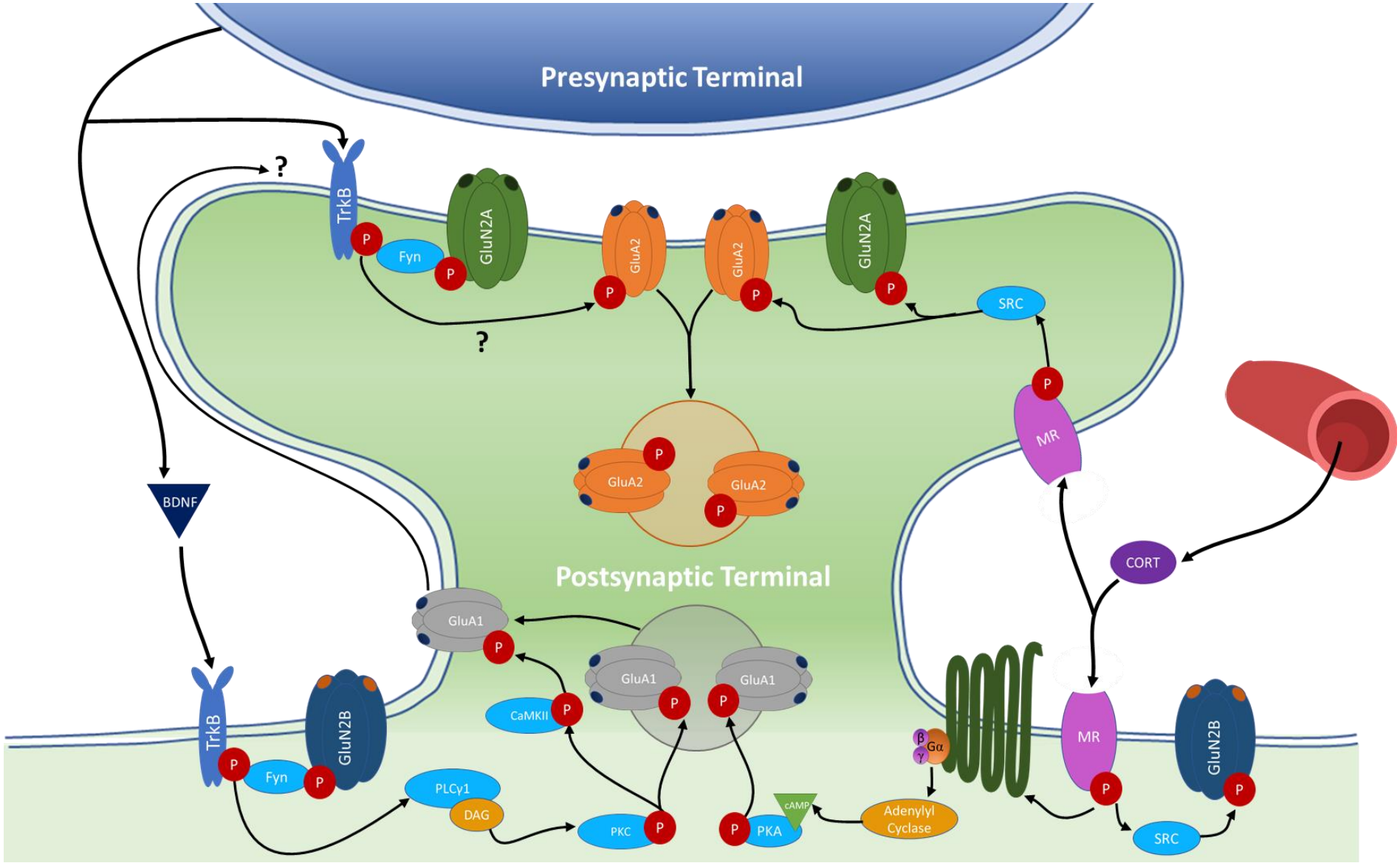
Presynaptic Terminal
?
TrkB
P
Fyn
P
GluN2A
GluA2
GluA2
GluN2A
P
P
P
?
SRC
P
MR
BDNF
GluA2
GluA2
P
Postsynaptic Terminal
CORT
GluA1
P
GluA1
GluA1
P
P
CaMKII
P
TrkB
P
Fyn
P
GluN2B
PLCγ1
DAG
PKC
P
P
PKA
cAMP
Adenylyl Cyclase
β
γ
Gα
MR
P
GluN2B
P
SRC

Figure 3.16

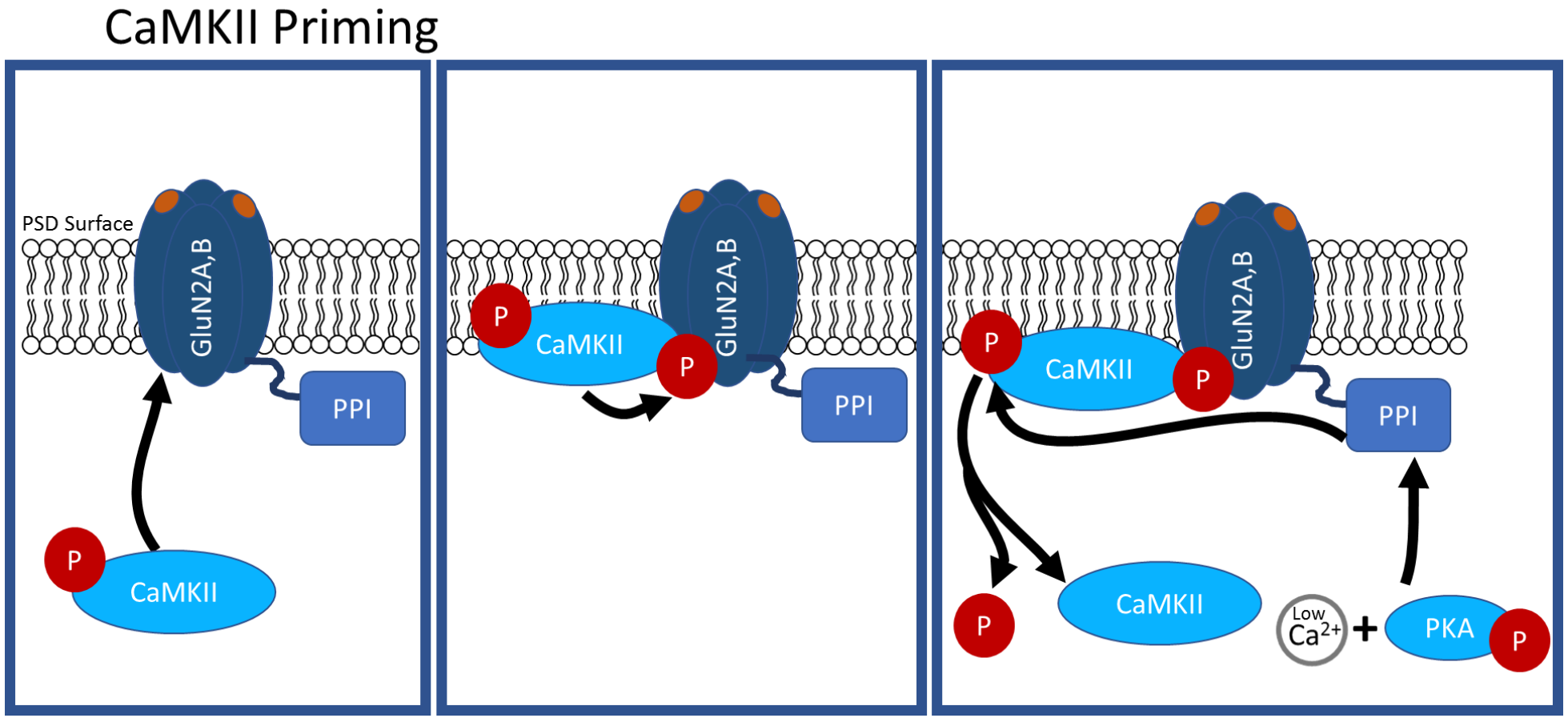
CaMKII Priming
PSD Surface
GluN2A,B
PPI
P
CaMKII
GluN2A,B
P
CaMKII
P
PPI
GluN2A,B
P
CaMKII
P
PPI
P
CaMKII
Low
Ca2+
+
PKA
P

4. A Novel Approach to Enrich Proteins Present at the Surface of Synaptic Terminals

Adapted from Submitted Manuscript: "Thacker JS., Xu Y., Fong T., Mielke JG. (2018). "A Novel Approach to Enrich Proteins Present at the Surface of Synaptic Terminals. Brain Res"

4.1 ABSTRACT

Although receptor trafficking is regarded as a key process in many forms of neuronal plasticity, studying the phenomenon is challenging, in part, due to the lack of techniques that effectively isolate the cell surface fraction of synapses. At present, the most common procedure for studying proteins at the neuronal surface is biotinylation, wherein biotin is conjugated with cell surface proteins and the complexes are covalently immobilized on beaded agarose, specifically avidin. Although highly sensitive, the biotinylation is not specific, and captures proteins from various cell types and neuronal sub-regions. One method for the isolation of synaptic terminals is a procedure that utilizes differential filtration to achieve intact synaptic terminals (i.e., a synaptoneurosome preparation; Syn). To more efficiently investigate receptor trafficking, we combined the biotinylation and Syn techniques (BioSyn) to enrich synaptic surface proteins. Tissue slices (350 µm) were prepared from Sprague-Dawley rats and incubated with 1 mg/mL of biotin for 40 minutes at 4^{o}C. Following homogenization, synaptoneurosomes were isolated and then incubated with NeutrAvidin beads for 4 h at 4^{o}C. The presumptive synaptic surface fractions were assessed via Western blotting. The data reveal that the BioSyn samples displayed an enrichment of proteins presumed to be found at the synaptic surface (GluN1, GluN2B, Neuroligin, NCAM), and the absence of internal neuronal proteins (actin, GAPDH) and glial specific proteins (GFAP). Moreover, we display the capacity of the technique to assess increased synaptic surface GluA1-containing AMPA receptors chemically-induced LTP.

Keywords: Receptor Trafficking, Plasticity, Biotinylation, Synaptoneurosome

4.2 INTRODUCTION

There is a general consensus that many forms of learning require long-term potentiation (LTP) of synapses (Bliss and Lomo, 1973; Rioult-Pedotti et al., 2000a; Whitlock et al., 2006), the earliest phases of which require the movement of proteins, particularly receptors, into and out of post-synaptic densities (Shi et al., 2001; Oh et al., 2006b). Furthermore, there is now wide acceptance that the trafficking and, consequently, altered surface expression of glutamatergic receptors is a key process in LTP (Bassani et al., 2013; Huganir and Nicoll, 2013; Blanco-Suarez and Hanley, 2014); however, there is a growing debate regarding the subcellular localization of specific glutamatergic receptor subunits, and the influence this location has on the relative contribution of these receptors to plasticity. For example, , NMDAR subunit composition is thought to influence the trafficking of the receptor either favor extra-synaptic, or synaptic membranes, which has led some to conclude an opposing involvement in either long-term potentiation (GluN2A), or depression (GluN2B) (Stocca and Vicini, 1998; Rumbaugh and Vicini, 1999; Tovar and Westbrook, 1999).

Previous work in this area often measured the movement of glutamatergic receptors by immunocytochemistry, real-time observation of fluorescently tagged proteins or, more recently, with the use of biarsenical dyes, which are not only expensive, but require a significant number of samples, and time to complete (Kohara et al., 2001; Malinow and Malenka, 2002; Song and Huganir, 2002; Ju et al., 2004). An ideal alternative to these methods would be one that measured receptor subunits in a high-throughput, objective manner that also retained the ability to reveal changes at the level of the synaptic surface. We sought to combine the sensitivity of biotinylation with the highly specific SNP to enrich the cell surface fraction of synaptic terminals; in effect creating a new preparative approach: a biotinylated synaptoneurosome (BioSyn). For example, the measurement of cell surface proteins is often conducted using biotinylation, which relies on the 3 characteristics native to the Sulfo-NHS conjugated biotin protein: (1) its membrane impermeability due to the highly charged Sulfo-NHS, as well as the (2) strong affinity and (3) incredibly stable non-covalent interaction of biotin with avidin (Elia, 2008). Briefly,

biotinylation involves the incubation of tissue slices, or cultured cells with biotin, which produces biotin-protein conjugates that can then be precipitated with the use of avidin conjugated beads. Although highly sensitive, biotinylation lacks specificity, capturing proteins from the surface of all cell types and membrane regions (e.g., the soma and all neurites). Additionally, techniques exist that can separate neurons into subcellular regions. For example, the high throughput, synaptoneurosome preparation (SNP) involves the use of differential filtration to enrich intact synaptic terminals. Unlike other forms of subcellular fractionation, such as the synaptosome preparation (which preferentially isolates presynaptic terminals) (Dodd et al., 1981), the SNP isolates both pre- and post-synaptic terminals (Hollingsworth et al., 1985; Johnson et al., 1997; Villasana et al., 2007). Synaptoneurosomes have been examined using electron microscopy and have been shown to be highly specific in yielding intact and enclosed synaptic terminals. The isolated terminals can be used in numerous applications, including being treated directly with drugs, electrophysiological clamping, or they can be lysed and analyzed by techniques such as Western Blot (Morrow and Paul, 1988; Kanhema et al., 2006; Chen et al., 2012). Herein, we provide a methodology to allow the combination of the biotinylation and synaptoneurosome techniques to achieve a simple, high-throughput, and reproducible sample that is enriched in proteins present at the synaptic surface.

4.3 METHODS

4.3.1 Animals

Male Sprague-Dawley rats (*Rattus norvegicus)* were purchased from Envigo™ at 6 weeks of age (weight 250-350 g). All animals were group housed in a temperature-controlled room on a reverse 12 : 12 light-dark cycle and allowed free access to both water and standard rodent chow. All animals were used in accordance with procedures approved by the University of Waterloo animal care and ethics committee.

4.3.2 Preparation of Cortical and Hippocampal Slices

On the day of sacrifice, rats were anesthetized with CO_2 and euthanized by decapitation. Brains were immediately removed and placed within an adult rat coronal brain matrix (Ted Pella, Inc., Redding, CA, USA) submerged in ice-cold artificial cerebral spinal fluid (ACSF) that contained (in mM): 127.0 NaCl (Sigma, Oakville, ON, Canada; all subsequent reagents from Sigma, unless otherwise noted), 26.0 $NaHCO_3$, 10.0 glucose, 2.0 $CaCl_2$, 2.0 KCl, 2.0 $MgSO_4$, and 1.2 KH_2PO_4 and was equilibrated with carbogen (95% O_2/5% CO_2), pH 7.37–7.43. The prefrontal cortex was largely removed by a coronal cut approximately 6 mm from the most rostral end of the brain; a position roughly corresponding to atlas plate 9 (Paxinos and Watson, 1982). The brain was then transferred to a Petri dish filled with ACSF and placed on ice, the cerebellum removed, and the brain hemisected.

After careful dissection, 8 slices (350 µm) were prepared from the septal (4 slices) and temporal (4 slices) region of each hippocampus each from individual rats using a McIllwain tissue chopper (Mickle Laboratory Engineering Co., Surrey, UK). To prepare slices of the sensorimotor cortex (SMCx), a previously established method was used (Thacker et al., 2018). Briefly, the hemisphere was placed on its mid-sagittal surface, and the ventral surface was removed with an axial cut along the rhinal sulcus. The remaining tissue was placed on the platform of a McIlwain Tissue chopper (mid-sagittal surface against the platform and rostral surface facing the blade), and 8 slices (350 µm) prepared. Slices were transferred to a Petri dish filled with chilled ACSF, and the presumptive motor region isolated by an axial cut along the apex of the corpus callosum. In a separate group of animals, both hippocampi were extracted from each hemisphere in a fashion similar to that previously described (Madison and Edson,

2001). All slices were subject to a 1-hour recovery period prior to the commencement of treatment.

4.3.3 Chemically-Induced Long-Term Potentiation (cLTP)

In an effort to prompt trafficking events within synapses, we administered cLTP within SMCx and HP, in a similar way as previously described with minor adaptation (Stewart et al., 2005). Following 1 hour of recovery, inserts were transferred to a mesh platform in a second incubation chamber containing modified ACSF, wherein $CaCl_2$ was adjusted to 4.0 mM, $MgSO_4$ to 0.0 mM, and tetraethylammonium (TEA) [25 mM] and glycine [200 µM] added. The cLTP chamber was continuously perfused with carbogen gas at 35°C ± 0.5°C similarly to the SHAM condition. In an effort to account for mechanical stress that cLTP slices may experience during the transfer, SHAM slices were exposed to the same movement procedure, but placed back into their original chamber. After 15 mins of cLTP, slices were transferred back into the original chamber and for 15 minutes under standard conditions. Following this brief period of washout, both SHAM and cLTP slices underwent biotinylation (Section 2.5).

4.3.4 Electrophysiological Recordings

Slices were transferred to a multi-electrode dish and placed such that an 8 x 8 electrode array (50 x 50 µm electrode diameter, inter-electrode distance: 100 µm) was next to the CA1 region. Prior to their initial use, MEDs was washed with deionized water and coated overnight with 0.1% polyethyleneimine in 25 mM borate buffer. Plastic wire mesh and a U-shaped weight were gently placed over each slice to improve contact with the microelectrodes. Carbogenated ACSF was continuously perfused (1.5-2 mL/minute) while warmed, humidified carbogen was directed over the slice. Experiments were conducted at 35 ±0.5 °C. Following a 20 min

stabilization period, biphasic constant current pulses (0.2 ms) were applied to individual electrodes along the Schaffer collateral pathway to identify the optimum CA1 stratum radiatum recording site. Upon selection of an electrode site, an input-output curve was completed in order to determine the stimulation intensity (30-50% of maximum). To obtain input-output (I–O) curves, stimuli of increasing intensities were applied (2–40 μA, in 5 μA steps) until signal saturation, or population spike generation. Data were imported into python (3.16) and analyzed using in-house generated scripts. In brief, offset of each trace was normalized to zero and amplitude (minimum value) of the field excitatory post-synaptic potential (fEPSP) response was extracted, and then normalized to the baseline.

4.3.5 Enrichment of Proteins Present at the Surface of Synaptic Terminals

Following either preparation or treatment, slices were individually placed within separate wells of a 96 well plate, wherein each well contained either 150 μL (SMCx), or 100 μL (HP) Sulfo-NHS-LL-biotin solution (1 mg/mL in ACSF) (Thermo Fisher Scientific, Massachusetts, USA). Following a 40-minute incubation at 4°C under gentle agitation, the biotin solution was removed and all slices were gently washed 3x with cold quenching buffer (ACSF with 50 mM Trizma base) over ice to stop the reaction. All slices were then placed in a 2 mL Potter-Elvehjem homogenizing tube containing 350 μL of ice-cold modified Krebs-Henseleit buffer (mKRBS) containing (in mM): 118.5 NaCl, 4.70 KCl, 1.18 $MgCl_2 \cdot 6H_2O$, 2.50 $CaCl_2 \cdot 2H_2O$, 1.18 KH_2PO_4, 24.90 $NaHCO_3$, 10.00 glucose, pH adjusted to ~7.40 using 1.0 N HCl. A protease inhibitor cocktail (104 mM AEBSF, 80 μM Aprotinin, 4 mM Bestatin, 1.4 mM E-64, 2 mM Leupeptin and 1.5 mM Pepstatin) and a tyrosine phosphatase inhibitor (200 mM Na_3VO_4) were included in the buffer to limit proteolysis and phosphatase activity. Slices were homogenized with 20 manual pestle strokes over ice, and the homogenate placed in a 1.5 mL microtube over ice for 10 minutes

to allow for gravity sedimentation. A small volume (50 µL) of the supernatant was extracted and designated as the whole homogenate (WH), and the remaining supernatant was used to prepare synaptoneurosomes.

Synaptoneurosomes were prepared by drawing the homogenate into a 1 cc Luer lock syringe and passing it through a 13 mm filter holder (XX3001200, EMD Millipore, Etobicoke, ON, Canada) containing 3 layers of pre-wetted (mKRBS) 100 µm pore nylon filters (NY1H02500, EMD Millipore). After this, 1 mL of air was passed through the filters (all filtrate was drawn in a small Petri dish placed over ice). The filtrate was then collected into a separate 1 cc Luer lock syringe and passed through a 13 mm filter holder containing a single pre-wetted (mKRBS) 5 µm nitrocellulose Durapore membrane filter (SVLP01300, Millipore) followed by 1 mL of air; samples were collected in a 1.5 mL microtube. Microtubes were then spun at 1000 x g for 15 minutes at 4ºC, supernatants were discarded and each pellet re-suspended in 200 µL non-ionizing lysis buffer (10 mM Tris, 25 mM EDTA, 100 mM NaCl, 1% [v/v] Triton X-100, and 1% [v/v] NP-40, pH 7.4) containing protease and phosphatase inhibitors; 180 µL was saved and designated as the synaptoneurosome preparation. Protein concentration was determined with the use of the Bio-Rad DC protein assay kit according to the manufacturer's recommended protocol.

In order to determine the ideal reagent concentration, two different NeutrAvidin™ agarose bead (Thermo-Fisher Scientific) to protein ratios were used. Specifically, either 40 µL, or 80 µL of NeutrAvidin™ beads were incubated with either 50 µg, or 100 µg of protein, respectively. Prior to use, NeutrAvidin™ beads were washed 3x with non-ionizing lysis buffer. Washed NeutrAvidin™ beads were incubated with the appropriate volume of homogenate for 4 h at 4ºC on a rocking platform. Bead-protein complexes were then washed 3x with non-ionizing lysis buffer and spun at 10,000 x g for 30 seconds. The pellet containing bead-protein complexes

was re-suspended and denatured using 50 µL of 1x sample buffer (0.0625 M Tris, 2% [v/v] glycerol, 5% [w/v] sodium dodecyl sulfate [SDS], 5% [v/v] b-mercaptoethanol, and 0.001% [w/v] bromophenol blue, pH 6.8) at 95ºC for 5 minutes. A final 10,000 x g spin (30 s) was completed, and the supernatant was designated the synaptic surface fraction (Refer to Fig. 1).

4.3.6 Western Blotting

Proteins were separated electrophoretically using a 10% SDS-polyacrylamide gel at 200 V for 1 h, and were then electroblotted onto PVDF membranes via wet transfer (350 mA at 4ºC for 2 h). Blots were then incubated with Ponceau S solution, washed with deionized water, air dried, and then imaged. Membranes were blocked using either 5% (w/v) bovine serum albumin (BSA), or 5% (w/v) non-fat milk in Tris-buffered saline with Tween-20 (TBST) for 1 h at room temperature. Next, antibodies directed at different neuronal and non-neuronal epitopes were used to evaluate the enriched synaptic surface fraction. Post-synaptic membrane-bound receptors, including GluN1 (mouse monoclonal, Millipore, cat. 05-432, 1:1000), GluN2A (rabbit polyclonal, Millipore, cat. 07-632, 1:1000), and GluN2B (mouse monoclonal, Millipore, cat. 05-920, 1:1000) were used as positive controls for the post-synaptic surface. The pan-synaptic structural protein neuroligin-1 (mouse monoclonal, Millipore, cat. MABN38, 1:1000) and neural cell adhesion molecules (NCAM; rabbit polyclonal, Santa Cruz, cat. SC-10735, 1:1000) were included as markers of membrane-bound structural proteins. Negative membrane controls included high abundant cytoskeletal proteins glyceraldehyde 3-phosphate dehydrogenase (GAPDH; rabbit monoclonal, Cell Signaling, cat. 14C10, 1:5000), actin (rabbit polyclonal, Sigma-Aldrich, cat. A2066, 1:2000), and post-synaptic density protein 95 (PSD-95) (mouse monoclonal, Millipore, cat. MABN68, 1:5000). The negative control was: glial fibrillary acidic protein (GFAP, a constituent of astrocytes; mouse monoclonal, Millipore, cat. MA3402, 1:1000).

All antibodies were diluted in 10 mL of blocking buffer and applied to blots for overnight incubation. Following incubation, blots were washed 3 x 10 minutes in TBST before being incubated with the appropriate secondary antibody (anti-rabbit immunoglobulin G-horseradish peroxidase [IgG-HRP], Santa Cruz Biotechnology, cat. SC 2004, 1:5000, or anti-mouse immunoglobulin G-horseradish peroxidase [IgG-HRP], Santa Cruz Biotechnology, cat. SC 2005, 1:5000) diluted in blocking buffer for 1 h at room temperature under gentle agitation. Chemiluminescence of secondary antibody-HRP conjugates was elicited by the use of Luminata Crescendo (receptor proteins), or Classico (structural proteins) electrochemiluminescent reagents (Millipore). All images were captured using the GeneSnap program and G6000 Gel Dock system (Synoptics, Cambridge, UK). Image analysis was conducted using the GeneTools companion program. Using the automated GeneTools function, antibody chemiluminescence imaged by GeneTools was quantified for each band at the correct molecular weight for the protein of interest. With regard to the staining methods, whole lane protein was evaluated by constructing peak bounds across the length of the band in an effort to capture total absorbance for each band. Whole protein stains were evaluated by using the GeneTools automated feature to extract optical densitometry from the entirety of each lane. Background subtraction was conducted using the embedded software within GeneTools; chemiluminescent bands used Rolling Disk, whereas whole protein bands required Lowest Slope. Optical densities were exported to Microsoft Excel for statistical analysis.

4.4 Summary of Results

4.4.1 BioSyn Characterization

We began by determining empirically the appropriate amount of starting protein required for a successful Western Blot, and tested two neutravidin pull-down protocols, (1) 40 µL of beads with 50 µg of protein, and (2) 80 µL of beads with 100 µg of protein. Western blot analysis revealed both bead/protein ratios were able to provide detectable Western blot signals of synaptic surface proteins, however, 100 µg of protein produced a more consistent signaling pattern (data not shown). For this reason, all subsequent steps used 100 µg of the starting material.

According to Western blotting data (Fig. 2), the BioSyn fraction appropriately enriched synaptic surface proteins, while excluding cytosolic proteins. Specifically, BioSyn homogenates clearly contained proteins known to be present at synapses (Sheng and Kim, 2011; Verpelli et al., 2012), including NMDAR subunits GluN1 and GluN2B. Moreover, BioSyn clearly enriched proteins expected to be only present at the synaptic surface, extracellular scaffolding proteins NCAM, Neuroligin-1, and intracellular scaffolding protein PSD95. Furthermore, BioSyn fractions contained little to no detectable signal of the highly abundant intracellular structural protein β-actin nor metabolic protein GAPDH. As well the glial-specific marker GFAP was not detected in either SNP, nor BioSyn.

Additional characterization of the technique was also performed. In particular, it was determined that the WH may be used in addition to BioSyn for the detection of either total homogenized proteins, or may also be subjected to neutravidin beads to explore total surface expressed proteins (data not shown). However, unlike traditional biotinylation protocols, the

cytosolic fractions following either SNP, or neutravidin pull-down do not yield sufficient protein for Western blot (data not shown). Therefore, the BioSyn protocol presented here yields 4 different, usable, subcellular fractions: (1) total tissue protein (WH), (2) total tissue surface proteins (Bio-WH), (3) total synaptic proteins (SNP), and (4) synaptic surface proteins (BioSyn).

4.4.2 cLTP leads to a robust and sustained potentiation in HP

To examine the ability of BioSyn to capture receptor trafficking events at synaptic sites, we subjected both SMCx and HP slices to cLTP treatment. Following the perfusion of cLTP-ACSF, we noticed a stark increase in fEPSPs recorded from the CA1 region of HP slices. Specifically, during the perfusion, we observed a 200% increase in recorded fEPSP's that saturates quickly. However, following washout with standard ACSF, the response to cLTP grew by another 100% (in total, 300% above baseline). Although there is a greater variability in response during this phase compared to the cLTP induction phase, the response remains relatively stable and decays slowly over time.

4.4.3 cLTP facilitates GluA1 incorporation in both SMCx and HP

There is now strong support for the trafficking of GluA1-containing AMPAR to the synaptic surface during LTP induction. In an effort to best capture these trafficking events, we prepared lysates at the point in time corresponding with the greatest response in fEPSP (15 min into washout). Following BioSyn preparation we were able to measure a detectable increase in the presence of GluA1 within the synaptic surface fraction of both SMCx (≈150%) and HP (≈120%). Our results demonstrate the utility of the BioSyn preparation in the assessment of acute receptor trafficking events.

4.5 Discussion

We have combined the sensitivity of biotinylation with the specificity of the synaptoneurosome technique to enrich proteins at the synaptic surface. In theory, BioSyn enriches the synaptic surface fraction by tagging all surface proteins with biotin, applying sequential filtration to sequester intact synaptoneurosomes, and then incubating the lysed synaptoneurosome with neutravidin beads followed by elution of neutravidin beads with sample buffer and heat (Figure 4.1). Herein, we provide convincing evidence that BioSyn provides a novel approach to evaluating various subcellular fractions, in particular, those proteins present at the synaptic surface. In addition, we display evidence that BioSyn is sensitive enough to measure changes occurring within the synaptic surface in response to cLTP. We believe BioSyn to be a powerful tool that will enhance the biochemical exploration of hypotheses relating to the movement/trafficking of proteins from one subcellular compartment to another. Moreover, BioSyn provides a simple, high-throughput and cost-effective alternative to the traditional techniques often employed to answer these research questions.

FIGURE LEGENDS

Figure 4.1. Illustration of the procedure for producing biotinylated synaptoneurosomes (BioSyn), which in theory yield an enriched homogenate of synaptic surface proteins. Slices (350 µm) from either SMCx, or HP were incubated with 1 mg/mL of biotin for 40 minutes at 4^{o}C. Following homogenization, the whole homogenate (WH) was passed through a sequence of filters to isolate the synaptoneurosome preparation. The SNPs were then lysed and homogenates incubated with neutravidin beads for 4 h at 4^{o}C under gentle agitation. Bead-biotin-protein complexes were dissociated by addition of Laemmli buffer at 95^{o}C for 5 min prior to gel electrophoresis.

Figure 4.2. Characterization of a BioSyn sample from the SMCx. The representative immunoblot displays various steps in the procedure, including WH, SNP, and BioSyn. Positive controls for synaptic surface included NMDA receptor subunits GluN1 and GluN2B, synaptic terminal protein PSD95 (intracellular), and synaptic surface structural proteins Neuroligin-1 and NCAM (extracellular). Negative control proteins included cytoskeletal protein β-actin and cytosolic metabolic protein GAPDH. Finally, the glial-specific marker GFAP is included as a cell-specific control.

Figure 4.3. (A) Electrophysiological recordings of HP CA1. Above graph, representative, to scale, timeline depicts the protocol. Delivery of cLTP for a total duration of 20 minutes facilitates electrophysiological recordings within HP. This potentiation is amplified during the first 15 minutes of washout, before decaying. This time point also corresponds with when lysates were sampled and processed by the BioSyn protocol. **(B)** Representative tracings for individually sampled points at baseline (1) and following 15 min washout post-cLTP induction.

Figure 4.5. Synaptic surface AMPAR subunit GluA1 expression in SMCx (n = 3) and HP (n = 2) following either SHAM or cLTP. Both SHAM and cLTP GluA1 are normalized to whole lane ponceau staining. Each cLTP GluA1 optical density is displayed relative to SHAM.

Figure 4.1

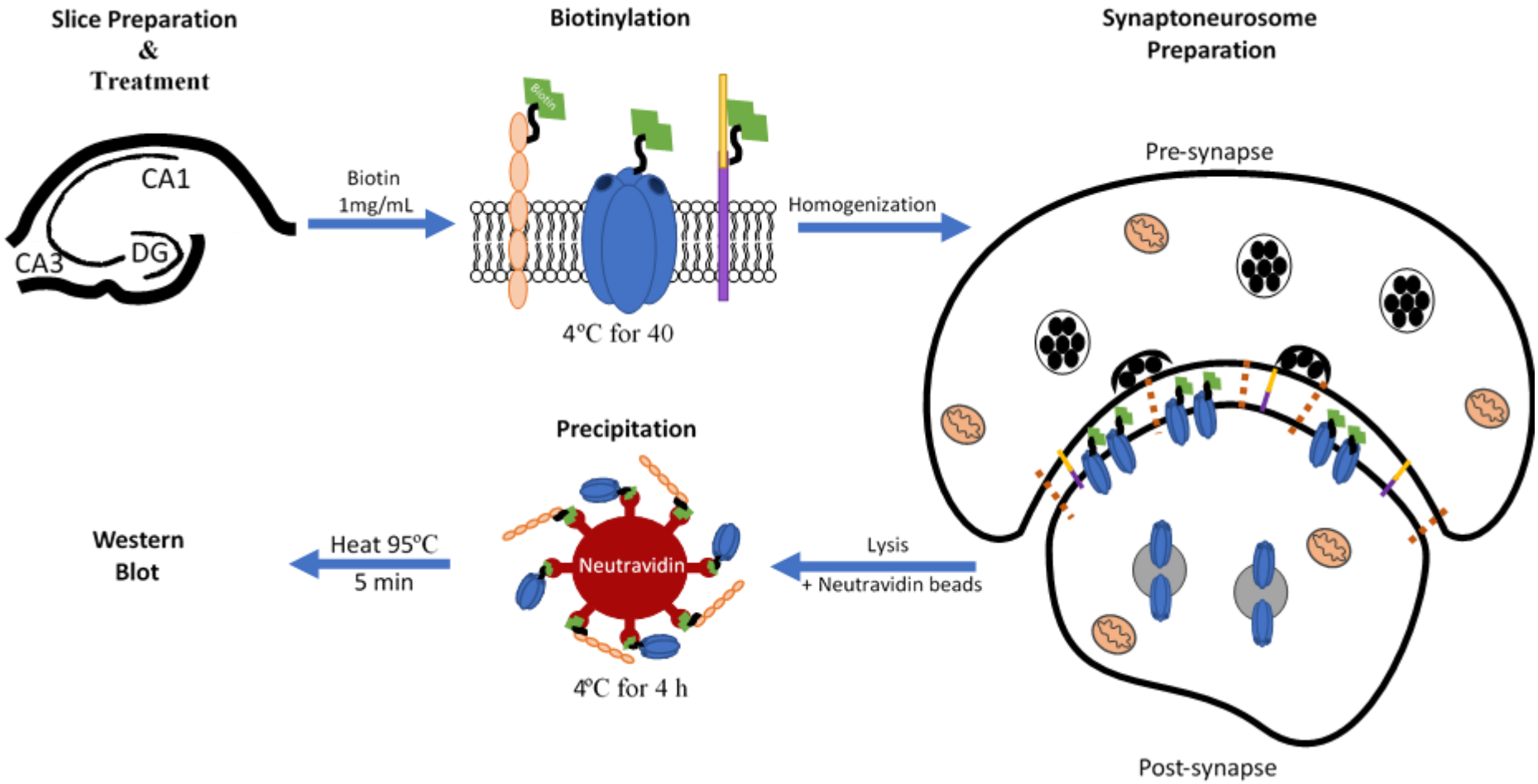
Slice Preparation
&
Treatment
CA1
CA3
DG
Biotin
1mg/mL
Biotinylation
Biotin
4°C for 40
Homogenization
Synaptoneurosome
Preparation
Pre-synapse
Post-synapse
Lysis
+ Neutravidin beads
Precipitation
Neutravidin
4°C for 4 h
Heat 95°C
5 min
Western
Blot

Figure 4.2

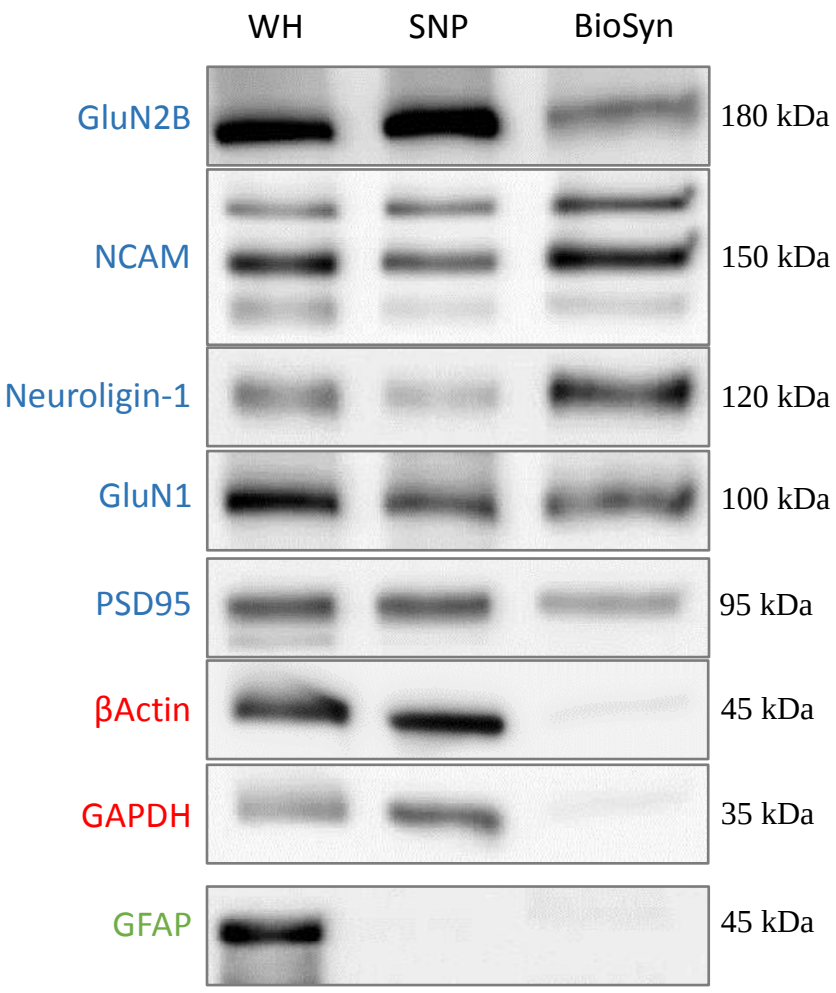
WH
SNP
BioSyn
GluN2B
180 kDa
NCAM
150 kDa
Neuroligin-1
120 kDa
GluN1
100 kDa
PSD95
95 kDa
βActin
45 kDa
GAPDH
35 kDa
GFAP
45 kDa

Figure 4.3

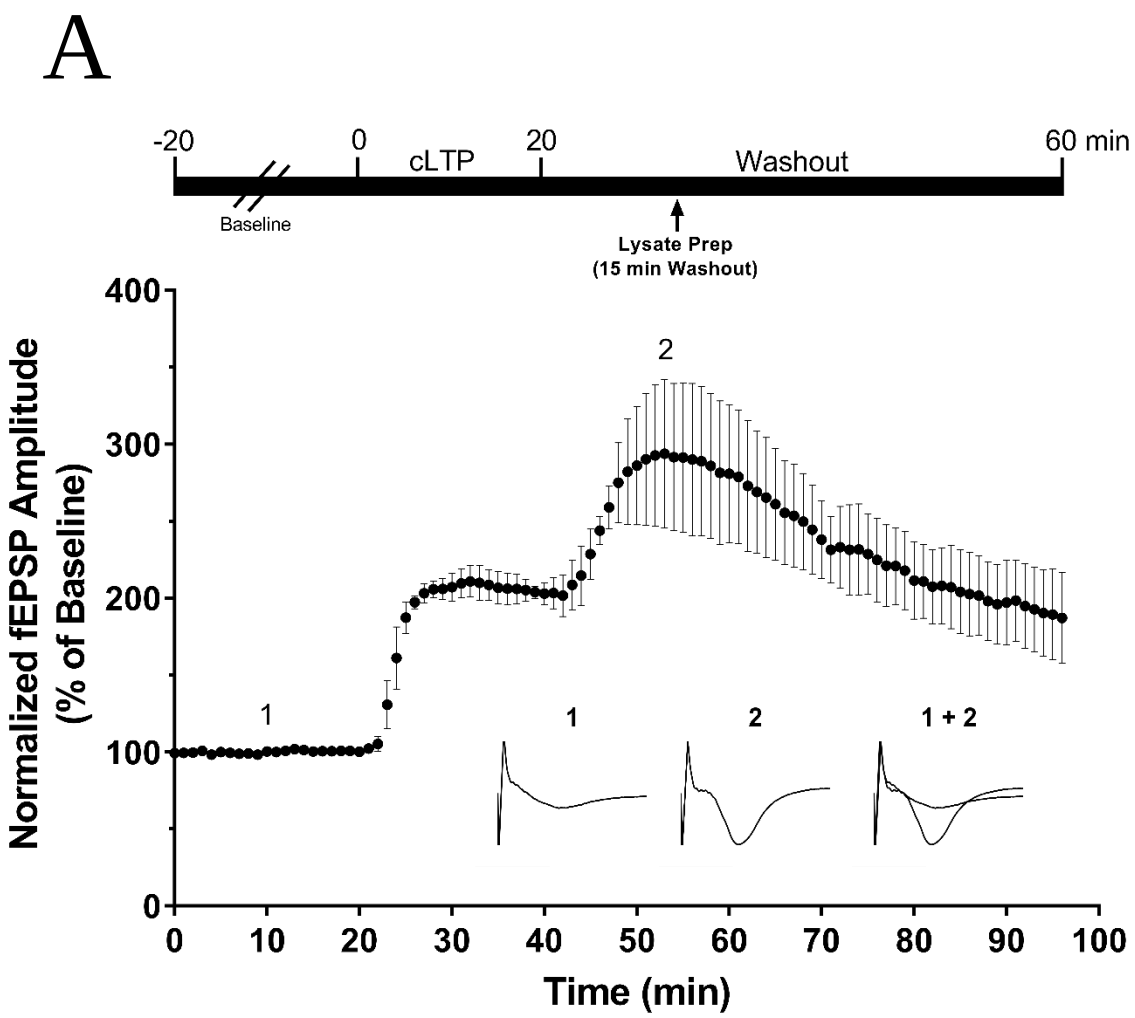
A
-20
0
cLTP
20
Washout
60 min
Baseline
Lysate Prep
(15 min Washout)
Normalized fEPSP Amplitude
(% of Baseline)
400
300
200
100
0
1
2
1
2
1 + 2
0
10
20
30
40
50
60
70
80
90
100
Time (min)

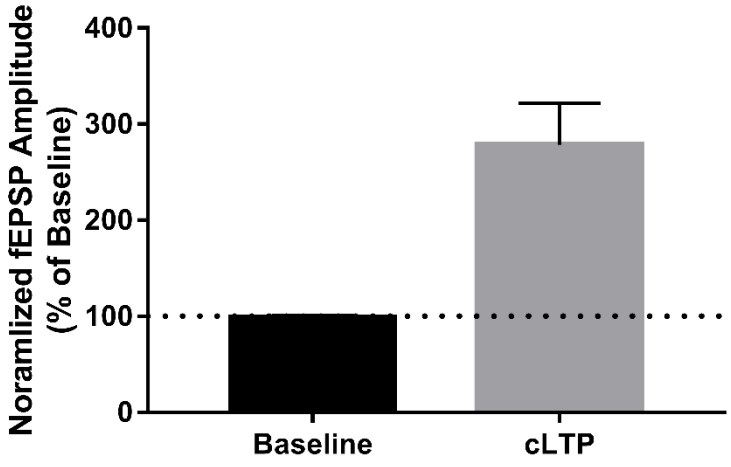
B
Noramlized fEPSP Amplitude
(% of Baseline)
400
300
200
100
0
Baseline
cLTP

Figure 4.4

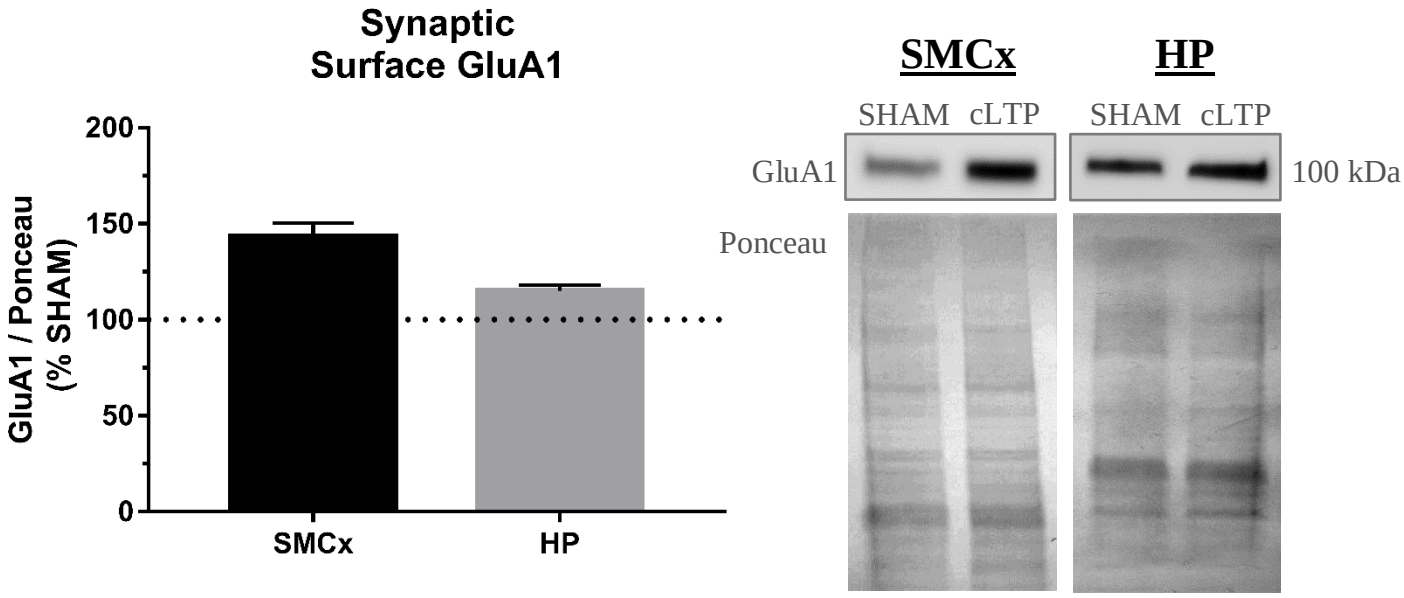
Synaptic
Surface GluA1
GluA1 / Ponceau
(% SHAM)
200
150
100
50
0
SMCx
HP
SMCx
HP
SHAM cLTP
SHAM cLTP
GluA1
100 kDa
Ponceau

5. The priming influence of CORT, BDNF, and CORT+BDNF on Plasticity-Related Receptor Phosphorylation and Trafficking at the Synaptic Surface in Sensorimotor Cortex

5.1 INTRODUCTION

Accumulating evidence suggests that pairing a single session of aerobic exercise with motor training enhances the acquisition of motor skill (Roig et al., 2012; McDonnell et al., 2013; Stavrinos and Coxon, 2014; Statton et al., 2015). Numerous studies exploring this phenomenon in humans mention an exercise-dependent "priming" effect; however, to date, the effects of a single session of exercise on LTP-related events are widely unexplored. Previous work in our lab (Chapter 4) has noted significant increases in neural tyrosine phosphorylation following brief (20 minutes), moderately intense exercise in a rodent model that may account for priming like events. Specifically, it was observed that moderately intense exercise enhanced the phosphorylation of GluA1 at Ser845 and Tyr869/873/876 of GluA2; others have shown changes at these sites to be related to the migration of these receptors (Oh et al., 2006a; Diering et al., 2016). The increased phosphorylation state of GluA1 and GluA2-containing AMPA receptors suggests that exercise may prime LTP by altering the composition of synaptic receptors, although this has yet to be explored.

As a first step, we sought to explore the exercise-dependent mechanisms through which changes in phosphorylation, and thus migration, of GluA1-containing AMPA receptors, occurs. Mechanisms to explain exercise-induced effects in the brain are the topic of fierce debate. There is a large body of research that supports a role for circulating neurotrophic factors, notably BDNF, in exercise-induced effects. Nearly 25 years ago it was discovered that BDNF protein expression is upregulated in physically active rodents within brain regions such as hippocampus, with more recent reports displaying significant increases in BDNF release, or conversion (proteolytic cleavage of proBDNF into mBDNF) following a single session of exercise (Neeper et al., 1995; Rojas Vega et al., 2006; Tang et al., 2008; Rasmussen et al., 2009). Strong evidence implicates

BDNF, via its receptor tropomyosin receptor kinase B (TrkB), in activity-dependent plasticity (Lu, 2003). In particular, BDNF application is associated with enhanced synaptic transmission, which was determined to be related to TrkB dependent phosphorylation of NMDA subunit GluN2B and GluA1-containing AMPA receptors (Levine et al., 1998; Lin et al., 1998; Crozier et al., 1999; Wu et al., 2004). Increased release of BDNF immediately following exercise, combined with evidence implicating BDNF as an active participant in many forms of activity-dependent glutamatergic plasticity, make BDNF a likely candidate for motor cortical priming following exercise.

Acute exercise in untrained animals, or sedentary humans is often associated with marked increases in glucocorticoids, notably corticosterone, or cortisol (CORT), respectively (Mastorakos et al., 2005). Glucocorticoid receptors have been traditionally regarded for their genomic influences, however recent evidence suggests that they (specifically the mineralocorticoid receptors) may display rapid (non-genomic), surface-expressed adaptations that favor plasticity (Groeneweg et al., 2011). Although the role that CORT plays in the brain following exercise has not been evaluated, it has been extensively studied following acute exposure to other forms of physical stress (McEwen, 2009; Kudielka and Wüst, 2010; Popoli et al., 2012). In particular, CORT evokes robust changes in GluA1 Ser845 phosphorylation that translate into enhanced LTP induction following 30 minutes of various stress exposures in rats (Pavlides et al., 1993; Whitehead et al., 2013; Godsil et al., 2016). Exposure to exogenous CORT in hippocampal slices promotes the migration of GluA1 into, and GluA2 out of, the synapse, possibly through surface expressed, mineralocorticoid receptor-dependent, lateral diffusion (Karst et al., 2005; Groc et al., 2008b; Kurgers et al., 2010; Groeneweg et al., 2011). These findings provide persuasive evidence that a single session of forced treadmill exercise may prime motor regions through the peripheral release of CORT and subsequent activation of surface expressed mineralocorticoid receptors.

In support of the possibility that either BDNF, and/or CORT mechanisms are operating following exercise are previous data (Chapter 4) displaying a steep rise in circulating CORT and a significant increase in central BDNF (in absence of increases in peripheral BDNF). However, it remains unclear from our data as to the relative contributions made by BDNF and CORT to enhanced AMPA phosphorylation, and whether they work independently, or in combination following exercise. There is evidence to support the latter possibility; intraperitoneal injections of dexamethasone (synthetic corticosterone derivative) in post-natal day 18 rats enhanced pTrkB phosphorylation (Y816) in both cortex and hippocampus in the absence of any changes in central BDNF (Jeanneteau et al., 2008). Moreover, recruitment of TrkB by exogenous glucocorticoid stimulation is associated with contextual fear memory consolidation in the hippocampus (Chen et al., 2012). This relationship appears bidirectional, whereby exogenous administration of BDNF leads to enhancements in both glucocorticoid and mineralocorticoid receptor phosphorylation (Arango-Lievano et al., 2015). These data suggest the possibility that exercise may enhance LTP via a synergistic CORT/BDNF mechanism. Herein, we propose exercise priming of motor cortical regions is achieved through the combined influence of peripherally derived CORT (due to increased HPA activity), and centrally activated BDNF (resulting from enhanced neuronal activity within sensorimotor cortex) during exercise. We hypothesized these effects are responsible for the enhanced phosphorylation, and thus increased inclusion, of GluA1-containing AMPARs at synapses, which would promote the induction of LTP in the sensorimotor cortex.

5.2 METHODS

5.2.1 Animals

Male Sprague-Dawley rats (*Rattus norvegicus)* were purchased from Envigo™ at 6 weeks of age (weight 250-350 g). All animals were group housed in a temperature-controlled room on a reverse 12 : 12 light-dark cycle and allowed free access to both water and standard rodent chow. Animals were used in accordance with procedures approved by the University of Waterloo animal care and ethics committee.

5.2.2 Preparation of Sensorimotor Slices

Prior to slice incubation, rats were anesthetized with CO_2 and euthanized by decapitation. Brains were immediately removed and placed within an adult rat coronal brain matrix (Ted Pella, Inc., Redding, CA, USA) submerged in ice-cold artificial cerebral spinal fluid (ACSF) containing (in mM): 127.0 NaCl (Sigma, Oakville, ON, Canada; all subsequent reagents from Sigma, unless otherwise noted), 26.0 $NaHCO_3$, 10.0 glucose, 2.0 $CaCl_2$, 2.0 KCl, 2.0 $MgSO_4$, and 1.2 KH_2PO_4 and equilibrated with carbogen (95% O_2/5% CO_2), pH 7.37–7.43]. The most rostral 6 mm of the cortex (prefrontal cortex) was removed by a coronal cut at a position roughly corresponding to atlas plate 9 (Paxinos and Watson, 1982). The brain was then transferred to a Petri dish placed on ice and filled with ACSF, the cerebellum removed, and the brain hemisected. To prepare slices of the sensorimotor cortex, the hemisphere was placed on its mid-sagittal surface, and the ventral surface removed with an axial cut along the rhinal sulcus. The remaining tissue is then placed on the platform of a McIlwain Tissue chopper (mid-sagittal surface against the platform and rostral surface facing the blade) for slice extraction. Transverse sensorimotor slices (350 µm) were allowed to recover in warmed (35 ºC) ACSF for 1 h under constant 95% O_2 / 5% CO_2 mixture.

5.2.3 Drug Application

Acute sensorimotor cortex slices were then incubated in an interface chamber containing oxygenated ACSF at 35°C ± 0.5°C. In order to determine the relative contribution of BDNF, or CORT, we performed experiments whereby we bath applied BDNF, or CORT (or a combination) for 30 minutes prior to). Specifically, CORT was applied at 200 nM for 30 minutes under steady carbogen perfusion, as previously reported (Whitehead et al., 2013). BDNF was applied at 20 ng/mL for 30 minutes under standard perfusion. The selection of 20 ng/mL for BDNF was determined by previous work suggesting this concentration is ideal for enhancing LTP induction in the absence of altering resting membrane potential (Kang and Schuman, 1995; Akaneya et al., 1997). Following the bath application, samples were assessed using a previously established method for the enrichment of synaptic surface proteins.

5.2.3 Surface Biotinylation & Synaptoneurosome Preparation

As described in Chapter 4, biochemical analysis of tissue slices was conducted by combining surface biotinylation with synaptoneurosome preparation and analyzing each fraction by Western blot. Briefly, following 1 hour of recovery, slices are individually placed within separate wells of a 96 well plate, wherein each well contains 150 µL Sulfo-NHS-LL-biotin solution (1 mg / mL in ACSF) (Thermo Fisher Scientific, Massachusetts, USA). Following a 40-minute incubation at 4°C under gentle agitation, the biotin solution is removed and all slices gently washed 3x with cold quenching buffer (ACSF with 50 mM Trizma base) over ice to stop the reaction. All slices from each structure are then be placed in 2 mL Potter-Elvehjem homogenizing tube containing 350 µL of ice-cold modified Krebs-Henseleit buffer (mKRBS) [containing (in mM): 118.5 NaCl, 4.70 KCl, 1.18 $MgCl_2 \cdot 6H_2O$, 2.50 $CaCl_2 \cdot 2H_2O$, 1.18 KH_2PO_4,

24.90 $NaHCO_3$, 10.00 glucose, pH adjusted to ~7.40 using 1.0 N HCl]. A protease inhibitor cocktail (104 mM AEBSF, 80 µM Aprotinin, 4 mM Bestatin, 1.4 mM E-64, 2 mM Leupeptin and 1.5 mM Pepstatin) and a tyrosine phosphatase inhibitor (200 mM Na_3VO_4) will be included in the buffer to limit proteolysis and phosphatase activity. Slices will be homogenized with 20 manual pestle strokes over ice, and the homogenate placed in a 1.5 mL microtube over ice for 10 minutes to allow for gravity sedimentation. A small volume (50 µL) of the supernatant will be extracted and designated as the whole homogenate (WH), and the remaining supernatant used to prepare synaptoneurosomes.

Synaptoneurosomes were prepared by drawing the homogenate into a 1 cc Luer lock syringe and passing it through a 13 mm filter holder (XX3001200, EMD Millipore, Etobicoke, ON, Canada) containing 3 layers of pre-wetted (mKRBS) 100 µm pore nylon filters (NY1H02500, EMD Millipore). After this, 1 mL of air is passed through the filters (all filtrate and collected in a small Petri dish placed over ice. The filtrate will be then collected into a separate 1 cc Luer lock syringe and passed through a 13 mm filter holder containing a single pre-wetted (mKRBS) 5 µm nitrocellulose Durapore membrane filter (SVLP01300, Millipore) followed by 1 mL of air and collected into a 1.5 mL microtube. Microtubes will be spun at 1000 x g for 15 minutes at 4°C, supernatants were discarded and pellet re-suspended in 200 µL non-ionizing lysis buffer (10 mM Tris, 25 mM EDTA, 100 mM NaCl, 1% [v/v] Triton X-100, and 1% [v/v] NP-40, pH 7.4) containing protease and phosphatase inhibitors; 150 µL will be saved and designated as the synaptoneurosome preparation (SNP). Protein concentration will be determined with the use of Bio-Rad DC protein assay kit according to the manufacturer's recommended protocol.

Prior to use, NeutrAvidin™ beads are washed 3x with non-ionizing lysis buffer. Washed NeutrAvidin™ beads are incubated with the appropriate volume of homogenate for 4 h at 4ºC on a rocking platform. Bead-protein complexes are then washed 3x with non-ionizing lysis buffer and spun at 10,000 x g for 30 seconds. The pellet containing bead-protein complexes are re-suspended and denatured using 50 µL of 1x sample buffer (0.0625 M Tris, 2% [v/v] glycerol, 5% [w/v] sodium dodecyl sulfate [SDS], 5% [v/v] b-mercaptoethanol, and 0.001% [w/v] bromophenol blue, pH 6.8) at 95°C for 5 minutes. A final 10,000 x g spin (30 s) was completed, and the supernatant will be designated the synaptic surface fraction (SSF). All homogenates were stored at -80ºC until use.

5.2.4 Western Blotting

Samples were thawed on ice and then denatured in sample buffer (0.0625 M Tris, 2% [v/v] glycerol, 5% [w/v] sodium dodecyl sulfate [SDS], 5% [v/v] β-mercaptoethanol, and 0.001% [w/v] bromophenol blue, pH 6.8) at 95ºC for 5 min. Proteins were electrophoretically separated using a 10 or 15% SDS-polyacrylamide gel at 200 or 150 V, respectively for 1 h, and then electroblotted onto PVDF membranes via wet transfer (350 mA at 4ºC for 2 h). Blots underwent staining with Ponceau S solution, washed with deionized water, air dried, and then imaged to determine transfer efficiency and normalized protein densitometric signals.

Membranes were blocked using either 5% (w/v) bovine serum albumin (BSA), or 5% (w/v) non-fat milk in Tris-buffered saline with Tween-20 (TBST) for 1 h at room temperature and incubated with relevant antibodies overnight. All primary antibodies are diluted to 1:1000 in block buffer specific to the application. All antibodies were purchased from Cell Signaling unless otherwise stated. The following polyclonal antibodies were used: anti-BDNF (SC-546) from Santa Cruz, anti-phospho (Y869, Y873, Y876)-GluA2 (#3921), anti-phosphoY1472-NMDAR2B

(#4208), anti-NMDAR2B (#4207). Monoclonal antibodies used included: anti-phosphotyrosine (#05-321X; from Millipore), anti-phosphoS845-GluA1 (#8084), anti-GluA1 (#13185S), anti-GluA2 (#13607). On the following day, membranes were incubated in either rabbit (SC-2004), or mouse (SC-2005) IgG antibodies (1:5000) conjugated to horseradish peroxidase from Santa Cruz and immunoblotted using Luminata Classico, or Crescendo ECL substrate (Millipore) for 2 minutes. Optical densities were captured, normalized to Ponceau staining and analyzed as previously described (Thacker et al., 2016, Appendix I). Optical densities will be captured, normalized to ponceau and analyzed as previously described (Thacker et al., 2016, Appendix 1).

5.2.5 Statistical Methods and Sample Size Calculations

Based on a similarly designed study by Whitehead and colleagues (2017), we were able to derive the sample size required for the current project. Specifically, the study used $N = 6$ ($\alpha = 0.05$, $\beta\text{-}1 = 0.95$), for each drug group (CORT, BDNF, CORT+BDNF) for a total of 18 animals. Each set of treatment slices were controlled for by a parallel set of slices in a SHAM condition. Thus, each measure within each treatment is taken as a ratio of treatment/sham. With regards to the statistical analysis, comparisons of optical densitometry were completed using the Wilcoxon-signed-ranked test with a hypothetical value of 100% set for SHAM slices within each animal. Practical significance was determined by considering the p-value statistics combined with standardized effect sizes (Cohen's d) in a similar way as previously described (Chapter 3).

5.3 RESULTS

Previous work in our lab suggests a unique biochemical signature in response to a single session of moderate aerobic exercise (MOD) that involves the phosphorylation status of plasticity-related proteins. Specifically, we observed increases in phosphorylation of GluN2A and GluN2B, GluA1 and GluA2, that appear to be related to an activated state of pPKA and suppression of pCaMKII. Herein we investigated whether bath application of CORT, BDNF or CORT+BDNF could mirror the phosphorylation signature produced by MOD and whether the individual or combined application of these molecules altered the surface expression of plasticity-related receptors in a way that could provide evidence in favor of exercise-induced priming.

5.3.1 CORT selectively enhances glutamate receptor subunit phosphorylation and promotes GluN2B migration

A number of studies have suggested that the peripheral release of CORT following acute stress may be responsible for enhanced plasticity within the hippocampus. More specifically, one study displays a direct link between CORT and GluA1-containing AMPAR phosphorylation, resulting in an increased surface expression of GluA1-containing AMPARs that is PKA dependent (Whitehead et al., 2013). Since a similar response may account for exercise-induced priming within SMCx we investigated the response of SMCx to CORT on its own. As expected, we saw large increases in pGluA1 (S845) following 30 minutes of CORT exposure ($\bar{X}$ = 196 ± 52%, p = 0.090, d = 0.78), although this increase was not associated with any increase in either synaptic accumulation of GluA1 ($\bar{X}$ = 92 ± 19%, p = 0.84, d = 0.19), or synaptic surface expression of GluA1 ($\bar{X}$ = 102 ± 9%, p = 0.84, d = 0.070). The phosphorylation of GluA1 at S845 is known to be related to increased PKA activity, however, we observed no changes in pPKA ($\bar{X}$ = 102 ± 4%, p = 0.63, d = 0.20), suggesting an alternative pathway of activation for

pGluA1 (S845). Additionally, it has been suggested that CORT may also prime plasticity by substituting GluA2-containing AMPARs for GluA1-containing AMPARs at the synaptic surface, a process dependent on the phosphorylation of GluA2. However, we failed to observe a notable CORT-mediated change in pGluA2 (Y869,873,876) ($\bar{X}$ = 115 ± 20%, p = 0.56, d = 0.31), within synapses, which was matched by no clear change in both the synaptic presence ($\bar{X}$ = 90 ± 8%, p = 0.31, d = 0.48) and placement at the synaptic surface ($\bar{X}$ = 112 ± 8%, p = 0.22, d = 0.60). We further determined that the relative presence of these two receptor subunits (GluA1/GluA2) at the synaptic surface remained unchanged following treatment ($\bar{X}$ = 0.84 ± 12%, p = 0.44, d = 0.31).

Although CORT application failed to affect AMPAR receptor trafficking, it does appear to alter NMDAR trafficking. Specifically, CORT application appears to promote the increased synaptic surface expression of GluN2B ($\bar{X}$ = 155 ± 26%, p = 0.16, d = 0.77), but not GluN2A ($\bar{X}$ = 116 ± 27%, p = 0.69, d = 0.24). This subunit preference was also reflected in their relative presence at the synaptic surface (GluN2A/GluN2B) ($\bar{X}$ = 72 ± 13%, p = 0.16, d = 0.87). Interestingly, CORT application selectively promoted phosphorylation of GluN2A (Y1246) ($\bar{X}$ = 139 ± 14%, p = 0.13, d = 1.20) but not pGluN2B (Y1472) ($\bar{X}$ = 112 ± 20%, p = 0.56, d = 0.37). Previous investigations have shown glucocorticoids can rapidly activate pCaMKII (T286) to facilitate PKC activation which is required for the trafficking of NMDARs towards synapses (Ahmed, 2006; Yan et al., 2011); we observed an increase in pCaMKII ($\bar{X}$ = 157 ± 37%, p = 0.22, d = 0.64) in the current study. Together, these data support that CORT may promote some, but not all, of the characteristics observed following moderate exercise.

5.3.2 BDNF broadly promotes the synaptic surface expression of glutamate receptor subunits

In response to increased activity, neurons release a host of factors that foster adaptation within a given network. One such factor is BDNF, which is released in an activity-dependent manner and can influence both rapid and delayed responses within neurons (Poo, 2001; Leal et al., 2015). Specifically, BDNF plays a critical role in altering (via TrkB) the biophysical and trafficking properties of both NMDAR and AMPARs in the hippocampus (Itoh et al., 2016c). For this reason, we investigated whether the exogenous application of BDNF would have a similar influence on NMDAR and AMPAR activity. We observed that BDNF application generally promoted the increased surface expression of NMDAR subunits, although the magnitude of effect seen with GluN2A ($\bar{X}$ = 242 ± 57%, p = 0.06, d = 1.03) was clearly greater than that observed with GluN2B ($\bar{X}$ = 171 ± 48%, p = 0.56, d = 0.75). Moreover, these changes were not associated with the phosphorylated state of the subunits, as there were no differences in pGluN2A(Y1246) ($\bar{X}$ = 93 ± 10%, p = 0.56, d = 0.28), or pGluN2B(Y1472) ($\bar{X}$ = 92 ± 6%, p = 0.31, d = 0.5), results not unexpected as these sites are more related to their respective biophysical properties than trafficking (unlike pGluA1(S845) and pGluA2(Y869,873,876) which are directly related to AMPAR trafficking). With regards to AMPARs, BDNF promoted the increased surface expression of both GluA1 ($\bar{X}$ = 115 ± 7%, p = 0.06, d = 0.97) and GluA2 ($\bar{X}$ = 111 ± 4%, p = 0.03, d = 1.13), which was supported by a marked increase in pGluA1(S845) ($\bar{X}$ = 150 ± 16%, p = 0.03, d = 1.29) and a lack of change to pGluA2(Y869,873,876) ($\bar{X}$ = 99 ± 8%, p = 0.99, d = 0.05). Previously, we had suggested that exercise may augment pGluA1 either through increased PKA activity, or pCaMKII (via PKC). The current investigation revealed no change to pPKA activity following BDNF ($\bar{X}$ = 98 ± 8%, p = 0.88, d = 0.08) treatment, but did note increases in pCaMKII ($\bar{X}$ = 150 ± 16%, p =

0.03, d = 1.29). Taken together, these data suggest that BDNF may be account for a number of biochemical features, especially AMPAR receptor phosphorylation, previously observed following certain forms of exercise.

5.3.3 CORT + BDNF specifically enhances GluN2A and GluA1 phosphorylation, but fails to alter synaptic surface expression of either AMPAR or NMDAR subunits

Our previous work suggests that a single session of moderately intense exercise yields conditions that are conducive for plastic change. In particular, we noted an enhanced pGluN2 and pGluA1-2 pattern that was related to an increase in pPKA and decreased pCaMKII signaling. These data, together with our observation of a significant rise in peripheral CORT and central BDNF, lead us to question whether a combination of these factors could yield a similar biochemical signature to that of exercise. In summary, the combination of CORT+BDNF did not alter the synaptic surface expression of either GluN2A ($\bar{X}$ = 93 ± 10%, p = 0.63, d = 0.30), GluN2B ($\bar{X}$ = 76 ± 13%, p = 0.56, d = 0.30), GluA1 ($\bar{X}$ = 108 ± 11%, p = 0.44, d = 0.37), or GluA2 ($\bar{X}$ = 95 ± 13%, p = 0.56, d = 0.41). However, BDNF+CORT produced a large increase in both pGluN2A ($\bar{X}$ = 95 ± 13%, p = 0.22, d = 0.83) and pGluA1 ($\bar{X}$ = 172 ± 33%, p = 0.03, d = 0.90), but not pGluN2B ($\bar{X}$ = 110 ± 15%, p = 0.69, d = 0.25), or pGluA2 ($\bar{X}$ = 93 ± 10%, p = 0.56, d = 0.29). Moreover, following CORT+BDNF neither pCaMKII ($\bar{X}$ = 120 ± 15%, p = 0.69, d = 0.29), nor pPKA ($\bar{X}$ = 117 ± 12%, p = 0.34, d = 0.58) were significantly altered. The data presented here suggest that the combination of CORT+BDNF may best account for the previously observed phosphorylation differences following a moderate bout of aerobic exercise, however, these changes do not appear to be associated with an increased level of trafficking of either NMDARs, or AMPARs at synaptic sites.

5.4 DISCUSSION

Our previous investigations support a mechanism of exercise-induced priming that is related to an increase in AMPAR and NMDAR phosphorylation (Chapter 4). However, from these investigations, it remains unclear as to whether these changes in phosphorylation are related to the robust release in peripheral CORT or an increase in the activity-dependent release of central BDNF, or some other factor released during exercise. If CORT and BDNF are active contributors to exercise-induced priming as our data suggests, it is important to examine whether these hormones alone, or in combination, promote synaptic trafficking in a way that could account for exercise-induced priming. For this reason, we selected doses of CORT (200 nM) and BDNF (20 ng/mL) that others have shown to not induce LTP but enhance LTP following either chemical or electrical stimulation. To date, there is a large body of research supporting the role of BDNF and CORT independently in hippocampal-dependent plasticity, however, it is unknown whether these effects are similar within SMCx.

5.4.1 CORT partially accounts for phosphorylation changes during exercise-induced priming

Based on the data presented in the current chapter, it is clear that CORT and BDNF each produce a unique set of biochemical changes within the SMCx that agree with some of the changes observed with exercise-induced priming. In particular, CORT appears to increase the phosphorylation of pGluA1 (S845) and pGluN2A (Y1246), which we observed following MOD exercise in SMCx. Additionally, we observed increased GluN2B trafficking towards the synaptic surface following CORT (155 ± 16%). There is a precedent for increased pGluA1 in response to either CORT, or acute stress treatment within the hippocampus (Whitehead et al., 2013). However,

unlike previous reports that suggested increases in pGluA1 contributed to changes in total surface GluA1 (Whitehead et al., 2013), we did not detect changes at the synaptic surface following CORT. Considering previous work mentions a saturation in total surface GluA1 after 30 minutes of CORT exposure using a protocol identical to ours (i.e., same dose and sampling point), our results suggest a delay may occur between the rise in total surface GluA1 and an increased presence of GluA1 at the synaptic surface. In favor of this possibility, is work that indicates a sequential pattern for GluA1-containing AMPAR trafficking. Briefly, increased phosphorylation of GluA1 at S845 promotes migration and insertion into the perisynaptic membrane (Shi et al., 2001), but capture by synapses relies on calcium-activated transmembrane AMPAR regulatory proteins (TARPs) (e.g., stargazin) (Chen et al., 2000; Groc et al., 2008a; Choquet, 2010). Therefore, CORT-induced priming may take shape as increased GluA1 perisynaptic insertion, a process that, in essence, would prime the synapse until a subsequent increase in synaptic activity drove them into the synaptic density. The possibility is further supported by data in hippocampal cultures showing 100 nM of CORT activates leads to an increase in total surface expression of GluA1 and GluA2, but their synaptic content only increases upon cLTP (glycine + picrotoxin) stimulation (Groc et al., 2008a). Additional support in favor of the proposed mechanism stems from evidence suggesting a dose-response with regards to membrane mineralocorticoid and glucocorticoid receptors; specifically, low doses (< 200 nM) of CORT favor the activation mineralocorticoid receptors and lead to increased neuronal excitability, whereas high doses (> 1 μM) promote AMPAR internalization (Martin et al., 2009; Prager and Johnson, 2009; Prager et al., 2010).

In addition to changes to GluA1-containing AMPARs, we observed a large increase in pGluN2A following CORT exposure. Unlike the phosphorylation of GluA1 at S845, which governs its trafficking, phosphorylation of Y1246 enhances the ability of GluN2A-containing

NMDARs to flux Ca^{2+} (Takasu et al., 2002). Although there is a large body of research suggesting that stress influences NMDAR function (Popoli et al., 2012; Mcewen et al., 2015), to date there is a limited amount of literature regarding whether NMDARs are directly influenced by the acute application of CORT. However, the reports that have investigated this effect consistently propose CORT influences NMDARs by activating membrane-bound glucocorticoid and mineralocorticoids in a dose-dependent manner (Prager and Johnson, 2009). In particular, the acute (10-20 min) application of CORT (1-100 µM) to cultured hippocampal neurons from postnatal rats caused a significant enhancement in Ca^{2+} influx following NMDA-induced stimulation (Takahashi et al., 2002), which our findings suggest may be related directly to enhanced phosphorylation at the Y1246 site of GluN2A. However, 400 nM CORT (for 30 min) applied to hippocampal slices from young-adult mice lead to a significant decrease in NMDA-stimulated Ca^{2+} flux (Sato et al., 2004), a change that could reasonably be associated with decreased pGluN2A (Y1246). The discrepancy between our pGluN2A data, and this other investigation may be attributed to a number of differences between the studies. For example, our study used SMCx where both others assessed hippocampus, a region that has been routinely demonstrated to have an increased susceptibility to stress (McEwen, 1999; Mikasova et al., 2017), suggesting that CORT sensitivity within SMCx may be substantially different or a concentration effect may be evident (400 nM vs 100 nM of the current study) that produces a distinct dose response.

Finally, we found an increase in synaptic surface GluN2B with no change in GluN2A following CORT exposure. Although debate continues regarding the relative contribution of GluN2B at synapses, there is a long-held view that synaptic GluN2B is required to form the anchoring assemblies critical for the capture of GluA1-containing AMPARs at synaptic sites (Lisman and Zhabotinsky, 2001; Lisman et al., 2002). Our observation of increased GluN2B is in

direct agreement with a recent report displaying acute CORT (100 nM) exposure specifically alters the synaptic surface accumulation of GluN2B, but not GluN2A (as measured by single quantum dot tracking in hippocampal cultures) (Mikasova et al., 2017). Interestingly, this investigation determined that CORT-mediated GluA1 synaptic insertion was delayed until 90 min post-treatment, and was dependent on an initial redistribution of NMDAR at synapses (Mikasova et al., 2017). Furthermore, it was discovered if the synaptic accumulation of GluN1 was hindered immediately before, or after CORT administration, the level of the GluA1 present at this delayed time point was significantly reduced (Mikasova et al., 2017). In our study, we also observed a small, but noticeable, rise in GluN1 immediately following CORT treatment. In combination with our previously discussed data, we propose a model whereby CORT may account for a portion of the exercise-induced priming we previously observed in SMCx. First, a steep rise in CORT during exercise perfuses brain at a dose within the range needed to stimulate mineralocorticoid receptors, which go on to cause a cascade of events resulting in the increased phosphorylation of GluA1 and GluN2A, while simultaneously activating the migration of GluN2B from perisynaptic sites into synapses. The outlined changes "prime" synapses to be more receptive to incoming activity-dependent plasticity through the following hypothesized series of events: (1) pGluN2A will facilitate a greater postsynaptic Ca^{2+} response to high-frequency stimulation, (2) high intracellular Ca^{2+} activates pCaMKII, (3) which targets TARPs for activation, as well as (4) binds to GluN2B, which is now present in greater density at synapses (5) prompting the formation of AMPAR-anchoring assemblies, (6) that when paired with increased activation of TARPs, promote the capture of GluA1-containing AMPARs at synaptic sites yielding a greater level of potentiation.

5.4.2 BDNF enhances receptor trafficking that may contribute to exercise-induced priming

In addition to CORT, we also assessed the contribution BDNF may make to exercise-induced priming. Although BDNF exerts a broad array of both short and long-term effects that foster adaptation within the brain (Yamada et al., 2002), surprisingly, we did not find that the neurotrophic factor altered the phosphorylation status of any of the measured proteins in a fashion similar to MOD exercise, with the exception of pGluA1. However, our data agree with a number of studies that have investigated the independent effect of BDNF on phosphorylation. With regards to GluA1, BDNF has been shown to actively upregulate the phosphorylation status of GluA1 by recruiting the TrkB-PI3K–AKT pathway (Nakata and Nakamura, 2007); it remains to be determined if BDNF activates GluA2 through a similar pathway. Moreover, studies investigating the influence BDNF application has on isolated cortical, or hippocampal post-synaptic densities reveal that BDNF fails to activate tyrosine phosphorylation of GluN2A, although it does appear to activate GluN2B in a dose-dependent pattern. Further, we note an increase in pCaMKII following BDNF application, which others have suggested is the result of the TrkB activated inositol triphosphate receptor promoting the release of Ca^{2+} from internal stores (Nakata and Nakamura, 2007). Together, these data suggest that BDNF alone likely accounts for, at most, only a limited segment of the phosphorylation differences observed following MOD.

Comparatively, BDNF in our study does appear to alter the synaptic surface expression of both NMDARs and AMPARs in a way that may account for exercise-induced priming. Specifically, we revealed that BDNF promotes the insertion of GluN2A, GluN2B, and GluN1 at synaptic terminals, in addition to, increases in the trafficking of GluA1 and GluA2. In so far as AMPAR trafficking is concerned, our data provide convincing evidence that BDNF influences the

movement of GluA1 and GluA2-containing AMPARs and that this is achieved by altering the phosphorylation state of GluA1 and GluA2 to favor synaptic accumulation (Narisawa-saito et al., 2002; Caldeira et al., 2007; Fortin et al., 2012). In contrast, there is less known regarding the role BDNF may play in NMDAR trafficking. One of the few studies in the area, by Caldeira and colleagues (2007), supports a role for BDNF in NMDAR trafficking, as its acute application to hippocampal cultures lead to significant increases in the surface content of GluN1 and GluN2B within 30 min, however, GluN2A surface expression required 24 hours of BDNF stimulation (Caldeira et al., 2007). The disparity between our GluN2A trafficking results and theirs may reflect the increased specificity of our biotinylated fraction (which would have contained only the synaptic surface region), or it is possible that GluN2A may be more responsive at lower doses of BDNF (100 ng/mL vs 20 ng/mL in the current study). The most likely mechanism through which TrkB alters NMDAR trafficking is similar to how the neurotrophin affects the AMPAR, in that BDNF-TrkB results in the downstream activation of PKC and CaMKII (Minichiello et al., 2002; Minichiello, 2009). In particular, PKC activation is strongly associated with the abrupt trafficking of NMDARs at synapses (Lan et al., 2001; Yan et al., 2011).

In summary, we provide evidence in support of a model in which BDNF contributes to exercise-induced priming within SMCx, albeit to a limited degree. Aerobic exercise requires a high level of neuronal activity, which leads to an increased activity-dependent release of central BDNF. The increased presence of BDNF around synaptic terminals might then be expected to cause the following cascade of events: (1) increased activation of IP-3 receptors, leading to an NMDAR-independent release of intracellular stores of Ca^{2+}, (2) spikes in intracellular Ca^{2+} that stimulate the activation of PKC and PKC-induced CaMKII activation, which causes (3) increased PKC-dependent phosphorylation of GluN1 and GluN2 that non-specifically drives GluN2A and

GluN2B into synapses where they associate with CaMKII forming additional anchoring assemblies, and (4) the simultaneous activation of GluA1 and GluA2 resulting in their migration to the perisynaptic membrane where they are captured by TARPs activated via IP-3 receptor-dependent Ca^{2+} release.

5.4.3 CORT+BDNF provides a potential mechanism for exercise-induced priming

Finally, we wanted to investigate the possibility that exercise-induced priming may be the result of a combination of CORT+BDNF. Previous reports, in conjunction with the present study, provide evidence in favor of these two molecules to account for exercise-induced priming. However, emerging data support a substantial crossover in effectors between BDNF and CORT (Gray et al., 2014), with some evidence suggesting that peripheral CORT can even upregulate pTrkB (Y816) activity (Jeanneteau et al., 2008; Jeanneteau and Chao, 2013). Since we observed a marked increase of both CORT and BDNF with MOD exercise, we hypothesized a combination of the two would provide the best account for exercise-induced priming. The present study revealed that the combination of CORT+BDNF produced a profile that reflected many aspects of our previously observed changes in phosphorylation to both AMPAR, NMDAR and kinase intermediaries following MOD (Table 1). Specifically, results show an increase in phosphorylation of GluN2A, GluA1, and PKA, which were all upregulated following MOD. Additional CORT+BDNF did not alter the surface expression to a meaningful degree of GluN2B, GluA2 and or the phosphorylation of CaMKII, although GluN2B and GluA2 phosphorylation changes were on average in a direction similar to MOD. Interestingly, we did not observe the previously mentioned BDNF-dependent changes in synaptic surface trafficking of any receptors. These data indicate that the addition of CORT may prevent BDNF-induced trafficking, which may be in response to a convergence of CORT and BDNF effects on TrkB. Moreover, there are a number of

factors that might contribute to why CORT+BDNF does not directly mirror MOD. First, the doses we used in this study were selected based on the likelihood that they would prime LTP induction in the hippocampus. Thus, our data would support that the dose used in the present study was sub-optimal for replicating findings of MOD, it remains unclear as to whether this combination of dose caused an over or under stimulation of either TrkB or glucocorticoid receptors. However, these effects are also likely to be related to the temporal nature of CORT+BDNF. During the current study, we investigated the immediate and simultaneous application of CORT and BDNF. This is in contrast to the *in vivo* state during exercise, whereby the initial increased activity of exercise results in an increased release of BDNF from neurons, followed by a ramping up of peripheral CORT. Microdialysis studies in hippocampus suggest that CORT levels peak 20 min after a noticeable rise in peripheral plasma levels following an acute stressor (Droste et al., 2008). Thus, it is possible that a pretreatment of BDNF followed by a simultaneous application of CORT may provide a more ideal model of *in vivo* exercise.

5.5 CONCLUSION

The present study provides evidence that both BDNF and CORT can have a priming influence over SMCx, although neither alone can account exclusive for exercise-induced priming following MOD. It remains unknown, but plausible that a combined CORT+BDNF mechanism best accounts for the priming influence observed following MOD. In addition, the current results provide the support in favor of the hypothesis that exercise-induced priming occurs via altered synaptic trafficking.

FIGURE LEGENDS

Figure 5.1 Timeline illustrating study protocol on the day of euthanasia. After preparation, each SHAM (n = 8 slices) and treatment (n = 8 slices) slice was allowed to recover for 1 hour. Each treatment CORT (200 nM), BDNF (20 ng/mL) or CORT+BDNF group (N = 6 animals), slices were incubated in a separated treatment chamber for 30 minutes. Following treatment, slices were immediately prepared using the BioSyn method presented in Chapter 4.

Figure 5.2 (A) Synaptic surface expression of NMDAR subunit GluN2A in sensorimotor cortex (n = 6/group). Each CORT, BDNF and CORT+BDNF sample is taken as the ratio of ponceau and then taken as a percentage of SHAM. (B) Y1246 phosphorylation site and total synaptic expression of the NMDAR subunit GluN2A in sensorimotor cortex (n = 6/group). Each CORT, BDNF, and CORT+BDNF sample pGluN2A optical density is taken as a ratio of total GluN2A and displayed relative to SHAM pGluN2A/GluN2A. Total GluN2A is taken as a ratio to ponceau and displayed relative to SHAM GluN2A/ponceau * denotes statistical significance ($p < 0.05$).

Figure 5.3 (A) Synaptic surface expression of NMDAR subunit GluN2B in sensorimotor cortex (n = 6/group). Each CORT, BDNF and CORT+BDNF sample is taken as the ratio of ponceau and then taken as a percentage of SHAM. (B) Y1472 phosphorylation site and total synaptic expression of the NMDAR subunit GluN2B in sensorimotor cortex (n = 6/group). Each CORT, BDNF, and CORT+BDNF sample pGluN2A optical density is taken as a ratio of total GluN2B and displayed relative to SHAM pGluN2B/GluN2B. * denotes statistical significance ($p < 0.05$) Total GluN2B is taken as a ratio to ponceau and displayed relative to SHAM GluN2B/ponceau.

Figure 5.4 Synaptic surface expression of NMDAR subunit GluN1 in sensorimotor cortex (n = 6/group). Each CORT, BDNF and CORT+BDNF sample is taken as the ratio of ponceau and then taken as a percentage of SHAM. * denotes statistical significance ($p < 0.05$).

Figure 5.5 (A) Synaptic surface expression of AMPAR subunit GluA1 in sensorimotor cortex (n = 6/group). Each CORT, BDNF and CORT+BDNF sample is taken as the ratio of ponceau and then taken as a percentage of SHAM. (B) S845 phosphorylation site and total synaptic expression of the AMPAR subunit GluA1 in sensorimotor cortex (n = 6/group). Each CORT, BDNF, and CORT+BDNF sample pGluA1 optical density is taken as a ratio of total GluA1 and displayed relative to SHAM pGluA1/GluA1. Total GluA1 is taken as a ratio to ponceau and displayed relative to SHAM GluA1/ponceau * denotes statistical significance ($p < 0.05$).

Figure 5.6 (A) Synaptic surface expression of AMPAR subunit GluA2 in sensorimotor cortex (n = 6/group). Each CORT, BDNF and CORT+BDNF sample is taken as the ratio of ponceau and then taken as a percentage of SHAM. (B) Y869,873,876 phosphorylation site and total synaptic expression of the NMDAR subunit GluA1 in sensorimotor cortex (n = 6/group). Each CORT, BDNF, and CORT+BDNF sample pGluA2 optical density is taken as a ratio of total GluA2 and displayed relative to SHAM pGluA2/GluA2. Total GluA2 is taken as a ratio to ponceau and displayed relative to SHAM GluA2/ponceau. * denotes statistical significance ($p < 0.05$).

Figure 5.7 T286 phosphorylation site and total synaptic expression of the CaMKII in sensorimotor cortex (n = 6/group). Each CORT, BDNF and CORT+BDNF sample pCaMKII optical density is

taken as a ratio of total CaMKII and displayed relative to SHAM pCaMKII/CaMKII. Total CaMKII is taken as a ratio to ponceau and displayed relative to SHAM pCaMKII/ponceau. * denotes statistical significance ($p < 0.05$).

Figure 5.8 T197 phosphorylation site and total synaptic expression of the PKA in sensorimotor cortex (n = 6/group). Each CORT, BDNF and CORT+BDNF sample pPKA optical density is taken as a ratio of total PKA and displayed relative to SHAM pPKA/PKA. Total PKA is taken as a ratio to ponceau and displayed relative to SHAM PKA/ponceau. * denotes statistical significance ($p < 0.05$).

Figure 5.1

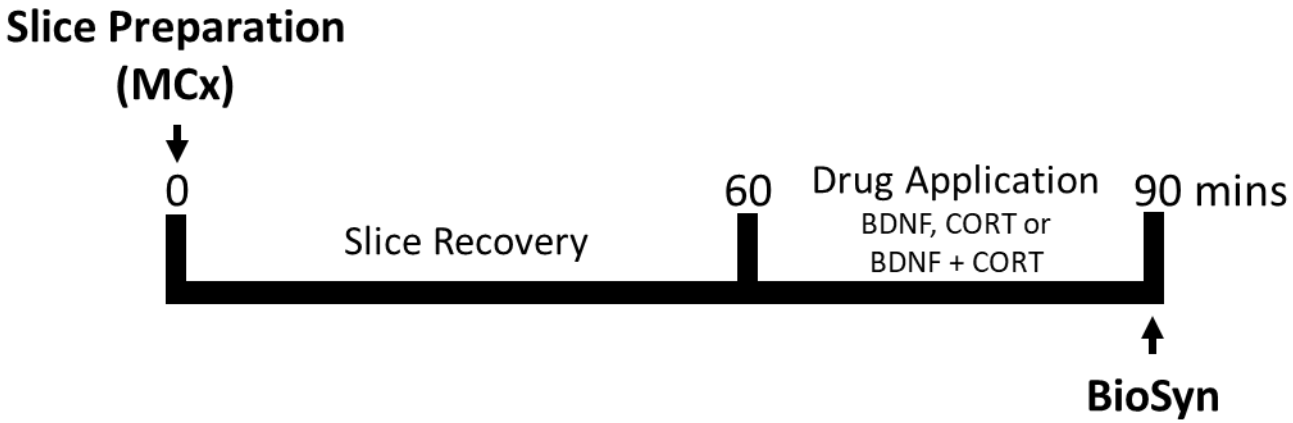
Slice Preparation
(MCx)
0
Slice Recovery
60
Drug Application
BDNF, CORT or
BDNF + CORT
90 mins
BioSyn

Figure 5.2

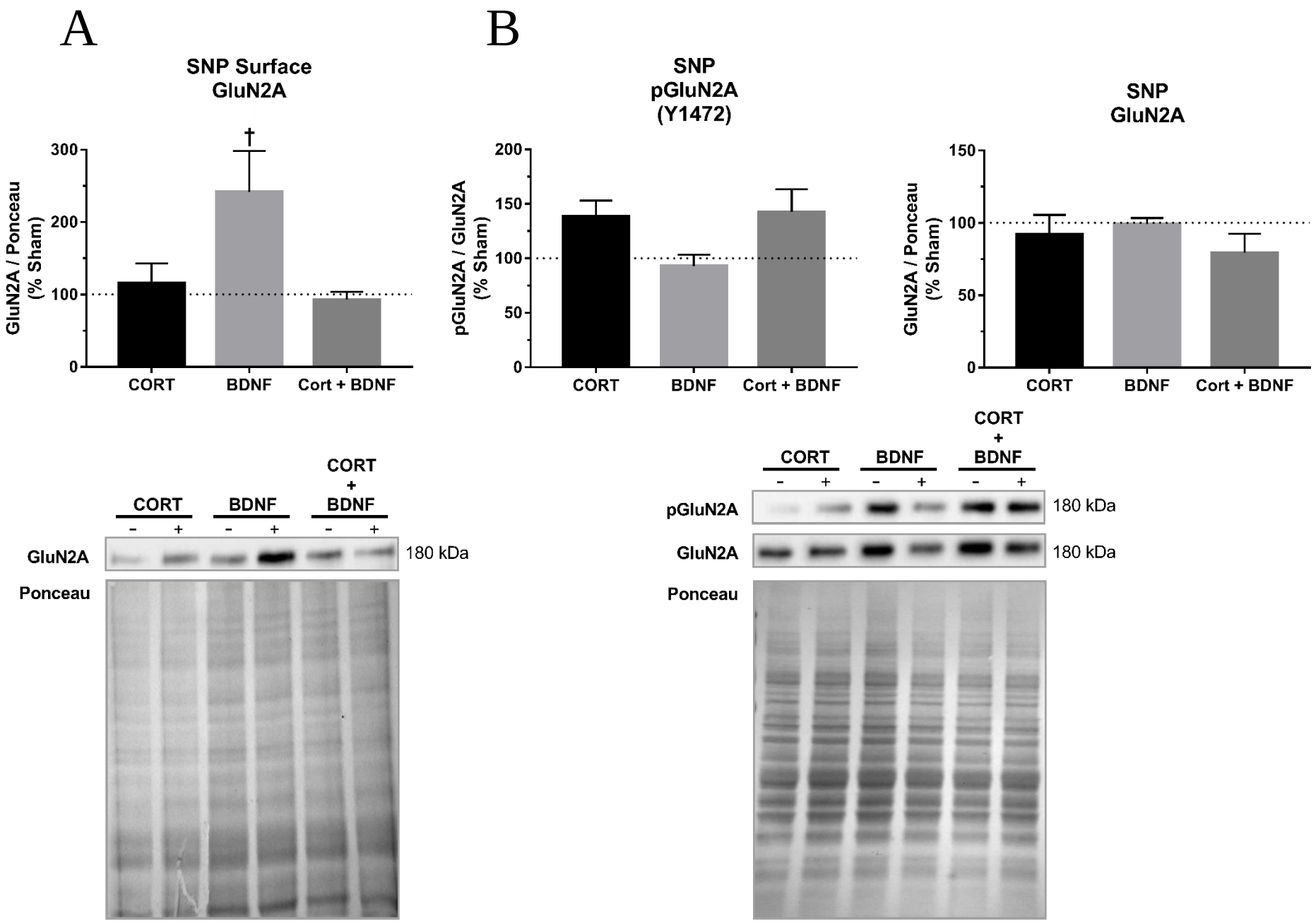
A
SNP Surface GluN2A
GluN2A / Ponceau (% Sham)
300
200
100
0
†
CORT
BDNF
Cort + BDNF
B
SNP pGluN2A (Y1472)
pGluN2A / GluN2A (% Sham)
200
150
100
50
0
CORT
BDNF
Cort + BDNF
SNP GluN2A
GluN2A / Ponceau (% Sham)
150
100
50
0
CORT
BDNF
Cort + BDNF
CORT
BDNF
CORT + BDNF
- + - + - +
GluN2A
180 kDa
Ponceau
CORT
BDNF
CORT + BDNF
- + - + - +
pGluN2A
180 kDa
GluN2A
180 kDa
Ponceau

Figure 5.3

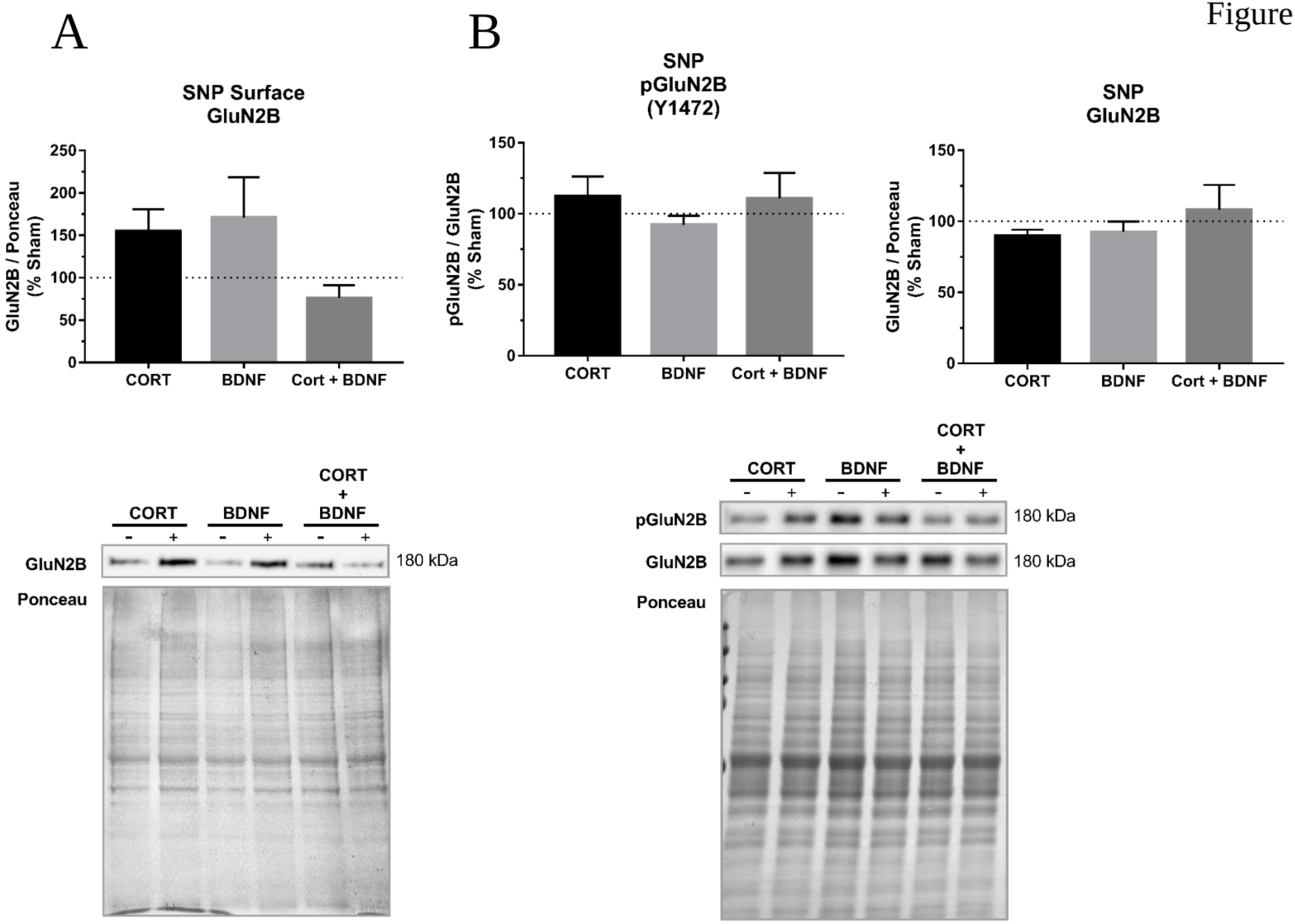
A
SNP Surface GluN2B
GluN2B / Ponceau (% Sham)
250
200
150
100
50
0
CORT
BDNF
Cort + BDNF
B
SNP pGluN2B (Y1472)
pGluN2B / GluN2B (% Sham)
150
100
50
0
CORT
BDNF
Cort + BDNF
SNP GluN2B
GluN2B / Ponceau (% Sham)
150
100
50
0
CORT
BDNF
Cort + BDNF
CORT
BDNF
CORT + BDNF
- + - + - +
GluN2B
180 kDa
Ponceau
CORT
BDNF
CORT + BDNF
- + - + - +
pGluN2B
180 kDa
GluN2B
180 kDa
Ponceau

Figure 5.4

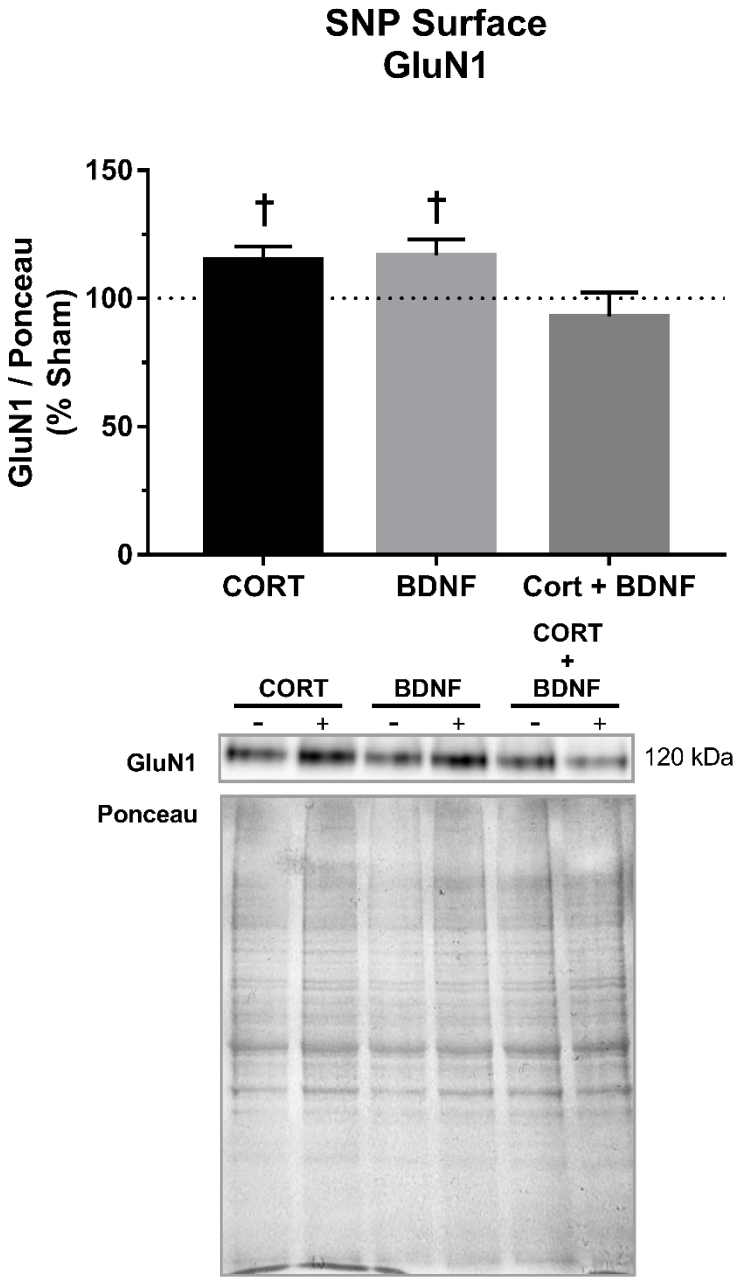
SNP Surface
GluN1
GluN1 / Ponceau
(% Sham)
150
100
50
0
†
†
CORT
BDNF
Cort + BDNF
CORT
BDNF
CORT
+
BDNF
-
+
-
+
-
+
GluN1
120 kDa
Ponceau

Figure 5.5

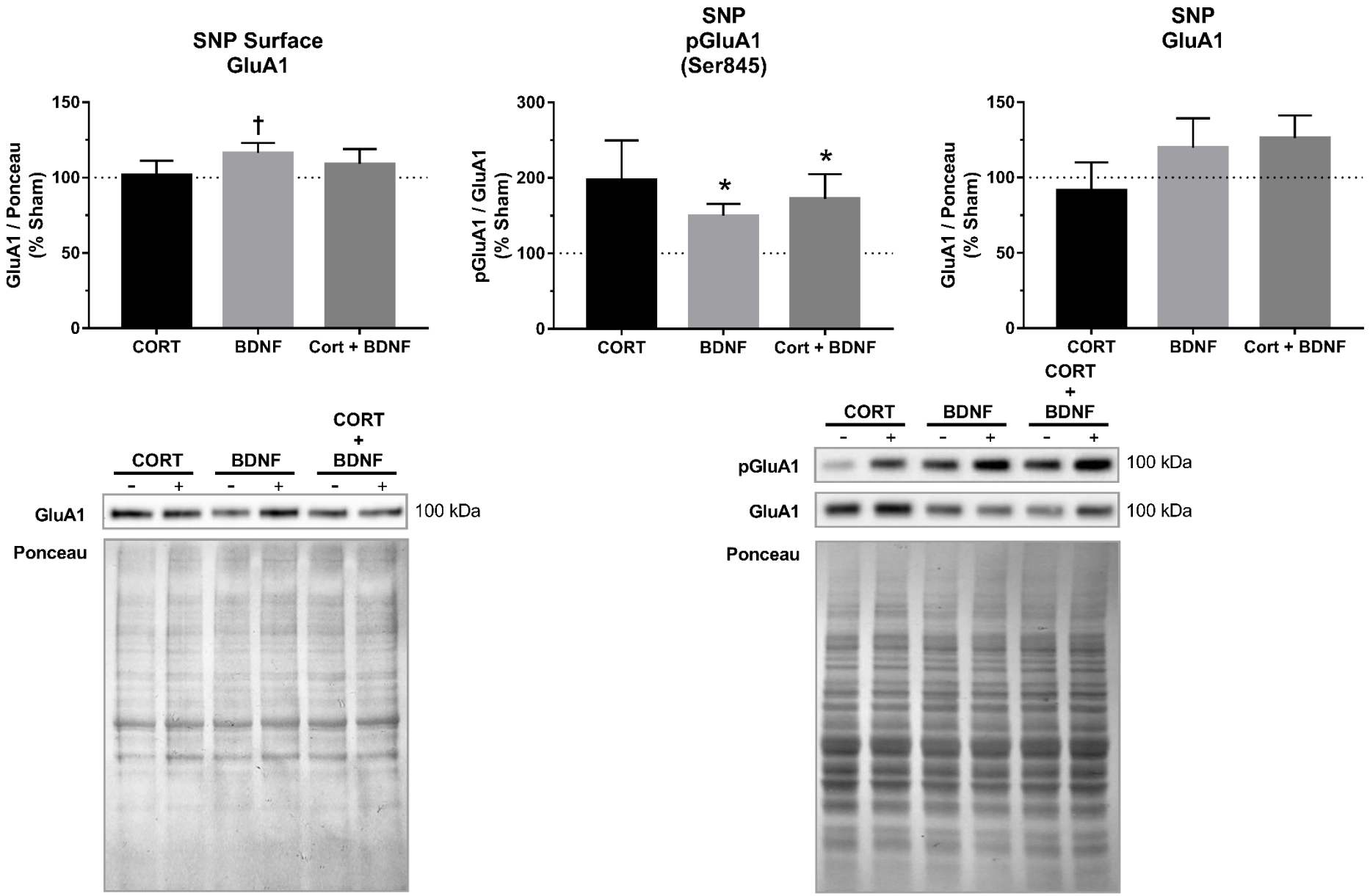
A
B
SNP Surface GluA1
GluA1 / Ponceau (% Sham)
150
100
50
0
†
CORT
BDNF
Cort + BDNF
SNP pGluA1 (Ser845)
pGluA1 / GluA1 (% Sham)
300
200
100
0
*
*
CORT
BDNF
Cort + BDNF
SNP GluA1
GluA1 / Ponceau (% Sham)
150
100
50
0
CORT
BDNF
Cort + BDNF
CORT
BDNF
CORT + BDNF
- + - + - +
GluA1
100 kDa
Ponceau
CORT
BDNF
CORT + BDNF
- + - + - +
pGluA1
100 kDa
GluA1
100 kDa
Ponceau

Figure 5.6

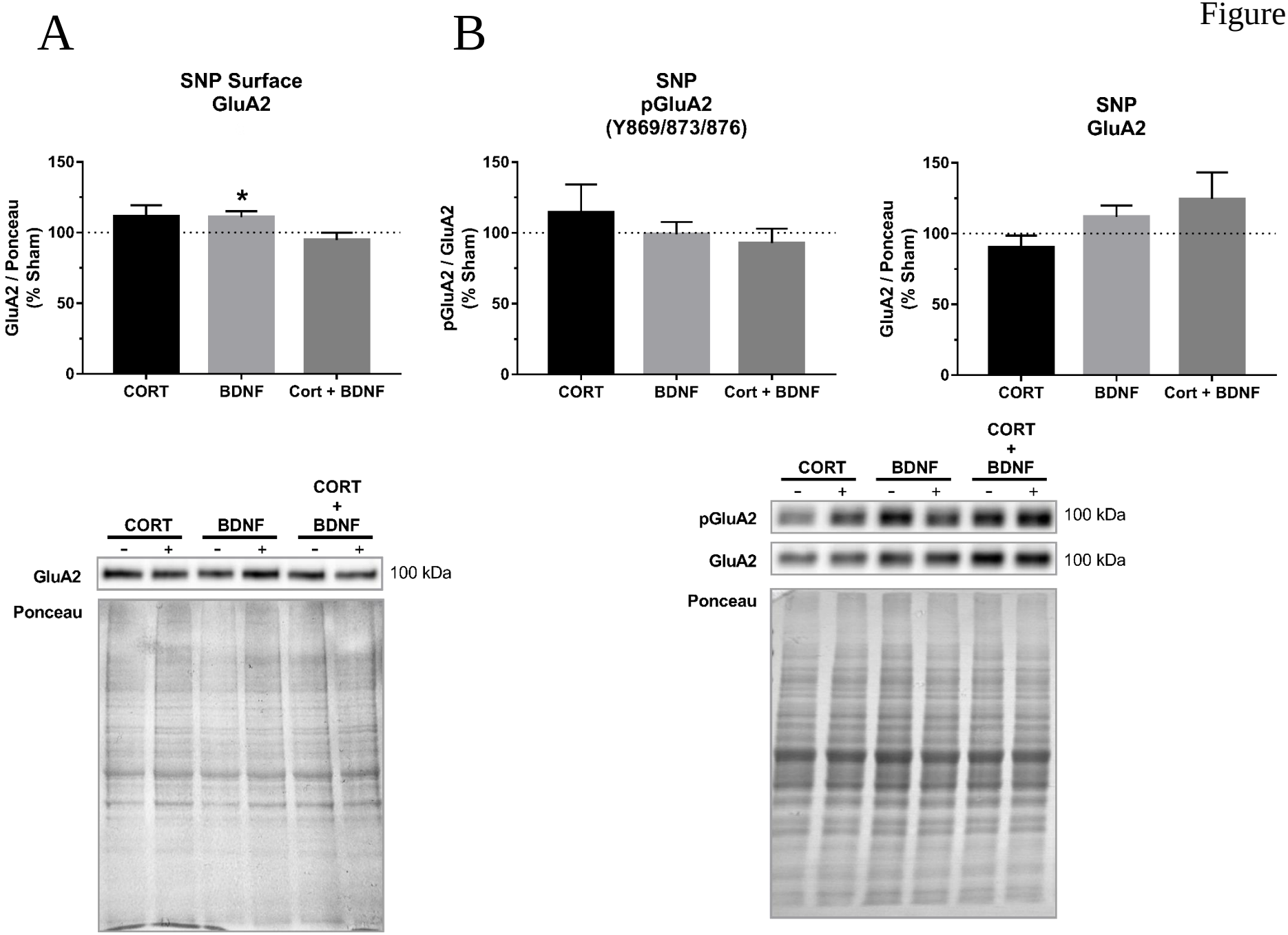
A
SNP Surface
GluA2
GluA2 / Ponceau
(% Sham)
150
100
50
0
*
CORT
BDNF
Cort + BDNF
CORT
+
BDNF
- + - + - +
GluA2
100 kDa
Ponceau
B
SNP
pGluA2
(Y869/873/876)
pGluA2 / GluA2
(% Sham)
SNP
GluA2
pGluA2
GluA2
100 kDa
100 kDa
Ponceau

Figure 5.7

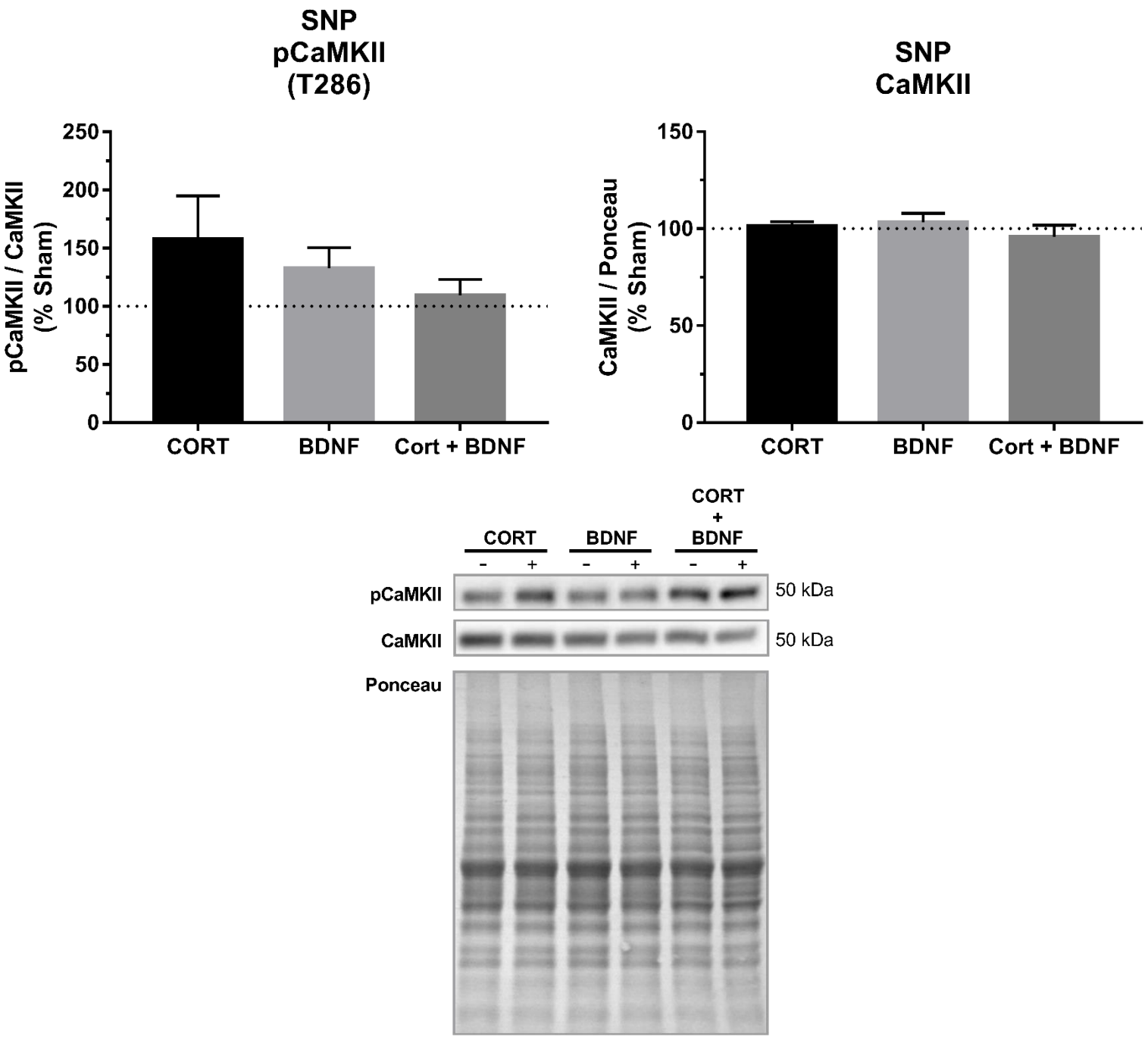
SNP
pCaMKII
(T286)
pCaMKII / CaMKII
(% Sham)
250
200
150
100
50
0
CORT
BDNF
Cort + BDNF
SNP
CaMKII
CaMKII / Ponceau
(% Sham)
150
100
50
0
CORT
BDNF
Cort + BDNF
CORT
+
BDNF
CORT
BDNF
- + - + - +
pCaMKII
50 kDa
CaMKII
50 kDa
Ponceau

Figure 5.8

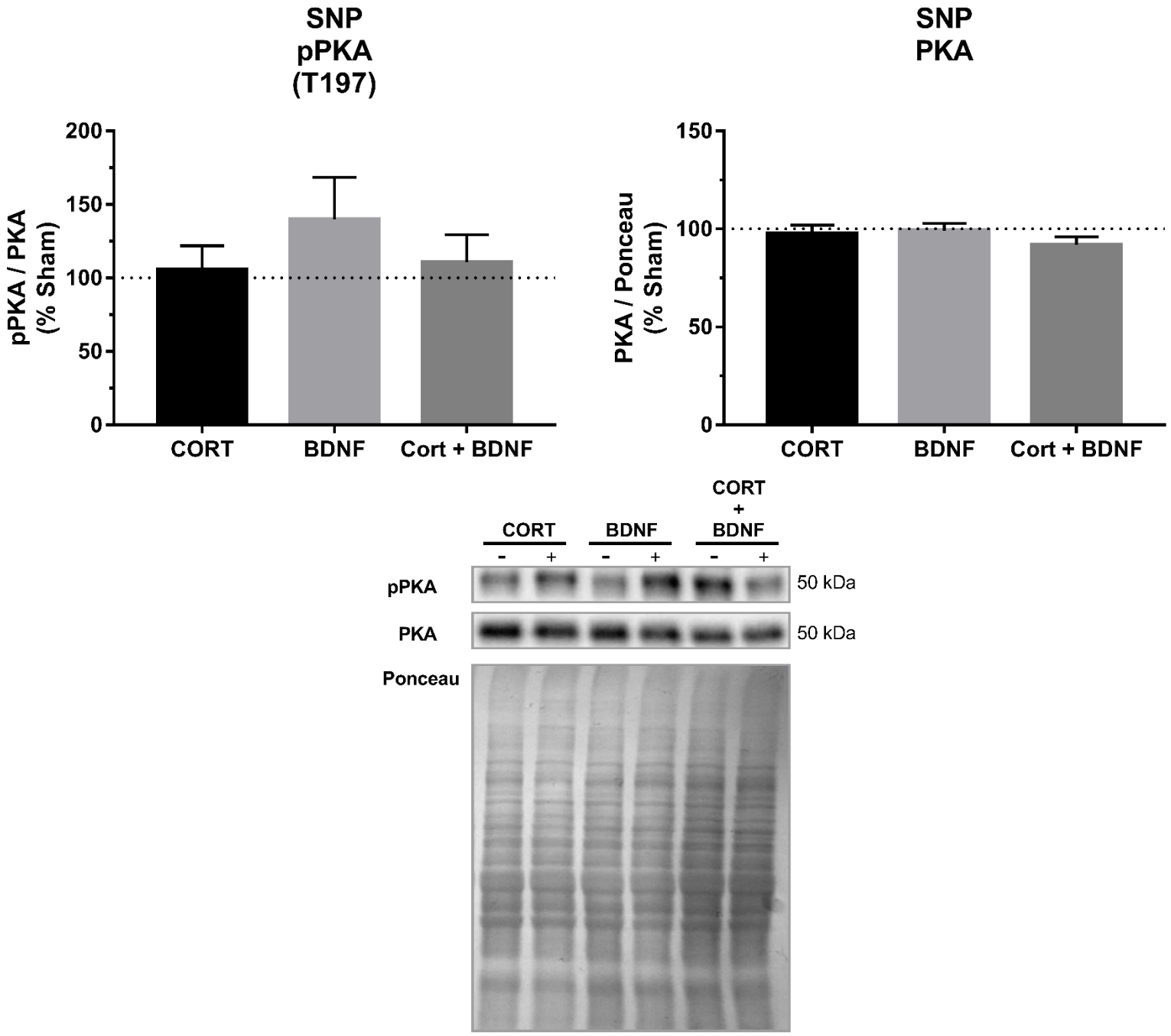
SNP
pPKA
(T197)
pPKA / PKA
(% Sham)
200
150
100
50
0
CORT
BDNF
Cort + BDNF
SNP
PKA
PKA / Ponceau
(% Sham)
150
100
50
0
CORT
BDNF
Cort + BDNF
CORT
BDNF
CORT
+
BDNF
- + - + - +
pPKA
50 kDa
PKA
50 kDa
Ponceau

Table 5.1 – Summary of effect sizes compared to MOD

Protein of Interest	MOD Exercise	CORT	BDNF	CORT+BDNF
pGluN2A	**↑**	**↑↑**	↔	**↑**
pGluN2B	**↑↑**	↔	↓	↔
pGluA1	**↑↑**	**↑**	**↑↑**	**↑**
pGluA2	**↑↑**	↔	↔	↔
pPKA	**↑**	↔	**↑↑**	↔
pCaMKII	**↓↓**	↑	↑	↔

Note: **Cohen's d: ↔ = ≤ 0.5, ↑ = 0.5-1.0, ↑↑ / ↓↓ = ≥ 1.0.**

Bold signifies whether direction matches MOD, while arrow describes the direction of effect.

Table 5.2 – Summary all synaptic surface data

Protein Target	Treatment	Mean ± SEM (%)	df	p	Effect Size (Cohen's d)
GluN2A	Cort	115 ± 27	5	0.69	0.24
	BDNF	242 ± 57	5	0.06	1.03
	Cort+BDNF	93 ± 11	5	0.63	0.30
GluN2B	Cort	155 ± 26	5	0.16	0.77
	BDNF	171 ± 48	5	0.56	0.75
	Cort+BDNF	76 ± 15	4	0.31	0.30
GluN1	Cort	112 ± 5	4	0.06	1.28
	BDNF	131 ± 16	5	0.03	0.82
	Cort+BDNF	118 ± 27	5	0.84	0.29
GluA1	Cort	101 ± 10	5	0.84	0.07
	BDNF	116 ± 7	5	0.06	0.97
	Cort+BDNF	109 ± 10	5	0.44	0.37
GluA2	Cort	112 ± 8	5	0.22	0.78
	BDNF	111 ± 4	5	0.03	1.12
	Cort+BDNF	95 ± 5	5	0.69	0.35

Table 5.3 – Summary all phospho- & total synaptic protein

Protein Target	Treatment	Mean ± SEM (%)	df	p	Effect Size (Cohen's d)
pGluN2A	Cort	139 ± 14	4	0.13	1.20
	BDNF	93 ± 10	5	0.56	0.28
	Cort+BDNF	143 ± 21	5	0.16	0.83
GluN2A	Cort	92 ± 14	5	0.56	0.24
	BDNF	99 ± 4	5	0.84	0.06
	Cort+BDNF	79 ± 13	5	0.22	0.65
pGluN2B	Cort	113 ± 14	5	0.56	0.37
	BDNF	92 ± 6	5	0.31	0.50
	Cort+BDNF	111 ± 18	5	0.69	0.25
GluA2B	Cort	90 ± 5	5	0.16	0.94
	BDNF	93 ± 7	5	0.44	0.42
	Cort+BDNF	108 ± 18	5	0.69	0.19
pGluA1	Cort	194 ± 54	5	0.09	0.75
	BDNF	136 ± 14	5	0.03	1.29
	Cort+BDNF	182 ± 30	5	0.03	0.90
GluA1	Cort	92 ± 19	5	0.84	0.19
	BDNF	120 ± 20	5	0.44	0.41
	Cort+BDNF	126 ± 15	5	0.09	0.73
pGluA2	Cort	115 ± 20	5	0.56	0.31
	BDNF	99 ± 9	5	0.99	0.05
	Cort+BDNF	93 ± 10	5	0.56	0.29
GluA2	Cort	90 ± 8	5	0.31	0.48
	BDNF	112 ± 8	5	0.31	0.59
	Cort+BDNF	125 ± 19	5	0.56	0.54
pCaMKII	Cort	158 ± 37	5	0.22	0.64
	BDNF	133 ± 18	5	0.16	0.76

	Cort+BDNF	113 ± 14	5	0.69	0.29
CaMKII	Cort	101 ± 2	5	0.56	0.25
	BDNF	103 ± 5	5	0.43	0.30
	Cort+BDNF	96 ± 6	5	0.84	0.29
pPKA	Cort	106 ± 16	5	0.69	0.15
	BDNF	140 ± 28	5	0.44	0.57
	Cort+BDNF	111 ± 19	5	0.69	0.24
PKA	Cort	98 ± 4	5	0.99	0.22
	BDNF	99 ± 4	5	0.84	0.09
	Cort+BDNF	92 ± 4	5	0.16	0.83

6. General Thesis Discussion

6.1 Summary of main findings

There is a growing body of literature that supports the use of acute aerobic exercise to prime motor regions of brain to be more receptive to the acquisition of skill following movement training (Ploughman et al., 2007; Roig et al., 2012; Mang et al., 2013a; Skriver et al., 2014; Statton et al., 2015). However, there remains a paucity of knowledge regarding the underlying cellular mechanisms that contribute to the exercise-induced priming phenomenon. The purpose of this dissertation was to identify a plausible mechanism to link previously observed exercise-induced priming effects with the biochemical correlates of learning; specifically, the subset of plasticity-related proteins, including glutamate receptors and related protein kinases, critical for the induction of LTP (the best characterized synaptic model of learning and memory).

We began in Chapter 2 by investigating the influence that a single session of aerobic exercise may have on the expression of key glutamatergic receptor subunit proteins (i.e., NMDAR and AMPAR subunits), in addition to the expression of a well-known plasticity-related intermediary kinase, CaMKII. To supplement our investigation, we devised a novel approach for the rapid and reproducible isolation of rat sensorimotor cortex. In addition, at the outset of this investigation, it was not known what would be the minimal amount of exercise required to induce plasticity-related changes within the motor cortex. Therefore, we explored the potential influence of treadmill acclimatization along with the outcome of a single session of exhaustive exercise on plasticity-related protein expression. We determined that both acclimatization and a single bout of exhaustive exercise failed to alter expression of either NMDAR, or AMPAR subunits, or CaMKII and concluded, as hypothesized, that the time-course required for changes in protein expression could not account for the exercise-induced priming previously observed immediately following exercise cessation, as has been suggested.

We next turned our investigation, in Chapter 3, towards the notion that a single session of exercise is more likely to enhance plasticity through changes at the level of existing proteins; that is, changes at the level of post-translational modifications (given that phosphorylation is markedly increased during, and critical for, early stages of LTP) (Wang and Salter, 1994; Hayashi et al., 2000; Soderling and Derkach, 2000). Thus, we assessed total tyrosine phosphorylation as a proxy for synaptic activity and determined a broad exercise-induced augmentation in tyrosine phosphorylation, particularly at molecular weights corresponding to the key, upstream plasticity-related proteins. Our follow-up experiments determined that both NMDAR and AMPAR subunit phosphorylation was elevated following moderate, but not exhaustive, exercise. Specifically, GluA1 (S845) and GluA2 (Y869,873,876) which govern the ability of these receptors to traffic towards, or away from synapses, was robustly affected following MOD, but not GXT, exercise. These data are in support of a hypothesis emerging from human studies showing that exercise-induced effects display a dependency on intensity in an inverted-U like pattern (Kamijo et al., 2004a, 2007; Lambourne and Tomporowski, 2010). Our investigation into the mechanisms underlying this unique pattern of phosphorylation led us to uncover a kinase-specific activation pattern following MOD, whereby PKA activity was upregulated and CaMKII was suppressed. Furthermore, we observed a large spike in peripheral corticosterone and central BDNF, but no change in peripheral BDNF, which has been shown to increase the following exercise in humans. Based on the findings from this study we posed two questions, (1) Does exercise-induced phosphorylation of AMPARs promote the trafficking and incorporation of these receptors at synapses? and (2) What are the relative contributions of BDNF and CORT to the observed pattern of exercise-induced phosphorylation?

In order to appropriately measure whether exercise not only promotes the trafficking of AMPARs, but also their presence at synaptic terminals, we required a technique that could isolate, with a high degree of specificity, the post-synaptic surface fraction of neurons. As a result, we developed an approach that combines two previously well-established techniques, biotinylation and synaptoneurosome enrichment. We conducted a series of experiments that convincingly led to a homogenate enriched with synaptic surface proteins. Moreover, we confirmed the sensitivity of the technique by showing its ability to capture the receptor trafficking that follows a chemical form of LTP induction. Together, we concluded that this "BioSyn" technique provides a powerful tool for the exploration of various sub-neuronal fractions, in addition to receptor trafficking events involved in plasticity.

The final chapter of this thesis investigated, with the aid of the BioSyn technique, changes to phosphorylation and trafficking of NMDAR and AMPAR subunits that follow the application of CORT, BDNF, and BDNF+CORT, in an effort to gauge their relative contributions to exercise-induced priming. The findings from Chapter 5 suggest that CORT and BDNF can reasonably be connected to the cellular-level changes believed to account for exercise-induced priming. Generally, it was discovered that CORT selectively increases phosphorylation status, whereas BDNF favors receptor trafficking of glutamatergic receptors. The combined CORT+BDNF data provide preliminary evidence that an interplay of these mechanisms may provide the best explanation for the occurrence of exercise-induced priming, however, it is likely that both the dose and temporality of drug application are important factors to consider when further examining the role of these hormones on underlying mechanisms.

6.2 Implications of current results and generalization of findings

As a whole, this thesis provides a foundation for the exploration of the cellular mechanisms underlying exercise-induced priming within the sensorimotor cortex. Herein, we propose a mechanism whereby forced treadmill exercise stimulates the release of CORT peripherally, and BDNF centrally, in a dose and possibly time-dependent pattern (not explored in this thesis), creating a unique set of conditions favoring the induction of sensorimotor cortical plasticity via enhanced glutamatergic signaling and trafficking. Alongside human studies using non-invasive stimulation (Singh et al., 2014a, 2014b; Neva et al., 2017), our results agree that the post exercise-induced priming within motor cortex appears to be more weighted towards LTP than LTD, which may argue for a temporary shift in the metaplastic state (i.e., altered ability/capacity to induce plasticity) following exercise. Thus, we provide further support for a potential use of the post-exercise time window to enhance the acquisition and consolidation of motor learning, or re-learning, which could have a profound impact on improving recovery following neurological injury.

6.2.1 Priming the brain to learn

The notion that the brain can be primed to learn is not new. There is a plethora of data supporting the use of preconditioning stimuli (including pharmacological, behavioral, and non-invasive electrical stimulation techniques) to improve behavioral outcomes following training (Schacter and Buckner, 1998; Cohen et al., 1999; Hallett, 2007; Schabrun and Chipchase, 2012; Cassidy et al., 2014). This thesis contributes to this growing body of research by outlining a cellular mechanism through which priming may occur. The possibility exists that, in addition to exercise, the priming phenomena observed in this study may be conserved across a number of other forms of priming. Specifically, phosphorylation changes at the level of AMPARs and NMDARs may

reflect the earliest adaptation to account for immediate priming following a variety of preconditioning stimuli (Klann, 2002; Yang et al., 2011; Rodríguez-Durán and Escobar, 2014). Although gene expression was not assessed in this thesis, as it was believed that changes of this nature would be to slow to account for exercise-induced priming, it is likely that changes in the level of gene expression, protein transcription and translation may be involved in the stability of priming phenomenon at delayed sampling points. In Chapter 5, we observed that BDNF and CORT, either alone or in combination, produced similar responses with regards to the phosphorylation status of GluA1(S845). These data are in further support for GluA1-containing AMPARs as primary sites to consider when evaluating the priming phenomenon. Overall, our understanding of how exercise-induced priming contributes to learning remains very much in its infancy, however, this thesis provides a foundation on which to build a new set of questions.

6.2.2 Divergent influence of single session exercise by brain region

Historically, there has been a strong bias towards using the HP as the primary model of neuronal function, and there is strong support for chronic exercise-induced effects within rodent hippocampus (Cotman and Engesser-Cesar, 2002; Redila and Christie, 2006; Patten et al., 2013). However, the unique nature of the hippocampus draws caution to its generalizability across other brain regions, as research over the past decade has revealed significant differences even within the hippocampal longitudinal axis (Ashton et al., 1989; Strange et al., 2014). For this reason, there is currently a lack of direct evidence in favor of mechanisms responsible for exercise-induced adaptation within motor cortex. This thesis sought to provide support for a discussion regarding the possibility of a divergent effect between cortical and hippocampal tissue. In Chapter 3, we note varying responses to exercise-induced phosphorylation between HP and the motor cortex. Most importantly, we noted a strong similarity in kinase related activity, but an opposing effect on

GluA1 phosphorylation. As previously mentioned, GluA1 phosphorylation may be one of the primary sites that can account for priming, and, as such, an observable increase in motor cortex and a decrease in HP could provide evidence that exercise favors different forms of plasticity (LTP vs LTD) in a regionally-specific way. Interestingly, both HP and motor cortex respond identically to maximally exhaustive exercise, which may, in part, account for a growing interest in a phenomenon known as central fatigue.

6.2.3 Novel techniques for the exploration of plasticity-related events

Receptor trafficking is now regarded as a key process in neuronal plasticity, however, studying the phenomenon is challenging due to the lack of techniques that effectively isolate the cell surface fraction of synapses. The current thesis (Chapter 4) provides a description of a novel technique that can both qualitatively and quantitively strengthen our understanding of synaptic protein dynamics. Our current investigations have shown this technique to be a powerful tool to assess the movement of receptors during chemical forms of LTP and to provide insights into how the application of hormones, or drugs may affect synaptic terminals. We believe this technique can easily be incorporated into a large number of studies to provide additional information regarding induced synaptic events. Although we used the technique in the current thesis following an acute exposure, the same method could provide interesting answers regarding chronic changes. In addition, the combined sensitivity and specificity of this technique lends itself well to providing insight regarding how genetic manipulations (such as those that might be induced using CRISPR-based technology) could alter the profile of proteins at the synaptic surface. Overall, we believe the technique can provide a robust tool for future explorations of synapse-specific protein dynamics, especially with regards to drug application, injury mechanisms, and behavioral correlates of learning.

6.3 Future Considerations

Within neuroscience, there is an emerging fascination regarding the use of short and long-term exercise to improve behavioral outcomes in both healthy, and a number of patient populations. Notably, a PubMed search for "brain" and "exercise" limited to only human subjects, generates roughly 1000 publications published in 2017, compared to less than 500/year a decade ago. With this kind of growth in interest towards exploiting the benefits of exercise, it is a surprise we understand so little regarding the mechanisms that connect exercise to learning. The lack of mechanistic support makes our interpretation of the current data sets difficult and limited, which may lead to misinformed decisions regarding the efficacy of certain exercise paradigms. Within this thesis, we provide evidence in support of a direct link between exercise and learning, which we believe will foster a number of new research avenues. Although the list of possible research avenues is great, here we will focus on a select few we regard as most important. First, in direct continuation of the work presented, it is imperative to link a single session of exercise with the improvement in the induction of plasticity, specifically, whether exercise favors either LTP or LTD, whether exercise alters the magnitude of that induction, and whether those effects differ by brain region (MCx or HP). Second, further support is needed in favor of BDNF and CORT as the potential mechanisms for the observed enhancement in glutamatergic phosphorylation following MOD exercise. In particular, identifying the temporality and quantity of CORT+BDNF release during exercise and following exercise, and how that temporal nature contributes to the interpretation of exercise intensity. Moreover, how this CORT+BDNF response changes with the addition of subsequent exercise training sessions. Finally, the discovery that we did not observe an exercise effect within GXT is fascinating. As mentioned in Chapter 4, this may be suggestive of a phenomenon known as central fatigue. Although central fatigue is a common theme within exercise research, the mechanisms underlying neurological fatigue following exercise are

essentially non-existent. Thus, it is our recommendation that GXT provides a template for the evaluation of both the effects and mechanisms that underlie a central fatigue effect.

7.4 Limitations

We took careful consideration from the beginning of this thesis to a examine the influence of exercise on the brain. First, we developed an in-house exercise model, whereby we controlled for various aspects of the acclimatization period, exposure and intensity. However, a possibility exists that the generalizability of the findings from this thesis is limited to only forced-treadmill exercise. First, treadmill exercise provides a lot of benefits over other forms of rodent exercise, such as running wheel, in controlling the duration and intensity of exercise. Nonetheless, treadmill exercise is not a natural form of exercise for rats, and as such, may produce a unique set of biochemical responses that would not otherwise be observed during exercise. Determining if similar effects can be observed in the brain following others types of rodent exercise, such as single session voluntary wheel running or forced-swim may help to address this generalizability.

Along with our consideration in the design of our experimental model to capture exercise effects, we aimed to select the most appropriate statistical test prior to our study. Based on the sample sizes we collected in our study (N = 5-7) and lack of previous data in this field, we could not with confidence assume a normally distributed data set, and thus decided to utilize non-parametric analysis to assess our data, specifically, the Wilcoxon-signed Rank (non-parametric t-test for dependent samples), Mann-Whitney U (non-parametric t-test for independent samples) and Kruskal-Wallis tests (non-parametric one-way ANOVA). In biomedical sciences, the use of non-parametric tests is often considered to be a very conservative approach, and as such, there is a chance that we have made type-II errors. For example, using the selection criteria of $\alpha = 0.05$, a number of findings in Chapter 4 and 5 were near to the statistical threshold, and by traditional

parametric tests, standards would have satisfied the rejection of the *null* hypothesis. We navigated the findings of marginal p values by taking them into consideration with both the mean and effect size (Cohen's d) to best capture patterns within our data. In addition, on a number of occasions we may be underpowered to draw conclusions from our non-parametric analysis, and thus the inclusion of larger sample sizes ($N \approx 10$) is recommended in future investigations.

7.5 Conclusions

As a collective, the 4 studies that comprise this thesis provide evidence in favor of a direct association between a single session of exercise and a mechanism underlying neuroplasticity. Specifically, these data highlight the ability of a single session of moderately intense exercise to augment glutamatergic phosphorylation possibly via a combined CORT+BDNF mechanism. Furthermore, through our investigations into exercise, we sponsored the development of a number of novel methodological approaches including preparation of motor cortex, the enrichment of synaptic surface proteins and a unique form of chemically-induced LTP. Overall, this thesis provides a number of foundational advances which we believe will be extremely valuable in the future of neuroscience research.

REFERENCES

Abraham WC (2008) Metaplasticity: tuning synapses and networks for plasticity. Nat Rev Neurosci 9:387.

Abraham WC, Mason-Parker SE, Bear MF, Webb S, Tate WP (2001) Heterosynaptic metaplasticity in the hippocampus in vivo: a BCM-like modifiable threshold for LTP. Proc Natl Acad Sci U S A 98:10924–10929.

Ahmed T (2006) Long-Term Effects of Brief Acute Stress on Cellular Signaling and Hippocampal LTP. J Neurosci 26:3951–3958.

Akaneya Y, Tsumoto T, Kinoshita S, Hatanaka H (1997) Brain-derived neurotrophic factor enhances long-term potentiation in rat visual cortex. J Neurosci 17:6707–6716.

Albensi BC, Oliver DR, Toupin J, Odero G (2007) Electrical stimulation protocols for hippocampal synaptic plasticity and neuronal hyper-excitability: Are they effective or relevant? Exp Neurol 204:1–13.

Aldridge GM, Podrebarac DM, Greenough WT, Weiler IJ (2008) The use of total protein stains as loading controls: an alternative to high-abundance single-protein controls in semi-quantitative immunoblotting. J Neurosci Methods 172:250–254.

Allen DG, Lamb GD, Westerblad H (2008) Skeletal muscle fatigue: cellular mechanisms. Physiol Rev 88:287–332.

Allen DG, Lamb GD, Westerblad H (2018) Impaired calcium release during fatigue. :296–305.

Andersen P, Bliss TVP, Skrede KK (1971) Lamellar organization of hippocampal excitatory pathways. Exp Brain Res 13:222–238.

Anggono V, Huganir RL (2012) Regulation of AMPA receptor trafficking and synaptic plasticity. Curr Opin Neurobiol 22:461–469.

Arango-Lievano M, Lambert WM, Bath KG, Garabedian MJ, Chao M V., Jeanneteau F (2015) Neurotrophic-priming of glucocorticoid receptor signaling is essential for neuronal plasticity to stress and antidepressant treatment. Proc Natl Acad Sci:201509045.

Aronsson M, Fuxe K, Dong Y, Agnati LF, Okret S, Gustafsson J a (1988) Localization of glucocorticoid receptor mRNA in the male rat brain by in situ hybridization. Proc Natl Acad Sci U S A 85:9331–9335.

Ashton D, Van Reempts J, Haseldonckx M, Willems R (1989) Dorsal-ventral gradient in vulnerability of CA1 hippocampus to ischemia: a combined histological and electrophysiological study. Brain Res 487:368–372.

Bailey CH, Kandel ER (1993) Structural Changes Accompanying Memory Storage. New York 55:397–426.

Bailey SJ, Vanhatalo A, Wilkerson DP, DiMenna FJ, Jones AM (2009) Optimizing the "priming" effect: influence of prior exercise intensity and recovery duration on O2 uptake kinetics and severe-intensity exercise tolerance. J Appl Physiol 107:1743–1756.

Bao JX et al. (1997) Involvement of pre- and postsynaptic mechanisms in posttetanic potentiation at Aplysia synapses. Science 275:969–973.

Barrès R, Yan J, Egan B, Treebak JT, Rasmussen M, Fritz T, Caidahl K, Krook A, O'Gorman DJ, Zierath JR (2012) Acute exercise remodels promoter methylation in human skeletal muscle. Cell Metab 15:405–411.

Barria A, Malinow R (2005) NMDA receptor subunit composition controls synaptic plasticity by regulating binding to CaMKII. Neuron 48:289–301.

Barria A, Muller D, Derkach V, Griffith LC, Soderling TR (1997) Regulatory Phosphorylation of AMPA-Type Glutamate Receptors by CaM-KII During Long-Term Potentiation. 276:2042–2046.

Bassani S, Folci A, Zapata J, Passafaro M (2013) AMPAR trafficking in synapse maturation and plasticity. Cell Mol Life Sci 70.

Bats C, Groc L, Choquet D (2007) The Interaction between Stargazin and PSD-95 Regulates AMPA Receptor Surface Trafficking. Neuron 53:719–734.

Bedford TG, Tipton CM, Wilson NC, Oppliger RA, Gisolfi C (1979) Maximum oxygen consumption of rats and its changes with various experimental procedures. J Appl Physiol 47:1278–1283.

Berridge MJ (2006) Calcium microdomains: Organization and function. Cell Calcium 40:405–412.

Betik AC, Thomas MM, Wright KJ, Riel CD, Hepple RT (2009) Exercise training from late middle age until senescence does not attenuate the declines in skeletal muscle aerobic function. Am J Physiol Regul Integr Comp Physiol 297:R744–R755.

Bishop DJ (2003) Warm up II - Performance changes following active warm up and how to structure the warm up Warm Up II Performance Changes Following Active Warm Up and How to Structure the Warm Up. Sport Med 33:483–498.

Blanco-Suarez E, Hanley JG (2014) Distinct subunit-specific α-amino-3-hydroxy-5-methyl-4-

isoxazolepropionic acid (AMPA) receptor trafficking mechanisms in cultured cortical and hippocampal neurons in response to oxygen and glucose deprivation. J Biol Chem 289:4644–4651.

Bliss T, Lomo T (1973) Long-Lasting Potentiation of Synaptic Transmission in the Dentate Area of the Anaesthetized Rabbit Following Stimulation of the Perforant Path. J Physiol 232:331–356.

Bliss T V, Collingridge GL (1993) A synaptic model of memory: long-term potentiation in the hippocampus. Nature 361:31–39.

Boulanger LM, Poo MM (1999) Presynaptic depolarization facilitates neurotrophin-induced synaptic potentiation. Nat Neurosci 2:346–351.

Bowery NGG, Hudson ALL, Price GWW (1987) GABAA and GABAB receptor site distribution in the rat central nervous system. Neuroscience 20:365–383.

Bramham CR, Messaoudi E (2005) BDNF function in adult synaptic plasticity: the synaptic consolidation hypothesis. Prog Neurobiol 76:99–125.

Bredt D, Nicholl R a (2003) AMPA Receptor Trafficking at Excitatory Synapses. Neuron 40:361–379.

Brodmann K, Garey LJ (2006) Brodmann's localisation in the cerebral cortex: The principles of comparative localisation in the cerebral cortex based on cytoarchitectonics.

Bruel-Jungerman E, Davis S, S L (2007) Brain Plasticity Mechanisms and Memory: a Party of Four: The Neuroscientist : a review journal bringing neurobiology, neurology and psychiatry. 13:492–505.

Caldeira M V, Melo C V, Pereira DB, Carvalho R, Correia SS, Backos DS, Luı A, Esteban A, Duarte CB (2007) Brain-derived Neurotrophic Factor Regulates the Expression and Synaptic Delivery of -Amino-3-hydroxy-5-methyl-4-isoxazole Propionic Acid Receptor Subunits in Hippocampal Neurons *. J Biol Chem 282:12619–12628.

Calvo AC, Moreno-Igoa M, Manzano R, Ordovás L, Yagüe G, Oliván S, Muñoz MJ, Zaragoza P, Osta R (2008) Determination of protein and RNA expression levels of common housekeeping genes in a mouse model of neurodegeneration. Proteomics 8:4338–4343.

Cao W, Duan J, Wang X, Zhong X, Hu Z, Huang F, Wang H, Zhang J, Li F, Zhang J, Luo X, Li C-Q (2014) Early enriched environment induces an increased conversion of proBDNF to BDNF in the adult rat's hippocampus. Behav Brain Res 265:76–83.

Carlin RK, Grab DJ, Cohen RS, Siekevitz P (1980) Isolation and characterization of postsynaptic densities from various brain regions: enrichment of different types of postsynaptic densities. J Cell Biol 86:831–843.

Cassidy JM, Gillick BT, Carey JR (2014) Priming the brain to capitalize on metaplasticity in stroke rehabilitation. Phys Ther 94:139–150.

Cassilhas RC, Lee KS, Fernandes J, Oliveira MGM, Tufik S, Meeusen R, de Mello MT (2012) Spatial memory is improved by aerobic and resistance exercise through divergent molecular mechanisms. Neuroscience 202:309–317.

Cauter E Van, Turek FW (1995) Endocrine and Other Biological Rhythms. Endocrinology 3:2497–2548.

Chang CL, Hsu SYT (2004) Ancient evolution of stress-regulating peptides in vertebrates.

Peptides 25:1681–1688.

Chen DY, Bambah-Mukku D, Pollonini G, Alberini CM (2012) Glucocorticoid receptors recruit the CaMKIIα-BDNF-CREB pathways to mediate memory consolidation. Nat Neurosci 15:1707–1714.

Chen L, Chetkovich DM, Petralia RS, Sweeney NT, Kawasaki Y, Wenthold RJ, Bredt DS, Nicoll RA (2000) Stargazin regulates synaptic targeting of AMPA receptors by two distinct mechanisms. Nature 408:936–943.

Chen N, Luo T, Raymond LA (1999) Subtype-Dependence of NMDA Receptor Channel Open Probability. J Neurosci 19:6844–6854.

Chen Z-Y, Ieraci A, Teng H, Dall H, Meng C-X, Herrera DG, Nykjaer A, Hempstead BL, Lee FS (2005) Sortilin controls intracellular sorting of brain-derived neurotrophic factor to the regulated secretory pathway. J Neurosci 25:6156–6166.

Cheung HH, Gurd JW (2001) Tyrosine phosphorylation of the N -methyl- d -aspartate receptor by exogenous and postsynaptic density-associated Src-family kinases. J Neurochem 78:524–534.

Choquet D (2010) Fast AMPAR trafficking for a high-frequency synaptic transmission. 32:250–260.

Chouinard P a, Paus T (2006) The primary motor and premotor areas of the human cerebral cortex. Neuroscientist 12:143–152.

Chung HJ, Xia J, Scannevin RH, Zhang X, Huganir RL (2000) Phosphorylation of the AMPA receptor subunit GluR2 differentially regulates its interaction with PDZ domain-containing

proteins. J Neurosci 20:7258–7267.

Clapham DE (2007) Calcium Signaling. Cell 131:1047–1058.

Cobb S, Buhl E, Halasy K, Paulsen O, Somogyi P (1995) Synchronization of neuronal activity in hippocampus by individual GABAergic interneurons. Lett to Nat:75–78.

Cohen AS, Coussens CM, Raymond CR, Abraham WC (1999) Long-lasting increase in cellular excitability associated with the priming of LTP induction in rat hippocampus. J Neurophysiol 82:3139–3148.

Colbran RJ (2004) Protein Phosphatases and Calcium / Calmodulin-Dependent Protein Kinase II-Dependent Synaptic Plasticity. 24:8404–8409.

Collingridge BYGL, Kehl SJ, Mclennan H (1983) Excitatory amino acids in synaptic transmission in the schaffer collateral-commissural pathway of the rat hippocampus. J Physiol 334:33–46.

Collingridge GL, Isaac JTR, Wang YT (20005) Receptor Trafficking and Synaptic Plasticity. Nat Rev Neurosci 5:952–962.

Cotman CW, Berchtold NC, Christie L-A (2007) Exercise builds brain health: key roles of growth factor cascades and inflammation. Trends Neurosci 30:464–472.

Cotman CW, Engesser-Cesar C (2002) Exercise enhances and protects brain function. Exerc Sport Sci Rev 30:75–79.

Crozier R a., Black IB, Plummer MR (1999) Blockade of NR2B-Containing NMDA Receptors Prevents BDNF Enhancement of Glutamatergic Transmission in Hippocampal Neurons. Learn Mem 6:257–266.

Cudmore SB, Gurd JW (1989) Postnatal Age and Protein Tyrosine Phosphorylation at Synapses in the Developing Rat Brain. :1240–1248.

Cui Z, Wang H, Tan Y, Zaia KA, Zhang S, Tsien JZ (2004) Inducible and reversible NR1 knockout reveals crucial role of the NMDA receptor in preserving remote memories in the brain. Neuron 41:781–793.

Cull-Candy S, Brickley S, Farrant M (2001) NMDA receptor subunits : diversity , development and disease. Curr Opin Neurobiol 11:18–20.

Cumming G, Finch S (2001) A primer on the understanding, use and calculation of confidence interval that are based on central and noncentral distributions. Educ Psychol Meas 61:532–574.

Dam AM (1979) The Denisty of Neurons in the Human Hippocampus. Neuropathol Appl Neurobiol 5:249–264.

de Kloet ER, Oitzl MS, Joëls M (1999) Stress and cognition: are corticosteroids good or bad guys? Trends Neurosci 22:422–426.

de Quervain DJ-F, Roozendaal B, McGaugh JL (1998) Stress and glucocorticoids impair retrieval of long-term spatial memory. Nature 394:787–790.

Dean AM, Thornton JW (2007) Mechanistic approaches to the study of evolution: the functional synthesis. Nat Rev Genet 8:675–688.

Demaria CD, Soong TW, Alseikhan BA, Alvania RS, Yue DT (2001) Calmodulin bifurcates the local Ca 2 + signal that modulates P/Q-type Ca2+ channels. Lett to Nat 411:484–489.

Derkach V a, Oh MC, Guire ES, Soderling TR (2007) Regulatory mechanisms of AMPA

receptors in synaptic plasticity. Nat Rev Neurosci 8:101–113.

Diamond DM, Bennett MC, Fleshner M, Rose GM (1992) Inverted-U relationship between the level of peripheral corticosterone and the magnitude of hippocampal primed burst potentiation. Hippocampus 2:421–430.

Diamond DM, Fleshner M, Ingersoll N, Rose GM (1996) Psychological stress impairs spatial working memory: Relevance to electrophysiological studies of hippocampal function. 110:661–672.

Diering GH, Heo S, Hussain NK, Liu B, Huganir RL (2016) Extensive phosphorylation of AMPA receptors in neurons. Proc Natl Acad Sci U S A 113:E4920-7.

Dietrich MO, Andrews ZB, Horvath TL (2008) Exercise-induced synaptogenesis in the hippocampus is dependent on UCP2-regulated mitochondrial adaptation. J Neurosci 28:10766–10771.

Ding Q, Ying Z, Gómez-Pinilla F (2011) Exercise influences hippocampal plasticity by modulating brain-derived neurotrophic factor processing. Neuroscience 192:773–780.

Dingledine R, Borges K, Bowie D, Traynelis S (1999) The glutamate receptor ion channels. Pharmacol Rev 51:7.

Dittmer A, Dittmer J (2006) Beta-actin is not a reliable loading control in Western blot analysis. Electrophoresis 27:2844–2845.

Dodd PR, Hardy JA, Oakley AE, Edwardson JA, Perry EK, Delaunoy JP (1981) A rapid method for preparing synaptosomes: Comparison, with alternative procedures. Brain Res 226:107–118.

Donoghue JP, Parham C (1983) Afferent Connections of the Lateral Agranular Field of the Rat Motor Cortex. J Comp Neurol 217:390–404.

Donoghue JP, Wise SP (1982) The Motor Cortex of the Rat: Cytoarchitecture and Microstimulation Mapping. J Comp Neurol 212:76–88.

Droste SK, De Groote L, Atkinson HC, Lightman SL, Reul JMHM, Linthorst ACE (2008) Corticosterone levels in the brain show a distinct ultradian rhythm but a delayed response to forced swim stress. Endocrinology 149:3244–3253.

Eccles J, McIntyre A (1951) Plasticity of Mammalian Monosynaptic Reflexes. Nature 167:466–468.

Egan MF, Kojima M, Callicott JH, Goldberg TE, Kolachana BS, Bertolino A, Zaitsev E, Gold B, Goldman D, Dean M, Lu B, Weinberger DR (2003) The BDNF val66met polymorphism affects activity-dependent secretion of BDNF and human memory and hippocampal function. Cell 112:257–269.

Ehlers MD (2000) Reinsertion or Degradation of AMPA Receptors Determined by Activity-Dependent Endocytic Sorting. Neuron 28:511–525.

Elbert T, Pantev C, Wienbruch C, Rockstroh B, Taub E (1995) Increased cortical representation of the fingers of the left hand in string players. Science (80-) 270:305–307.

Elia G (2008) Biotinylation reagents for the study of cell surface proteins. Proteomics 8:4012–4024.

Eliot LS, Kandel ER, Hawkins RD (1994) Modulation of spontaneous transmitter release during depression and posttetanic potentiation of Aplysia sensory-motor neuron synapses isolated

in culture. JNeurosci 14:3280–3292.

Erickson KI, Voss MW, Prakash RS, Basak C, Szabo A, Chaddock L, Kim JS, Heo S, Alves H, White SM, Wojcicki TR, Mailey E, Vieira VJ, Martin S a, Pence BD, Woods J a, McAuley E, Kramer AF (2011) Exercise training increases size of hippocampus and improves memory. Proc Natl Acad Sci U S A 108:3017–3022.

Ernfors P, Bramham CR (2003) The coupling of a trkB tyrosine residue to LTP. Trends Neurosci 26:171–173.

Erreger K, Dravid SM, Banke TG, Wyllie DJA, Traynelis SF (2005) Subunit-specific gating controls rat NR1 / NR2A and NR1 / NR2B NMDA channel kinetics and synaptic signalling profiles. J Physiol 2:345–358.

Esteban JA, Shi S, Wilson C, Nuriya M, Huganir RL, Malinow R (2003) PKA phosphorylation of AMPA receptor subunits controls synaptic trafficking underlying plasticity. Nat Neurosci 6:136–143.

Fajardo VA, Smith IC, Bombardier E, Chambers PJ, Quadrilatero J, Tupling AR (2016) Diaphragm assessment in mice overexpressing phospholamban in slow-twitch type I muscle fibers. Brain Behav 6:1–10.

Fanselow MS, Dong HW (2010) Are the Dorsal and Ventral Hippocampus Functionally Distinct Structures? Neuron 65:7–19.

Farmer J, Zhao X, Praag HVAN (2004) Effects of voluntary exercise on synaptic plasticity and gene expression in the dentate gyrus of adult male Sprague-Dawley rats in vivo. Neuroscience 124:71–79.

Fernandez-Monreal M, Brown TC, Royo M, Esteban A (2012) The Balance between Receptor Recycling and Trafficking toward Lysosomes Determines Synaptic Strength during Long-Term Depression. J Neurosci 32:13200–13205.

Ferreira AFB, Real CC, Rodrigues AC, Alves AS, Britto LRG (2010) Moderate exercise changes synaptic and cytoskeletal proteins in motor regions of the rat brain. Brain Res 1361:31–42.

Ferris LT, Williams JS, Shen C-L (2007) The effect of acute exercise on serum brain-derived neurotrophic factor levels and cognitive function. Med Sci Sports Exerc 39:728–734.

Fiuza-Luces C, Garatachea N, Berger NA, Lucia A (2013) Exercise is the real polypill. Physiol 28:330–358.

Fluck M (2006) Functional, structural and molecular plasticity of mammalian skeletal muscle in response to exercise stimuli. J Exp Biol 209:2239–2248.

Flück M, Hoppeler H (2003) Molecular basis of skeletal muscle plasticity-from gene to form and function. Rev Physiol Biochem Pharmacol:159–216.

Fortin DA, Srivastava T, Dwarakanath D, Pierre P, Nygaard S, Derkach VA, Soderling TR (2012) BDNF activation of CaM-kinase kinase via TRPC channels induces the translation and synaptic incorporation of GluA1 containing calcium-permeable AMPARs. J Neurosci 32:8127–8137.

Foster KA, Mclaughlin N, Edbauer D, Phillips M, Bolton A, Constantine-paton M, Sheng M (2010) Distinct Roles of NR2A and NR2B Cytoplasmic Tails in Long-Term Potentiation. 30:2676–2685.

Fountoulakis M, Tsangaris GT, Maris A, Lubec G (2005) The rat brain hippocampus proteome. J

Chromatogr B Anal Technol Biomed Life Sci 819:115–129.

Fox CJ, Russel KI, Wang YT, Christie BR (2007) Contribution of NR2A and NR2B NMDA Subunits to Bidirectional Synaptic Plasticity in the Hippocampus In Vivo. Hippocampus 16:907–915.

Freund TF, Gulyás a I (1997) Inhibitory control of GABAergic interneurons in the hippocampus. Can J Physiol Pharmacol 75:479–487.

Frisone DF, Frye CA, Zimmerberg B (2002) Social isolation stress during the third week of life has age-dependent effects on spatial learning in rats. Behav Brain Res 128:153–160.

Fujimura H, Altar CA, Chen R, Nakamura T, Nakahashi T, Kambayashi J, Sun B, Tandon NN (2002) Brain-derived Neurotrophic Factor Is Stored in Human Platelets and Released by Agonist Stimulation. Thromb Haemostasis-stuttgart 87:728–734.

Funder JW (1997) GLUCOCORTICOID AND MINERALOCORTICOID RECEPTORS : Biology and Clinical Relevance. 1985.

Gallagher D, Belmonte D, Deurenberg P, Wang Z, Krasnow N, Pi-Sunyer FX, Heymsfield SB (1998) Organ-tissue mass measurement allows modeling of REE and metabolically active tissue mass. Am J Physiol - Endocrinol Metab 275:E249–E258.

Garcia R (2001) Stress, hippocampal plasticity, and spatial learning. Synapse 40:180–183.

Geiger JRP, Melcher T, Koh DS, Sakmann B, Seeburg PH, Jonas P, Monyer H (1995) Relative abundance of subunit mRNAs determines gating and Ca2+ permeability of AMPA receptors in principal neurons and interneurons in rat CNS. Neuron 15:193–204.

Gibson BYIM, Mcilwain H, Hospital M (1965) Potential in Mammalian Cerebral Tissues in

Vitro ; Recovery After Depolarization By Added Substances. J Physiol 176:261–283.

Giese KP, Fedorov NB, Filipkowski RK, Silva AJ (1998) Autophosphorylation at Thr286 of the alpha calcium-calmodulin kinase II in LTP and learning. Science 279:870–873.

Godsil BP, Caudal D, Rame M (2016) Dynamic Regulation of AMPAR Phosphorylation In Vivo Following Acute Behavioral Stress. Cell Mol Neurobiol 36:1331–1342.

Goebel DJ, Poosch MS (1999) NMDA receptor subunit gene expression in the rat brain: A quantitative analysis of endogenous mRNA levels of NR1(Com), NR2A, NR2B, NR2C, NR2D and NR3A. Mol Brain Res 69:164–170.

Gómez-Pinilla F, Ying Z, Roy RR, Molteni R, Edgerton VR (2002) Voluntary exercise induces a BDNF-mediated mechanism that promotes neuroplasticity. J Neurophysiol 88:2187–2195.

Gray JD, Milner TA, McEwen BS (2014) Dynamic Plasticity: The role of glucocorticoids, brain-derived neurotrophic factor and other trophic factors. Neuroscience:214–227.

Groc L, Choquet D, Chaouloff F (2008a) The stress hormone corticosterone conditions AMPAR surface trafficking and synaptic potentiation. Nat Neurosci 11:868–870.

Groc L, Choquet D, Chaouloff F (2008b) The stress hormone corticosterone conditions AMPAR surface trafficking and synaptic potentiation. Nat Neurosci 11:868–870.

Groeneweg FL, Karst H, de Kloet ER, Joëls M (2011) Rapid non-genomic effects of corticosteroids and their role in the central stress response. J Endocrinol 209:153–167.

Gruhzit OM, Fisken A, Cooper BJ (1947) Tetraethylammonium Chloride. Acute and Chronic Toxicity in Experimental Animals. J Pharmacol Exp Ther:103–107.

Gulyás AI, Megías M, Emri Z, Freund TF (1999) Total Number and Ratio of Excitatory and

Inhibitory Synapses Converging onto Single Interneurons of Different Types in the CA1 Area of the Rat Hippocampus. J Neurosci 19:10082–10097.

Guo W, Ji Y, Wang S, Sun Y, Lu B (2014) Neuronal activity alters BDNF-TrkB signaling kinetics and downstream functions. J Cell Sci 127:2249–2260.

Hackney AC (2006) Exercise as a stressor to the human neuroendocrine system. Medicina (Kaunas) 42:788–797.

Hall RD, Lindholm EP (1974) Organization of motor and somatosensory neocortex in the albino rat. Brain Res 66:23–38.

Hallett M (2007) Transcranial magnetic stimulation: a primer. Neuron 55:187–199.

Hanawalt PC, Hanawalt PC (1993) Mineralocorticoids, Glucocorticoids, Receptors and Response Elements. Science (80-) 259:1957–1958.

Hanisch U-KK, Kettenmann H (2007) Microglia: active sensor and versatile effector cells in the normal and pathologic brain. Nat Neurosci 10:1387–1394.

Harrington RD, Hooton TM (1985) Simultaneous determination of blood levels of corticosterone and growth hormone in the male rat: relation to sleep-wakefulness cycle. J Gender-Specific Med 41:125–130.

Hayashi-Takagi A, Yagishita S, Nakamura M, Shirai F, Wu YI, Loshbaugh AL, Kuhlman B, Hahn KM, Kasai H (2015) Labelling and optical erasure of synaptic memory traces in the motor cortex. Nature 525:333–338.

Hayashi T, Huganir RL (2004) Tyrosine phosphorylation and regulation of the AMPA receptor by SRC family tyrosine kinases. J Neurosci 24:6152–6160.

Hayashi Y, Ishida A, Katagiri H, Mishina M, Fujisawa H, Manabe T, Takahashi T (1997) Calcium- and calmodulin-dependent phosphorylation of AMPA type glutamate receptor subunits by endogenous protein kinases in the post-synaptic density. Mol Brain Res 46:338–342.

Hayashi Y, Shi SH, Esteban J a, Piccini a, Poncer JC, Malinow R (2000) Driving AMPA receptors into synapses by LTP and CaMKII: requirement for GluR1 and PDZ domain interaction. Science 287:2262–2267.

Heffner TG, Hartman JA, Seiden LS (1980) A rapid method for the regional dissection of the rat brain. Pharmacol Biochem Behav 13:453–456.

Henley JM, Barker EA, Glebov OO (2012) Routes , destinations and delays : recent advances in AMPA receptor trafficking. Trends Neurosci 34:258–268.

Herring BE, Nicoll RA (2016) Long-Term Potentiation: From CaMKII to AMPA Receptor Trafficking. Annu Rev Physiol 78.

Hillman CH, Erickson KI, Kramer AF (2008) Be smart, exercise your heart: exercise effects on brain and cognition. Nat Rev Neurosci 9:58–65.

Hilty MR, Groth H, Moore RL, Musch TI (1989) Determinants of VO2max in rats after high-intensity sprint training. J Appl Physiol 66:195–201.

Hirano M, Rakwal R, Shibato J, Agrawal GK, Jwa N-S, Iwahashi H, Masuo Y (2006) New protein extraction/solubilization protocol for gel-based proteomics of rat (female) whole brain and brain regions. Mol Cells 22:119–125.

Hollingsworth E, McNeal E, Burton JL, Williams RJ, Daly J, Creveling C (1985) Biochemical

Characterization of a Filtered Synaptoneurosome Preparation from Guinea Pig Cerebral Cortex : Cyclic Adenosine. J Neurosci 5:2240–2253.

Holman D, Feligioni M, Henley JM (2007) Differential redistribution of native AMPA receptor complexes following LTD induction in acute hippocampal slices. Neuropharmacology 52:92–99.

Høydal MA, Wisløff U, Kemi OJ, Ellingsen O (2007) Running speed and maximal oxygen uptake in rats and mice: practical implications for exercise training. Eur J Cardiovasc Prev Rehabil 14:753–760.

Huang C, Hsu K (2014) Protein tyrosine kinase is required for the induction of long-term potentiation in the rat hippocampus. J Physiol 520:783–796.

Huang Y-Z, Edwards MJ, Rounis E, Bhatia KP, Rothwell JC (2005) Theta burst stimulation of the human motor cortex. Neuron 45:201–206.

Huang YY, Kandel ER (1998) Postsynaptic induction and PKA-dependent expression of LTP in the lateral amygdala. Neuron 21:169–178.

Huganir RL, Nicoll RA (2013) AMPARs and synaptic plasticity: the last 25 years. Neuron 80:704–717.

Hulme SR, Jones OD, Abraham WC (2013) Emerging roles of metaplasticity in behaviour and disease. Trends Neurosci 36:353–362.

Hunter T (2010) Tyrosine phosphorylation : thirty years and counting. 21:140–146.

Iriki A, Pavlides C, Keller A (1989) Long-Term Potentiation in the Motor Cortex. Am Assoc Adv Sci 245:1385–1387.

Isaac JTR, Nicoll RA, Malenka RC (1995) Evidence for silent synapses: Implications for the expression of LTP. Neuron 15:427–434.

Ito I, Futai K, Katagiri H, Watanabe M, Sakimura K, Mishina M, Sugiyama H (1997) Synapse-selective impairment of NMDA receptor functions in mice lacking NMDA receptor epsilon 1 or epsilon 2 subunit. J Physiol 500:401–408.

Ito I, Kawakami R, Sakimura K, Mishina M, Sugiyama H (2000) Input-specific targeting of NMDA receptor subtypes at mouse hippocampal CA3 pyramidal neuron synapses. Neuropharmacology 39:943–951.

Ito R, Lee ACH (2016) The role of the hippocampus in approach-avoidance conflict decision-making: Evidence from rodent and human studies. Behav Brain Res 313:345–357.

Itoh N, Enomoto A, Nagai T, Takahashi M, Yamada K (2016a) Molecular mechanism linking BDNF/TrkB signaling with the NMDA receptor in memory: The role of Girdin in the CNS. Rev Neurosci 27:481–490.

Itoh N, Enomoto A, Nagai T, Takahashi M, Yamada K (2016b) Molecular mechanism linking BDNF/TrkB signaling with the NMDA receptor in memory: the role of Girdin in the CNS. Rev Neurosci 0:481–490.

Itoh N, Enomoto A, Nagai T, Takahashi M, Yamada K (2016c) Molecular mechanism linking BDNF/TrkB signaling with the NMDA receptor in memory: the role of Girdin in the CNS. Rev Neurosci 0.

Jeanneteau F, Chao M V (2013) Are BDNF and glucocorticoid activities calibrated? Neuroscience 6:173–195.

Jeanneteau F, Garabedian MJ, Chao M V (2008) Activation of Trk neurotrophin receptors by glucocorticoids provides a neuroprotective effect. Proc Natl Acad Sci U S A 105:4862–4867.

Ji K, Akgul G, Wollmuth LP, Tsirka SE (2013) Microglia Actively Regulate the Number of Functional Synapses. PLoS One 8.

Joels M, Sarabdjitsingh RA, Karst H (2012) Unraveling the Time Domains of Corticosteroid Hormone Influences on Brain Activity: Rapid, Slow, and Chronic Modes. Pharmacol Rev 64:901–938.

Johansson B (2000) Brain Plasticity and Stroke Rehabilitation: The Willis Lecture. Stroke 31:223–230.

Johnson MW, Chotiner JK, Watson JB (1997) Isolation and characterization of synaptoneurosomes from single rat hippocampal slices. J Neurosci Methods 77:151–156.

Johnston M V. (2004) Clinical disorders of brain plasticity. Brain Dev 26:73–80.

Jonas P, Racca C, Sakmann B, Seeburg PH, Monyer H (1994) Differences in Ca2+ permeability of AMPA-type glutamate receptor channels in neocortical neurons caused by differential GluR-B subunit expression. Neuron 12:1281–1289.

Ju W, Morishita W, Tsui J, Gaietta G, Deerinck TJ, Adams SR, Garner CC, Tsien RY, Ellisman MH, Malenka RC (2004) Activity-dependent regulation of dendritic synthesis and trafficking of AMPA receptors. 7:244–253.

Kamijo K, Nishihira Y, Hatta A, Kaneda T, Kida T, Higashiura T, Kuroiwa K (2004a) Changes in arousal level by differential exercise intensity. Clin Neurophysiol 115:2693–2698.

Kamijo K, Nishihira Y, Hatta A, Kaneda T, Wasaka T, Kida T, Kuroiwa K (2004b) Differential influences of exercise intensity on information processing in the central nervous system. Eur J Appl Physiol 92:305–311.

Kamijo K, Nishihira Y, Higashiura T, Kuroiwa K (2007) The interactive effect of exercise intensity and task difficulty on human cognitive processing. Int J Psychophysiol 65:114–121.

Kang H, Schuman EM (1995) Long-Lasting Neurotrophin-Induced Enhancement of Synaptic Transmission in the Adult Hippocampus Author (s): Hyejin Kang and Erin M . Schuman Published by : American Association for the Advancement of Science Stable URL : http://www.jstor.org/stable/2886. Science (80-) 267:1658–1662.

Kanhema T, Dagestad G, Panja D, Tiron A, Messaoudi E, Håvik B, Ying SW, Nairn AC, Sonenberg N, Bramham CR (2006) Dual regulation of translation initiation and peptide chain elongation during BDNF-induced LTP in vivo: Evidence for compartment-specific translation control. J Neurochem 99:1328–1337.

Karst H, Berger S, Turiault M, Tronche F, Schütz G, Joëls M (2005) Mineralocorticoid receptors are indispensable for nongenomic modulation of hippocampal glutamate transmission by corticosterone. Proc Natl Acad Sci U S A 102:19204–19207.

Keller A (1993) Intrinsic Synaptic Organization of the Motor Cortex. Cereb Cortex 3:430–441.

Kermani P, Rafii D, Jin DK, Whitlock P, Schaffer W, Chiang A, Vincent L, Friedrich M, Shido K, Hackett NR, Crystal RG, Rafii S, Hempstead BL (2005) Neurotrophins promote revascularization by local recruitment of TrkB + endothelial cells and systemic mobilization of hematopoietic progenitors. J Clin Invest 115:653–663.

Kim J, Yoon KS (1998) Stress: Metaplastic effects in the hippocampus. Trends Neurosci 21:505–509.

Kim K, Saneyoshi T, Hosokawa T, Okamoto K, Hayashi Y (2016) Interplay of enzymatic and structural functions of CaMKII in long-term potentiation. J Neurochem:959–972.

Kirkwood A, Dudek SM, Gold JT, Aizenman CD, Bear MF (1993) Common Forms of Synaptic Plasticity in the Hippocampus and Neocortex in Vitro. Science (80-) 260:1518–1521.

Kiuchi T, Lee H, Mikami T (2012) Regular exercise cures depression-like behavior via VEGF-Flk-1 signaling in chronically stressed mice. Neuroscience 207:208–217.

Klann E (2002) Metaplastic protein phosphatases. Learn Mem 9:153–155.

Kleim J a, Barbay S, Cooper NR, Hogg TM, Reidel CN, Remple MS, Nudo RJ (2002) Motor learning-dependent synaptogenesis is localized to functionally reorganized motor cortex. Neurobiol Learn Mem 77:63–77.

Kleim J a, Hogg TM, VandenBerg PM, Cooper NR, Bruneau R, Remple M (2004) Cortical synaptogenesis and motor map reorganization occur during late, but not early, phase of motor skill learning. J Neurosci 24:628–633.

Kleim J a, Lussnig E, Schwarz ER, Comery T a, Greenough WT (1996) Synaptogenesis and Fos expression in the motor cortex of the adult rat after motor skill learning. J Neurosci 16:4529–4535.

Kleim JA, Barbay S, Nudo RJ (1998) Functional Reorganization of the Rat Motor Cortex Following Motor Skill Learning. J Neurophysiol 80:3321–3325.

Kleim JAJA, Chan S, Pringle E, Schallert K, Procaccio V, Jimenez R, Cramer SCSC (2006)

BDNF val66met polymorphism is associated with modified experience-dependent plasticity in human motor cortex. Nat Neurosci 9:735–737.

Klien D, Kern RM, Sokol RZ (1995) A method for the quantification and correction of proteins after transfer to immobilization membranes. Biochem Mol Biol Int 36:59–66.

Knaepen K, Goekint M, Heyman EM, Meeusen R (2010) Neuroplasticity - exercise-induced response of peripheral brain-derived neurotrophic factor: a systematic review of experimental studies in human subjects. Sports Med 40:765–801.

Kohara K, Kitamura a, Morishima M, Tsumoto T (2001) Activity-dependent transfer of brain-derived neurotrophic factor to postsynaptic neurons. Science 291:2419–2423.

Köhler C (1985) A projection from the deep layers of the entorhinal area to the hippocampal formation in the rat brain. Neurosci Lett 56:13–19.

Korte M, Carroll P, Wolf E, Brem G, Thoenen H, Bonhoeffer T (1995) Hippocampal long-term potentiation is impaired in mice lacking brain-derived neurotrophic factor. Proc Natl Acad Sci U S A 92:8856–8860.

Kovalchuk Y, Hanse E, Kafitz KW, Konnerth A (2002) Postsynaptic Induction of BDNF-Mediated Long-Term Potentiation. Science (80-) 295:1729–1734.

Kudielka BM, Wüst S (2010) Human models in acute and chronic stress: assessing determinants of individual hypothalamus-pituitary-adrenal axis activity and reactivity. Stress 13:1–14.

Kumar SS, Huguenard JR (2003) Pathway-specific differences in subunit composition of synaptic NMDA receptors on pyramidal neurons in neocortex. J Neurosci 23:10074–10083.

Kurgers HJ, Hoogenraad CC, Groc L (2010) Stress hormones and AMPA receptor trafficking in

synaptic plasticity and memory. Nat Rev Neurosci 11:675–681.

Lambourne K, Tomporowski P (2010) The effect of exercise-induced arousal on cognitive task performance: a meta-regression analysis. Brain Res 1341:12–24.

Lan J, Skeberdis VA, Jover T, Grooms SY, Lin Y, Araneda RC, Zheng X, Bennett MVL, Zukin RS (2001) Protein kinase C modulates NMDA.

Lau CG, Zukin RS (2007) NMDA receptor trafficking in synaptic plasticity and neuropsychiatric disorders. Nat Rev Neurosci 8:413–426.

Law AJ, Weickert CS, Webster MJ, Herman MM, Kleinman JE, Harrison PJ (2003) Expression of NMDA receptor NR1, NR2A and NR2B subunit mRNAs during development of the human hippocampal formation. Eur J Neurosci 18:1197–1205.

Lawson LJ, Perry VH, Dri P, Gordon S (1990) Heterogeneity in the distribution and morphology of microglia in the normal adult mouse brain. Neuroscience 39:151–170.

Leal G, Afonso PM, Salazar IL, Duarte CB (2015) Regulation of hippocampal synaptic plasticity by BDNF. Brain Res 1621:82–101.

Lee SH, Simonetta A, Sheng M (2004) Subunit rules governing the sorting of internalized AMPA receptors in hippocampal neurons. Neuron 43:221–236.

Lee T-H, Kim K, Shin M-S, Kim C-J, Lim B-V (2015) Treadmill exercise alleviates chronic mild stress-induced depression in rats. J Exerc Rehabil 11:303–310.

Lester RA, Clements JD, Westbrook GL, Jahr CE (1990) Channel kinetics determine the time course of NMDA receptor-mediated synaptic currents. Nature 346:565–567.

Levine ES, Crozier R a, Black IB, Plummer MR (1998) Brain-derived neurotrophic factor

modulates hippocampal synaptic transmission by increasing N-methyl-D-aspartic acid receptor activity. Proc Natl Acad Sci U S A 95:10235–10239.

Lin SY, Wu K, Levine ES, Mount HTJ, Suen PC, Black IB (1998) BDNF acutely increases tyrosine phosphorylation of the NMDA receptor subunit 2B in cortical and hippocampal postsynaptic densities. Mol Brain Res 55:20–27.

Linthorst ACE, Flachskamm C, Barden N, Holsboer F, Reul JMHM (2000) Glucocorticoid receptor impairment alters CNS responses to a psychological stressor: An in vivo microdialysis study in transgenic mice. Eur J Neurosci 12:283–291.

Lisman J, Schulman H, Cline H (2002) The Molecular Basis of CaMKII Function in Synaptic and Behavioural Memory. Nat Rev Neurosci 3:175–190.

Lisman J, Yasuda R, Raghavachari S (2012) Mechanisms of CaMKII action in long-term potentiation. Nat Rev Neurosci 13:169–182.

Lisman JE, Zhabotinsky AM (2001) A Model of Synaptic Memory. Neuron 31:191–201.

Liu L, Wong TP, Pozza MF, Lingenhoehl K, Wang Y, Sheng M, Auberson YP, Wang YT (2004) Role of NMDA Receptor Subtypes in Governing the Direction of Hippocampal Synaptic Plasticity. Science (80-) 304:1021–1024.

Lømo T (2003) The discovery of long-term potentiation. Philos Trans R Soc Lond B Biol Sci 358:617–620.

Lorente De Nó R (1934) Studies on the structure of the cerebral cortex. II. Continuation of the study of the ammonic system.

Lorente De Nó R (1939) Transmission of impulses through cranial motor nuclei. J Neurophysiol.

Lou S, Liu J, Chang H, Chen P (2008) Hippocampal neurogenesis and gene expression depend on exercise intensity in juvenile rats. Brain Res 1210:48–55.

Lu B (2003) BDNF and activity-dependent synaptic modulation. Learn Mem 10:86–98.

Lu B, Pang PT, Woo NH (2005) The yin and yang of neurotrophin action. Nat Rev Neurosci 6:603–614.

Luo Y, Kuang S, Li H, Ran D, Yang J (2017) cAMP/PKA-CREB-BDNF signaling pathway in hippocampus mediates cyclooxygenase 2-induced learning/memory deficits of rats subjected to chronic unpredictable mild stress. Oncotarget 8:35558–35572.

Lupien SJ, McEwen BS, Gunnar MR, Heim C (2009) Effects of stress throughout the lifespan on the brain, behaviour and cognition. Nat Rev Neurosci 10:434–445.

Madison D V, Edson EB (2001) Preparation of hippocampal brain slices. Curr Protoc Neurosci Chapter 6:Unit 6.4.

Mahanty NK, Sah P (1998) Calcium-permeable AMPA receptors mediate long-term potentiation in interneurons in the amygdala. Nature 394:683–687.

Makatsori A, Duncko R, Schwendt M, Moncek F, Johansson BB, Jezova D (2003) Voluntary wheel running modulates glutamate receptor subunit gene expression and stress hormone release in Lewis rats. Psychoneuroendocrinology 28:702–714.

Malinow R, Mainen ZF, Hayashi Y (2000) LTP mechanisms: From silence to four-lane traffic. Curr Opin Neurobiol 10:352–357.

Malinow R, Malenka RC (2002) AMPA RECEPTOR TRAFFICKING AND SYNAPTIC PLASTICITY. Annu Rev Neurosci 25:103–126.

Maloney SJ, Turner AN, Fletcher IM (2014) Ballistic Exercise as a Pre-Activation Stimulus: A Review of the Literature and Practical Applications. Sport Med 44:1347–1359.

Mang CS, Campbell KL, Ross CJD, Boyd L a (2013a) Promoting Neuroplasticity for Motor Rehabilitation After Stroke: Considering the Effects of Aerobic Exercise and Genetic Variation on Brain-Derived Neurotrophic Factor. Phys Ther.

Mang CS, Snow NJ, Campbell KL, Ross CJD, Boyd L a (2013b) Promoting neuroplasticity for motor rehabilitation after stroke: considering the effects of aerobic exercise and genetic variation on brain-derived neurotrophic factor. Phys Ther 93:1707–1716.

Martens U, Capito B, Wree A, The A, Leeuwen V, Ruiz G (1998) Septotemporal distribution of [3 H] MK-801 , [3 H] AMPA and [3 H] Kainate binding sites in the rat hippocampus. Anat Embryol (Berl) 198:195–204.

Martin LJ, Blackstone CD, Levey a I, Huganir RL, Price DL (1993) AMPA glutamate receptor subunits are differentially distributed in rat brain. Neuroscience 53:327–358.

Martin S, Henley JM, Holman D, Zhou M, Wiegert O, van Spronsena M, Joëls M, Hoogenraad CC, Krugers HJ (2009) Corticosterone alters AMPAR mobility and facilitates bidirectional synaptic plasticity. PLoS One 4:1–8.

Massey P V. (2004) Differential Roles of NR2A and NR2B-Containing NMDA Receptors in Cortical Long-Term Potentiation and Long-Term Depression. J Neurosci 24:7821–7828.

Mastorakos G, Pavlatou M, Diamanti-kandarakis E, Chrousos GP (2005) Exercise and the Stress System. Hormones 4:73–89.

Mattson MR (2007) Calcium and neurodegeneration. Aging Cell 6:337–350.

McDonnell MN, Buckley JD, Opie GM, Ridding MC, Semmler JG (2013) A single bout of aerobic exercise promotes motor cortical neuroplasticity. J Appl Physiol 114:1174–1182.

McEwen B (2009) Stress and Neuronal Plasticity. Stress Sci Neuroendocrinol:455–458.

McEwen BS (1999) Stress and Hippocampal Plasticity. Annu Rev Neurosci 22:105–122.

Mcewen BS, Bowles NP, Gray JD, Hill MN, Hunter RG, Karatsoreos IN, Nasca C (2015) Mechanisms of stress in the brain. Nat Neursoscience 18:1353–1363.

Mcewen BS, Magarinos ANAM (1997) Stress Effects on Morphology and Function of the Hippocampus. Ann New York Acad Sci 821:271–284.

McEwen BS, Weiss JM, Schwartz LS (1969) Uptake of corticosterone by rat brain and its concentration by certain limbic structures. Brain Res 16:227–241.

McIlwain H (1951) A Means of Metabolic Investigation of Small Portions of the Central Nervous System in an Active State. J Biochem 50:132–140.

Meeusen R, Meirleir K De (1995) Exercise and Brain Neurotransmission. Sport Med 20:160–188.

Meeusen R, Piacentini MF, De Meirleir K (2001) Brain microdialysis in exercise research. Sports Med 31:965–983.

Melling CWJ, Thorp DB, Milne KJ, Krause MP, Noble EG (2007) Exercise-mediated regulation of Hsp70 expression following aerobic exercise training. 7:3692–3698.

Mendel C (1992) The free hormone hypothesis distinction from the free hormone transport hypothesis. J Androl 13:107–116.

Mikasova L, Xiong H, Kerkhofs A, Bouchet D, Krugers HJ, Groc L (2017) Stress hormone rapidly tunes synaptic NMDA receptor through membrane dynamics and mineralocorticoid signalling. Sci Rep 7:8053.

Miller S, Kennedy MB (1986) Regulation of brain Type II Ca2+/calmodulin-dependent protein kinase by autophosphorylation: A Ca2+-triggered molecular switch. Cell 44:861–870.

Milne KJ, Noble EG, Kevin J, Exercise-induced EGN (2002) Exercise-induced elevation of HSP70 is intensity dependent. J Appl Physiol 7:561–568.

Minichiello L (2009) TrkB signalling pathways in LTP and learning. Nat Rev Neurosci 10:850–860.

Minichiello L, Calella AM, Medina DL, Bonhoeffer T, Klein R, Korte M (2002) Mechanism of TrkB-mediated hippocampal long-term potentiation. Neuron 36:121–137.

Molteni R, Ying Z, Gomez-Pinilla F (2002) Differential effects of acute and chronic exercise on plasticity-related genes in the rat hippocampus revealed by microarray. Eur J Neurosci 16:1107–1116.

Momiyama A (2000) Distinct synaptic and extrasynaptic NMDA receptors identified in dorsal horn neurones of the adult rat spinal cord. J Physiol 523 Pt 3:621–628.

Monyer H, Burnashev N, Laurie DJ, Sakmann B, Seeburg PH (1994) Developmental and regional expression in the rat brain and functional properties of four NMDA receptors. Neuron 12:529–540.

Morimoto M, Morita N, Ozawa H, Yokoyama K, Kawata M (1996) Distribution of glucocorticoid receptor immunoreactivity and mRNA in the rat brain: An

immunohistochemical and in situ hybridization study. Neurosci Res 26:235–269.

Morris RGM (2013) NMDA receptors and memory encoding. Neuropharmacology 74:32–40.

Morrow AL, Paul SM (1988) Benzodiazepine Enhancement. :302–306.

Moser EI, Moser MB, Andersen P (1993) Spatial learning impairment parallels the magnitude of dorsal hippocampal lesions, but is hardly present following ventral lesions. J Neurosci 13:3916–3925.

Muellbacher W, Ziemann U, Wissel J, Dang N, Kofler M, Facchini S, Boroojerdi B, Poewe W, Hallett M (2002) Early consolidation in human primary motor cortex. Nature 415:640–644.

Murdoch K, Buckley JD, McDonnell MN (2016) The Effect of Aerobic Exercise on Neuroplasticity within the Motor Cortex following Stroke. PLoS One 11:e0152377.

Murphy JA, Stein IS, Lau CG, Peixoto RT, Aman TK, Kaneko N, Aromolaran K, Saulnier JL, Popescu GK, Sabatini BL, Hell JW, Zukin RS (2014) Phosphorylation of Ser1166 on GluN2B by PKA Is Critical to Synaptic NMDA Receptor Function and Ca^{2+} Signaling in Spines. J Neurosci 34.

Murray E, Oulter JD (1981) Organization of Corticospinal Neurons in the Monkey. J Comp Neurol 195:339–365.

Nadel J, Huang T, Xia Z, Burlin T, Zametkin A, Smith CB (2013) Voluntary exercise regionally augments rates of cerebral protein synthesis. Brain Res 1537:125–131.

Nadel L (1968) Dorsal and Ventral Hippocampal Lesions and Behavior'. Physiol Behav 3:891–900.

Nader K, Schafe GE, Le Doux JE (2000) Fear memories require protein synthesis in the

amygdala for reconsolidation after retrieval. Nature 406:722–726.

Nafstad PHJ (1967) An electron microscope study on the termination of the perforant path fibres in the hippocampus and the fascia dentata. Zeitschrift f??r Zellforsch und Mikroskopische Anat 76:532–542.

Nakahashi T, Fujimura H, Altar C a, Li J, Kambayashi J, Tandon NN, Sun B (2000) Vascular endothelial cells synthesize and secrete brain-derived neurotrophic factor. FEBS Lett 470:113–117.

Nakata H, Nakamura S (2007) Brain-derived neurotrophic factor regulates AMPA receptor trafficking to post-synaptic densities via IP3R and TRPC calcium signaling. FEBS Lett 581:2047–2054.

Narisawa-saito M, Iwakura Y, Kawamura M, Araki K, Kozaki S, Takei N, Nawa H (2002) Brain-derived Neurotrophic Factor Regulates Surface Expression of -Amino-3-hydroxy-5-methyl-4-isoxazoleproprionic Acid Receptors by Enhancing the N -Ethylmaleimide-sensitive Factor / GluR2 Interaction in Developing Neocortical Neurons *. 277:40901–40910.

Neeper S a, Gómez-Pinilla F, Choi J, Cotman CW (1996) Physical activity increases mRNA for brain-derived neurotrophic factor and nerve growth factor in rat brain. Brain Res 726:49–56.

Neeper S, Gomez-Pinilla F, Chol J, Cotman C (1995) Exercise and brain neurotrophins. Nature 373:109–109.

Neva JL, Brown KE, Mang CS, Francisco BA, Boyd LA (2017) An acute bout of exercise

modulates both intracortical and interhemispheric excitability. Eur J Neurosci 45:1343–1355.

Nguyen P V, Abel T, Kandel ER (2016) Requirement of a Critical Period of Transcription for Induction of a Late Phase of LTP. Science (80-) 265:1104–1107.

Nicoll RA, Roche KW (2013) Neuropharmacology Long-term potentiation : Peeling the onion. Neuropharmacology 74:18–22.

Nudo RJ, Milliken GW (1996) Reorganization of Movement Representations in Primary Motor Cortex Following Focal Ischemic Infarcts in Adult Squirrel Monkeys. J Neurosci 75:2144–2149.

Obermeier a, Halfter H, Wiesmüller KH, Jung G, Schlessinger J, Ullrich a (1993) Tyrosine 785 is a major determinant of Trk--substrate interaction. EMBO J 12:933–941.

Oh MC, Derkach VA, Guire ES, Soderling TR (2006a) Extrasynaptic Membrane Trafficking Regulated by GluR1 Serine 845 Phosphorylation Primes AMPA Receptors for. J Biol Chem 281:752–758.

Oh MC, Derkach VA, Guire ES, Soderling TR (2006b) Extrasynaptic membrane trafficking regulated by GluR1 serine 845 phosphorylation primes AMPA receptors for long-term potentiation. J Biol Chem 281:752–758.

Olah M, Biber K, Vinet J, Boddeke HWGM (2011) Microglia phenotype diversity. CNS {&} Neurol Disord drug targets 10:108–118.

Opazo P, Choquet D (2011) Molecular and Cellular Neuroscience A three-step model for the synaptic recruitment of AMPA receptors. Mol Cell Neurosci 46:1–8.

Otmakhova N a, Otmakhov N, Mortenson LH, Lisman JE (2000) Inhibition of the cAMP pathway decreases early long-term potentiation at CA1 hippocampal synapses. J Neurosci 20:4446–4451.

Pang PT, Teng HK, Zaitsev E, Woo NT, Sakata K, Zhen S, Teng KK, Yung W-H, Hempstead BL, Lu B (2004) Cleavage of proBDNF by tPA/plasmin is essential for long-term hippocampal plasticity. Science 306:487–491.

Paoletti P, Bellone C, Zhou Q (2013) NMDA receptor subunit diversity: impact on receptor properties, synaptic plasticity and disease. Nat Rev Neurosci 14:383–400.

Pardridge WM (1981) Transport of protein-bound hormones into tissues in vivo. Endocr Rev 2:103–123.

Park J-K, Lee S-J, Kim T-W (2014) Treadmill exercise enhances NMDA receptor expression in schizophrenia mice. J Exerc Rehabil 10:15–21.

Parker D (2001) Spinal-Cord Plasticity. Mol Neurobiol 22:55–80.

Patapoutian a., Reichardt LF (2001) Trk receptors: Mediators of neurotrophin action. Curr Opin Neurobiol 11:272–280.

Patel PD, Lopez JF, Lyons DM, Burke S, Wallace M, Schatzberg a F (2001) Glucocorticoid and mineralocorticoid receptor mRNA expression in squirrel monkey brain. J Psychiatr Res 34:383–392.

Patten AR, Sickmann H, Hryciw BN, Kucharsky T, Parton R, Kernick A, Christie BR (2013) Long-term exercise is needed to enhance synaptic plasticity in the hippocampus. :642–647.

Pavlides C, Watanabe Y, Magariños A, McEwen B (1995) Opposing roles of type I and type II

adrenal steroid receptors in hippocampal long-term potentiation. Neuroscience 68:387 394.

Pavlides C, Watanabe Y, McEwen BS (1993) Effects of glucocorticoids on hippocampal long-term potentiation. Hippocampus 3:183–192.

Paxinos G, Watson C (1982) The Rat Brain in Stereotaxic Coordinates. Academic Press.

Paxinos G, Watson C (1997) The Rat Brain in Stereotaxic Coordinates.

Paxinos G, Watson C, Pennisi M, Topple A (1985) Bregma , lambda and the interaural midpoint in stereotaxic surgery with rats of different sex , strain and weight. 13:139–143.

Pellegrini-Giampietro DE, Gorter JA, Bennett MVL, Zukin RS (1997) The GluR2 (GluR-B) hypothesis: Ca2+-permeable AMPA receptors in neurological disorders. Trends Neurosci 20:464–470.

Penfield W, Boldrey E (1937) Somatic Motor and Sensory Representation in the Cerebral Cortex of Man as Studied by Electrical Stimulation. Brain 60:389–443.

Pereira AC, Huddleston DE, Brickman AM, Sosunov A a, Hen R, McKhann GM, Sloan R, Gage FH, Brown TR, Small S a (2007) An in vivo correlate of exercise-induced neurogenesis in the adult dentate gyrus. Proc Natl Acad Sci U S A 104:5638–5643.

Perogamvros I, Ray DW, Trainer PJ (2012) Regulation of cortisol bioavailability – effects on hormone measurement and action. Endocrinology:717–727.

Petralia RS, Esteban JA, Wang YX, Partridge JG, Zhao HM, Wenthold RJ, Malinow R (1999) Selective acquisition of AMPA receptors over postnatal development suggests a molecular basis for silent synapses. Nat Neurosci 2:31–36.

Petriz BA, Gomes CPC, Almeida JA, de Oliveira GP, Ribeiro FM, Pereira RW, Franco OL

(2017) The Effects of Acute and Chronic Exercise on Skeletal Muscle Proteome. J Cell Physiol 232:257–269.

Piepmeier AT, Etnier JL (2015) Brain-derived neurotrophic factor (BDNF) as a potential mechanism of the effects of acute exercise on cognitive performance. J Sport Heal Sci 4:14–23.

Pierotti MA, Greco A (2006) Oncogenic rearrangements of the NTRK1/NGF receptor. Cancer Lett 232:90–98.

Plant K, Pelkey KA, Bortolotto ZA, Morita D, Terashima A, Mcbain CJ, Collingridge GL, Isaac JTR (2006) Transient incorporation of native GluR2-lacking AMPA receptors during hippocampal long-term potentiation. Nat Neurosci 9:602–604.

Plautz EJ, Milliken GW, Nudo RJ (2000) Effects of repetitive motor training on movement representations in adult squirrel monkeys: role of use versus learning. Neurobiol Learn Mem 74:27–55.

Ploughman M, Attwood Z, White N, Doré JJE, Corbett D (2007) Endurance exercise facilitates relearning of forelimb motor skill after focal ischemia. Eur J Neurosci 25:3453–3460.

Poduslo JF, Curran GL (1996) Molecular Permeability at the blood-brain and blood-nerve barriers of the. Mol Brain Res 36.

Poo MM (2001) Neurotrophins as synaptic modulators. Nat Rev Neurosci 2:24–32.

Popoli M, Yan Z, McEwen BS, Sanacora G (2012) The stressed synapse: the impact of stress and glucocorticoids on glutamate transmission. Nat Rev Neurosci 13:22–37.

Pozzo-Miller LD, Gottschalk W, Zhang L, McDermott K, Du J, Gopalakrishnan R, Oho C,

Sheng ZH, Lu B (1999) Impairments in high-frequency transmission, synaptic vesicle docking, and synaptic protein distribution in the hippocampus of BDNF knockout mice. J Neurosci 19:4972–4983.

Prager EM, Brielmaier J, Bergstrom HC, McGuire J, Johnson LR (2010) Localization of mineralocorticoid receptors at mammalian synapses. PLoS One 5:1–10.

Prager EM, Johnson LR (2009) Stress at the synapse: Signal transduction mechanisms of adrenal steroids at neuronal membranes. Sci Signal 2.

Prybylowski K, Chang K, Sans N, Kan L, Vicini S, Wenthold RJ (2005) The synaptic localization of NR2B-containing NMDA receptors is controlled by interactions with PDZ proteins and AP-2. Neuron 47:845–857.

Radak Z, Taylor AW, Ohno H, Goto S (2001) Adaptation to exercise-induced oxidative stress: from muscle to brain. Exerc Immunol Rev 7:90–107.

Rami A, Ausmeir F, Winckler J, Krieglstein J (1997) Differential effects of scopolamine on neuronal survival in ischemia and glutamate neurotoxicity : relationships to the excessive vulnerability of the dorsoseptal hippocampus. J Chem Neuroanat 13:201–208.

Rasmussen P, Brassard P, Adser H, Pedersen M V, Leick L, Hart E, Secher NH, Pedersen BK, Pilegaard H (2009) Evidence for a release of brain-derived neurotrophic factor from the brain during exercise. Exp Physiol 94:1062–1069.

Real CC, Ferreira AFB, Hernandes MS, Britto LRG, Pires RS (2010) Exercise-induced plasticity of AMPA-type glutamate receptor subunits in the rat brain. Brain Res 1363:63–71.

Real CC, Garcia PC, Britto LRG, Pires RS (2015) Different protocols of treadmill exercise

induce distinct neuroplastic effects in rat brain motor areas. Brain Res 1624:188–198.

Redila VA, Christie BR (2006) Exercise-induced changes in dendritic structure and complexity in the adult hippocampal dentate gyrus. Neuroscience 137:1299–1307.

Ren L, Lubrich B, Biber K, Gebicke-Haerter PJ (1999) Differential expression of inflammatory mediators in rat microglia cultured from different brain regions. Brain Res Mol Brain Res 65:198–205.

Reul JMHM, De Kloet ER (1985) 2 Receptor Systems for Corticosterone in Rat-Brain - Microdistribution and Differential Occupation. Endocrinology 117:2505–2511.

Rioult-Pedotti M-S, Friedman D, Donoghue JP (2000a) Learning-Induced LTP in Neocortex. Science (80-) 290:533–537.

Rioult-Pedotti MS, Friedman D, Donoghue JP (2000b) Learning-induced LTP in neocortex. Science 290:533–536.

Ritter LM, Unis AS, Meador-Woodruff JH (2001) Ontogeny of ionotropic glutamate receptor expression in human fetal brain. Dev Brain Res 127:123–133.

Rockl KS, Witczak CA, Goodyer LJ (2008) Signaling Mechanisms in Skeletal Muscle: Acute Responses and Chronic Adaptations to Exercise. Int Union Biochem Mol Biol 60:145–153.

Rodríguez-Durán LF, Escobar ML (2014) NMDA receptor activation and PKC but not PKA lead to the modification of the long-term potentiation in the insular cortex induced by conditioned taste aversion: Differential role of kinases in metaplasticity. Behav Brain Res 266:58–62.

Roig M, Skriver K, Lundbye-Jensen J, Kiens B, Nielsen JB (2012) A single bout of exercise

improves motor memory. PLoS One 7:e44594.

Rojas Vega S, Hollmann W, Strüder HK (2012) Influences of exercise and training on the circulating concentration of prolactin in humans. J Neuroendocrinol 24:395–402.

Rojas Vega S, Strüder HK, Vera Wahrmann B, Schmidt A, Bloch W, Hollmann W (2006) Acute BDNF and cortisol response to low intensity exercise and following ramp incremental exercise to exhaustion in humans. Brain Res 1121:59–65.

Romero-Calvo I, Ocón B, Martínez-Moya P, Suárez MD, Zarzuelo A, Martínez-Augustin O, de Medina FS (2010) Reversible Ponceau staining as a loading control alternative to actin in Western blots. Anal Biochem 401:318–320.

Roth-Alpermann C, Morris RGM, Korte M, Bonhoeffer T (2006) Homeostatic shutdown of long-term potentiation in the adult hippocampus. Proc Natl Acad Sci U S A 103:11039–11044.

Roth RH, Zhang Y, Huganir RL (2017) Dynamic imaging of AMPA receptor trafficking in vitro and in vivo. Curr Opin Neurobiol 45:51–58.

Ruan W, Lai M (2007) Actin, a reliable marker of internal control? Clin Chim Acta 385:1–5.

Rumbaugh G, Vicini S (1999) Distinct synaptic and extrasynaptic NMDA receptors in developing cerebellar granule neurons. J Neurosci 19:10603–10610.

Russell V a, Zigmond MJ, Dimatelis JJ, Daniels WMU, Mabandla M V (2014) The interaction between stress and exercise, and its impact on brain function. Metab Brain Dis 29:255–260.

Sage MD (2015) Priming the Brain for Recovery from Stroke : The Role of Aerobic Exercise as an Adjunct to Upper-Limb Therapy by Priming the Brain for Recovery from Stroke : The

Role of Aerobic Exercise as an Adjunct to Upper-Limb Therapy.

Salter MW, Kalia L V (2004) Src kinases: a hub for NMDA receptor regulation. Nat Rev Neurosci 5:317–328.

Sandi C (2011) Glucocorticoids act on glutamatergic pathways to affect memory processes. Trends Neurosci 34:165–176.

Sandi C, Pinelo-nava MT (2007) Stress and Memory : Behavioral Effects and Neurobiological Mechanisms. 2007.

Sanes JN, Donoghue JP (2000) Plasticity and Primary Motor Cortex. Annu Rev Neurosci 23:393–415.

Saoudi M, Abdelmouleh A, El Feki A (2010) Tetrodotoxin: a potent marine toxin. Toxin Rev 29:60–70.

Sapolsky RM, Romero LM, Munck a. U (2000) How Do Glucocorticoids Influence Stress Responses ? Preparative Actions *. Endocr Rev 21:55–89.

Sato S, Osanai H, Monma T, Harada T, Hirano A, Saito M, Kawato S (2004) Acute effect of corticosterone on. 321:510–513.

Savchenko VL, Nikonenko IR, Skibo GG, McKanna JA (1997) Distribution of microglia and astrocytes in different regions of the normal adult rat brain. Neurophysiology 29:343–351.

Scannevin RH, Huganir RL (2000) Postsynaptic organization and regulation of excitatory synapses. Nat Rev Neurosci 1:133–141.

Schabrun SM, Chipchase LS (2012) Priming the brain to learn: The future of therapy? Man Ther 17:184–186.

Schacter DL, Buckner RL (1998) DUPLICATE-Priming and the Brain Review. Neuron 20:185–195.

Schieber MH (2001) Constraints on Somatotopic Organization in the Primary Motor Cortex. J Neurophysiol 86:2121–2143.

Schmolesky MT, Webb DL, Hansen R a (2013) The effects of aerobic exercise intensity and duration on levels of brain-derived neurotrophic factor in healthy men. J Sports Sci Med 12:502–511.

Segal R a., Bhattacharyya A, Rua L a., Alberta J a., Stephens RM, Kaplan DR, Stiles CD (1996) Differential utilization of Trk autophosphorylation sites. J Biol Chem 271:20175–20181.

Selmaoui B, Touitou Y (2003) Reproducibility of the circadian rhythms of serum cortisol and melatonin in healthy subjects: A study of three different 24-h cycles over six weeks. Life Sci 73:3339–3349.

Shamloo M, Wieloch T (1999) Changes in Protein Tyrosine Phosphorylation in the Rat Brain After Cerebral Ischemia in a Model of Ischemic Tolerance. J Cereb Blood Flow Metab 19:173–183.

Shen C, Tsimberg Y, Salvadore C, Meller E (2004) Activation of Erk and JNK MAPK pathways by acute swim stress in rat brain regions. BMC Neurosci 5:1–13.

Sheng M, Cummings J, Roldan L a, Jan YN, Jan LY (1994) Changing subunit composition of heteromeric NMDA receptors during development of rat cortex. Nature 368:144–147.

Sheng M, Kim E (2011) The postsynaptic organization od synapses. Cold Spring Harb Perspect Biol 3:a005678.

Shi S-H, Hayashi Y, Esteban JA, Malinow R (2001) Subunit-Specific Rules Governing AMPA Receptor Trafficking to Synapses in Hippocampal Pyramidal Neurons. Cell 105:331–343.

Shi SH et al. (1999) Rapid spine delivery and redistribution of AMPA receptors after synaptic NMDA receptor activation. Science 284:1811–1816.

Shors TJ (2001) Acute stress rapidly and persistently enhances memory formation in the male rat. Neurobiol Learn Mem 75:10–29.

Simonsen H, Jeune B (1972) Origin and termination of the hippocampal perforant path in the rat studied by silver impregnation. J Comp Neurol 144:215–232.

Singh AM, Duncan RE, Neva JL, Staines WR (2014a) Aerobic exercise modulates intracortical inhibition and facilitation in a nonexercised upper limb muscle. BMC Sports Sci Med Rehabil 6:23.

Singh AM, Neva JL, Staines WR (2014b) Acute exercise enhances the response to paired associative stimulation-induced plasticity in the primary motor cortex. Exp Brain Res 232.

Singh AM, Staines WR (2015) The Effects of Acute Aerobic Exercise on the Primary Motor Cortex. J Mot Behav:1–12.

Skriver K, Roig M, Lundbye-Jensen J, Pingel J, Helge JW, Kiens B, Nielsen JB (2014) Acute exercise improves motor memory: Exploring potential biomarkers. Neurobiol Learn Mem.

Smith AE, Goldsworthy MR, Garside T, Wood FM, Ridding MC (2014) The influence of a single bout of aerobic exercise on short-interval intracortical excitability. Exp brain Res.

Soderling TR, Derkach VA (2000) Postsynaptic protein phosphorylation and LTP. Trends Neurosci 23:75–80.

Sokoloff L (1960) Metabolism of the central nervous system in vivo. In: Handbook of Physiology, pp 1843–1864.

Somogyi P, Tamás G, Lujan R, Buhl EH (1998) Salient features of synaptic organisation in the cerebral cortex. Brain Res Rev 26:113–135.

Song I, Huganir RL (2002) Regulation of AMPA receptors during synaptic plasticity. Trends Neurosci 25:578–588.

Soya H, Mukai A, Deocaris CC, Ohiwa N, Chang H, Nishijima T, Fujikawa T, Togashi K, Saito T (2007) Threshold-like pattern of neuronal activation in the hypothalamus during treadmill running: establishment of a minimum running stress (MRS) rat model. Neurosci Res 58:341–348.

Squire LR (1992) Memory and the Hippocampus : A Synthesis From Findings With Rats, Monkeys, and Humans. Psychol Rev 99:195–231.

Statton MA, Encarnacion M, Celnik P, Bastian AJ (2015) A Single Bout of Moderate Aerobic Exercise Improves Motor Skill Acquisition. PLoS One 10:e0141393.

Stavrinos EL, Coxon JP (2014) High-intensity Interval Exercise Promotes Motor Cortex Disinhibition and Early Motor Skill Consolidation. :593–604.

Steward O (1976) Topographical organization of the Projections from the Entorhinal Area to the Hippocampal Formation of the Rat. J Comp Neurol 167:285–314.

Stewart MG, Medvedev NI, Popov VI, Schoepfer R, Davies HA, Murphy K, Dallérac GM, Kraev I V., Rodríguez JJ (2005) Chemically induced long-term potentiation increases the number of perforated and complex postsynaptic densities but does not alter dendritic spine

volume in CA1 of adult mouse hippocampal slices. Eur J Neurosci 21:3368–3378.

Stocca G, Vicini S (1998) Increased contribution of NR2A subunit to synaptic NMDA receptors in developing rat cortical neurons. J Physiol 507:13–24.

Stranahan AM, Khalil D, Gould E (2006) Social isolation delays the positive effects of running on adult neurogenesis. Nat Neurosci 9:526–533.

Stranahan AM, Khalil D, Gould E (2007) Running Induces Widespread Structural Alterations in the Hippocampus and Entorhinal Cortex. Hippocampus 1022:1017–1022.

Strange BA, Witter MP, Lein ES, Moser EI (2014) Functional organization of the hippocampal longitudinal axis. Nat Rev Neurosci 15:655–669.

Sun L, Shipley MT, Lidow MS (2000) Subunits of the NMDA Receptor in the Cerebral Cortex and Olfactory Bulb of Adult Rat. Synapse 35:212–221.

Sun Y, Xu Y, Cheng X, Chen X, Xie Y, Zhang L, Wang L, Hu J, Gao Z (2018) The differences between GluN2A and GluN2B signaling in the brain. J Neurosci Res:1430–1443.

Sutton MA, Schuman EM (2005) Local translational control in dendrites and its role in long-term synaptic plasticity. J Neurobiol 64:116–131.

Sutton MA, Schuman EM (2006) Dendritic Protein Synthesis, Snaptic Plasticity, and Memory. Cell 127:49–58.

Swanson L, Cowan W (1977) An Autoradiographic Study of the Organization of the Efferent Connections of the Hippocampal Formation in the Rat. J Comp Neurol 172:49–84.

Takahashi T, Kimoto T, Tanabe N, Hattori T, Yasumatsu N (2002) Corticosterone acutely prolonged N -methyl- D -aspartate receptor-mediated Ca 2 + elevation in cultured rat

hippocampal neurons. :1441–1451.

Takasu MA, Dalva MB, Zigmond RE, Greenberg ME (2002) Modulation of NMDA Receptor – Dependent Calcium Influx and Gene Expression Through EphB Receptors. Science (80-) 295:491–496.

Takumi Y, Ramirez-Leon V, Laake P, Rinvik E, Ottersen OP (1999) Different modes of expression of AMPA and NMDA receptors in hippocampal synapses. Nat Neurosci 2:618–24.

Tang SW, Chu E, Hui T, Helmeste D, Law C (2008) Influence of exercise on serum brain-derived neurotrophic factor concentrations in healthy human subjects. Neurosci Lett 431:62–65.

Tang Y, Nyengaard JR, De Groot DMG, Gundersen HJG (2001) Total regional and global number of synapses in the human brain neocortex. Synapse 41:258–273.

Tasker JG, Di S, Malcher-Lopes R (2006) Minireview: Rapid glucocorticoid signaling via membrane-associated receptors. Endocrinology 147:5549–5556.

Taylor SC, Berkelman T, Yadav G, Hammond M (2013) A defined methodology for reliable quantification of western blot data. Mol Biotechnol 55:217–226.

Teyler TJ (1980) Brain slice preparation: hippocampus. Brain ResBull 5:391–403.

Teyler TJ, DiScenna P (1987) Long-Term Potentiation. Annu Rev Neurosci 10:131–161.

Thacker JS, Middleton LE, Mcilroy WE, Staines WR (2014) The influence of an acute bout of aerobic exercise on cortical contributions to motor preparation and execution. Physiol Rep 2:1–11.

Thacker JS, Yeung D, Chambers PJ, Tupling AR, Staines WR, Mielke JG (2018) Single Session, High-Intensity Aerobic Exercise Fails to Affect Plasticity-Related Protein Expression in the Rat Sensorimotor Cortex. Behav Brain Res:0–1.

Thacker JS, Yeung DH, Staines WR, Mielke JG (2016) Total protein or high-abundance protein: Which offers the best loading control for Western blotting? Anal Biochem 496:76–78.

Tillerson J., Caudle W., Reverón M., Miller G. (2003) Exercise induces behavioral recovery and attenuates neurochemical deficits in rodent models of Parkinson's disease. Neuroscience 119:899–911.

Tomita S, Adesnik H, Sekiguchi M, Zhang W, Wada K, Howe JR, Nicoll R a, Bredt DS (2005) Stargazin modulates AMPA receptor gating and trafficking by distinct domains. Nature 435:1052–1058.

Tong L, Shen H, Perreau VM, Balazs R, Cotman CW (2001) Effects of exercise on gene-expression profile in the rat hippocampus. Neurobiol Dis 8:1046–1056.

Tovar KR, Westbrook GL (1999) The incorporation of NMDA receptors with a distinct subunit composition at nascent hippocampal synapses in vitro. J Neurosci 19:4180–4188.

Tovar KR, Westbrook GL (2002) Mobile NMDA receptors at hippocampal synapses. Neuron 34:255–264.

Tsien JZ (2000) Linking Hebb's coincidence-detection to memory formation. Curr Opin Neurobiol 10:266–273.

van Praag H, Christie BR, Sejnowski TJ, Gage, F. H. (1999) Running enhances neurogenesis, learning, and long-term potentiation in mice. Proc Natl Acad Sci USA 96:13427–13431.

van Strien NM, Cappaert NLM, Witter MP (2009) The anatomy of memory: an interactive overview of the parahippocampal-hippocampal network. Nat Rev Neurosci 10:272–282.

Vaynman S (2003) Interplay between brain-derived neurotrophic factor and signal transduction modulators in the regulation of the effects of exercise on synaptic-plasticity. Neuroscience 122:647–657.

Vaynman S (2005) License to Run: Exercise Impacts Functional Plasticity in the Intact and Injured Central Nervous System by Using Neurotrophins. Neurorehabil Neural Repair 19:283–295.

Verpelli C, Schmeisser MJ, Sala C, Boeckers TM (2012) Synaptic Plasticity.

Villasana LE, Klann E, Tejada-Simon MV (2007) Rapid isolation of synaptoneurosomes and postsynaptic densities from adult mouse hippocampus. J Neurosci Methods 158:30–36.

Vissel B, Krupp JJ, Heinemann SF, Westbrook GL (2001) A use-dependent tyrosine dephosphorylation of NMDA receptors is independent of ion flux. Nat Neurosci 4:587–596.

Voss MW, Vivar C, Kramer AF, van Praag H (2013) Bridging animal and human models of exercise-induced brain plasticity. Trends Cogn Sci 17:525–544.

Walters TJ, Ryan KL, Tehrany MR, Jones MB, Paulus LA, Mason PA (1998a) HSP70 expression in the CNS in response to exercise and heat stress in rats. J Appl Physiol 84:1269–1277.

Walters TJ, Ryan KL, Tehrany MR, Jones MB, Paulus LA, Mason PA, Air B, Base F, Ryan KL, Tehrany MR, Jones MB, Paulus LA, Hsp PAM (1998b) HSP70 expression in the CNS in response to exercise and heat stress in rats. :1269–1277.

Wang JQ, Guo ML, Jin DZ, Xue B, Fibuch EE, Mao LM (2014) Roles of subunit phosphorylation in regulating glutamate receptor function. Eur J Pharmacol 728:183–187.

Wang YT, Salter MW (1994) Regulation of NMDA receptors by tyrosine kinases and phosphatases. Lett to Nat 369:233–235.

Watanabe M, Inoue Y, Sakimura K, Mishina M (1992) Developmental changes in distribution of NMDA receptor channel subunit mRNAs. Neuroreport 3:1138–1140.

Welinder C, Ekblad L (2011) Coomassie staining as loading control in Western blot analysis. J Proteome Res 10:1416–1419.

Wenthold RJ, Prybylowski K, Standley S, Sans N, Petralia RS (2003) Trafficking of NMDA Receptors. Annu Rev Pharmacol Toxicol 43:335–358.

Wenzel A, Scheurer L, Kunzi R, Fritschy JM, Mohler H, Benke D (1995) Distribution of NMDA receptor subunit proteins NR2A, 2B, 2C and 2D in rat brain. Neuroreport 7:45–48.

White WF, Nadler J V, Hamberger A, Cotman CW, Cummins JT (1977) Glutamate as transmitter of hippocampal perforant path. Nature 270:356–357.

Whitehead G, Jo J, Hogg EL, Piers T, Kim D, Seaton G, Seok H, Bru-mercier G, Son GH, Regan P, Hildebrandt L, Waite E, Kim B, Kerrigan TL, Kim K, Whitcomb DJ, Collingridge GL, Lightman SL, Cho K (2013) Acute stress causes rapid synaptic insertion of Ca 2 + -permeable AMPA receptors to facilitate long-term potentiation in the hippocampus. Brain 136:3753–3765.

Whitlock JR, Heynen AJ, Shuler MG, Bear MF (2006) Learning induces long-term potentiation in the hippocampus. Science 313:1093–1097.

Wigstrom H, Gustafsson B (1983) Facilitated induction of long-lasting potentiation during blockade of inhibition. Nature 301:1983.

Willingham D (1998) A Neuropsychological Theory of Motor Skill Learning. Psychol Rev 105:558–584.

Wilson S a, Thickbroom GW, Mastaglia FL (1993) Transcranial magnetic stimulation mapping of the motor cortex in normal subjects. The representation of two intrinsic hand muscles. J Neurol Sci 118:134–144.

Winder DG, Sweatt JD (2001) Roles of serine/threonine phosphatases in hippocampel synaptic plasticity. Nat Rev Neurosci 2:461–474.

Windle RJ, Wood SA, Shanks N, Lightman SL, Ingram CD (1998) Ultradian rhythm of basal corticosterone release in the female rat: Dynamic interaction with the response to acute stress. Endocrinology 139:443–450.

Winter B, Breitenstein C, Mooren FC, Voelker K, Fobker M, Lechtermann A, Krueger K, Fromme A, Korsukewitz C, Floel A, Knecht S (2007) High impact running improves learning. Neurobiol Learn Mem 87:597–609.

Wisløff U, Helgerud J, Kemi OJ, Ellingsen Ø, Helgerud JAN, Kemi OLEJ (2001) Intensity-controlled treadmill running in rats : VO2 max and cardiac hypertrophy. Am J Physiol Hear Circ Physiol 280:1301–1310.

Witter MP (2006) Connections of the subiculum of the rat: Topography in relation to columnar and laminar organization. Behav Brain Res 174:251–264.

Witzmann FA, Arnold RJ, Bai F, Hrncirova P, Kimpel MW, Mechref YS, McBride WJ,

Novotny M V., Pedrick NM, Ringham HN, Simon JR (2005) A proteomic survey of rat cerebral cortical synaptosomes. Proteomics 5:2177–2201.

Wrann CD, White JP, Salogiannnis J, Laznik-Bogoslavski D, Wu J, Ma D, Lin JD, Greenberg ME, Spiegelman BM (2013) Exercise induces hippocampal BDNF through a PGC-1α/FNDC5 pathway. Cell Metab 18:649–659.

Wranne and R. D. Woodson. B (2013) A graded treadmill test for rats: maximal work performance in normal and anemic animals. J Appl Physiol 34:732–735.

Wu K, Len GW, McAuliffe G, Ma C, Tai JP, Xu F, Black IB (2004) Brain-derived neurotrophic factor acutely enhances tyrosine phosphorylation of the AMPA receptor subunit GluR1 via NMDA receptor-dependent mechanisms. Mol Brain Res 130:178–186.

Wyllie DJA, Livesey MR, Hardingham GE (2013) Influence of GluN2 subunit identity on NMDA receptor function. Neuropharmacology 74:4–17.

Xu B (2013) BDNF (I)rising from exercise. Cell Metab 18:612–614.

Xu T, Yu X, Perlik AJ, Tobin WF, Zweig JA, Tennant K, Jones T (2009) Rapid formation and selective stabilization of synapses for enduring motor memories. Nature 462:915–919.

Yamada K, Mizuno M, Nabeshima T (2002) Role for brain-derived neurotrophic factor in learning and memory. Life Sci 70:735–744.

Yamada K, Nabeshima T (2003) Brain-derived neurotrophic factor/TrkB signaling in memory processes. J Pharmacol Sci 91:267–270.

Yamaguchi T, Fujiwara T, Liu W, Liu M (2012) Effects of pedaling exercise on the intracortical inhibition of cortical leg area. Exp Brain Res 218:401–406.

Yamamoto C, McIlwain H (1966) Potentials evoked in vitro in Preparations from the Mammalian Brain. J Neurochem 13:1333–1343.

Yan JZ, Xu Z, Ren SQ, Hu B, Yao W, Wang SH, Liu SY, Lu W (2011) Protein kinase C promotes N-methyl-D-aspartate (NMDA) receptor trafficking by indirectly triggering calcium/calmodulin-dependent protein kinase II (CaMKII) autophosphorylation. J Biol Chem 286:25187–25200.

Yang K, Trepanier C, Sidhu B, Xie Y-F, Li H, Lei G, Salter MW, Orser BA, Nakazawa T, Yamamoto T, Jackson MF, Macdonald JF (2011) Metaplasticity gated through differential regulation of GluN2A versus GluN2B receptors by Src family kinases. EMBO J 31:805–816.

Yang S, Roselli F, Patchev A V, Yu S, Almeida OF (2013) Non-receptor-tyrosine Kinases Integrate Fast Glucocorticoid Signaling in Hippocampal Neurons. J Biol Chem 288:23725–23739.

Yarom O, Maroun M, Richter-levin G (2008) Exposure to Forced Swim Stress Alters Local Circuit Activity and Plasticity in the Dentate Gyrus of the Hippocampus. Neural Plast 2008:1–8.

Yuen EY, Liu W, Karatsoreos IN, Feng J, MCEWEN BS, Yan Z (2009) Acute stress enhances glutamatergic transmission in prefrontal cortex and facilitates working memory. Proc Natl Acad Sci 106:14075–14079.

Zakiewicz IM, Dongen YC Van, Leergaard TB, Bjaalie JG (2011) Workflow and Atlas System for Brain-Wide Mapping of Axonal Connectivity in Rat. PLoS One 6.

Zhang J, Zhang W (2016) Can irisin be a linker between physical activity and brain function? Biomol Concepts 7:253–258.

Zhao MG, Toyoda H, Lee YS, Wu LJ, Ko SW, Zhang XH, Jia Y, Shum F, Xu H, Li BM, Kaang BK, Zhuo M (2005) Roles of NMDA NR2B subtype receptor in prefrontal long-term potentiation and contextual fear memory. Neuron 47:859–872.

Zheng Z, Keifer J (2009) PKA has a critical role in synaptic delivery of GluR1- and GluR4-containing AMPARs during initial stages of acquisition of in vitro classical conditioning. J Neurophysiol 101:2539–2549.

Ziemann U, Ilić T V, Iliać T V, Pauli C, Meintzschel F, Ruge D (2004) Learning modifies subsequent induction of long-term potentiation-like and long-term depression-like plasticity in human motor cortex. J Neurosci 24:1666–1672.

Zilles K (1985) The Cortex of the Rat: A Stereotaxic.

Zoladz J, Pilc A (2010) The Effect of Physical Activity on the Brain Derived Neurotrophic Factor: From Animal to Human Studies. Jounral Physiol Pharmacol 61:533–541.

Zucker RS, Regehr WG (1989) Short-Term Synaptic Plasticity. Annu Rev Physiol 12:355–405.

7. Appendix I: Total protein, or high abundance protein: which offers the best loading control for Western blotting?

Adapted from Manuscript: "Thacker JS., Yeung, D., Staines WR., Mielke JG. (2016). Total protein, or high abundance protein: which offers the best loading control for Western blotting? Anal Biochem 496:76–78."

i.1 ABSTRACT

Western blotting routinely involves a control for variability in the amount of protein across immunoblot lanes. Normalizing a target signal to one found for an abundantly expressed protein is widely regarded as a reliable loading control; however, this approach is being increasingly questioned. As a result, we compared blotting for two high abundance proteins (actin, GAPDH) and two total protein membrane staining methods (Ponceau, Coomassie Brilliant Blue) to determine the best control for loading variability. We found Coomassie staining optimally balanced accuracy and precision, and suggest this approach be considered as an alternative to normalizing with a high abundance protein.

i.2 INTRODUCTION

Immunoblotting is a semi-quantitative technique widely used to assess the relative expression of specific proteins in a tissue homogenate, or cell lysate. Samples are denatured, separated electrophoretically, and then transferred onto a protein-absorbing medium, such as polyvinylidene fluoride (PVDF) membrane. The membranes are then incubated with one (or more) antibodies directed at specific target epitopes, and the resulting immunocomplex allows for proteins of interest to be compared across samples using the optical density of observed signals. Notably, the comparison across samples rests on the assumption that an equal amount of total protein has been used for each one. To account for the possibility that the same amount of total protein for each sample may not have been placed onto a gel, a loading control is typically used. For example, one common approach involves the use of antibodies directed at high abundance (i.e., "housekeeping") proteins, such as actin and glyceraldehyde 3-phosphate dehydrogenase (GAPDH), which are critical for cell structure and/or metabolism.

In usual practice, the densitometric value obtained for a protein of interest is divided by the value obtained for the loading control in the same lane, which reflects the assumption that variability in the amount of sample present will be seen in the loading control values. However, two primary concerns exist with this method of controlling for technical variability in the amount of protein present on an immunoblot. First, is the assumption that the expression of the presumptive loading control will not be affected by the experimental conditions. Evidence exists to suggest that the commonly used "housekeeping" proteins can fluctuate in response to various stimuli, different stages of cellular growth and differentiation, and certain disease states (see reviews by Ruan and Lai, 2007 and Li and Shen, 2013; also, Calvo et al., 2008 and Ferguson et al., 2005). Second, when proteins of interest are not abundantly expressed, and therefore require a high loading concentration, one runs the risk of normalizing a target protein's densitometric value to a

"housekeeping" protein densitometric value that is outside the linear range of detection (that is, saturated). Since a saturated signal will not reveal differences in the amount of protein loaded, such a normalization method may lead to the erroneous conclusion that equal amounts of protein are present, which may allow for a false treatment effect to be found.

As an alternative to high abundance proteins, total protein stains have been considered (Klien et al., 1995). For example, Aldridge et al. (2008) were able to show that total protein stains, relative to GAPDH, were more suitable as a loading control, since they were more accurately able to detect differences among serial dilutions of brain samples and showed reduced variability. In addition, Romero-Calvo et al. (2010) used 10 to 140 µg of either liver, or kidney homogenate and found the densitometric signal for actin saturated at around 40 µg of loaded protein, while the Ponceau S signal remained relatively linear. Lastly, Welinder and Ekblad (2011) observed that total protein staining with Coomassie Brilliant Blue was a desirable alternative to GAPDH, which failed to detect differences among increasing protein concentrations. Taken together, previous reports indicate total protein staining should be more broadly applied as an alternative to "housekeeping" proteins.

We sought to contribute to the discussion regarding what approach might offer the best loading control by directly comparing several approaches with rat brain tissue homogenates. We measured differences between increasingly higher concentrations of hippocampal homogenate using the most commonly employed "housekeeping" proteins, actin and GAPDH, as well as two whole proteins stains, Ponceau S and Coomassie Brilliant Blue. In addition, we assessed the precision and accuracy of each loading control method by conducting an experiment where we simulated a "treatment effect" by loading two clearly distinct concentrations of motor cortex homogenate, and then probing for a growth factor receptor (Tropomyosin receptor kinase B; Trk-

B). In summary, our study compared the general characteristics of commonly used loading control methods and, using a simulated experiment, provides evidence for the loading control method that yields the most reliable and reproducible results.

i.3 METHODS

i.3.1 Electrophoresis

Protein homogenates were prepared from either cortex, or hippocampus of male Sprague-Dawley rats (weight: 250-350 g); all animals were used in accordance with procedures approved by the University of Waterloo animal care and ethics committee. Dissected tissue was placed in 3 mL of non-ionizing lysis buffer [10 mM Tris, 25 mM EDTA, 100 mM NaCl, 1% (v/v) Triton X-100, 1% (v/v) NP-40, pH 7.40; all reagents from Sigma-Aldrich unless stated otherwise], manually homogenized over ice with a Potter-Elvehjem homogenizer, and then centrifuged at 1000 x g for 10 min at 4°C. Supernatants were collected, protein concentrations determined with a BioRad DC protein assay kit according to the manufacturer's recommended protocol, and aliquots stored at -80°C. Samples were thawed on ice and then denatured in sample buffer [0.0625 M Tris, 2% (v/v) glycerol, 5% (w/v) SDS, 5% (v/v) β-mercaptoethanol, 0.001% (w/v) bromophenol blue, pH 6.80] at 95°C for 5 minutes before being separated electrophoretically with a 10% SDS-polyacrylamide gel at 200 V for 1 hour. Following electrophoresis, proteins were electroblotted onto PVDF membranes via wet transfer (35 V at 4°C for 16 hours).

i.3.2 Membrane Staining

Blots (N = 5) were incubated with Ponceau S solution for 7 minutes at room temperature with gentle agitation, washed with deionized water for 2 minutes, air dried, and then imaged. After immunoblotting (see following section), membranes were incubated with Coomassie Brilliant

Blue G solution for 5 minutes, washed twice for 5 minutes in 50% (v/v) methanol, air dried, and then imaged.

i.3.3 Immunoblotting

Membranes were blocked with 5% (w/v) non-fat milk in tris-buffered saline with Tween-20 (TBS-T) for 1 hour at room temperature. Antibodies directed at two highly abundant proteins were used: actin (rabbit polyclonal, Sigma-Aldrich, A2066, 1:5000) and GAPDH (rabbit monoclonal, Cell Signaling, 14C10, 1:1000). All antibodies were diluted in 10 mL of 5% milk/TBST before use for overnight incubation (16 hours). Following incubation, blots were washed 3x 10 minute in TBS-T before being incubated with secondary antibody (anti-rabbit IgG-HRP, Santa Cruz Biotechnology Inc, SC 2004, 1:5000) diluted in blocking buffer for 1 hour at room temperature under gentle agitation. Chemiluminescence of secondary antibody conjugates was elicited by the use of Luminata™ Classico electrochemiluminescent reagents (EMD Millipore Corporation).

Imaging

All images were captured using the GeneSnap program and G6000 Gel Dock system (Synoptics, Cambridge, UK). Image analysis was conducted using the GeneTools companion program. Using the automated GeneTools function, antibody chemiluminescence imaged by GeneTools was quantified for each band at the correct molecular weight for the protein of interest for each amount of protein loaded. With regards to the staining methods, whole lane protein was evaluated by constructing peak bounds across the length of the band in an effort to capture total absorbance for each band. The “housekeeping” proteins were evaluated by using the GeneTools automated feature to extract optical densitometry from the entirety of each lane. Optical densities were exported to Microsoft Excel for statistical analysis.

i.3.4 Statistics

Coefficient of variation was conducted on all data sets by calculating the ratio of standard deviation to the mean (CV= standard deviation/mean).

i.4 RESULTS & DISCUSSION

In this study, the approaches commonly used to control for loading variability in Western blotting were evaluated. In our first experiment, hippocampal homogenates of increasing protein concentration were loaded in an effort to evaluate how typical "housekeeping" proteins, such as GAPDH and actin, would compare to total protein stains, such as Ponceau S and Coomassie Brilliant Blue. The purpose of the experiment was to assess the linear range of detection and variability associated with each loading control method, particularly, with regards to neural tissue. A comparison of the relative optical densities derived from the blots revealed that normalizing to the GAPDH signal presented the least desirable option as a loading control, for it had the smallest range (5-10 µg) before signal saturation, which agrees with previous research (Aldridge et al., 2008; Welinder and Ekblad, 2011; Taylor et al., 2013). Notably, Dittmer and Dittmer (2006) have proposed that GAPDH may be suitable as a loading control when less than 7.5 µg of a protein homogenate is used. In addition to signal saturation, GAPDH displayed a dramatic increase in the degree of signal variability as more tissue homogenate was loaded. Actin appeared to be a better alternative, as the variability remained relatively consistent with increasing protein concentration; however, the linear range of actin detection appeared to end around 30 µg, suggesting that actin may not be suitable as a loading control with higher protein concentrations. In contrast to the high abundance proteins, whole protein stains appeared much more suitable as loading controls, for they displayed limited variability across increasing protein concentrations and gave no indication of signal saturation. Given that Coomassie Brilliant Blue staining presented a profile more accurate

(depicted by a slope closer to 1) than that of Ponceau S staining, Coomassie staining appeared to offer the best option as a loading control.

The results from our initial evaluation of loading control methods were tested with a simulated experiment to determine which approach would be best suited to distinguish a clear experimental effect on a target protein. Ideally, a loading control should be able to robustly distinguish between variations in loading concentration in a reproducible manner (i.e., be both accurate and precise). To recreate a "treatment effect," we compared the level of TrkB present in 10 µg and 20 µg of motor cortex homogenate using actin immunolabeling and both Ponceau S and Coomassie Brilliant Blue staining. Notably, due to its poor overall performance, GAPDH immunolabeling was not included in the experiment. We observed that normalizing the TrkB signal to actin was most accurately able to distinguish between the "treatment" and "control" conditions (approximately 1.98-fold). Coomassie Brilliant Blue staining was slightly less effective (an approximate 1.80 times increase in the "treatment" condition), while normalizing our antibody densitometry values to Ponceau S staining provided the poorest outcome (an approximate 1.39 times increase with our "treatment" condition). At first glance, the results seemed to suggest that actin may be the best candidate as a loading control, but when the variability of each method was considered, an important trade-off was revealed. Values from TrkB normalized to actin displayed the greatest variability, and therefore the least amount of precision (Coefficient of variation = 0.38), followed by values normalized to Coomassie Brilliant Blue staining (Coefficient of variation = 0.20). Notably, values normalized to Ponceau S staining were the least variable (Coefficient of variability = 0.06). The lower variability generally observed with the whole protein stains may be related to the fact that they do not rely on specific proteins, which makes them relatively more resistant to treatment effects, as suggested by others (Romero-Calvo et al., 2010).

In summary, while traditional “housekeeping” proteins are often used to control for loading variation, they should be carefully validated for a particular application. For example, with neural tissue, GAPDH may not be suitable as a loading control for any experiment that requires greater than 5 µg to 10 µg of homogenate to be loaded. In addition, while actin may be suitable over a greater concentration range, its accuracy is likely to be counterbalanced by a high degree of variability. Lastly, although whole protein stains would appear to provide a good alternative to high abundance proteins, in general, even they need to be properly characterized. Specifically, considering both accuracy and precision, we would conclude that Coomassie Brilliant Blue provides the best option as a loading control method when using brain homogenate.

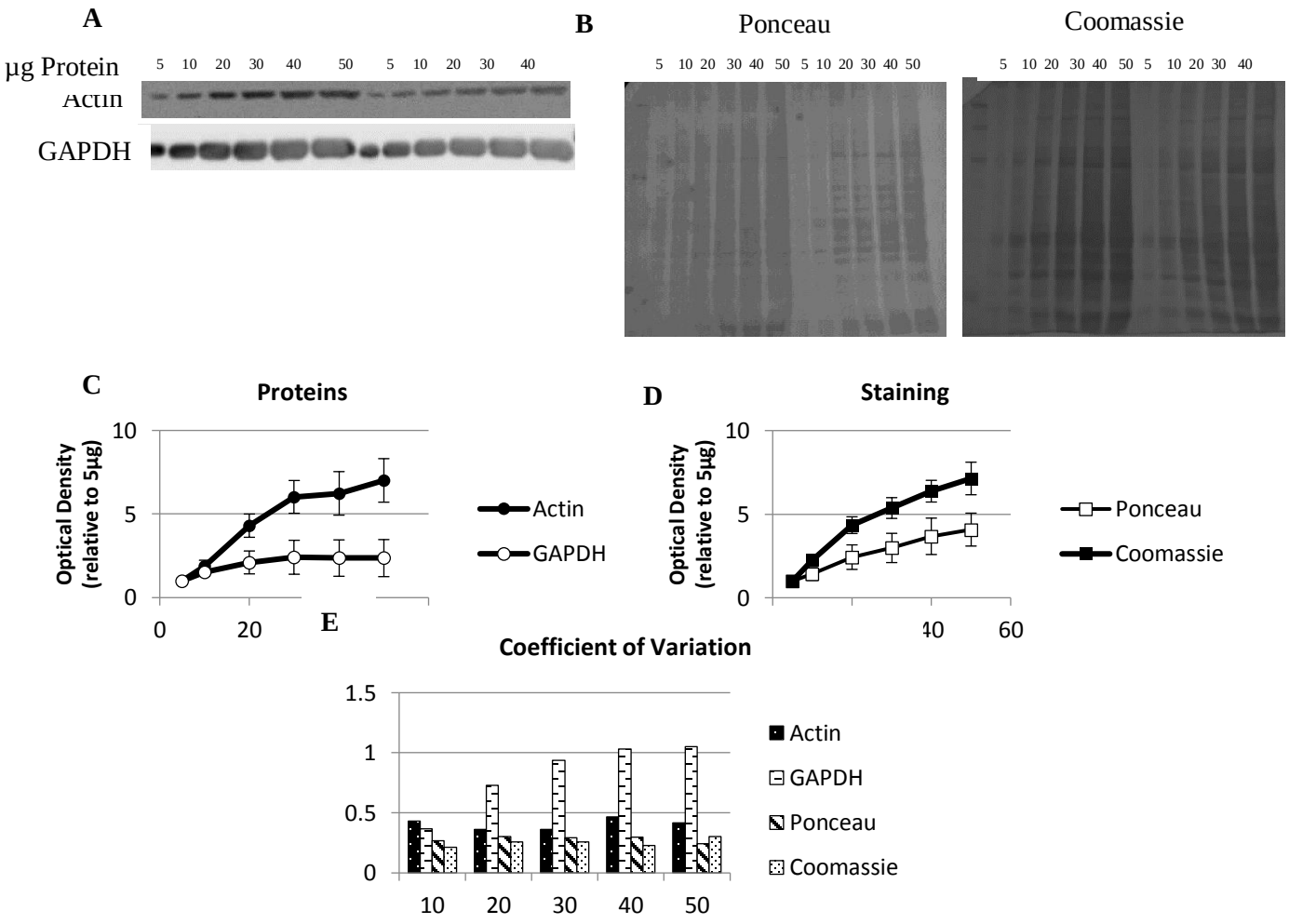

Figure 1: Evaluation of actin and GAPDH immunodetection versus Coomassie Brilliant Blue and Ponceau S membrane staining. (A) The representative blots display increasing protein concentrations examined with Western blotting using either anti-actin, or anti-GAPDH antibodies. (B) Blots stained with either Ponceau S, or Coomassie Brilliant Blue matched to blots in A (the Ponceau S stained membrane matches the actin immunoblot and the Coomassie Brilliant Blue stained membrane matches the GAPDH immunoblot). (C, D) Graphs display average relative optical density recorded for each method (bars present mean + SEM; N = 5 separate blots) for increasing protein concentrations normalized to the 5-µg sample. Line of best fit analysis (not displayed) reported that Ponceau S ($R^2 = 0.9810$, slope = 0.0694) and Coomassie ($R^2 = 0.9536$, slope = 0.1337) were most linear followed by actin ($R^2 = 0.9176$, slope = 0.1362) and GAPDH ($R^2 = 0.7430$, slope = 0.0285). (E) Coefficient of variation for each loading control method across increasing concentrations of protein.

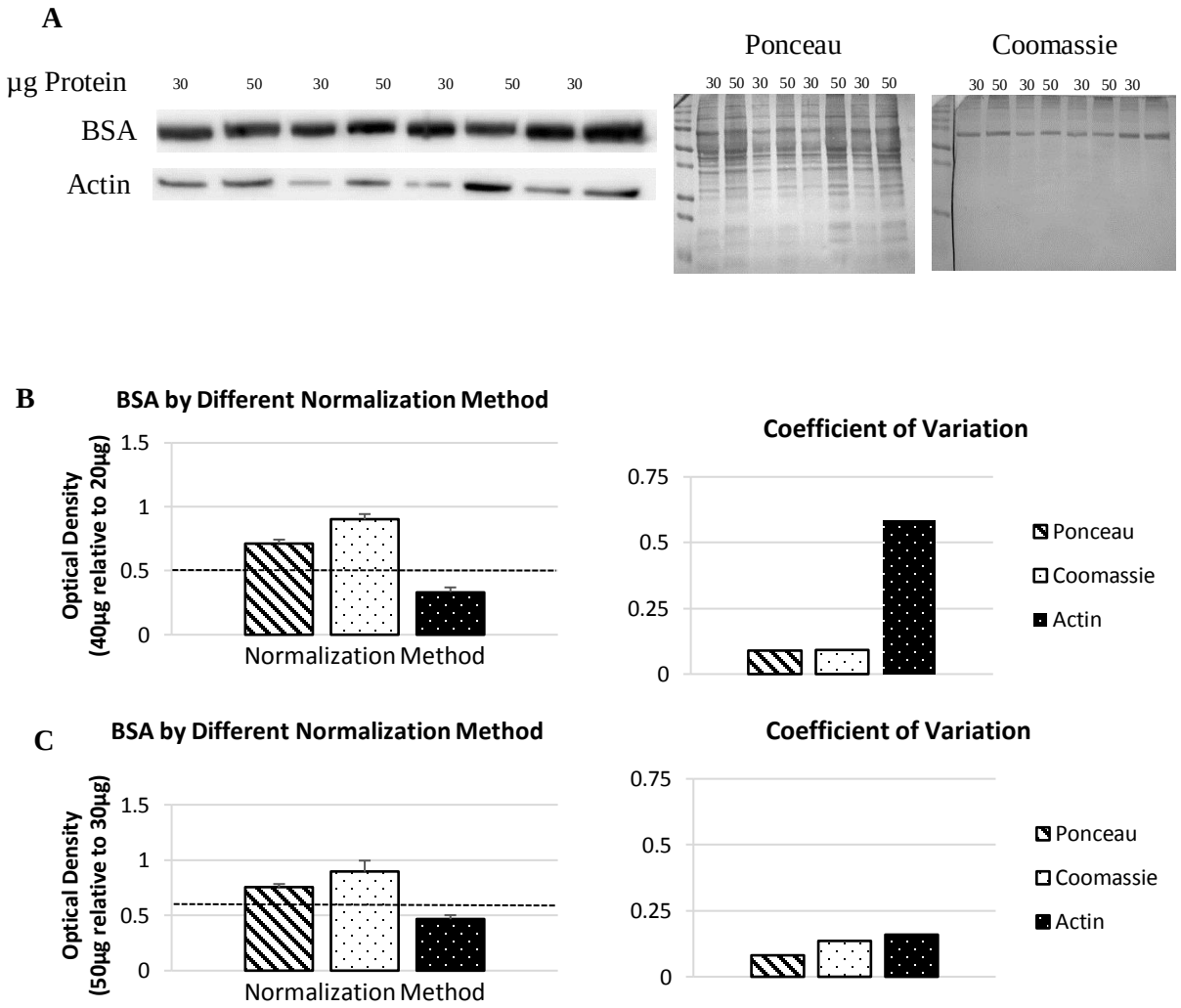

Figure 2: (A) Simulated experiment to assess various loading control methods with a protein of interest (TrkB). Images are from a single blot with protein homogenate loaded at 2 known concentrations (10 µg, 20 µg). (B) The graph displays how well each of the 3 loading control methods measured the known concentration difference (i.e., 2:1) (bars present mean + SEM; N = 5 separate blots). (C) Coefficient of variation by loading control method.